ISSN 0367-2026

ФИЗИКА ЭЛЕМЕНТАРНЫХ ЧАСТИЦ и АТОМНОГО ЯДРА

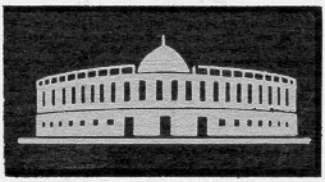

ЭЧАЯ

1995 том 26 выпуск 2

JOINT INSTITUTE FOR NUCLEAR RESEARCH

PHYSICS OF ELEMENTARY PARTICLES AND ATOMIC NUCLEI

PARTICLES & NUCLEI

SCIENTIFIC REVIEW JOURNAL

Founded in December 1970
VOL.26
PART 2
Six issues per year

DUBNA 1995

ОБЪЕДИНЕННЫЙ ИНСТИТУТ ЯДЕРНЫХ ИССЛЕДОВАНИЙ

ФИЗИКА ЭЛЕМЕНТАРНЫХ ЧАСТИЦ И АТОМНОГО ЯДРА

ЭЧАЯ

НАУЧНЫЙ ОБЗОРНЫЙ ЖУРНАЛ

Основан в декабре 1970 года

ТОМ 26

ВЫПУСК 2

Выходит 6 раз в год

ДУБНА 1995

Редактор **Е.К.Аксенова, тел. 65-165**
Э.В.Ивашкевич

«ФИЗИКА ЭЛЕМЕНТАРНЫХ ЧАСТИЦ И АТОМНОГО ЯДРА»
1995, ТОМ 26, ВЫП.2

УДК 539.1.01

FUNDAMENTAL SYMMETRY BREAKING IN NUCLEAR REACTIONS

V.E.Bunakov

Joint Institute for Nuclear Research, Dubna*

A theoretical review is given of P- and (or) T-invariance violating effects in nuclear reactions. It is demonstrated that all of them are characterized by 2 major enhancement factors — dynamical and resonance ones. The net enhancement effect reaches 5—6 orders of magnitude. Both enhancements are caused by quantum chaoticity (complexity) of compound-nucleus resonances. This complexity, however, demands statistical methods of analysis of observed data in order to extract information on symmetry-breaking interaction strength constants. These methods are also presented and discussed in the review.

Дан теоретический обзор эффектов P- и (или) T-несохранения в ядерных реакциях. Показано, что все они характеризуются двумя основными механизмами усиления — динамическим и резонансным. Полное усиление при этом достигает 5—6 порядков. Оба механизма усиления являются следствием квантовой хаотичности (сложности) структуры резонансов компаунд-ядра. Эта хаотичность, однако, приводит к необходимости использования статистических методов анализа экспериментальных данных для извлечения из них информации о силовых константах, нарушающих симметрию взаимодействий. Эти статистические методы также обсуждаются в обзоре.

It is frequently pointed that discovery of America by Columbus nicely illustrated transformation of scientific hypothesis into discovery. Colubmbus cherished the idea that Earth is round and hoped to reach East India by sailing to the West. Notice that:

a. His idea was by no means original, but he received new information.

b. He faced enormous difficulties both in search for subsidies and in carrying on with his experiment.

c. He did not find a new way to India, but discovered a new continent instead.

---

*On leave of absence from St. Petersburg Nuclear Physics Institute, 188350, Gatchina, Russia.

d. In spite of all the arguments to the contrary he continued believing that he discovered a new way to the East.

e. He got neither special respect nor substantial reward in his lifetime.

f. Since then it was proved without doubt that he was not the first European to reach America.

(«Physicists Joking». Mir, Moscow, 1966, p.66)

I. INTRODUCTION

The phase «fundamental symmetry» in the title is the frequently used shorthand for *P*- and *T*-invariance. It just reminds us of old times, when both those symmetries were considered to be most unbreakable. Since then *P*-invariance lost a good deal of its glamour. Its fundamentality was shaken by the discovery of *P*-violation first in β-decay and then in nucleon-nucleon interactions. For a certain time it seemed possible that weak interaction which caused *P*-violation in those two cases might be different for leptonic and baryonic processes. This could have added interest to nuclear *P*-violation studies. However the electroweak interacrtion theory of Weinberg and Salam closed this possibility. The *T*-invariance fortress remains much more invincible. The only experimental fact known by now is CP-violation in *K*-mesons decays discovered 30 years ago. On the basis of the CPT-theorem this implies *T*-violation, which can be explained theoretically in an infinite number of ways. All this makes further search of *T*-violation a much more exciting problem of general importance in physics. In other words, *T*-invariance is much more fundamental nowadays than the *P*-one.

The present wave of interest to *P*-violation in nuclear reactions was boosted by the theoretical predictions [1,2] of possible huge (6 orders of magnitude) enhancement of these effects in the vicinity of compound-nucleus resonances which were almost immediately confirmed experimentally [3]. A year later the same huge enhancements were predicted [4] for the effects violating both *P*- and *T*-invariance. Similar enhancements of *P*-conserving *T*-violating effects were predicted a few years later [5,6]. It seemed to us at that time (and still seems to me now), that those huge enhancements should be primarily used in experimental search of *T*-violating effects, since even establishing new upper bounds on *CP*-interaction constants might help a lot in selecting the most promising models of *CP*-violation.

However this natural way of reasoning does not seem to be well understood and shared. The major part of experimental and theoretical efforts up to now was concentrated on *P*-violation effects. Even there a good deal of energy was wasted on sensation-hunting and theoretical re-discovering of facts known for years.

One of the reasons for this is, according to my experience, a poor understanding of basic and quite general physics, which governs the above enhancements even by those, who work in the field. Lots of them naively believe that one can professionally discuss and analyze symmetry breaking in nuclear reactions without any knowledge of nuclear reaction theory or, at best, with rudimentary knowledge of Breit-Wigner formula. This strange belief is partially explained by bad traditions in nuclear physics, where nuclear structure studies were always considered to be of major importance in spite of the fact that most information for those studies was obtained from nuclear reactions. On deeper level it comes from the fact that quantum mechanics of bound states is in all respects much simpler than for continuum. Therefore it is quite tempting (and often quite misleading) to oversimplify the description of the process by using well-known bound-state analogies.

This unprofessional approach and naive clinging to the bound-state analogies create a fragmentary and wrong impression about the enhancement mechanisms for different observable quantities. For instance, very popular interpretation of neutron transmission enhancement in terms of «structural» enhancement factor $(kR)^{-1}$ does not allow one to understand the significance of P-odd correlation asymmetry measurements in inelastic channels, where the effects might be even larger [7,8] but could not be understood in terms of bound-state parallels. Exactly the same applies to T-violation tests of detailed balance in isolated resonance regime, where the net enhancements might be orders of magnitude larger [6,9] than in transmission experiments and are practically bound only by the experimental energy-resolution. All this leads to prejudiced distortion of the «priority scale» for different observables and often makes the experimentalists to choose rather difficult experiments, which in reality promise no enhancements whatsoever.

Only when the results start to deviate from naive expectations, people start reading papers on nuclear reaction theory. And the lack of professionalism again shows itself — people start mixing one mechanism with the other, reinvent models, which were longly discarded with by professionals or invent «home-brew» models whose validity was never checked in description of nonexotic reaction processes. This in turn often leads to aggressively incompetent statements of the type — «Live me alone with all your fancy reaction models, I had already wasted several days reading some of them and I'm sure, that you are overcomplicating quite simple things».

In view of all this, my present review is primarily addressed to those unprejudiced readers, who realize that nuclear reaction theory is a special branch of nuclear physics developed by generations of professionals. It has only few features in common with the bound-state spectroscopic theories, and I shall try to emphasize them.

Therefore I shall start with brief reminding of P-violation theory in cases of bound states (Sec.II) with special emphasis on its specific enhancements.

Then I shall switch over to my main topic of nuclear reactions for isolated resonances when the average resonance spacing d is much larger than average resonance width Γ (Sec.III).

I shall start this Section by short reminder of some results of nuclear reaction theory for isolated resonances (III, 1), which will be essential for all the further analysis, namely the structure of the wave functions for a system of incident (outgoing) particle and a target (residual) nucleus. In doing this I shall use the best and most physical version of nuclear reaction theory, namely the shell-model with continuum, developed by Mahaux and Weidenmüller [10] as the natural realization of Feshbach's unified theory of nuclear reactions. The advantage of this approach over the more popular R-matrix one lies in much more physical treatment on continuum wave-functions, which allows one to describe both the direct and compound processes in a unified way.

A fairly large Subsection III.2 discusses all the aspects of P-violation in nuclear reactions. Paragraph 2.1 contains the analysis of possible P-violating observables. In paragraph 2.2. a short historical background is given with special emphasis on how erroneous the bound-state parallels might be. The rather lengthy paragraph 2.3 contains the analysis of all the possible mechanisms of P-violation in nuclear reactions (all the 32 terms contributing to P-violating scattering amplitude). Mark that the absolute magnitudes of the corresponding effects are defined by nucleon-nucleon weak-interaction constants, on which up to now we have only educated guesses and whose extraction from experimental observables should be the ultimate aim of our P-violating investigations. Therefore only estimates of relative contributions coming from different mechanisms and of their energy behaviour are meaningful in the analysis of different competing mechanisms. For this reason I expand in paragraph 2.3 on this kind of analysis and emphasize the generality of various enhancement effects specific for each mechanism. It turns out that only 2 major enhancement factors govern the P-violating amplitudes — dynamical enhancement $\tilde{v}/d \sim \sqrt{N}$ ($\tilde{v}$ is the variance of strong interaction matrix element between compound states and $N \sim 10^6$ is the number of basic components, which define the complexity of the compound state wave function) and resonance enhancement d/Γ. While the former enhancement is well-known in the bound-state P-violating theory, the resonance enhancement is a specific feature of continuum spectra, which has no bound-state analogous. After analyzing the energy behaviour of P-violating amplitudes we are forced to come back to observables (paragraph 2.4) in order to investigate their rather complicated energy dependence, caused by the combined influence of P-violating amplitudes in their numerators and P-invariant ones in their denominators. This

allows us to compare the specific enhancements of all the *P*-violating observables in different energy regions and to understand in quite general terms the «priority hierarchy» of observables, which is confirmed by experiments. We also show that the «structural» enhancement factor $(kR)^{-1}$ is an artifact of presenting the auxiliary quantities instead of the really observed ones.

Subsection III.3 deals with *T*-violation. In paragraph 3.1 we discuss specific hidden dangers, which make true *T*-invariance investigations much more subtle than the *P*-invariance ones, and present the list of «true» *T*-violating observables. The theory of *T*-violation in nuclear reactions dates back to late 50-ies and is rather dramatic. However only few people know about it. Therefore I present a short survey of its development in 3.2. Paragraph 3.3 deals with the most important theoretically *P*-odd *T*-odd «triple correlation» (TC). The analysis of possible TC enhancements is given in it together with analysis of specific difficulties in its experimental observation. In 3.4 we analyze the *P*-even *T*-odd correlation (FC) in neutron transmission, demonstrating both its advantages and drawbacks. In 3.5 we analyze the possibilities of *T*-violation detailed balance tests (TVDB) for 2 close-lying resonances, when average spacing d in much larger than average Γ. In paragraph 3.6, we briefly summarize our results on *T*-violation effects showing that all of them are governed by the same dynamical and resonance enhancement effects as the *P*-violating ones. In complete analogy to *P*-violation we present the «priority hierarchy» of *T*-violating observables and conclude that most promising results in the near future might be expected from TVDB tests of paragraph 3.5.

In Section IV the statistical approach to compound-resonance measurements is discussed. In Subsection IV.1 it is demonstrated that both dynamical and resonance enhancements are quite general consequences of quantum chaos characteristic of compound nucleus, which was faced and physically understood in «strong» symmetry-breaking from the dawn of nuclear physics. Therefore the meaningful analysis of weak symmetry-breaking (WSB) matrix elements extracted from experiments should be done with exactly the same mathematical methods which were successfully applied in studies of «strong» symmetry-breaking, namely with the use of randon-matrix theory and Gaussian ensembles of Wigner and Dyson. Since historically such methods were first applied to calculation of energy-averaged WSB quantities, I discuss in Subsection IV.2 the practical disadvantages of «unbiased» energy-averaging and come to the idea of «biased» on-resonance ensemble averaging, which is fully described in Subsection IV.3. In IV.4, I discuss how should one apply the on-resonance theory of IV.3 to the realistic case of necessarily imperfect experimental measurements (small number of independent on-resonance observations with poor experimental accuracy), concluding that the only appropriate way in this case is given by Bayesian statistics (BS) based on the use of standard conditional prob-

ability theory. I also discuss the parallels and differences between BS results and empirical maximum-likelihood method (MLM), which is applied in experimental analysis of *P*-violating effects during recent 5 years. Most obvious disadvantages and nuisances of MLM are shown, especially in the typical case when the spins of observed resonances are unknown. In view of this, I only briefly analyze in Subsection IV.5 the sensational «sign-correlation» effect observed in *P*-violating experiments on ^{232}Th target, and conclude that its statistical significance was greatly exaggerated and is highly questionable.

In Section V, I present a short summary of the most important and general conclusions and recommendations for future.

II. *P*-VIOLATION IN THE CASE OF NUCLEAR BOUND STATES

We shall start with brief reminding of the «classical» *P*-violation experiments in low-energy physics when only the mixing of bound states was considered. Pretty early (see, e.g., [11]) it was realized that the experimental observation of the interference-type phenomena (i.e., observation of *P*-odd correlations in the amplitudes of different processes) has an advantage over the «brute force» violation of probabilities (e.g., *P*-forbidden α-decay) because the latter are quadratic in weak interaction strength constant *F*. There are several possible *P*-odd correlations (see the list in [11]), among them the correlation $(\boldsymbol{\sigma}_\gamma \cdot \mathbf{p}_\gamma) = h_\gamma$ between the spin and momentum of γ-quanta emitted by the excited unpolarized nuclei. The value h is called helicity and leads to circular polarization of the emitted γ-quanta which can be observed experimentally (see, e.g., [12]). Let us consider this experiment in more detail in order to demonstrate various enhancement mechanisms, which might manifest themselves in it. The wave function Ψ_i of the decaying excited state might be presented as a sum

$$\Psi_i = \psi_1 + \alpha \psi_2. \tag{1}$$

Here ψ_1 and ψ_2 are the states of opposite parity, while the coefficient α describes the admixture of the state ψ_2 caused by *P*-violating weak interaction V_W. Standard first-order perturbation theory gives

$$\alpha = \frac{\langle \psi_1 | V_W | \psi_2 \rangle}{E_1 - E_2}. \tag{2}$$

Circular polarization appears as an interference of the electric E_λ and magnetic M_λ transitions of the same multipolarity λ. Therefore

$$h = 2\alpha \langle \psi_f | \hat{O}_\lambda | \psi_1 \rangle \langle \psi_f | \hat{O}'_\lambda | \psi_2 \rangle, \tag{3}$$

where $\hat{O}_\lambda$ is the «regular» γ-transition operator, which connects the main component ψ_1 of Ψ_i with the final state Ψ_f; $\hat{O}'$ is the «irregular» transition operator which, due to P-selection rules, connects only ψ_2 component with Ψ_f. Then the degree of circular pluralization observed will be defined by

$$\delta = \frac{h}{|\langle \psi_f|\hat{O}_\lambda|\psi_1\rangle|^2 + \alpha^2|\langle \psi_f|\hat{O}'_\lambda|\psi_2\rangle|^2} \simeq \alpha \frac{\langle \psi_f|\hat{O}'_\lambda|\psi_2\rangle}{\langle \psi_f|\hat{O}_\lambda|\psi_1\rangle}. \tag{4}$$

It is important to note that δ like *any other observable*, which measures the degree of any symmetry breaking, is always normalized by the *total transition probability*. Therefore, in general, the denominator of (4) contains a sum over all the allowed transitions $\sum_\lambda |\langle \psi_f|\hat{O}_\lambda|\psi_1\rangle|^2$:

$$\delta = \frac{h}{\sum_\lambda |\langle \psi_f|\hat{O}_\lambda|\psi_1\rangle|^2 + \alpha^2|\langle \psi_f|\hat{O}'_\lambda|\psi_2\rangle|^2}. \tag{4a}$$

Only this kind of normalization for observables has real physical meaning — the maximal value of δ is unity, meaning 100% parity violation. This almost trivial rule is taken for granted in all fields of physics, from optics to elementary particles, and all the meaningful enhancements appear only within this normalization. Of course some odd personalities might introduce the normalization of their own by, say, retaining only the weakest term in the normalization sum. If this term is really small, this would immediately enhance the newly introduced quantity. But such a fictitious «enhancement» would have nothing to do with the physics of the process. I have to mention this triviality only because, as we shall see below, even this standard rule is unprofessionally violated all the time in the majority of experimental (and, alas, even theoretical) publications on P-noninvariance in nuclear reactions.

Coming back to ex.(4), we can analyze its structure in order to see the role of different enhancement mechanisms. First of all, we observe that α increases with decreasing level spacing $D = |E_1 - E_2|$ — a natural result of perturbation theory. Therefore naively one should expect the average effect to increase linearly with increasing state density $\rho = 1/d$ of the system (d here is the average level spacing). However the increase of ρ is closely connected with increasing complexity of the mixing states ψ_1 and ψ_2. In terms of basic (so-called «simple configurations») components, which build up the compound state wave function ψ, this means increasing number N of this components and simultaneously the random signs for their admixture coefficients in ψ. Therefore the average value

of $\langle \psi_2 | V_W | \psi_1 \rangle \equiv v_p$ matrix element will be zero in proper statistical treatment (see Sec.IV below), and we can speak only in terms of its variance

$$\tilde{v}_p = \sqrt{(\overline{v}_p^2)}. \tag{5}$$

Using the simple scaling procedure we can express v_p in terms of the strong interaction matrix element v:

$$v_p = F \cdot v, \tag{6}$$

where F is the characteristic ratio of the strengths for weak and strong interaction, which is given by the phenomenological models as $F \approx 10^{-7} \div 10^{-8}$.

The average value of $\tilde{v}$ can be estimated from the usual expression for the spreading width Γ_{spr} of the single-particle resonance (which roughly equals the imaginary part W of optical model potential and in the limit of black nucleus approaches the single-particle level spacing d_0):

$$\Gamma_{spr} = \frac{2\pi \tilde{v}^2}{d} \approx W \sim d_0. \tag{7}$$

This gives us

$$\tilde{v}_p = F_p = \sqrt{\frac{\Gamma_{spr} d}{2\pi}} \approx F_p \sqrt{d_0 d}. \tag{8}$$

Therefore the variance of α in (2) can be estimated as:

$$\tilde{\alpha} = \frac{\tilde{v}_p}{D} = F_p \frac{\tilde{v}}{D} = F_p \sqrt{\frac{\Gamma_{spr}}{2\pi D}} \approx F_p \sqrt{\frac{d_0}{d}} = F_p \sqrt{N}. \tag{9}$$

Thus we see, that the many-body aspect of the compound nuclear system manifests itself in the systematic enhancement of P-violating effect by roughly a factor of $\sqrt{N}$, where N is the number of basic components forming the compound states. The namber N increases with increasing excitation energy E^* and nuclear mass number and reaches $\sim 10^6$ for $E^* \approx B_n$ (B_n is the neutron binding energy) in medium and heavy nuclei. This sort of enhancement was considered several times [13,14,15,16] and received the name [15] of «*dynamical enhancement*».

One can also see from (4) that increasing the value of «irregular» amplitude and decreasing the value of «regular» one leads to the additional enhancement of the effect. This usually happens, when for purely structural reasons the «regular» component is strongly forbidden, while the «irregular» one is favoured. Therefore this kind of enhancement was called (see [15]) «*structural enhancement*».

These enhancements made possible one of the earliest *P*-violating observation in γ-channel [17] on the level of $6 \cdot 10^{-6}$. However even earlier [18], similar experiments were done in (n,γ) reaction with thermal neutrons showing the effects up to ~ 10^{-4}. As we shall see below, these more impressive results can be easily understood in the framework of nuclear reaction theory.

As we see, the general trick of any enhancement mechanism is to make the numerator of the observable (4) as large as possible and the denominator small. The same trick will be used in case of nuclear reactions. Since however both the numerators and denominators of observables in that case are rapidly varying functions of energy, this allows a much larger variety of situations and leads to quite specific enhancements, with we consider in the next sections.

III. NUCLEAR REACTIONS (ISOLATED RESONANCES)

1. Elements of Nuclear Reaction Theory for Isolated Resonances. We shall introduce the basic results of nuclear reaction theory which will be extensively used in all our further applications. In doing this, we shall follow the approach of Mahaux and Weidenmüller [10], which is a projection of Feshbach's unified theory of nuclear reactions on the realistic shell-model basis.

The most essential for our purposes result of this approach is that in the region of isolated resonances, where $\Gamma << d$, the wave function of the system of incident (outgoing) particle plus target (residual) nucleus is given by:

$$\Psi^{(\pm)}_{i,f}(E) = \sum_k a^{(\pm)}_{k(i,f)}(E)\varphi_k + \sum_c \int b^{(\pm)}_{c(i,f)}(E,E')\chi^{(\pm)}_c(E')dE'. \qquad (10)$$

Here φ_k is the wave function of the so-called «bound state embedded in continuum» (BSEC) or, roughly speaking, the wave function of the k-th compound state, where all the nucleons of the system occupy only the bound states in average nuclear potential, but are not allowed to collect all the excitation energy via pair-wise collisions on a single particle. The $\chi_c(E)$ is the continuum c-th channel wave function which, describes the (infinite) motion of a particle in the average field of the target (residual) nucleus. In the particular case of a neutron incident on the ground state target (elastic channel $c = i$), χ_i is the antisymmetrized product of the target nucleus wave function in its ground state times the wave function of a neutron moving in the average field of the target. The φ_k and χ_c correspond to Feshbach's projections on closed (Q) and open (P) channels, respectively. Mind that unless you switch on the pair-wise residual interactions V between the channels (PHQ = QHP in Feshbach's notations), you do not allow the incident neutron to share its energy with the

target nucleons. This does not allow this neutron to form a compound resonance. Therefore in the absence of pair-wise interaction V the BSEC's would never decay, while χ's would describe only potential scattering in the mean field. This unphysical situation changes as soon as we switch on the residual interaction V. Then each resonance k receives partial decay widths $\Gamma_k^{i,f}$ with amplitudes:

$$(\Gamma_k^{i,f})^{1/2} = \gamma_k^{i,f} = (2\pi)^{1/2} \langle \chi_{i,f}(E)|V|\varphi_k \rangle. \tag{11}$$

In other words, the pair-wise residual interaction allows the nucleons of BSEC to collect their total excitation energy on one of the particles and emit it into the open channel i or f.

For the expansion coefficients a and b in this case the theory gives rather transparent expressions:

$$a_{k(i,f)}^{(\pm)}(E) = \frac{\exp(\pm i\delta_{i,f})}{\sqrt{2\pi}} \frac{\gamma_k^{i,f}}{E - E_k + i\Gamma_k/2}. \tag{12}$$

Here E_k is the energy of a given compound resonance, $\Gamma_k = \sum \Gamma_k^c$ is its total width.

The open channel wave functions (second part of (10)) are governed by the coefficients:

$$b_c^{(\pm)}(E,E') = \delta_{c(i,f)}\delta(E - E')\exp(\pm i\delta_c) + \\ + \frac{1}{E^{\pm} - E'} \sum_k a_k^{\pm}(E) \langle \chi_c(E')|V|\varphi_k \rangle. \tag{13}$$

Here $E^{\pm} = E \pm i\varepsilon$ is the usual notation for pole shifts in the complex energy plane.

Let us now simplify the picture, neglecting all the BSEC's in the sums of (10) and (13) besides the one, whose energy E_k is the closet to the energy E of the incident neutron (this might always be done when Γ_k is much smaller than the distance between resonances of the same spin and parity). Let us also consider the case when only the neutron elastic scattering channel is open ($c = i = f$). In this case the continuum term in (10) can be written as:

$$e^{i\delta_i}\chi_i(E) + a_{k(i)}^{+}(E) \int \frac{dE'}{E + i\varepsilon - E'} \langle \chi_i(E')|V|\varphi_k \rangle = e^{i\delta_i}\chi_i(E) + \\ + a_{k(i)}^{+}(E)\left[i\pi \langle \chi_i(E)|V|\varphi_k \rangle \chi_i(E) + \mathcal{P}\int \frac{dE'\chi_i(E)}{E - E'} \langle \chi_i(E')|V|\varphi_k \rangle \right], \tag{14}$$

where $\mathcal{P}$ stands for the integral principal value.

The first term in (14) describes the potential elastic scattering of a neutron. The resonance behaviour of $a_k(E)$ (see (12)) shows that the two terms in square brackets of (14) are the «imprints» of compound resonance at $E = E_k$ on the elastic continuun. Using eq.(11) one can express the first of these terms as

$$i\sqrt{\frac{\pi}{2}}\,\gamma_k^i\,\chi_i(E). \tag{15}$$

Recollecting now that $\chi_i(E)$ describes the single neutron *(valence* particle) in the mean field of a ground-state target, we see that ex.(15) is exactly what was called the single-particle (or *valence*) component u of the compound resonance wave function in the simplified R-matrix theory. The wave function $\chi_i(E)$ belongs to the continuum, as it should. However, if it has a potential resonance at $E = E_0$ with (single-particle) width Γ_0, one can use the approximate expression (see [19]) valid inside the nuclear potential radius R (for simplicity we suppress the coordinates of the target nucleons):

$$\chi(E) \simeq \sqrt{\frac{\Gamma_0}{2\pi}}\,\frac{u_0(r)}{E - E_0 + i\,\Gamma_0/2}\,.$$

Here $u_0(r)$ is the solution of the Schrödinger equation describing particle motion in average field, which is normalized to unity inside the nuclear volume $r \le R$. Substituting this expression into (15), we get in the Γ_0 vicinity of $E \approx E_0$

$$i\sqrt{\frac{\pi}{2}}\,\gamma_k^i\chi_i(E) \simeq \left(\frac{\Gamma_k^i}{\Gamma_0}\right)^{1/2} u_0(r), \tag{16}$$

restoring thus the approximate result of R-matrix approach. The quantity

$$S_k^n = \frac{\Gamma_k^n}{\Gamma_0} \approx \frac{1}{N}$$

is usually called the spectroscopic factor. It defines the probability of finding a single-particle (valence) component in the compound-resonance state, and is equal in the black-nucleus approximation to $1/N \sim (d/\tilde{\nu})^2$, that is, to the inverse square of the dynamical enhancement factor of (9).

Adding up this term (16) to the BSEC's wave function φ just gives us the R-matrix compound resonance wave function:

$$\Phi_k = \varphi_k + \sqrt{S_k^i}\,u_0. \tag{17}$$

Therefore the wave function (10) of the system in the vicinity of isolated compound resonance E_k can be expressed as:

$$\Psi_i^{(\pm)}(E) = a_{k,i}^{\pm}(E)\left[\varphi_k + \sqrt{S_k^i}\, u_0\right] + e^{i\delta_i}\chi_i(E) +$$

$$+ a_k^{\pm}(E)\, \mathcal{P}\int \frac{dE'\chi_i(E')}{E-E'} \langle \chi_i(E')|V|\varphi_k\rangle = a_k^{\pm}(E)\Phi_k + e^{i\delta_i}\chi_i(E) +$$

$$+ a_{k,i}^{\pm}(E)\, \mathcal{P}\int \frac{dE'\chi_i(E')}{E-E'} \langle \chi_i(E')|V|\varphi_k\rangle. \qquad (18)$$

2. *P*-Violation Let us consider now the case of *P*-violation in neutron-induced reactions, which would demonstrate all the specific features of any symmetry-breaking in them.

We shall first discuss the *P*-violating quantities, which might be observed experimentally in these reactions.

2.1. P-Violating Observables in Neutron-Induced Reactions. Using the polarized neutron beam, one can observe the P-violating correlation $(\boldsymbol{\sigma}_n \cdot \mathbf{k}_n)$ between the spin $\boldsymbol{\sigma}_n$ and momentum $\mathbf{k}_n$ of a neutron. There are several possibilities of doing it. One can consider the transmission of neutrons with opposite helicities through a target sample and measure the difference of the corresponding total cross-sections:

$$\Delta_{\text{tot}}^{P} = \sigma_{\text{tot}}^{+} - \sigma_{\text{tot}}^{-} = \frac{4\pi}{k}\,\text{Im}(f_+ - f_-). \qquad (19)$$

Here $f_{\pm}$ defines the forward scattering amplitudes for neutrons with opposite helicities. To obtain the second equality we used the optical theorem.

The corresponding dimensionless measure of this transmission asymmetry effect is

$$P = \frac{\Delta_{\text{tot}}^{P}}{\sigma_{\text{tot}}^{+} + \sigma_{\text{tot}}^{-}} \simeq \frac{\Delta_{\text{tot}}^{P}}{2\sigma_{\text{tot}}}. \qquad (20)$$

One should point (see, e.g., [20]) that in reality the experimentalists do measure the numbers $N_{\pm}$ of neutrons with opposite helicities transmitted through the target sample with thickness x and calculate the ratio:

$$P_{\text{exp}} = \frac{N_+ - N_-}{N_+ - N_-}. \qquad (21)$$

Now for counter efficiency $\varepsilon = 1$

$$N(x) = N_0\, e^{-x\sigma_{\text{tot}}\rho}, \qquad (22)$$

where N_0 is the intensity of the incident beam and ρ is the density of nuclei in a target sample. Expressing $\sigma^{\pm}_{tot}$ as

$$\sigma^{\pm}_{tot} = \sigma^{0}_{tot} \pm \frac{\Delta^{P}_{tot}}{2} \tag{23}$$

one can write

$$N_{+} - N_{-} = N_0 e^{-x\sigma^{0}_{tot}\rho}(e^{+x\Delta^{P}_{tot}\rho/2} - e^{-x\sigma^{P}_{tot}\rho/2}) \simeq N_0 e^{-x\sigma^{0}_{tot}\rho} \cdot \Delta^{P}_{tot} \cdot x \cdot \rho. \tag{24}$$

Therefore

$$P_{exp} \simeq \frac{\Delta^{P}_{tot}}{2} x\rho. \tag{25}$$

It seems from (25) that since the experimentally observed effect increases with x, one should use very thick targets. However (see (22)) the counting rates $N(x)$ go down exponentially with increasing x. The relative counting statistical error equals $1/\sqrt{N}$ and increases exponentially with x:

$$\frac{1}{\sqrt{N}} = \frac{1}{\sqrt{N_0}} e^{\sigma_{tot}\rho x/2}. \tag{26}$$

In order to maximize (25) retaining the minimal possible error (26) one has to choose $x\rho \approx (1/\sigma_{tot})$. Thus *really measured* quantity (25) coincides with the expression (25):

$$P_{exp} = \frac{\Delta^{P}_{tot}}{2\sigma_{tot}} \equiv P. \tag{27}$$

One can easily see [21] that the same quantity could be obtained with unpolarized neutron beam. Then P is just a measure of the longitudinal polarization of the initially unpolarized beam arising after passing a distance in the sample equal to mean free path (hence the symbol P, denoting this quantity). Sometimes one measures the difference in radiative capture cross sections $\sigma^{(\pm)}_{n\gamma}$ and gives the quantity:

$$A = \frac{\sigma^{+}_{n\gamma} - \sigma^{-}_{n\gamma}}{\sigma^{+}_{n\gamma} + \sigma^{-}_{n\gamma}}. \tag{28}$$

The same $(\boldsymbol{\sigma}_n \cdot \mathbf{k}_n)$ correlation in the elastic scattering amplitude also causes the rotation of the neutron polarization around $\mathbf{k}_n$. The angle of this rotation per unit length of the target sample is defined [22] as follows:

$$\frac{d\Phi}{dz} = \frac{2\pi\rho}{k} \mathrm{Re}\,(f_+ - f_-), \tag{29}$$

where ρ is the density of nuclei in the sample. For the same reasons of better statistics the experimentally defined angle Φ is measured for neutrons, which travelled the distance z equal to mean free path $1/\rho\sigma_{tot}$ in the target:

$$\Phi = \frac{1}{\rho\sigma_{tot}} \frac{d\Phi}{dz} = \frac{\mathrm{Re}\,(f_+ - f_-)}{\mathrm{Im}\,(f_+ + f_-)}. \tag{30}$$

One can also look for inelastic reaction (n,f) and measure the P-odd correlation $(\boldsymbol{\sigma}_n \cdot \mathbf{k}_f)$ between the initial neutron polarization and the momentum $\mathbf{k}_f$ of the outgoing particle in channel f. This is done by measuring the asymmetry of the final products with respect to $\boldsymbol{\sigma}_n$:

$$\Delta_{nf} = \frac{d\sigma_{nf}}{d\Omega}\uparrow\uparrow - \frac{d\sigma_{nf}}{d\Omega}\uparrow\downarrow. \tag{31}$$

The corresponding dimensionless degree of asymmetry is:

$$\alpha_{nf} = \frac{\Delta_{nf}}{\frac{d\sigma_{nf}}{d\Omega}\uparrow\uparrow + \frac{d\sigma_{nf}}{d\Omega}\uparrow\downarrow}. \tag{32}$$

2.2. Historical Background. The possibility of using low energy neutron-nucleus interactions and all sorts of neutron coherent scattering processes (neutron optics) in studies of P-violation was considered long ago (see [21,22,23,24]). But these theoretical investigations were concerned only with potential scattering models completely disregarding the presence of compound-resonances. Some of these approaches ([23,24]) made a point of possible enhancement of the effects in the vicinity of potential (single-particle) p-wave resonance. The first theoretical paper [25] mentioning the possible enhancement of γ-ray circular polarization in the vicinity of compound resonance remained unnoticed. The first simplified approach to compound resonance analysis which really encouraged the experimental investigations was done only in 1980 ([1], see also [26]). In this approach the p-wave compound resonance was treated in complete analogy with the bound-state case above (see Sec.II). Indeed, Sushkov and Flambaum took the case of two closely-lying bound states (imitating p- and s-resonances) with corresponding wave functions ψ_1 and ψ_2. Then in complete analogy to (1), the p-resonance wave function, which takes into account the possible parity admixture, looks like:

$$\Psi(E_p) = \Psi_p + \alpha\Psi_s. \tag{33}$$

Now one might just say that in case of elastic scattering both states decay by neutron emission and substitute the γ-ray transition probabilities in (3) and (4) by the corresponding partial neutron widths Γ_s^n and Γ_p^n. Then one immediately obtains for, say, *P*-value in analogy to (4):

$$P \approx \alpha \frac{\sqrt{\Gamma_s^n}}{\sqrt{\Gamma_p^n}}. \tag{34}$$

In slow neutron case $\Gamma_p^n \approx (kR)^2 \Gamma_s^n$, where $(kR)^2$ comes from the centrifugal barrier penetration factor. Thus

$$P \approx \frac{\alpha}{kR}. \tag{35}$$

The typical value of (kR) for eV energy region in medium and heavy nuclei is ~ 10^{-3}. Thus in addition to the dynamical enhancement contained in α, they got a particular case of «structural enhancement» factor ~ 10^3.

This way of arguing *sometimes* gives, as we shall see later, the correct order of magnitude estimate of the effect, but is quite misleading. To start with, the initial equation (33) for the continuum wave function is meaningless, since each continuum wave function with fixed momentum $\mathbf{k}_n$ *is always* a linear superposition of states with opposite parities (i.e., superposition of partial waves). Therefore the compound nucleus wave function $\Psi(E)$ even in the simplest case of slow neutron elastic scattering without any *P*-violating forces is a sum of *p*- and *s*-compound resonance wave functions Ψ_p and Ψ_s with corresponding «mixture» coefficients (see eq.(10) or any sound reaction theory):

$$\frac{e^{i\delta_p}(\Gamma_p^n)^{1/2}}{E - E_p + i\Gamma_p/2} \quad \text{and} \quad \frac{e^{i\delta_s}(\Gamma_s^n)^{1/2}}{E - E_s + i\Gamma_s/2}.$$

Thus even in the maximum of *p*-resonance ($E = E_p$) we have:

$$\Psi(E_p) \sim \Psi_p + \alpha' \Psi_s,$$

where

$$\alpha' = i \frac{\Gamma_p}{2D} \left(\frac{\Gamma_s^n}{\Gamma_p^n} \right)^{1/2}.$$

Proceeding now with the bound-state arguments which lead us from (33) to (34), we obtain

$$|P| = |\alpha'| \left(\frac{\Gamma_s^n}{\Gamma_p^n} \right)^{1/2} = \left(\frac{\Gamma_s^n}{\Gamma_p^n} \right) \frac{\Gamma_p}{2D} \approx \frac{1}{(kR)^2} \frac{\Gamma_p}{2D} \sim 10^6 \frac{\Gamma}{D}.$$

For the famous *La* case this would give us $P \approx 10^3$ *without any weak interaction!*

There are also other striking absurdities in (34), (35): a) Consider its energy behaviour. Since all the E dependence enters (34), (35) essentially through the energy dependence of partial widths, we see that the effect (35) blasts to infinity for very small E (small k). b) We know that neutron partial widths vary in a rather wide range obeying Porter-Thomas law. Eq.(34) clearly indicates that the largest P effects would be observed for the smallest Γ_p^n possible — the less observable p-resonance is in total cross-section the more it would stick out in P-violation. Even more tempting is to repeat the whole above reasoning for mixing of resonances in higher partial waves (say, $l = 3$ ones) with s-wave resonance. (This is perfectly legitimate if one considers the target with spin $I \geq 2$). Then the «regular» neutron partial widths would be even smaller ($\Gamma_l^n \approx (kR)^{2l} \Gamma_s^n$) and for $l = 3$ we obtain «structural enhancement» factor $1/(kR)^3 \sim 10^9$ in eq. (39). This allows the quantity P, which by definition (20) cannot exceed unity, to reach the value 10^5. Obviously Sushkov and Flambaum were too good theorists to be caught into such traps, but I have seen an experimental proposal with clearly stated intentions to hunt for the weakest p-resonances in order to obtain maximal P effects. I also know experimental group, which made special efforts to perform transmission experiments with thermal neutrons and was quite disappointed when the effect turned out to be about 10^{-6} instead of huge increase predicted by eq. (35). To mix up things even more, the above «structural enhancement» of Sushkov — Flambaum nowadays is called in a lot of experimental papers «the kinematic enhancement» (originally this name was given by Shapiro [15] to the typical ratio of electric to magnetic transition amplitudes, which might really cause additional enhancement of P-violating observables in γ-transitions).

In spite of all these inconsistencies, these theoretical results, as I had already pointed out, greatly encouraged the preparation of on-resonance experimental measurements of the Dubna group [3].

The first proper theoretical treatment of the problem in the framework of nuclear reaction theory was given by us in the beginning of 1981 [2]. We had derived the expressions for Δ_{tot}^P and $\text{Re}(f_- - f_+)$ essential for the description of P-violation in neutron transmission. Since the Dubna on-resonance measurements were still in preparation at that time, we had to check our theory [2] by comparing the theoretical relations between P and Φ values at thermal energies

with the existing experimental measurements in *Sn* performed by the Grenoble group [27]. A few months later Dubna group has performed the first on-resonance observations in *Sn* [3] and checked our expression for $P(E)$ by comparing their on-resonance results with thermal-energy ones, obtained by Lobashov's group in Gatchina [28]. This was the first experimental confirmation of the resonance enhancement mechanism. Ironically enough that, although our expressions for $\Delta^{P}_{\mathrm{tot}}(E)$ derived in [2] clearly manifested the resonance enhancement parameter D/Γ, we fully understood its physical meaning and generality only a year later, while finishing a big paper on general theory of *P*- and *T*-violating effects [7]. Some of our expressions obtained in that paper were re-derived later on in the framework of *R*-matrix theory [29,30]. Quite apart stands the theoretical investigation [31] of the $\alpha_{n,f}$-type correlation in the particular case of $(\mathbf{p}, \alpha)$ reactions. The authors obtained fairly large estimates, but did not realize that they hitted the new far-leading enhancement mechanism for $\alpha_{n,f}$ correlation. This fact, together with principal possibility of observing *P*-violating effects of the order of unity, was pointed out in [8].

2.3. P-Mixing Mechanisms and Specific Enhancements in Neutron-Induced Reactions. Any proper treatment of *P*-violation in nuclear reactions consists of two steps: 1. Expressing the observed quantity in terms of the *P*-violating part of *T*- (or *S*) matrix T_W. 2. Calculating T_W in the first-order Born approximation with respect to weak interaction V_W.

The first part of the task involves the standard theory of reaction kinematics with polarized beams (see, e.g., [32,21,22]). As it is usual in any of angular correlations, this gives rather awkward combinations of vector-coupling coefficients, which are all of the order of unity and which do not contribute to the understanding of essential physics. The general expressions for them can be found in [7,29,30] (two latter references even give numerical values for some target spins). We shall further on omit them in the majority of expressions. The effects also depend linearly on the incoming beam polarization p, which will be set to unity in all the further expressions. In case of slow neutrons one can also restrict the neutron angular momenta by $l_n = 0$ and $l_n = 1$.

With these remarks one obtains the following expressions:

$$\Delta^{P}_{\mathrm{tot}} = \frac{\pi}{k^2} \mathrm{Im}\,[\langle p, j = 1/2 | T_W | s \rangle + \langle s | T_W | p, j = 1/2 \rangle], \tag{36}$$

$$\frac{d\Phi}{dz} = \frac{2\pi\rho}{k^2} \mathrm{Re}\,[\langle p, j = 1/2 | T_W | s \rangle + \langle s | T_W | p, j = 1/2 \rangle], \tag{37}$$

$$\Delta_{nf} = \frac{2\pi}{k^2} \sum_{l_f, l_n} \mathrm{Im}\,\{\langle l_f, f | T | l_n \rangle \langle (l_f + 1), f | T_W | l_n \rangle\}. \tag{38}$$

Here $\langle l_f+1, f|T_W|l_n\rangle$ means the parity violating element of T-matrix describing the transition from initial state with $l_n = 0,1$ (s-, p-correspondingly) to the final state with angular momentum (l_f+1); f means all the additional quantum numbers defining the channel f (j in case of elastic p-wave); $\langle l_f, f|T|l_n\rangle$ defines the corresponding P-allowed transition.

Now one can use the Born approximation to calculate the P-forbidden transition

$$T_W = \langle \Psi_f^{(-)}|V_W|\Psi_i^{(+)}\rangle. \tag{39}$$

To simplify the problem even more, we shall retain only one s- and p-wave resonance in expressions (18) for the initial and final states. In this case the first-order Born amplitude (39) contains 9 terms:

$$\begin{aligned}
T_W = \langle \Psi_s^{(-)}|V_W|\Psi_p^{(+)}\rangle &= a_p^+(E)\langle \Psi_s|V_W|\Psi_p\rangle a_s^+(E) + \\
&+ e^{i\delta_s} a_p^+(E)\langle \Psi_p|V_W|\chi_s(E)\rangle + \\
&+ a_p^+(E)a_s^+(E)\,\mathcal{P}\int \frac{dE'}{E-E'}\langle \Phi_p|V_W|\chi_s(E')\rangle\langle \chi_s(E')|V|\varphi_s\rangle + \\
&+ e^{i\delta_p}\langle \chi_p(E)|V_W|\Phi_s\rangle a_s^+(E) + e^{i(\delta_s+\delta_p)}\langle \chi_p(E)|V_W|\chi_s(E)\rangle + \\
&+ e^{i\delta_p} a_s^+(E)\,\mathcal{P}\int \frac{dE'}{E-E'}\langle \chi_p|V_W|\chi_s(E')\rangle\langle \chi_s(E')|V|\varphi_s\rangle + \\
&+ a_p^+(E)a_s^+(E)\,\mathcal{P}\int \frac{dE'}{E-E'}\langle \varphi_p|V|\chi_p(E')\rangle\langle \chi_p(E')|V_W|\varphi_s\rangle + \\
&+ a_p^+(E)\,e^{i\delta_s}\,\mathcal{P}\int \frac{dE'}{E-E'}\langle \varphi_p|V|\chi_p(E')\rangle\langle \chi_p(E')|V_W|\chi_s\rangle + \\
&+ a_p^+(E)a_s^+(E)\,\mathcal{P}\int \frac{dE'dE''}{(E-E')(E-E'')}\langle \varphi_p|V|\chi_p(E')\rangle \times \\
&\times \langle \chi_p(E')|V_W|\chi_s(E'')|V|\varphi_s\rangle .
\end{aligned} \tag{40}$$

In order to understand the physical meaning of each term it is useful to introduce the graphical technique with the following correspondence rules: the wavy line with indices (p- or s-) means an $l=1$ or $l=0$ neutron in the mean field of the target; thin solid line means the ground state target; empty circles correspond to strong interaction amplitudes $\gamma_s^n \exp i\delta_s/\sqrt{2\pi}$ and $\gamma_p^n \exp i\delta_p/\sqrt{2\pi}$; crossed circles correspond to weak interaction matrix

elements; double solid lines with indices correspond to resonance propagators $1/[E-E_s)+i\,\Gamma_s/2]$ or $1/[E-E_p)+i\,\Gamma_p/2]$ for s- or p- BSEC's φ_s or φ_p; the boldface solid lines mean the same propagators, but for the «full» compound-resonance wave functions Φ_s or Φ_p (see eq.(17)); the closed loop of neutron and target lines implies the principal value integration over neutron energy.

The first term in (40)

$$T_1=\frac{e^{i\delta_p}\gamma_p^n}{\sqrt{2\pi}}\,\frac{1}{(E-E_p)+i\,\Gamma_p/2}\,\langle\,\Phi_p|V_W|\Phi_s\,\rangle\,\frac{1}{(E-E_s)+i\,\Gamma_s/2}\,\frac{e^{i\delta_s}\gamma_s^n}{\sqrt{2\pi}} \tag{41}$$

describes (see diagram 1 of Fig.1) the p-neutron strong absorption into compound resonance Φ_p, p-resonance propagation, its weak-interaction mixing with compound resonance Φ_s, propagation of s-resonance and its strong decay.

The second term

$$T_2=\frac{e^{i\delta_p}\gamma_p^n}{\sqrt{2\pi}}\,\frac{1}{(E-E_p)+i\,\Gamma_p/2}\,\langle\,\Phi_p|V_W|\chi_s(E)\,\rangle \tag{42}$$

describes (diagram 2 of Fig.1) the p-neutron strong absorption into compound resonance Φ_p, p-resonance propagation and its subsequent «weak» decay into the s-wave continuum state.

The third term

$$T_3=\frac{e^{i\delta_p}\gamma_p^n}{\sqrt{2\pi}}\,\frac{1}{(E-E_p)+i\,\Gamma_p/2}\,\mathcal{P}\int\frac{dE'}{E-E'}\,\langle\,\Phi_p|V_W|\chi_s(E')\,\rangle\times$$

$$\times\,\langle\,\chi_s(E')|V|\Phi_s\,\rangle\,\frac{1}{(E-E_s)+i\,\Gamma_s/2}\,\frac{e^{i\delta_s}\gamma_s^n}{\sqrt{2\pi}} \tag{43}$$

describes (diagram 3 of Fig.1) p-neutron strong absorption, p-resonance propagation of Φ_p, its «weak» decay into s-neutron continuum with immediate strong reabsorption of s-neutron into the s-resonance state Φ_s. Then follows s-resonance propagation of Φ_s, and its strong neutron decay. We see that this is another way of mixing p- and s-resonance (compare with T_1) by virtual emission and reabsorption of s-wave neutron. The processes of this type were first encountered in isospin symmetry breaking, where they played an important role. Historically they were first analyzed in terms of R-matrix theory and called «external mixing» processes, contrary to the «internal mixing» of T_1.

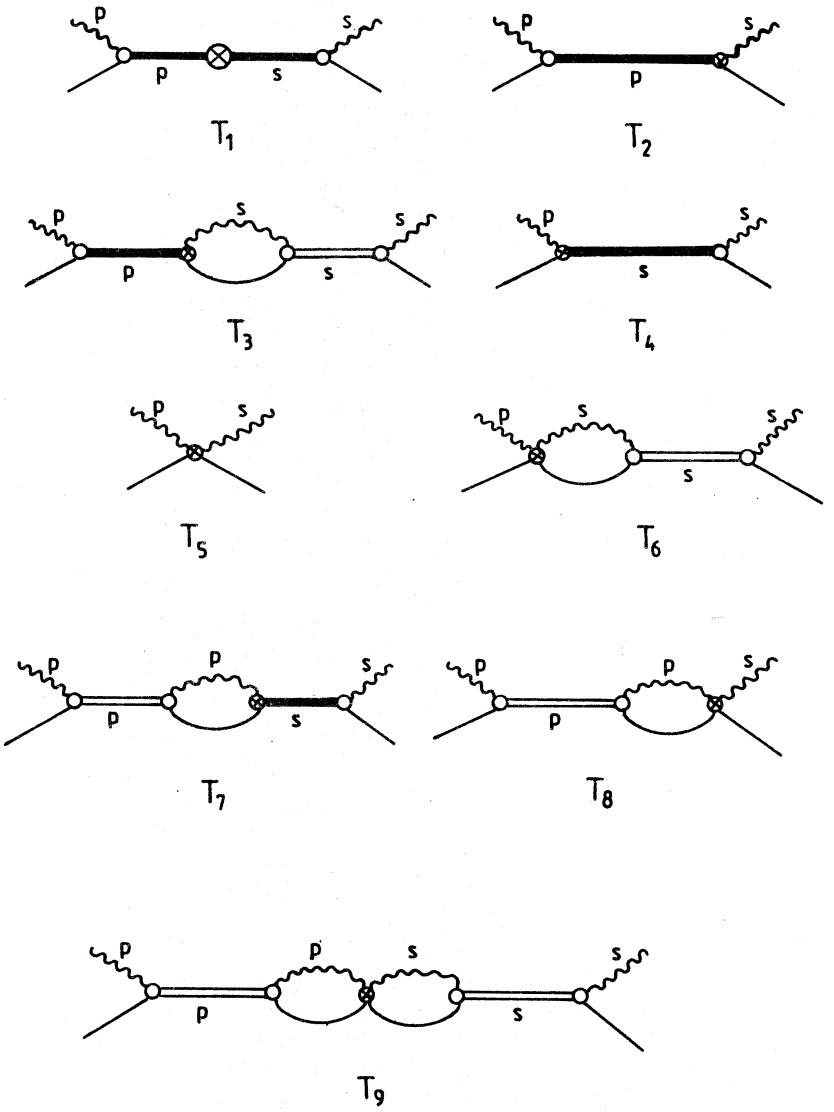

Fig. 1. Diagrams of possible processes contributing to p-violation in neutron-nucleus elastic scattering

The fourth term T_4 describes p-neutron «weak» absorption forming s-resonance compound state Φ_s which then decays in a normal «strong» way. It is obvious (see Fig.1) that this amplitude closely resembles the T_2 amplitude.

The fifth term T_5 describes just the potential scattering of p-wave neutron in the weak mean field of the target. This type of process was historically discussed in P-violation first of all (see, e.g., [22]) and is important, since all the specific enhancements below should be defined with respect to this simplest amplitude.

The term T_6 describes re-scattering of p-wave neutron in the weak mean field of the target with subsequent «strong» absorption of the created s-neutron forming the s-resonance BSEC φ_s. This resonance propagates and then decays in a normal «strong» way governed by γ_s^n amplitude. This process is topologically close to the process T_8 (see below).

The term T_7 describes strong p-neutron absorption into p-compound BSEC φ_p, resonance propagation and strong decay, which is followed by «weak» re-absorption of neutron into s-compound resonance state Φ_s. This state then decays in a normal «strong» way. Obviously T_7 is very similar to the above T_3 one.

We have already mentioned that T_8 is very similar to T_6. It describes the strong formation of the p-resonance BSEC and its strong decay followed by weak re-scattering in the target field. Exactly this amplitude was considered recently by Weidenmüller and Lewenkopf [33,34].

Finally T_9 describes «strong» p-compound formation of Φ_p and its «strong» decay, which is followed by «weak» re-scattering in the target mean field. The s-neutron created in this re-scattering is then «strongly» re-absorbed into s-compound BSEC, which finally decays in a normal «strong» way.

Now, as we know all the essential mechanisms contributing to P-violation in slow neutron-nucleus elastic scattering, it is high time to estimate which of them gives the most important contribution and why. In doing this estimates we shall drop all the phase shift exponentials because in the energy region of interest to us $\delta_s \sim (kR) \sim 10^{-3}$, $\delta_p \sim (kR)^2 \sim 10^{-6}$. Since the total resonance widths in this region are defined essentially by γ-emission we shall assume that $\Gamma_s \approx \Gamma_p = \Gamma$. For simplicity we shall denote $|E_s - E_p|$ as D and assume that $D \sim d$.

We shall tell the reader in advance the result of our analysis carried out back in 1982 (see [7]) — the dominant contribution comes from the mechanism

of T_1, which is usually called compound-compound (c-c) mixing. Other mechanisms' contributions are smaller by, at any rate, the above factor of dynamical enhancement $v/D \sim \sqrt{N} \sim 10^3$ (see eq.(9)). Therefore we shall estimate the ratios of T_1 to all other amplitudes in (40).

We shall start with standard weak potential scattering T_5, which defines the process in the simplest systems of n—p type. In order to estimate T_5 we shall first take the weak interaction scaling factor F out of $\langle \chi_p(E)|V_W|\chi_s(E) \rangle$. Then we shall proceed by removing the extra barrier penetration factor out of the amplitude, thus converting T_5 into the strong interaction amplitude $\langle \chi_s(E)|V|\chi_s(E) \rangle$, which roughly equals the s-wave phase shift $\delta_s \sim (kR)$. Thus:

$$\langle \chi_p(E)|V_W|\chi_s(E) \rangle \approx F \cdot (kR)^2. \tag{44}$$

The exact calculation of T_5 done in [34] shows that ex.(44) is correct to within a constant factor of ~ 7. Now we can estimate the ratio

$$\frac{T_1}{T_5} \approx \frac{\gamma_p^n \gamma_s^n \langle \Phi_p|V_W|\Phi_s \rangle}{(E-E_p+i\,\Gamma_p/2)(E-E_s+i\,\Gamma_s/2)} \cdot \frac{1}{F(kR)^2} \approx$$

$$\approx \frac{S_n \Theta_0^2 v}{(E-E_p+i\,\Gamma_p/2)(E-E_s+i\,\Gamma_s/2)}. \tag{45}$$

Here we have done the scaling (see eq.(6)) of weak interaction matrix element $v_p = Fv$ and used the standard estimates of neutron partial widths, factoring out the barrier penetration $(kR)^{2l+1}$, spectroscopic factor S_n and the «single-particle reduced width» $\Theta_0^2 = 2\hbar^2/mR^2$. The resonance denominators of T_1 give the smallest ratio (45) exactly between the E_s and E_p. In this energy point (we consider the case of $D >> \Gamma$):

$$\frac{T_1}{T_s} \approx \frac{S_n \Theta_0^2 v}{D^2} \approx \frac{\Theta_0^2 v}{d_0 D} \approx \frac{v}{D} \sim \sqrt{N}. \tag{46}$$

In estimating (46) we assumed that $S_n \sim d/d_0$, where the single-particle level spacing d_0 was taken to be roughly equal to Θ_0^2 (see, e.g., [12]). Thus we see that under the worst «off-resonance» conditions c-c mixing mechanism T_1 gives us the dynamical enhancement factor. We also see that this enhancement disappears for the simplest systems with $N \sim 1$. This, however, is not the whole story. We also see from (41), (45) that in the vicinity of each

resonance pole ($E \approx E_s$ or E_p) T_1 presents us with extra resonance enhancement factor D/Γ, providing thus for the overall enhancement of the ratio

$$\left(\frac{T_1}{T_5}\right)_{\text{res}} \approx \frac{v}{D}\frac{D}{\Gamma} = \frac{v}{\Gamma}. \tag{47}$$

The above *resonance enhancement* is a specific feature of nuclear reactions which has no analogues in case of bound states. Its meaning is, however, quite transparent — the magnitude of P-violating effects is proportional to the time τ spent by incident neutron in the weak-interaction field of the target. The role of the complicated compound resonance is to capture the neutron and keep it inside the compound system for a long time $\tau = h/\Gamma$. This kind of effect was first mentioned by Mahaux and Weidenmüller [35].

Consider now the ratio of T_1 to T_2:

$$\frac{T_1}{T_2} \approx \frac{\gamma_s^n \langle \Phi_p | V_W | \Phi_s \rangle}{(E - E_s + i\,\Gamma_p/2)\langle \Phi_p | V_W | \chi_s \rangle} \approx \frac{v}{(E - E_s + i\,\Gamma_p/2)}. \tag{48}$$

In performing the estimate we introduced the scaling $\langle \Phi_p | V_W | \chi_s \rangle \sim$ $\sim F \langle \Phi_s | V | \chi_s \rangle \approx F \cdot \gamma_s^n$. We see again that even in the worst case of $E = E_p$ the T_1 dominates by the dynamical enhancement factor v/D, while at $E = E_s$ the resonance enhancement D/Γ is added.

Since T_4 amplitude is topologically close to T_2 the ratio T_1/T_4 demonstrates exactly the same enhancements with exchange of E_s by E_p.

All the remaining diagrams in Fig.1 contain closed loops of principal value integrals. In estimating those loops we shall follow the arguments of Weidenmüller and Lewenkopf [34,35] carried for the case of T_8. Crudely their argument was that the main E' dependence in the integral

$$\mathcal{P} \int \frac{dE'}{E - E'} \langle \varphi_p | V | \chi_p(E') \rangle \langle \chi_p(E') | V_W | \chi_s(E) \rangle \tag{49}$$

comes from the barrier penetration factor $(kR)^{2l+1}$ of $|\chi_p(E')|^2$. This allows one to drop the principal-value symbol and carry the integrands at $E' = E$ out of the integral. Thus (49) becomes:

$$\langle \varphi_p | V | \chi_p(E) \rangle \langle \chi_p(E) | V_W | \chi_s(E) \rangle \int \frac{dE'}{E'} \frac{\chi_p^2(k'R)}{\chi_p^2(kR)}. \tag{50}$$

In case of square well potential $\chi_p(kR) \sim j_l(kR)$, and one gets the analytical result

$$\langle \varphi_p | V | \chi_p(E) \rangle \langle \chi_p(E) | V_W | \chi_s(E) \rangle \cdot \frac{3\pi}{(kR)^3} \approx \gamma_p^n \frac{F}{(kR)} . \tag{51}$$

In order to obtain the final result we used the above estimate (44) for weak-interaction amplitude. More exact numerical calculations of [34] for Woods-Saxon potential show that instead of 3π one gets the value $C = 3.1$. This obviously does not affect our order-of-magnitude estimates.

Now we can estimate the ratio of T_1 to

$$T_8 \simeq \frac{\Gamma_p^n F}{(E - E_p + i\Gamma_p/2)(kR)} . \tag{52}$$

We see that this ratio is

$$\frac{T_1}{T_8} \approx \frac{\gamma_s^n}{\gamma_p^n} \frac{(kR)v}{(E - E_s + i\Gamma_s/2)} \approx \frac{v}{(E - E_s + i\Gamma_s/2)} . \tag{53}$$

Again we observe that even at $E = E_p$ the T_s is smaller by the dynamical enhancement factor $v/D \sim \sqrt{N}$.

Since T_6 is topologically close to T_8, the same dynamical enhancement is lacking in T_6 even at $E = E_s$, while at $E = E_p$ the resonance enhancement of T_1 is added to the ratio T_1/T_6.

Now we can use the above procedure for estimation of the principal value integral in T_3 (see (43)):

$$\mathcal{P} \int \frac{dE'}{E - E'} \langle \Phi_p | V_W | \chi_s(E') \rangle \langle \chi_s(E') | V | \varphi_s \rangle \approx \langle \Phi_p | V_W | \chi_s(E) \rangle \times$$

$$\times \langle \chi_s(E') | V | \varphi_s \rangle \int \frac{dE'}{E'} \frac{\chi_s^2(k'R)}{\chi_s^2(kR)} \approx \frac{F \cdot \gamma_s^n \gamma_s^n]}{kR} . \tag{54}$$

Therefore

$$T_3 \approx \frac{\gamma_p^n F (\gamma_s^n)^3}{(E - E_p + i\Gamma_p/2)(E - E_s + i\Gamma_s/2)(kR)} \tag{55}$$

and

$$\frac{T_1}{T_3} \approx \frac{(kR)v}{\Gamma_s^n} \approx \frac{v}{S_n \Theta_0^2} \approx \frac{d_0}{\Theta_0^2} \frac{v}{d} \approx \frac{v}{d} . \tag{56}$$

In doing this estimate we used the same factorization as in (45), (46) for neutron width Γ_s^n.

In the same way we get the same estimate (55) for T_7 and (56) for the ratio T_1/T_7.

The only remaining term now is T_9. Each integral in it can be estimated in the way we have already used several times, giving:

$$\mathcal{P}\int \frac{dE'dE''}{(E-E')(E-E'')} \langle \varphi_p|V|\chi_p(E')\rangle\langle \chi_p(E')|V_W|\chi_s(E'')\rangle\langle \chi_s(E'')|V|\varphi_s\rangle \approx$$

$$\approx \gamma_p^n \langle \chi_p(E)|V_W|\chi_s(E)\rangle \gamma_s^n \frac{1}{(kR)^4} \approx \gamma_p^n\gamma_s^n \frac{F}{(kR)^2}. \tag{57}$$

Therefore

$$T_9 \approx \frac{\Gamma_p^n F \Gamma_s^n}{(kR)^2(E-E_p+i\Gamma_p/2)(E-E_s+i\Gamma_s/2)} \tag{58}$$

and

$$\frac{T_1}{T_9} \approx \frac{(kR)^2 v}{\gamma_p^n\gamma_s^n} \approx \frac{v}{S_n\Theta_0^2} \approx \frac{d_0}{\Theta_0^2}\frac{v}{d} \approx \frac{v}{d}. \tag{59}$$

To finish with our analysis we shall recollect that some of the above amplitudes (T_1, T_2, T_3, T_4 and T_7) contained the «full» compound nucleus functions $\Phi_k = \varphi_k + (S_k^n)^{1/2}u$. Substitution of φ_k instead of Φ_k in the above amplitudes would not affect, as long as we see, the above estimates of their relative contribution to (40). The additional valence terms $(S^n)^{1/2}u$ would give us seven more amplitudes with the exchange of corresponding Φ by $(S^n)^{1/2}u$. All of them would contain at any rate the additional small factor $\sqrt{S^n} \approx 1/\sqrt{N}$ (inverse dynamical enhancement). Therefore in all the amplitudes but T_1 they should be disregarded as small additions to the *already small* amplitudes. In the case of T_1 there will be 2 «mixed» terms containing the products $(\varphi\cdot\sqrt{S^n}u)$ and one term of the form:

$$T_{10} = \frac{\Gamma_p^n}{(\Gamma_p^0)^{1/2}} \frac{\langle u_p|V_W|u_s\rangle}{(E-E_p+i\Gamma_p/2)(E-E_s+i\Gamma_s/2)} \frac{\Gamma_s^n}{(\Gamma_s^0)^{1/2}}. \tag{60}$$

Since this term contains extra smallness $S^n \sim 1/N$ in comparison with T_1 it seems that it should be dropped first of all. However the compound-compound matrix element v_p (to be exact, its variance $\tilde{v}_p$) of (41) goes down with increasing complexity N of the wave function Φ_k as $d_0/\sqrt{N}$ (see eq.(9)). Therefore the «single-particle» matrix element $\langle u_p|V_W|u_s\rangle$ should be larger than $\tilde{v}_p$ by roughly a factor of $\sqrt{d_0/d} \approx \sqrt{N}$. Thus the overall ratio of T_1/T_{10} is $1/\sqrt{N}$ rather than $1/N$.

An important point is that, contrary to partial amplitudes γ^n of (41), whose signs vary randomly from resonance to resonance, all the partial widths in (60) are positive. Similarly, contrary to randomly varying sign of v_p in (41), the sign of single-particle matrix element in (60) (defined by u_p, u_s) might vary only over the energy range of single-particle levels spacing d_0. The overall sign of (60) at a given resonance, say E_p, seems to be also defined by the sign of $(E_p - E_s)$. If, however, we switch over to multi-resonance case, we should sum T_{10} at E_p over all the s-resonances which might mix with a given p-one:

$$\sum_s T_{10} = \frac{\Gamma_p^n}{(\Gamma_p^0)^{1/2}} \frac{\langle u_p | V_W | u_s \rangle}{(E - E_p + i\,\Gamma_p/2)} \frac{\Gamma_s^0}{(\Gamma_s^0)^{1/2}} \sum_s \frac{S_n(s)}{E - E_s} . \qquad (60a)$$

Since the spectroscopic factor saturates to unity over the energy range Γ_{spr} around the position E_{s0} of a single-particle level:

$$\sum_s T_{10} \approx \frac{\Gamma_p^n \langle u_p | V_W | u_s \rangle}{(E - E_p + i\,\Gamma_p/2)} \left(\frac{\Gamma_s^0}{\Gamma_p^0} \right)^{1/2} \frac{1}{E - E_{s0}} , \qquad (60b)$$

therefore the overall sign of the effect caused by valence neutron remains constant over the range d_0. However the same is true for mechanisms of T_9 and T_8 (see (58), (52)). All these mechanisms, which essentially sprang to life because of the single-particle (valence) contributions $\chi(E)$ to the BSEC wave functions ϕ_k would provide for the constant sign contributions to the effect. But as we pointed already in [7] *all of them lack the factor of dynamical enhancement* $v/D \sim \sqrt{N}$ and should be dropped on this grounds. We shall briefly come back to this problem in discussing the «sign correlation effect» below (see Sec. IV. 5).

Up to now we considered (see (40) and Fig.1) only the case, when the initial p-wave neutron is transformed by weak interaction into the final state s-one — i.e., the second term in (36). Repeating the above analysis for the first term of (36) will add 16 more amplitudes similar to those of Fig.1. One can easily see that diagrams 1,3,5,7 and 9 are symmetric with respect to the exchange of s- and p-neutron states. Therefore such an exchange will just double the contributions of corresponding mechanisms to (36). The same exchange in amplitudes 2, 8 of Fig.1 would shift their resonance poles to E_s. However the poles of T_4 and T_6 after this exchange would be shifted to E_p. Therefore the addition of the first term in (36) would just completely restore the symmetry of the whole expression (36) with respect to the exchange of initial and final states,

which is expected for *any* elastic scattering T-invariant amplitude. The relative dominance of c–c mixture amplitude T_1 remains unaltered.

To sum up, we have seen that proper nuclear reaction theory allows us to find all the contributions to the weak interaction elastic scattering amplitude of neutrons on a nuclear target. The leading contribution to this amplitude comes from compound-compound mixing mechanism T_1 of eq.(41). This mechanism shows two kinds of enhancement factors: a) the dynamical enhancement factor $v/D \sim \sqrt{N}$; b) the resonance enhancement factor D/Γ. The physical reason of both enhancements is the complexity (or quantum chaoticity) of the compound nucleus resonances. The lack of symmetries characteristic of quantum chaotic system (see, e.g., [36]) removes all the degeneracies of the independent particles' shell-model and thus exponentially decreases the resonance spacing. At the same time it complicates the structure of the compound-resonance wave function, hindering in this way all the decay processes and reducing the total resonance width Γ.

One should also mention that in our analysis we met no traces of the mystical «structural enhancement factor» $1/(kR)$. As is mentioned above, theoretically this factor is a false result of inconsistent application of bound-state theory to the continuum nuclear reaction case.

2.4. Back to Observables. In the previous paragraph we performed an analysis of all possible P-violating amplitudes in the simplest case of elastic neutron-nucleus scattering, understood the physics of their enhancements and have chosen our «favourite» — c–c mixing amplitude T_1, which exceeds the others by at any rate dynamical enhancement factor of $\sqrt{N} \sim 10^3$.

Inserting T_1 into eqs. (36), (37) we obtain

$$\Delta^{P}_{\text{tot}} = \frac{2\pi}{k^2} \frac{\gamma_p^n \cdot v_p \cdot \gamma_s^n \cdot e^{i(\delta_s + \delta_p)}}{[(E - E_p)^2 + \Gamma_p^2/4]\,[(E - E_s)^2 + \Gamma_s^2/4]} \times$$

$$\times [(E - E_s)\,\Gamma_p + (E - E_p)\,\Gamma_s], \tag{61}$$

$$\frac{d\Phi}{dz} = \frac{4\pi\rho}{k^2} \frac{\gamma_p^n \cdot v_p \cdot \gamma_s^n \cdot e^{i(\delta_s + \delta_p)}}{[(E - E_p)^2 + \Gamma_p^2/4]\,[(E - E_s)^2 + \Gamma_s^2/4]} \times$$

$$\times \left[(E - E_s)\,(E - E_p) - \frac{\Gamma_s\,\Gamma_p}{4} \right]. \tag{62}$$

Here v_p stands for the weak interaction matrix element $i\langle \Phi_p | V_W | \Phi_s \rangle$. The presence of Breit — Wigner denominators shows that both effects de-

monstrate symmetric resonance enhancements in the vicinities of both *s*- and *p*-resonances. Δ^{p}_{tot} reaches its maxima at E_s and E_p:

$$\Delta^{P}_{\text{tot}}(E_{\text{res}}) \approx \frac{8\pi}{k^2} \frac{\gamma_p^n \gamma_s^n}{\Gamma} \frac{v}{D} . \tag{63}$$

The quantity (62), however, changes sign at points $E \approx E_{s,p} + \Gamma_s \Gamma_p / 4D \approx E_{s,p}$ and reaches its maxima

$$\left(\frac{d\Phi}{dz} \right)_{\text{res}} \approx \pm \frac{8\pi p}{k^2} \frac{\gamma_p^n \gamma_s^n}{\Gamma} \frac{v}{D} \tag{64}$$

at points $E \approx E_{s,p} \pm \Gamma_{s,p}/2$. For the characteristic curves of the energy behaviour of (61), (62) see our paper [2].

Provided that the asymmetry in total cross-sections Δ^{p}_{tot} is dominated by resonance-resonance mixture of T_1, we can write (see, e.g., [2]) for the asymmetry $\Delta^{p}_{n,\gamma}$ in the denominator of ex. (28):

$$\Delta^{p}_{n,\gamma} = \sigma^{+}_{n,\gamma} - \sigma^{-}_{n,\gamma} \approx \frac{\Gamma_\gamma}{\Gamma} \Delta^{p}_{\text{tot}} \approx \Delta^{p}_{\text{tot}} . \tag{61a}$$

Mind that for other mixture mechanisms this might be not true. Even in this case the last equality holds only for low-energy neutrons incident on non-fissioning target.

We have not yet performed the analysis of the *P*-violating amplitudes in the inelastic channels, which are essential for calculation of the quantity $\Delta_{n,f}$ of eq. (38). This can be easily done on the same lines as the previous paragraph. Those, who are interested in more details, might look through our papers [7] and [8]. The net result of such an analysis is again the conclusion that *c*–*c* mixture amplitudes are dominant. For incident $l_n = 0$ and $l_n = 1$ those amplitudes are (see Fig.2):

$$T^{(1)}_{nf} = \langle\, l_f + 1, f | T_W | 0 \,\rangle = i \frac{\gamma_s^{n} \cdot v_p \cdot \gamma_p^{f} \cdot e^{\,i(\delta_s^n + \delta^f_{l_f+1})}}{(E - E_s + i\,\Gamma_s/2)\,(E - E_p + i\,\Gamma_p/2)} ,$$

$$T^{(2)}_{nf} = \langle\, l_f, f | T_w | 1 \,\rangle = i \frac{\gamma_p^{n} \cdot v_p \cdot \gamma_s^{f} \cdot e^{\,i(\delta_p^n + \delta^f_{l_f})}}{(E - E_s + i\,\Gamma_s/2)\,(E - E_p + i\,\Gamma_p/2)} . \tag{65}$$

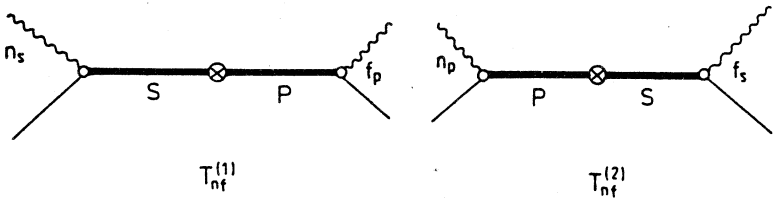

Fig. 2. Two P-violating compound-compound mixing processes in (n, f) inelastic channel

Both amplitudes demonstrate resonance enhancement of D/Γ at E_s and E_p plus the dynamical enhancement of v/D. However their ratio is

$$\frac{T^{(2)}}{T^{(1)}} = \frac{\gamma_p^n \gamma_s^f}{\gamma_s^n \gamma_p^f} \sim (kR) \frac{\gamma_s^f}{\gamma_p^f}.$$

Therefore for low-energy ($E \leq 1$ Mev) neutrons the second diagram contains «*the initial channel hindrance*» factor (kR) (see [7]), which again has no bound-state analogues, but can be easily understood in terms of nuclear reaction theory. Contrary to P-violating elastic amplitudes of the above paragraph the inelastic amplitudes are not symmetric with respect to the exchange of s- and p-neutron waves, and it is highly preferable to excite the s-wave compound resonance in the initial neutron channel rather than p-wave one. This initial channel hindrance leads to even more general and important consequences (see below), making the «inelastic» observables more preferable in general than the «transmission» ones. The corresponding «allowed» reaction amplitudes are:

$$\langle l_f, f | T | 0 \rangle = \frac{\gamma_s^n \cdot \gamma_s^f \cdot e^{i(\delta_s^n + \delta_{l_f}^f)}}{(E - E_s + i\Gamma_s/2)}, \tag{66}$$

$$\langle l_f, f | T | 1 \rangle = \frac{\gamma_p^n \cdot \gamma_p^f \cdot e^{i(\delta_p^n + \delta_{l_f}^f)}}{(E - E_p + i\Gamma_p/2)}. \tag{67}$$

Inserting (65)—(67) into (38) and retaining only the largest terms, we obtain:

$$\Delta_{nf} = \frac{2\pi}{k^2} \sum_{l_f} \frac{\gamma_s^f \cdot v_p \cdot \gamma_p^f}{[(E - E_s)^2 + \Gamma_s^2/4]\,[(E - E_p)^2 + \Gamma_p^2/4]} \times$$

$$\times \operatorname{Re}\left[(E - E_p)\, \Gamma_s^n \cdot e^{i(\delta_{l_f}^f - \delta_{l_{f+1}}^f)} \right]. \tag{68}$$

In this expression we already neglected the neutron potential phase shifts δ_s, δ_p. When the final channel is a γ-emission one, we get:

$$\Delta_{n\gamma_0} = \frac{2\pi}{k^2} \frac{\gamma_s^n \cdot v_p \cdot \gamma_p^f}{[(E-E_s)^2 + \Gamma_s^2/4]\,[(E-E_p)^2 + \Gamma_p^2/4]} (E-E_p)\,\Gamma_s^n. \qquad (69)$$

Mind that γ_0 here denotes the *particular* γ-transition (say, to the ground state of initial nucleus). Mark also, that the effect changes its sign in close vicinity to $E = E_p$ in analogy to $d\Phi/dz$ of eq. (62).

Generally speaking, the most nontrivial part of P-violation theory ends with expressions (61), (62), (61a), (68) and (69) for Δ^p_{tot}, $d\Phi/dz$, $\Delta^p_{n,\gamma}$ and $\Delta_{n,f}$. In order to find the dimensionless ratios P, Φ, A and $\alpha_{n,f}$ observed experimentally, one should just divide those expressions by $2\sigma_{\text{tot}}$, $2\sigma_{n,\gamma}$ or $2d\sigma_{n,f}/d\Omega$, respectively. However it turns out that even this seemingly simple arithmetical operation is full of intricate tricks, because, as we have already mentioned, the denominators also exhibit rapid and sometimes complicated energy dependencies.

Indeed, even in the simplest case of one s- and one p-compound resonances the simplified (i.e., without interference terms) expression for σ_{tot} is:

$$\sigma_{\text{tot}}(E) \approx \sigma_s(E) + \sigma_{\text{pot}}(E) + \sigma_p(E) \approx$$

$$\approx \frac{2\pi}{k^2}\left[\frac{\Gamma_s^n \Gamma_s}{(E-E_s)^2 + \Gamma_s^2/4} + 4(kR)^2 + \frac{\Gamma_p^n \Gamma_p}{(E-E_p)^2 + \Gamma_p^2/4}\right]. \qquad (70)$$

Here σ_s, σ_p and σ_{pot} are the contributions to total cross-section coming from s-, p-compound resonances and potential elastic scattering. As is pointed above, the numerators Δ^p_{tot}, $d\Phi/dz$ display resonance enhancement *both* in s- and p-resonances. However in the energy region of major interest to us (from thermal neutrons to few eV) $\sigma_{\text{tot}}(E)$ and $\sigma_{n,f}(E)$ are dominated by s-resonance contribution: $\sigma_s(E)/\sigma_{\text{tot}}(E) \sim 1$; $\sigma^s_{n,f}(E)/\sigma_{n,f}(E) \sim 1$. Therefore in this region the resonance enhancement at $E \approx E_s$ is completely cancelled from the «observable» ratios:

$$P(E) \approx \frac{\gamma_p^n}{\gamma_s^n} \frac{v_p}{(E-E_p)^2 + \Gamma_p^2/4} \frac{[(E-E_s)\,\Gamma_p + (E-E_p)\,\Gamma_s]}{2\Gamma_s}, \qquad (71)$$

$$\Phi(E) \approx \frac{\gamma_p^n}{\gamma_s^n} \frac{v_p}{(E-E_p)^2 + \Gamma_p^2/4} \frac{(E-E_s)(E-E_p) - \Gamma_s\Gamma_p/4}{\Gamma_s}, \qquad (72)$$

$$\alpha_{n\gamma_0} \approx \frac{\gamma_p^{\gamma_0}}{\gamma_s^{\gamma_0}} \frac{v_p}{(E-E_p)^2+\Gamma_p^2/4} \frac{(E-E_p)}{2}. \tag{73}$$

Since the p-resonance contribution to cross-section is usually *only a small bump* on the large smooth tail of s-resonance (and σ_{pot} background of σ_{tot}) all the observables demonstrate characteristic resonance enhancement in the vicinity of E_p, although the latter two change their signs at $E \approx E_p$ and therefore display more complicated patterns typical of optical dispersion rather than simple Breit — Wigner ones. The largest among them is the «inelastic channel» observable (73) which reaches at $E \approx E_p \pm \Gamma_p/2$ the value:

$$\alpha_{n,\gamma_0} \sim \frac{\gamma_p^{\gamma_0}}{\gamma_s^{\gamma_0}} \frac{v_p}{\Gamma}. \tag{73a}$$

And here come a few more specific features of nuclear reactions. Consider now the ratio of observables at maximum $E \approx E_p \pm \Gamma_p/2$:

$$\left(\frac{P(E)}{\alpha_{n\gamma_0}(E)}\right)_{\max} \approx \frac{\gamma_p^n}{\gamma_s^n} \frac{\gamma_s^{\gamma_0}}{\gamma_p^{\gamma_0}} \frac{D}{\Gamma} \sim (kR) \frac{\gamma_s^{\gamma_0}}{\gamma_p^{\gamma_0}} \frac{D}{\Gamma},$$

$$\left(\frac{\Phi(E)}{\alpha_{n\gamma_0}(E)}\right)_{\max} \approx \frac{\gamma_p^n}{\gamma_s^n} \frac{\gamma_s^{\gamma_0}}{\gamma_p^{\gamma_0}} \frac{D}{\Gamma} \sim (kR) \frac{\gamma_s^{\gamma_0}}{\gamma_p^{\gamma_0}} \frac{D}{\Gamma}. \tag{73b}$$

We see that both observables P and Φ connected with the elastic channel correlation $(\boldsymbol{\sigma}_n \cdot \mathbf{k}_n)$ contain the already familiar entrance channel hindrance factor (kR). This demonstrates a very *general law* — if any symmetry-breaking correlation contains a certain power of $\mathbf{k}_n$, all the corresponding observables will contain hindrance factors (k_nR) of at least the same power. (We shall return to this point in our discussion of T-violation below). This fact puts *all the «transmission» observables of symmetry-breaking into unfavourable position with respect to inelastic channel ones* from the very beginning.

Thus we at last encountered the factor (kR) in the observables (71), (72). But, contrary to naive expectations of bound-state parallels, it is a *hindrance* factor rather than enhancement one.

On the other hand, we have a factor γ_p^f/γ_s^f in inelastic channel observables, which in general might play both ways, but for some special cases might serve a role of the only true «structural enhancement» factor (see,e.g.,[8]) increasing the *P-violation effects in inelastic channels practically to 100% level.*

We also see that the interference patterns of resonance enhancement are rather complicated, which often results in extra resonance enhancements D/Γ (see, e.g., Φ and P observables). These extra enhancement factors in most favourable on-resonance situations (see below) might almost compensate the general smallness (kR) pertinent to transmission experiments.

Since historically P-nonconserving effects were first observed at thermal energies, it is instructive to classify the magnitudes of these effects at $E = E_{th}$:

$$P(E_{th}) \approx -\frac{\gamma_p^n}{\gamma_s^n}\frac{v_p}{E_p^2}\frac{E_s\Gamma_p + E_p\Gamma_s}{2\Gamma_s} \approx -\frac{\gamma_p^n}{\gamma_s^n}\frac{v_p}{E_p}\frac{E_s + E_p}{E_p}, \tag{74}$$

$$\Phi(E_{th}) \approx \frac{\gamma_p^n}{\gamma_s^n}\frac{v_p}{E_p^2}\frac{E_s E_p - \Gamma_s\Gamma_p/4}{2\Gamma_s} \approx \frac{\gamma_p^n}{\gamma_s^n}\frac{v_p}{E_p}\frac{E_s}{\Gamma_s}, \tag{75}$$

$$\alpha_{n\gamma_0}(E_{th}) \approx -\frac{\gamma_p^{\gamma_0}}{\gamma_s^{\gamma_0}}\frac{v_p}{E_p^2}\frac{1}{2}. \tag{76}$$

We see that both P and Φ contain the above strong hindrance factor $\gamma_p^n/\gamma_s^n \sim (kR) \sim 10^{-4}$, which is not present in inelastic case of α_{n,γ_0}. Therefore the «inelastic» value α_{nf} is the largest ($10^{-3} + 10^{-4}$) at thermal energies and was experimentally observed for γ's and fission fragments in almost «prehistoric» times (see [18,37]). It was exactly those unbelievably large (compared to $10^{-7} \div 10^{-8}$ effects in n–p scattering) effects observed in neutron-induced fission that initiated the theoretical studies of Sushkov — Flambaum and Bunakov — Gudkov, which led both groups to the prediction of p-resonance enhancements. Next in magnitude (typically 10^{-5}) comes the value of Φ, which contains additional large factor E_s/Γ_s. The P value containing instead the factor $(E_s + E_p)/E_p$ is usually smaller (typically 10^{-6}). Consequently the first experimental observations for them were done later (see [27,28]). Comparison with experiment nicely confirms the above «hierarchy» of observables (see, e.g., [2,7]).

Let us come back to the behaviour of P in the vicinity of p-resonance:

$$P(E) \approx \frac{2\pi}{k^2}\frac{v_p}{D}\frac{\Gamma_p}{(E - E_p)^2 + \Gamma_p^2/4}\frac{\gamma_p^n \cdot \gamma_s^n}{\sigma_{tot}(E)}. \tag{77}$$

Mind that this expression is valid *only* for $D > \Gamma_s/2$.

Since *even at its maximum p-resonance contributes only a small fraction to* $\sigma_{tot}(E_p)$, the overall behaviour of $\sigma_{tot}(E)$ in the vicinity of *p*-resonance *is quite smooth*. Therefore the resonance enhancement of $P(E)$, represented by Breit — Wigner denominator of (77) fully displays itself in experiment. Seemingly everything is clear — we have both this resonance enhancement mechanism plus a familiar factor v_p/D of dynamical enhancement in (77).

Nevertheless, here starts the «mythology» of experimentalists, which prefer to stick to naive bound-state analogies, whose physical inconsistency we have already analyzed at length. *Instead* of presenting the observable P, given by (77), they prefer to introduce the *auxiliary* quantity $\mathcal{P}$ by relating observed Δ^P_{tot} to a *small fraction* of the observed σ_{tot}, namely to the *p*-resonance contribution $\sigma_p(E)$ (see third term in ex. (70)):

$$\mathcal{P} = \frac{\Delta^P_{tot}}{2\sigma_p(E)} = P\frac{\sigma_{tot}}{\sigma_p}. \tag{78}$$

The *purely technical* reason for such a renormalization is explained as follows. We have already mentioned that the really measured quantity (25) is:

$$P_{exp}(E) = \Delta^P_{tot}(E) \cdot C,$$

where the constant C depends linearly on the target sample thickness x. In order to optimize the statistical significance of measurements this x is chosen in such a way that $C \approx 1/2\sigma_{tot}$. While measuring $P_{exp}(E)$ in the Γ_p vicinity of E_p, the experimentalists do not re-adjust x for each energy point (again because the *smallness* of σ_p/σ_{tot} ratio allows this). Therefore the measured value $P_{exp}(E)$ performs a «full-scale» resonance behaviour of Δ^P_{tot} in the vicinity of *p*-resonance:

$$\Delta^P_{tot}(E) \approx \frac{2\pi}{k^2}\frac{v_p}{D}\frac{\gamma_s^n \gamma_p^n \Gamma_p}{(E-E_p)^2 + \Gamma_p^2/4}. \tag{79}$$

In order to avoid quoting a whole set of numbers $P_{exp}(E)$ at all the energy point E measured on the resonance curve (79), the experimentalist prefers to *cancel* the resonance behaviour of the effect by normalizing it to $\sigma_p(E)$. This allows one to present only one value of $\mathcal{P}$ instead of the whole resonance curve.

Of course this makes some sense, although one might rather use the knowledge of C to quote directly the measured matrix elements v_p — that will be again one number and exactly the only one we are looking for in performing our experiments. One should, however, realize that this *artificial normalization* by one of the weakest components of the total cross-section gives you *only the*

auxiliary quantity without much physical meaning (see eq. (4a) of Sec.II and the discussion which follows it). The non-physical normalization of this quantity produces fictitious enhancement which has nothing to do with reality — one might as well normalize Δ^{p}_{tot} by the neutrino cross-section and surprise the world with huge unobservable effects. To mix up things even more, nowadays all the experimental papers use for this auxiliary quantity of eq. (78) the same notation as for the physical observable P, which was defined already for 20 years by eq. (20). Dubna experimental group in the past at any rate bothered to introduce different notations for those two quantities, although they never advertised the difference between them and always presented $\mathcal{P}$ as the *observed* result. The main reason for such an «absent-minded» mixing of two physically different quantities becomes quite obvious when one presents (78) in a slightly different form:

$$\mathcal{P} = \frac{v_p}{D}\frac{\gamma_s^n}{\gamma_p^n} \sim \frac{v_p}{D}\frac{1}{(kR)} . \tag{80}$$

This is exactly the result which was so easily obtained (see (34), (35)) in a simple but inconsistent attempt to apply bound-state perturbation theory to the reaction continuum case. The physically meaningful resonance enhancement mechanism is «swallowed» in it by the renormalization of $\mathcal{P}$, while instead of it out of nowhere appears the misleading factor of «structural enhancement» $(kR)^{-1}$. If one recollects that the majority of experimental papers and reviews practically start with quoting the simple bound-state expressions (33), (34), one realizes how tempting it is to make a small step, substituting the observed P by the auxiliary $\mathcal{P}$: no need to study reaction theory with its strange terminology of continuum spectra, all the theory you need to understand the results boils down to the above 2 simple expressions (33) and (34). This is exactly the case to apply the Russian proverb: «Simplicity worse than robbery».

To summarize, we have shown that the «structural (or kinematical) enhancement factor» $(kR)^{-1}$ is an artifact produced by renormalization (78). It immediately disappears when you come back to the observable

$$P(E) \equiv \mathcal{P}\frac{\sigma_p(E)}{\sigma_{\text{tot}}(E)} \approx P_{\text{exp}} \tag{81}$$

which always contains a small factor $\sigma_p(E)/\sigma_{\text{tot}}(E) \sim (\Gamma_p^n/\Gamma_s^n) \sim (kR)^2$, overcompensating the above «structural enhancement».

As to the resonance enhancement mechanism sitting in resonance denominator of (77), one often hears naive statements: «Why, it is quite trivial, everybody knows that compound-resonance effects are of Breit — Wigner shape, and we do not need your fancy theories to prove it». This is again a

wrong nonprofessional statement which might lead to erroneous conclusions. To begin with, the energy behaviour of Δ^{n}_{tot} in eq. (61) is more complicated than simple Breit — Wigner formula combined with bound-state perturbation theory, as it might seem from, say, eq. (79). When one divides it by the energy-dependent $\sigma_{\text{tot}}(E)$ the resulting expression becomes even more complicated (see, e.g., [7,8]). For instance, the observable P at the p-resonance maximum is given by:

$$P(E_p) \approx 8 \frac{\gamma_p^n}{\gamma_s^n} \frac{\nu_p}{\Gamma_p} \frac{(E_p - E_s)}{\Gamma_s} \left[1 + \frac{\sigma_p}{\sigma_s} + \frac{\sigma_{\text{pot}}}{\sigma_s} \right]^{-1}. \qquad (82)$$

Suppose now that we face a situation when s- and p-resonances almost overlap $E_s \approx E_p$ (the normal Wigner repulsion does not apply to resonances of opposite parity, so this can easily happen). Then the maximal observed effect *goes down* linearly with decreasing spacing $D = |E_s - E_p|$, contrary to naive expectations of bound-state perturbation theory and even to our eq. (77) which was valid only for $D > \Gamma/2$. All these intricacies become quite essential in the attempts to calculate the energy-averaged effects (see below). Another illuminating example is provided by the «capture transmission» observable A of eq. (28). In view of eq. (61a) we can write this observable at $E = E_p$ as

$$A \approx \frac{\sigma^s_{n,\gamma}(E_p)\, \sigma^p_{n,\gamma}(E_p)}{\sigma^s_{n,\gamma}(E_p) + \sigma^p_{n,\gamma}(E_p)} B.$$

One can see that, in analogy to all the interference type quantities, A would be maximal when the s-resonance contribution σ^s to the (n, γ) cross-section at $E = E_p$ exactly equals the p-resonance one σ^p. Then and only then A would reach its maximal possible value

$$A^{\max} \approx 2 \frac{\nu_p}{\Gamma}.$$

The observable $P(E)$ differs from A by a factor of $\sigma_{n,\gamma}/\sigma_{\text{tot}}$. Therefore $P^{\max}$ would *never* reach $2\nu_p/\Gamma$. However (see [7,8,38]) the most optimal situation for $P(E_p)$ happens again when $\sigma_s(E_p) = \sigma_p(E_p)$. Then

$$P^{\max}(E_p) \approx 2 \frac{\nu_p}{\Gamma} \frac{\sigma_{n,\gamma}}{\sigma_{\text{tot}}}.$$

The famous *La* resonance with $\mathcal{P} \approx 10\%$ satisfies this condition: $\sigma_p(E_p) \approx \sigma_s(E_p) \approx \sigma_{\text{pot}}(E_p)$, thus providing for the observed $P \approx 3\%$.

Eqs. (78), (81) and above considerations show that for *strong* observable *p*-resonances (present beam intensities force us to select just those for measurements) the enhancement of P would be maximal. Since in those cases $\sigma_p(E_p)/\sigma_{tot}(E_p)$ is about $0.1 \div 0.3$, the difference between quoted $\mathcal{P}$ and observed P would not be too large, although $\mathcal{P}$ values already sound more impressive than the really measured P. However with increasing intensities experimentalists will start observing effects on weaker *p*-resonances, and this difference might rise to orders of magnitude. The impressive 10% effects, recently observed in ^{232}Th, when expressed in terms of physical observables P, turn out to be more modest 1% effects. So it is high time to stop mixing the 2 quantities and fooling each other.

To finish this paragraph we should mention that we paid special attention to transmission measurements of quantity P (E) since this type of experiments is most popular nowadays. This feeds a constant stream of publications, where the same physical errors in interpretation are repeated again and again.

A special case is *P*-violation in neutron-induced fission. I am not going to expand on it for several reasons. First of all, this interesting subject is worth a separate review. I shall only mention that there are 2 theoretical approaches to it. Sushkov and Flambaum (see, e.g., [26]), likewise in case of *P*-quantites, used intuitive bound-state analogies to construct $\alpha_{n,\,fis}$. Gudkov and I (see [7] and especially [39]) tried to apply the general expression (68) to this case. However the most striking fact connected with experimental observation of $\alpha_{n,\,fis}$ dates back to the midst of 50-ies, when it was discovered (see [40,41]) that, in spite of the fact that all the experimental observables in fission are sums over the enormous amount of outgoing reaction channels seemingly with random signs of γ_f, this summation does not destroy the interference effects in (*n*, *fission*) cross-section. This difficulty was bypassed at that time by the fission transition-state hypothesis of A.Bohr (see [42,43]). Now the *same* story repeated in the measurements of $\alpha_{n,\,fis}$. This quantity is also an interference type phenomenon (see eq.(68)) and again the summation over all the outgoing channels γ_f does not destroy the *P*-violation effects caused by *c*–*c* mixing mechanism in each channel. In view of this common origin of the difficulty we tried to resolve it by generalizing Bohr's hypothesis of transition states. Sushkov and Flambaum used instead of it a purely classical model of fission-fragments motion plus a hypothesis of pear-like shape of the fissioning nuclei *at the saddle-point*. Both approaches have their weaknesses. Applying the classical trajectory notion to the analysis of quantum interference effects seems quite hazardous to us. Moreover, while most people agree that for asymmetric fission the fissioning nucleus has a pear-like shape *near the scission-point,* the same assumption *on*

the top of fission barrier seems quite dubious and contradicts some experimental evidence (see [7,39]). We are, however, not very happy with our's (or, rather, with A.Bohr's) transition-state hypothesis because it seems up to now a rather artificial construction in the framework of quantum reaction theory. I am sure that *P*-violation in fission is just an additional guide-light in search for yet nonexistant quantum theory of fission.

3. *T*-Violation

3.1. Specific Intricacies of T-Invariance and Observables. One of the greatest dangers in the analysis of *T*-violation is to follow too closely the parallels with *P*-violation — these parallels might be quite wrong. To demonstrate this point we shall consider the cases of *P*-odd and *T*-odd correlations. Everybody knows the mnemonic rule — if the transition operator $\hat{T}$ changes sign under the space reflection operation $\mathcal{P}$ (is *P*-odd), then it has nonzero matrix elements between states of opposite parity. This is perfectly true. Therefore if you observe nonzero amplitude of *P*-odd correlation (say, $\sigma \cdot \mathbf{k}$) this means *P*-violation. However, if you observe nonzero amplitude of *T*-odd correlation, this fact in itself in the majority of cases has nothing to do with *T*-violation. In order to understand this let us see, how *P*-violation is mathematically connected with *P*-odd operators (or correlations) $\hat{T}$. Acting by unitary transformation operator $\mathcal{P}$ on a state $|A\rangle$ we get a number π_A (parity quantum number) equal to + 1 or − 1:

$$\mathcal{P}|A\rangle = \pi_A |A\rangle. \tag{83}$$

For operators the space reflection looks like:

$$\mathcal{P}\hat{T}\mathcal{P}^{-1} = \pi_T \hat{T}. \tag{84}$$

Consider now the transition amplitude:

$$\langle B|\hat{T}|A\rangle = \langle B|\mathcal{P}^{-1}\mathcal{P}\hat{T}\mathcal{P}^{-1}\mathcal{P}A\rangle = \pi_B \pi_T \pi_A \langle B|\hat{T}|A\rangle. \tag{85}$$

The first line in this equation uses the fact that $\mathcal{P}\mathcal{P}^{-1} = 1$. The second line makes use of (83), (84) and the unitarity of $\mathcal{P}$. The whole equation gives us a selection rule:

$$\pi_A \pi_B \pi_T = 1. \tag{86}$$

Thus the *P*-odd operator ($\pi_T = -1$) leads to nonzero amplitudes only in case when $|A\rangle$ and $|B\rangle$ are of opposite parity.

However the action of time-reversal operator $\mathcal{T}$ changes the signs of momenta and spins and exchanges the initial and final states. Therefore its action on any state $|A\rangle$ cannot be expressed in terms of eigenvalues, like (83). If one also adds that $\mathcal{T}$ is not unitary, one sees that it is impossible to construct (85) for $\mathcal{T}$ and get selection rule (86).

Therefore $\mathcal{T}$-invariance leads only to 2 immediate consequences (see, e.g., [11,12]). The first is the detailed-balance principle. For binary process $A + a \to B + b$ it looks like:

$$\frac{(2s_a + 1)\,(2s_A + 1)\,k_a^2\, d\sigma_{ab}/\, d\Omega}{(2s_b + 2)\,(2s_B + 1)\,k_b^2\, d\sigma_{ba}/\, d\Omega} = 1. \tag{87}$$

Here s_i are the corresponding particles' spins.

The other consequence is the so-called P–A theorem which connects the polarization P and asymmetry A. For elastic scattering of spin 1/2 particles it states:

$$P = A. \tag{88}$$

However lots of papers seriously discussed T-odd correlations, hoping to measure T-violation. Was it completely meaningless? The answer is no, but the arguments are quite subtle and tricky (see, e.g., [44,45,46]). We start with unitarity of S-matrix:

$$SS^{\dagger} = 1.$$

Inserting this into the expression

$$S = 1 + i\hat{T}$$

for the transition matrix, we get:

$$\hat{T} - \hat{T}^{\dagger} = i\,\hat{T}\hat{T}^{\dagger}. \tag{89}$$

In case of transition from the initial state $|i\rangle$ to final state $|f\rangle$ this looks like:

$$\langle f|\hat{T}|i\rangle - \langle f|\hat{T}^{\dagger}|i\rangle = i\sum_n \langle f|\hat{T}|n\rangle\,\langle n|\hat{T}^{\dagger}|i\rangle, \tag{90}$$

where $|n\rangle$ forms a complete set of all possible intermediate states. Up to this point everything was quite exact. And now starts the approximation. Suppose that the interaction which defines our transition T contains a small parameter F. Then the l.-h. side of (90) is linear in F, while the r.-h. side is quadratic. Therefore in the first-order approximation

$$\langle f|\hat{T}|i\rangle \approx \langle i|\hat{T}^{*}|f\rangle. \tag{91}$$

This means that matrix $\hat{T}$ is Hermitean. Let us now combine (91) with the condition of T-invariance (see definition of $\mathcal{T}$-operation above):

$$\langle f|\hat{T}|i\rangle = \langle -i|\hat{T}|-f\rangle. \tag{92}$$

Here minus signs mean changes of signs for momenta and spins.

Eqs. (91) and (92) give us:

$$\langle f|\hat{T}|i\rangle = \langle -f|\hat{T}|-i\rangle^{*}, \tag{93}$$

or

$$|\langle f|\hat{T}|i\rangle|^2 = |\langle -f|\hat{T}|-i\rangle|^2. \tag{94}$$

The last equation means that in case of $\mathcal{T}$-invariance (92) the transition probability should be an even function under the sign exchange of all spins and momenta. Now (93) shows that sign-inversion operation for initial and final states means just complex conjugation. Therefore the overall sign of transition probability under this sign inversion is completely defined by the sign of transition operator $\hat{T}$. If this operator is T-odd, (94) demands that transition probability should be zero.

Thus we have seen that nonzero T-odd correlations *are* connected to T-violation only when the transition matrix $\hat{T}$ is approximately Hermitean and *within the accuracy of this approximation*. The last point is very delicate. Consider it in more detail, taking as an example the T-odd correlation $\sigma_n \cdot [\mathbf{k}_e \times \mathbf{k}_\nu]$, which is measured in neutron β-decay. Seemingly this is a weak interaction process, which is governed by weak interaction constant F and therefore deviations from Hermiticity are

$$T - T^\dagger \sim F^2.$$

However we should not forget about final-state electromagnetic interaction (Coulomb scattering of electron on proton). This means that the non-Hermitean r.-h. side of (90) should contain terms of the type:

$$i\langle pe\tilde{\nu}|\hat{T}|p'e'\tilde{\nu}\rangle\langle p'e'\tilde{\nu}|\hat{T}^\dagger|n\rangle. \tag{95}$$

While the second amplitude in (95) is really of the order of F, the first one is proportional to the fine-structure constant α. Therefore the deviation of $\hat{T}$ from Hermiticity is of the order of αF, and this would imitate T-violation even when it does not exist (see also [44]). In principle one can calculate this final-state interaction correction and subtract it from the experimentally observed value of T-odd correlation. However all the existing experiments of this type were giving only the experimental upper bounds on the effect. While experimental accuracy is more or less easily defined, the accuracy of theoretical estimates of final-state interactions is usually much less reliable. This makes the estimates of the upper bounds on «real» T-violation correspondingly unreliable. Therefore experiments of this type are gradually dying out.

If strong interaction is present in the process, the final-state interaction corrections become of the same order as the Hermitean part of the amplitude, and situation becomes completely hopeless.

The only exclusion, when T-odd correlation is a *direct* evidence of T-violation, is the transmission-type experiment. Then the σ_{tot} quantity, which

defines the transmission, is expressed via the optical theorem (see, e.g., eq. (19)) as the imaginary part of zero-angle elastic scattering amplitude $f(0)$. In this case the initial and final states coincide $|i\rangle = |f\rangle$ and the T-invariance conidition (92) by itself (*without approximation of (91)*) immediately gives us (93) and (94).

There exist 2 types of those «true» T-odd correlations in elastic forward scattering amplitude, which can manifest themselves in neutron transmission experiments with nonzero target spins I.

One of them is the correlation $\sigma_n \cdot (\mathbf{k}_n \times \mathbf{I})\,(\mathbf{k}_n \cdot \mathbf{I})$. One can measure this correlation in polarized neutron transmission through the oriented-nuclei samples. Observing that this correlation depends on the angle θ between $\mathbf{k}_n$ and the target alignment axis as $\sin 2\theta$, one immediately sees that the best observation conditions would be for $\theta = 45°$ and neutron spins σ_n directed parallel or antiparallel to $(\mathbf{k}_n \times \mathbf{I})$ axis. The presence of T-violating interaction would cause the difference in σ_{tot} for those two choices of neutron polarization

$$\Delta^T = \sigma_{\rightarrow} - \sigma_{\leftarrow} \,. \tag{96}$$

Using the optical theorem, one can express this quantity in terms of T-violating part of the scattering amplitude f_T :

$$\Delta^T = \frac{4\pi}{k}\ \mathrm{Im}\, f_T \tag{97}$$

in complete analogy with eqs. (19), (36). Since the experimentalists would always prefer to measure relative quantities rather than absolute ones (see (20)—(27)), the experimentally observed T-violation effect will be:

$$\beta = \frac{\Delta^T}{\sigma_{\rightarrow} + \sigma_{\leftarrow}} \simeq \frac{\Delta^T}{2\sigma_{tot}} \,. \tag{98}$$

Observe that the above correlation is T-violating but P-conserving. The conventional name for it is «five-fold correlation» (FC).

There also exists another correlation, namely $\sigma_n\,[\mathbf{k}_n \times \mathbf{I}]$, which is both P- and T-violating. This «triple correlation» (TC) should be measured with polarized neutron beam and polarized target nuclei. Performing transmission experiments with beam polarization parallel or antiparallel to $[\mathbf{k}_n \times \mathbf{I}]$ axis, one might observe the cross-section difference:

$$\Delta_{PT} = \sigma_{\uparrow} - \sigma_{\downarrow} = \frac{4\pi}{k}\ \mathrm{Im}\,(f_{\uparrow} - f_{\downarrow}) \tag{99}$$

and the corresponding P- and T-violation effect:

$$\eta = \frac{\Delta_{PT}}{\sigma_{\uparrow} + \sigma_{\downarrow}} \simeq \frac{\Delta_{PT}}{2\sigma_{\text{tot}}} . \tag{100}$$

In complete analogy with P-violating effects (see (29)), this correlation also causes the precession of neutron spin around the $[\mathbf{k}_n \times \mathbf{I}]$ axis. The corresponding value of the rotation angle χ per unit length in a target sample is:

$$\frac{d\chi}{dz} = \frac{4\pi\rho}{k} \text{Re}\,(f_{\uparrow} - f_{\downarrow}). \tag{101}$$

In the optimal experimental conditions $z = 1/N\sigma_{\text{tot}}$ the corresponding angle of rotation is:

$$\chi = \frac{\text{Re}\,(f_{\uparrow} - f_{\downarrow})}{\text{Im}\,(f_{\uparrow} + f_{\downarrow})} . \tag{102}$$

3.2. Historical Background. Although the general remark that nuclear reactions of strong dynamical complexity are most likely to be sensitive to T-violation was done by Henley and Jackobsohn [47] long ago, this remark seemingly passed unnoticed till the experimental discovery [48] of CP-violation in K-meson decay. In the framework of CPT theorem that meant T-violation. This discovery brought a new wave of experimental and theoretical studies of T-violation in nuclear reactions. First experimental tests of T-violation in detailed balance (TVDB, see (87)) were carried out [49] in 1966. Simultaneously appeared first publications on nuclear-reaction theory in the presence of T-violation [50,35]. Mahaux and Weidenmüller [35] obtained the theoretical expression for T-violating amplitudes in case of two near-lying compound resonances and were the first to understand the above mechanism of resonance enhancement. However both experimental and theoretical efforts at that time were concentrated on the energy domain of overlapping resonances $\Gamma >> d$ (Ericson regime). Therefore Ericson [50] claimed the enhancement parameter to be $\sqrt{(W/\Gamma)} \sim 10$, where W was supposed to be of the order of spreading width of eq. (7). Mahaux and Weidenmüller [35] pointed out that W should be much smaller, reducing the enhancement factor $\sqrt{W/\Gamma}$ to unity. Thus the possibilities of isolated resonance region with really large resonance enhancements $d/\Gamma >> 1$ remained unnoticed. Much later Pearson and Richter [51] considered TVDB for *one* isolated resonance. This case (for its analogues in P-violation see diagrams T_2 and T_4 of Fig.1) in principle contains resonance enhancement but lacks the dynamical enhancement factor $\sqrt{N}$ typical for 2-resonance interaction. Moreover, in case of TVDB experimental observable (see below) this resonance enhancement is completely cancelled by the resonance enhancement of the T-invariant cross-section in the denominator. Therefore this mechanism remained unnoticed and main theoretical investigations of TVDB

[52,53,54,16] were centered on energy-averaged quantities for strongly-overlapping resonances.

The full significance of both dynamical and resonance enhancements in T-violation was first realized by Gudkov and the author [4,7] in 1982, when we started the theoretical analysis of the newly suggested [55,56] P- and T-violating triple correlation in neutron transmission and predicted 5 + 6 orders of possible enhancement for this effect on p-resonances interacting with near-lying s-ones. Later on we [57,38] studied the resonance enhancement of P-conserving five-fold correlations (96)—(98). The same investigations were done independently by Barabanov [58]. Ironically enough, in both investigations the resonance-resonance T-violating term in the amplitude (analogue of T_1 term in P-violation) was unnoticed and only analogues of T_2 and T_4 were considered. This mistake was finally corrected in 1988 by the author [8], who realized the possibilities of both dynamical and resonance enhancements for this type of correlation. Since however the FC contains an extra $|\mathbf{k}|$ factor in comparison to TC, this results in the extra hindrance factor (see eqs. (74)—(76) and the discussion following them) of (kR) order which reduces the overall enhancement of FC to more modest 2 + 4 orders of magnitude.

Detailed balance tests for a close-lying pair of resonances in isolated resonance regime was first considered by Weidenmüller and the author [6]. Both dynamical and resonance enhancement effects were found in that case together with possible «true» structural enhancement. However, the measured quantities in TVDB show even more complicated interference energy behaviour and the conditions for observing the maximal possible effect are even more involved. The net enhancement in realistic conditions was found to essentially depend on experimental energy resolution and was estimated by us as $10^3 + 10^4$. However, recently Mitchel and co-workers [9] generalized our analysis by including the angular dependence of observable quantities. This led to even more complicated two-dimensional picture for the effect as a function of energy and angle. However, this more complicated analysis brought even more optimistic estimates. Analyzing their own high-resolution experimental data on (p, p) and (p, α) reactions, obtained at Duke, the authors proved that it is possible to obtain enhancements up to $10^4 + 10^5$. This fact together with various difficulties characteristic of other types of T-violating experiments (see below) makes the TVDB tests for interfering resonances perhaps the best possible way of T-noninvariance observation in the nearest future.

3.3. T- and P-Violation (Triple Correlation). The triple correlation quantities Δ_{PT} and $d\chi/dz$ of (99) and (100) can be analyzed in complete analogy to P-odd quantities Δ_P and $d\Phi/dz$ (see [3,7]) by substituting the T- and P-violating interaction iV_{PT} instead of P-violating weak interaction V_W into the Born

amplitude (39). Analysis of the resulting analogue of eq. (40) shows again that c–c mixing amplitude

$$T_1^{PT} \approx \frac{\gamma_p^n \cdot v_{PT} \cdot \gamma_s^n}{(E - E_p + i\,\Gamma_p/2)\,(E - E_s + i\,\Gamma_s/2)} \tag{103}$$

dominates, since it contains both factors of dynamical v/D and resonance D/Γ enhancement.

Inserting this amplitude into (99) gives [3,7]:

$$\Delta_{PT} = \frac{2\pi}{k^2}\, G_J\, \frac{\gamma_p^n \cdot v_{PT} \cdot \gamma_s^n}{[(E - E_p)^2 + \Gamma_p^2/4]\,[(E - E_s)^2 + \Gamma_s^2/4]} \times$$

$$\times\,[(E - E_s)\,\Gamma_p + (E - E_p)\,\Gamma_s] \tag{104}$$

with

$$G_J = \frac{1}{2}\sqrt{\frac{3}{2(2I+1)}}\left[\sqrt{\frac{2I+1}{2I+3}}\,\delta_{J,I+1/2}\,\delta_{c,I-1/2} + \right.$$

$$\left. + \sqrt{\frac{I}{I+1}}\,\delta_{J,I-1/2}\,\delta_{c,I+1/2}\right]. \tag{105}$$

Here J is the total compound resonance spin and c is the channel spin.

In p- and s-resonance points we have maxima:

$$(\Delta_{PT})_{\text{res}} \approx \frac{8\pi}{k^2}\, G_J\, \frac{v_{PT}}{D}\, \frac{\gamma_p^n \cdot \gamma_s^n}{\Gamma}. \tag{106}$$

Exactly in the same way we obtain:

$$\frac{d\chi}{dz} = -\frac{4\pi}{k^2}\, G_J\, \frac{\gamma_p^n \cdot v_{PT} \cdot \gamma_s^n}{[(E - E_p)^2 + \Gamma_p^2/4]\,[(E - E_s)^2 + \Gamma_s^2/4]} \times$$

$$\times\left[(E - E_p)\,(E - E_s) - \frac{\Gamma_s\,\Gamma_p}{4}\right]. \tag{107}$$

Observe that (107) changes sign at $E \approx E_p$ or E_s and shows maxima at $E_{p,s} \pm \Gamma_{p,s}/2$:

$$\left(\frac{d\chi}{dz}\right)_{\text{res}} \approx \frac{8\pi}{k^2}\, G_J\, \frac{v_{PT}}{D}\, \frac{\gamma_p^n \cdot \gamma_s^n}{\Gamma}. \tag{108}$$

Introducing the scaling factor λ between the P-, T-violating interaction $\tilde{v}_{PT}$ and the weak one $\tilde{v}_p$, we see that in average the P-, T-violating observed effects will be enhanced in the same p-resonances as P-violating ones:

$$\eta \approx \lambda P, \tag{109}$$

$$\chi \approx \lambda \Phi. \tag{110}$$

It is worth mentioning that all the present gauge-invariant theoretical models consider only the simultaneous P- and T-violation giving a wide range of λ between 10^{-4} and 10^{-15} (see, e.g., [46, 59]). Since the existing experimental constraints on the theory are given only by the case of K-meson decay and by the upper bound on neutron electric dipole moment (EDM), there is a special branch of CP-violation theory called «model-building» — anybody can construct his own branch of CP-violation theory provided that it does not contradict the above 2 experimental constraints. Moreover, λ enters those constraints in a model-dependent way. Thus *any* additional constraint on λ obtained from TC measurements could help a lot in narrowing the class of acceptable CP-violation models. It also seems that after 3 decades of constant improving the methodics of EDM measurements, the experimentalists had already exhausted their possibilities there. Mind also, that EDM does not contain the above 6 orders of enhancement, which somewhat resemble the good old Wolfenstein enhancement of CP-violation in K-mesons. Therefore FC measurements might rank as highest-priority ones from the point of view of its «fundamentality».

There are however grave difficulties with the idealized transmission experiments we were analyzing above in search for FC, and we ourselves were the first to realize their presence [60]. Indeed, the simplest way seems to choose $\mathbf{I}$ and $\mathbf{k}$ directions along, say, x and z axes, while directing $\boldsymbol{\sigma}$ parallel or anti-parallel to y axis. However, in order to polarize the target we need external (and rather strong) magnetic field $\mathbf{H}$. This field would cause Larmour precession of $\boldsymbol{\sigma}$ around $\mathbf{H}$ as soon as the neutron enters the target. This precession in its turn produces non-zero helicities (of different signs for initial cases of $\boldsymbol{\sigma} \uparrow\uparrow \mathbf{y}$ and $\boldsymbol{\sigma} \uparrow\downarrow \mathbf{y}$). Those helicities would cause the P-odd difference in transmission coming from «normal» weak interaction and considered in the previous subsection. Moreover, this weak interaction would start rotating $\boldsymbol{\sigma}$ around the $\mathbf{k}$ direction as well (see ex. (62)). Therefore the neutron spin starts wobbling in 3 dimensions in almost unpredictable way. Since all the CP-violating theories agree that $\lambda << 1$, those effects would completely camouflage the T-odd correlation we are looking for. To make the situation worse, even if we manage to keep the target polarized without the strong external magnetic field, we still will face the so-called «nuclear pseudo-magnetism» (see [61]). This is the phenomenon caused by $\boldsymbol{\sigma} \cdot \mathbf{I}$ dependent part of nuclear strong interaction, which imitates the external magnetic field causing the $\boldsymbol{\sigma}$ precession around $\mathbf{I}$. Since this effect arises from nuclear interaction, it is quite strong (usually equivalent to several KG of magnetic field).

The only crude remedy we could suggest in 1984 (see [60]) was to compensate the nuclear pseudomagnetic field by fine-tuning the external field **H** (this is in principle possible since the direction of pseudomagnetic precession is not correlated with neutron magnetic moment). We fully realized that such a solution is rather awkward in practice, since one needs to control this compensation by measuring neutron spin rotation angle with high precision $-\delta\phi \sim 10^{-(3+5)}$. In principle much higher precision of 10^{-6} was reached [27] in measurements of P-violating value Φ of eq. (75), but in our case one should do these high-precision measurements simultaneously with the measurements of FC itself.

On publishing this kind of «experimental» proposal [60] we expected to hear the reaction of professional experimentalists. Our expectations lasted for about a decade. Only in 1993 we received first response. One suggestion was presented by KEK group of Masuda [62] and actually contains a refined version of our magnetic field fine-tuning. The other suggestion came from PNPI group of Serebrov [63]. It involves the simultaneous measurements of polarization and asymmetry in transmission of initial longitudinally-polarized neutrons, and seem to be free of the above camouflaging effects. It remains, however, to check the energy dependence of the much more complicated observable suggested in this experiment in order to see whether the above enhancement effects survive in it and to estimate the accuracy of this experiment in realistic conditions.

3.4. P-Conserving T-Violating Transmission (Five-Fold) Correlation. We shall start with the T-violating part of the scattering amplitude f_T in eq. (97). It can be expressed (see [57,58]) for low-energy neutrons ($l = 0, 1, 2$):

$$f_T = \frac{A}{k}\Bigg[3\sqrt{2} \begin{Bmatrix} I & 2 & I \\ I-1/2 & J & I+1/2 \end{Bmatrix} [\langle I+1/2,\ 1|T^{TJ}|I-1/2,\ 1\rangle - \langle I-1/2,\ 1|T^{TJ}|I+1/2,\ 1\rangle] +$$

$$+ (-1)^{2I}\sqrt{\frac{3}{2I}}\,[\langle I+1/2,\ 2|T^{TJ}|I-1/2,\ 0\rangle - \langle I-1/2,\ 0|T^{TJ}|I+1/2,\ 2\rangle]\,\delta_{J,I-1/2} +$$

$$+ (-1)^{2I}\sqrt{\frac{3}{2(I+1)}}\,[\langle I+1/2,\ 2|T^{TJ}|I-1/1,\ 0\rangle - \langle I-1/2,\ 0|T^{TJ}|I+1/2,\ 2\rangle]\,\delta_{J,I+1/2}, \qquad (111)$$

$$A = (2J+1)\sqrt{\frac{5I(2I-1)}{(2I+1)(2I+3)}}\,(-1)^{I+3/2-J}.$$

Here $T = 1 - S$, S being the scattering matrix. Notation $\langle c', l'|T|c, l \rangle$ is used for transition matrix elements, where l and l' are orbital momenta of the initial and final channels, c and c' are the corresponding channel spins and J is the compound system spin. Upper T indices denote T-violating part of the T-matrix.

One might introduce, following Mahaux and Weidenmüller [35], the quantity $\delta S_{\lambda\mu} = S_{\lambda\mu} - S_{\mu\lambda}$ arising in the presence of T-noninvariant part V_T in the Hamiltonian, and consider the matrix $\delta S_{\lambda\mu} = -T^T_{\lambda\mu}$ in case of two interacting resonances, using the wave function expressions (18) for the initial and final channels μ and λ. This would give us the whole set of amplitudes similar to those of Fig.1 — the role of parity quantum number is «mimicked» in our case by channel spins. The analysis of different contributions to $T^T_{\lambda\mu}$ gives us essentially the same results as in P-violation. This analysis was schematically mentioned in connection with detailed-balance tests already in [35] and later in [5,6]. As usual, it boils down [5] to the dominant contribution of c–c mixing term, which demonstrates both dynamical and resonance enhancements:

$$T^T_{\lambda\mu} = 4\sqrt{2\pi}\cdot i \; \frac{\gamma_{1\mu}\,\gamma_{2\lambda}\,(V_T)_{12} + \gamma_{2\mu}\,\gamma_{1\lambda}\,(V_T)_{21}}{(E - E_1 + i\,\Gamma_1/2)\,(E - E_2 + i\,\Gamma_2/2)} \,. \tag{112}$$

Here E_i, Γ_i are the energies and total widths of the mixing compound resonances. The T-violating matrix elements between the compound states Φ_1 and Φ_2 $(V_T)_{12} = \langle \Phi_1|V_T|\Phi_2 \rangle = -(V_T)_{21}$ are purely imaginary

$$(V_T)_{12} = iv_T \,. \tag{113}$$

Therefore:

$$\mathrm{Im}\; T^T_{\lambda\mu} = \frac{(\gamma_{1\mu}\,\gamma_{2\lambda} - \gamma_{2\mu}\,\gamma_{1\lambda})\,v_T}{[(E - E_1)^2 + \Gamma_1^2/4]\,[(E - E_2)^2 + \Gamma_2^2/4]} \times$$

$$\times\,[(E - E_1)\,\Gamma_2 + (E - E_2)\,\Gamma_1] \,. \tag{114}$$

Substituting (114) into (111) and (97), we get the terms of p–p resonance mixing (we omit the geometrical factors):

$$\Delta_T(p_1, p_2) \approx \frac{4\pi}{k^2} \; \frac{(\gamma^n_{1(-)}\,\gamma^n_{2(+)} - \gamma^n_{2(-)}\,\gamma^n_{1(+)})\cdot v_T}{[(E - E_1)^2 + \Gamma_1^2/4]\,[(E - E_2)^2 + \Gamma_2^2/4]} \times$$

$$\times\,[(E - E_1)\,\Gamma_2 + (E - E_2)\,\Gamma_1] \tag{115}$$

and s–d resonance mixing terms:

$$\Delta_T(s, d) \approx \frac{4\pi}{k^2} \frac{(\gamma^n_{s(-)}\,\gamma^n_{d(+)} - \gamma^n_{s(+)}\,\gamma^n_{d(-)}) \cdot v_T}{[(E - E_s)^2 + \Gamma_s^2/4]\,[(E - E_d)^2 + \Gamma_d^2/4]} \times$$

$$\times [(E - E_s)\,\Gamma_d + (E - E_d)\,\Gamma_s]. \qquad (116)$$

The indices (+) and (−) stand for the channel spins. The order-of-magnitude estimates for the brackets with γ-amplitudes in (115), (116) are $(\gamma^n_p)^2$ and $\gamma^n_S\,\gamma^n_d$, respectively. Comparing this with the value Δ^p_{tot} of (61), we see that in both cases Δ_T is smaller by roughly (kR) factor arising from extra $|\mathbf{k}|$ value in FC. Otherwise both (115) and (116) show dynamical and resonance enhancements. However the optimal conditions for maximal observable $\beta(E)$ of eq. (98) differ from those of $P(E)$. Detailed analysis (see, e.g., [5]) demonstrates that observations in strong isolated p-resonance (when $\sigma_p(E_p) \approx \approx \sigma_{\text{tot}}(E_p)$) are most favourable. In this case the overall $(kR)^2$ smallness is compensated by resonance enhancement $(D/\Gamma)^2$ to give:

$$\beta_{\max}(E_p) \approx \frac{v_T}{D_{12}} \frac{\sigma_p(E_p)}{\sigma_{\text{tot}}(E_p)}. \qquad (117)$$

In the vicinity of s-resonance one gets from (116):

$$\beta(E_s) \approx \frac{\gamma^n_d}{\gamma^n_s} \frac{v_T}{D_{sp}} \sim (kR)^2 \frac{v_T}{D_{sp}}. \qquad (118)$$

The additional small (kR) factor makes those observations impractical. The main trouble with observations of (116) in d-resonance lies in the fact that exceedingly small Γ^n_d values make those resonances unobservable in σ_{tot}. If only we knew E_d in advance, then:

$$\beta(E_d) \approx \frac{\gamma^n_d}{\gamma^n_s} \frac{v_T}{\Gamma_d} \frac{D_{sp}}{\Gamma_s} \frac{\sigma_s(E_d)}{\sigma_{\text{tot}}(E_d)} \sim (kR)^2 \frac{v_T}{D_{sd}} \left(\frac{D_{sd}}{\Gamma}\right)^2. \qquad (119)$$

Observe that for very small D_{sd} (119) decreases drastically and transforms into (118) for $D_{sd} \approx \Gamma$. If the d-resonance lies sufficiently far away from s-resonance (say, $D_{sd} \sim 10$ eV) then the resonance enhancement factor $(D_{sd}/\Gamma)^2$ in (119) might almost compensate the smallness of $(kR)^2 \sim$ $\sim 10^{-5} \div 10^{-6}$. Since, however, the E_d are not known in advance, the d-resonance enhancement seems to be of purely academic interest, as it was

pointed in my ref. [5]. This point was misunderstood by the authors of ref. [30] who «re-discovered» the *s–d* mixing two years later (see also [64]). Unfortunately the only known target of ^{165}Ho suitable for FC measurements does not show any *p*-wave resonances [64]. Therefore the above possibilities of resonance enhancement (117) in FC were not used by the experimentalists up to now.

3.5. Detailed Balance Tests (TVDB). The simplest quantity, which describes the *T*-violation in detailed balance (TVDB) is (see eq. (87)):

$$\Delta_{DB}(E, \theta) = 2 \frac{\sigma_{ab}(E, \theta) - \sigma_{ba}(E, \theta)}{\sigma_{ab}(E, \theta) + \sigma_{ba}(E, \theta)} . \tag{120}$$

Since, as usual, the Δ_{DB} value is a ratio of experimentally measured quantities, we included the kinematic factors $k_a^2 (2s_a + 1) (2s_A + 1)$ into the value $\sigma_{ab}(E, \theta) = k_a^2 (2s_a + 1) (2S_A + 1) d\sigma_{ab}/d\Omega (E, \theta)$. To simplify our analysis we shall also restrict ourselves with only E dependence of the cross section, omitting the θ dependence for the time being. Thus (120) would read:

$$\Delta_{DB}(E) = 2 \frac{\sigma_{ab}(E) - \sigma_{ba}(E)}{\sigma_{ab}(E) + \sigma_{ba}(E)} . \tag{121}$$

Any statistically meaningful deviation of this quantity from 0 would mean *T*-violation. However the experimental accuracy for absolute cross-section measurements is much less than for relative ones. Therefore it is preferable to do measurements at any rate in 2 different energy points E_I and E_{II} and construct a quantity:

$$\tilde{\Delta}_{DB}(E_I, E_{II}) = \frac{\sigma_{ab}(E_I)\, \sigma_{ba}(E_{II})}{\sigma_{ab}(E_{II})\, \sigma_{ba}(E_I)} - 1. \tag{122}$$

Here one of the points, say E_I, is chosen for the normalization of the ratio. This allows one to cancel out most of systematic errors. This can be seen, since to first order in $\Delta(E)$ we have:

$$\tilde{\Delta}_{DB}(E_I, E_{II}) \simeq \Delta_{DB}(E_I) - \Delta_{DB}(E_{II}). \tag{123}$$

Therefore in most cases we shall proceed working with the simplest form (121). In doing so we shall use the general expression obtained in [35] for the difference $\delta S_{ab} = S_{ab} - S_{ba}$ between *S*-matrix elements, connecting channels *a* and *b* and caused by the presence of *T*-violating part V_T in the Hamiltonian. As usual, we shall consider the situation for only a pair of close-lying compound resonances 1 and 2. As we have already mentioned in the previous paragraph, the use of the wave functions (18) would give to first order in V_T

amplitudes similar to those considered in P-violation (Figs.1,2). These amplitudes are characterized by the same dynamical v/D and resonance D/Γ enhancement factors. Therefore the dominant contribution to δS_{ab} would come from c–c mixing amplitude of type T_1:

$$\delta S_{ab} = 4\sqrt{2\pi}\ \frac{(\gamma_{2a}\,\gamma_{1b} - \gamma_{2b}\,\gamma_{1a})\cdot v_T}{(E - E_1 + i\,\Gamma_1/2)\,(E - E_2 + i\,\Gamma_2/2)}\,. \tag{124}$$

Here $v_T = -\,i\,\langle\,\Phi_1|V_T|\Phi_2\,\rangle = i\,\langle\,\Phi_2|V_T|\Phi_1\,\rangle$ is the matrix element of V_T interaction between the compound resonances' wave functions Φ_1 and Φ_2 (see (17)).

Now, for the numerator of (121) we have:

$$\sigma_{ab} - \sigma_{ba} = 2\,[\mathrm{Re}\,(\delta S_{ab})\ \mathrm{Re}\,(S^0_{ab}) + \mathrm{Im}\,(\delta S_{ab})\ \mathrm{Im}\,(S^0_{ab})]. \tag{125}$$

While the corresponding expression for the denominator is:

$$\frac{1}{2}\,(\sigma_{ab} + \sigma_{ba}) = |S^0_{ab}|^2 = \left|\frac{\gamma_{1a}\,\gamma_{1b}}{E - E_1 + i\,\Gamma_1/2} + \frac{\gamma_{2a}\,\gamma_{2b}}{E - E_2 + i\,\Gamma_2/2}\right|^2. \tag{126}$$

Then for the case of two weakly overlapping resonances ($\Gamma < |E_1 - E_2| \equiv D$) we get (see [6]):

$$\Delta_{DB}(E) = \frac{v_T\cdot(|\gamma_{1b}\,\gamma_{2a}| - |\gamma_{2b}\,\gamma_{1a}|)\,(\Gamma_1\,|\gamma_{2a}\,\gamma_{2b}| + \Gamma_2\,|\gamma_{1a}\,\gamma_{1b}|)}{[(E - E_2)\,|\gamma_{1a}\,\gamma_{1b}| + (E - E_1)\,|\gamma_{2a}\,\gamma_{2b}|]^2 + 1/4\,(\Gamma_2|\gamma_{1a}\,\gamma_{1b}| + \Gamma_1|\gamma_{2a}\,\gamma_{2b}|)^2}\,. \tag{127}$$

The analysis of this expression shows that it reaches its maximal value in the interference minimum of the cross-sections $|S^0_{ab}|^2$, i.e., when

$$E = E_0 \equiv \frac{|\gamma_{1a}\,\gamma_{1b}|\,E_2 + |\gamma_{2a}\,\gamma_{2b}|\,E_1}{|\gamma_{1a}\,\gamma_{1b}| + |\gamma_{2a}\,\gamma_{2b}|}\,. \tag{128}$$

In case of $\Gamma_1 \approx \Gamma_2 = \Gamma$ this yields for (127):

$$\Delta_{DB}(E_0) \simeq 4\,\frac{v_T}{\Gamma}\,\frac{|\gamma_{2b}\,\gamma_{1a}| - |\gamma_{1b}\,\gamma_{2a}|}{|\gamma_{1a}\,\gamma_{1b}| - |\gamma_{2a}\,\gamma_{2b}|}\,. \tag{129}$$

Supposing for simplicity $\Gamma_{1a}\,\Gamma_{1b} \approx \Gamma_{2a}\,\Gamma_{2b}$ (i.e., equally strong resonances) we obtain:

$$\Delta_{DB}(E_0) = 2\,\frac{v_T}{\Gamma}\left[\left|\frac{\gamma_{2b}}{\gamma_{1b}}\right| - \left|\frac{\gamma_{2a}}{\gamma_{1a}}\right|\right] \equiv \frac{v_T}{\Gamma}\,f, \tag{130}$$

where $f = 2\,[|\gamma_{2b}/\gamma_{1b}| - |\gamma_{2a}/\gamma_{1a}|]$, and the position of the interference dip of σ_{ab} is given by:

$$E_0 \approx \frac{1}{2}(E_1 + E_2).$$

Thus we observe how the already familiar factors of dynamical and resonance enhancement give in (130) the overall enhancement factor v/Γ. We also see that (130) can be sometimes enhanced even more by the «real» structural enhancement factor f (compare with eq. (73a) for the «inelastic channel» observable α_{nf} in P-violation). To be realistic however, one should take into account the finite experimental energy resolution ΔE, which usually exceeds Γ and smears the whole interference picture, bringing the observed effect down to $(v_T/\Delta E)\,f$. Making now a conservative assumption $f \approx 1$, we get the overall enhancement factor in $\Delta_{DB}(E_0)$ to be

$$\frac{\tilde{v}}{\Delta E}. \tag{131}$$

Remember that $\tilde{v}$ is the variance of strong-interaction matrix element (see (9)) which is of the order of 1 MeV. Therefore the net enhancement of TVDB is about 10^3.

This was essentially the result of our analysis with Weidenmüller [6]. As I already mentioned, recently the TUNL-Duke group [9], which is the world authority in fine-resolution experiments, generalized our approach to include the θ-dependence of eq. (120) in it. After performing a tedious analysis of their own experimental data on (p, p) and (p, α) reactions, they concluded that there are *real experimental* situations when the enhancement in TVDB reaches $10^4 + 10^5$. In view of specific difficulties which mark the TC and FC experiments, this seems to be the most realistic experimental way of T-invariance measurements in the nearest future.

3.6. Brief Summary of Possible Enhancements. Thus we have seen that the dominant contribution to all the above effects of T-violation comes from c–c mixing amplitude of the type T_1 in Fig.1. This amplitude contains two basic enhancement mechanisms — dynamical enhancement $\tilde{v}/D$ and resonance enhancement D/Γ. Since however the experimental observables are different, those mechanisms manifest themselves in different manner. Therefore in the optimal conditions we might have the following enhancements:

For TC in the vicinity of E_p, provided that $\sigma_s(E_p) \approx \sigma_p(E_p) \geq \sigma_{\text{pot}}$ (see (82a)):

$$\eta_{\max} \sim \frac{\tilde{v}}{\Gamma}, \qquad \chi_{\max} \sim \frac{\tilde{v}}{\Gamma}. \tag{132}$$

For FC in the vicinity of strong isolated p-resonance $(\sigma_p(E_p) \geq \geq \sigma_s(E_p) + \sigma_{pot}(E_p))$:

$$\beta_{max} \sim \frac{\tilde{v}}{D}. \tag{133}$$

In this case the extra (kR) factor with respect to FC cancels D/Γ.

For TVDB in interference minimum of two close-lying resonances:

$$\Delta_{DB}^{max} \sim \frac{\tilde{v}}{\Gamma} f_1(\theta), \tag{134}$$

where $f_1(\theta)$ might serve as an additional enhancement factor. In realistic conditions, when experimental energy resolution $\Delta E > \Gamma$, we have:

$$\Delta_{DB}^{max} \sim \frac{\tilde{v}}{\Delta E} f_1(\theta). \tag{135}$$

Of greatest interest to the «high-brow» gauge theories of CP-violation is TC, since it is both T- and P-violating. However, I remind that estimates (152) were obtained by us [4,7] for idealized experimental case without Larmour and pseudomagnetic effects.

Among the remaining, purely T-violating effects, TVDB has obvious advantages compared to transmission FC. Its enhancements (135) for already known experimental cases reach $10^4 \div 10^5$, while the only available target for FC shows no p-resonances and therefore lacks even the enhancement of (133).

IV. STATISTICAL APPROACH TO COMPOUND-RESONANCE MEASUREMENTS

1. Nuclear Chaos and Necessity of Statistical Approach. The analysis of the previous section shows that in the isolated resonance regime $\Gamma << d$ (d is the *average* spacing between compound resonances of the same spin) the symmetry breaking interaction of a pair of close-lying resonances with energy separation D leads to two major enhancements — dynamical enhancement v/D and resonance enhancement D/Γ, which very often combine with other specific factors of nuclear reaction theory to produce the net enhancement v/Γ, reaching $5 \div 6$ orders of magnitude. Both enhancements result from a complexity of nuclear compound resonances and practically disappear in simple nucleon-nucleon scattering (see eq. (47)). To be more specific, they manifest quantum chaos, whose idea is still rejected by the majority of professional «chaotists», but accepted (at any rate on intuitive level) by all the nuclear

physicists. Establishing the connection between the fully recognized chaos of classical mechanics and quantum chaos of nuclear physics is an interesting and perspective problem (see, e.g., [36]), whose solution shows that a generic feature of any chaoticity (both in quantum and classical mechanics) is the lack of symmetries in the Hamiltonian of the system. In compound nucleus this lack of symmetries is caused in the first place by the strong pair-wise «residual» interactions, which remove practically all the degeneracies connected with the mean field symmetries (let us call it «strong» chaos) and thus lead to the exponential increase of level density $1/d$. This chaoticity also increases the complexity N of the compound resonance wave function and randomizes the signs of its basic («simple») components' amplitudes. In plain words this means that the incident nucleon quickly distributes its energy among the target nucleons and gets entrapped in a compound system. This, together with small barrier penetration factors, strongly reduces the contribution of particle-emission channels to the resonance total width Γ leaving only the γ-emission. The same complexity of the resonance wave functions considerably reduces the gamma widths. All this results in large compound-resonance lifetimes $\tau \sim 1/\Gamma$ which enter the above enhancement factors. This seems to be a rare occasion, when complexity helps us, leading directly to 6 orders of magnitude enhancement of the experimentally observed effects.

However, one has to pay for everything. The above complexity of compound resonance wave functions Φ makes the head-on calculations of the «weak chaos» symmetry-breaking (WSB) matrix elements $\langle \Phi_1 | V_{SB} | \Phi_2 \rangle$ completely hopeless. Therefore even if we observe the WSB effect and manage to extract the corresponding v_{WSB} out of it (which might be a problem in itself), we seem to learn nothing about the strength constant of the WSB interaction. Coming back to the origin of strong chaos, we see that the above problem with weak interaction matrix elements v_{WSB} differs from the same problem with strong interaction ones only by the strength constants F (see (6)—(9)) which we are hunting for. The problem of strong quantum chaos and strong symmetry breaking matrix elements was faced and physically understood at the dawn of nuclear physics and led to Niels Bohr's hypothesis of compound nucleus, which does not «remember» its formation, and to Weisskopf's idea of black absorbing nucleus. A more refined mathematical technique of nuclear Hamiltonian random matrices was developed by Wigner, Dyson, Mehta and other outstanding physicists in 50-ies. In this approach the expansion coefficients c_i of Φ as well as the matrix elements $\langle \Phi_i | V | \Phi_k \rangle$ are considered to be random numbers varying from resonance to resonance while the value v for the ensemble of individual resonances obeys the normal distribution law with zero mean and variance $\tilde{v} = \sqrt{\langle v^2 \rangle}$. This led to various statistical predictions concerning the properties of

resonances which were all brilliantly confirmed experimentally: the Wigner distribution law for level spacing, the Porter-Thomas law for neutron width distribution and corresponding laws for γ-widths distributions. Therefore the problem of WSB presented practically nothing new to us. This fact was intuitively recognized in the analysis of WSB for a pair of isolated bound states or resonances from the very beginning (see, e.g., the conception of dynamical enhancement factor $\sim \sqrt{N}$ in [15]). Therefore all the order-of-magnitude theoretical estimates of enhancements from the very beginning (see, e.g., [26,4,7]) were done actually for ensemble-averaged variance. We also predicted the sign randomness of the observed effects in c–c mixing mechanism and possible constancy of sign (connected however with loss of dynamical enhancement factor) for valence mechanism [7]. However the intricacies of specific nuclear reaction enhancements for various observables discussed above were so exciting, while the statistics of experimental observations was so meager, that we were postponing the problem of meaningful analysis for experimentally observed values.

2. Energy Averaging. In the meanwhile a highly professional and sophisticated statistical theory of symmetry breaking in nuclear reactions was developing. For purely historical reasons it was essentially concentrated on TVDB effects. After the observation was made [47] that in the two-channel case detailed balance follows from unitary alone (without T-invariance), theoretical [50,52,53,54] and experimental [49,65] interest shifted to the domain of many open channels and strongly overlapping resonances ($\Gamma >> d$). Even the explicit appearance of Γ in the denominator of TVDB energy-averaged expression [50] remained unnoticed. Mahaux and Weidenmüller derived the two-resonance expression (112), (124) which allowed 2 decades later me [5], Weidenmüller and me [6] to see the large enhancements in FC and TVDB, discussed in the previous section. But they also applied it to $\Gamma >> d$ regime of Ericson fluctuations to show that the only enhancement in this regime is the structural factor f (see eq. (130)). Later on Moldauer [52] obtained the same results in R-matrix formalism, again sticking to $\Gamma >> d$ region. He also considered TVDB in direct reactions (see also [66]) proving that direct reaction mechanism contribution to T-violation is 3 orders of magnitude smaller than that of compound resonance mechanism for $\Gamma >> d$ (unfortunately, on obtaining this result he formulated it in a somewhat misleading way — the direct reaction sensitivity to T-violation is 3 orders of magnitude smaller than that of compound resonance reactions).

A new wave of statistical approach to energy-averaged TVDB which involved a full scale mathematics of random-matrix theory developed in [67,68] started with the papers [53,54]. Only in 1989 the technique developed in those papers was first applied by Davis [69] to numerical calculations of energy-averaged FC and TVDB — numerical since the method involved the computation of rather complicated multi-dimensional integrals. «An informed

guess» allowed Davis to approximate in semi-analytical form the results of exact numerical integration for the energy-averaged values of $\langle \Delta_T^2 \rangle$ (see eq. (115) for FC) and $\langle (\sigma_{ab} - \sigma_{ba})^2 \rangle$ (see eqs. (124)—(125) for TVDB) in the limit of isolated resonances $\Gamma < 0.1d$. The corresponding expression for FC was given (omitting the trivial $4\pi/k^2$ factor) as

$$\langle \Delta_T^2 \rangle \approx 4T_{n(-)}T_{n(+)} \frac{2\pi^2 \langle v_T^2 \rangle}{d^2} \frac{(0.35 - 0.17 \ln t)}{t}, \qquad (136)$$

where the neutron transmission coefficients for channel spins (±) are given by

$$T_{(\pm)} = \frac{2\pi \Gamma_{n(\pm)}}{d}; \qquad t = \frac{2\pi \Gamma}{d}.$$

Since by this time the resonance enhancement effect for 2 interacting isolated resonances was already recognized, ref. [69] was the first recognition of the fact that resonance enhancement survives also in *energy-averaged* effects. Moreover, the necessity to pay attention to the isolated resonance regime ($\Gamma << d$) was also accepted. However a statement was made in favour of using *energy-averages* of observables for this regime as opposed to the statistics of individual *on-resonance* observations, which I (and the experimentalists) kept in mind all the time. It took me some time and a bit of reasoning to persuade the author of [69] that his point of view is rather academic than practical. My arguments were as follows: Consider the FC expression (115) in the Γ-vicinity of each resonance energy assuming the typical case $(E_1 - E_2) \approx d$, $\Gamma_1 \approx \Gamma_2 \approx \Gamma$:

$$\bar{\Delta}_T^{res} \approx 4 \frac{v_T}{d} \frac{a_{12}}{\Gamma}. \qquad (137)$$

Here $a_{12} = \gamma_{1(-)}^n \gamma_{2(+)}^n - \gamma_{2(-)}^n \gamma_{1(+)}^n$ and the $4\pi/k^2$ factor is omitted for the sake of comparison with (136). The same expression for (113) in a typical situation between the resonances $|E - E_1| \approx |E - E_2| \sim d$ would be:

$$\bar{\Delta}_T = 2 \frac{v_T}{d} \frac{a_{12}}{d} \frac{\Gamma}{d}. \qquad (138)$$

This expression is a factor of $(d/\Gamma)^2$ smaller than Δ_T^{res}. Let us estimate in a simple-minded way the energy-averaged effect (136) starting from (137) and (138) and averaging their squares over an interval d. Then the $(\Delta^{res})^2$ contribution should be weighed by roughly a factor of Γ/d, while the $(\bar{\Delta})^2$ should have a weighing factor $(d - \Gamma)/d \approx 1$:

$$\langle \Delta_T^2 \rangle \approx (\Delta_T^{res})^2 \frac{\Gamma}{d} + \bar{\Delta}_T^2 \approx 16 \frac{v_T^2}{d^2} \frac{a_{12}^2}{\Gamma^2} \frac{\Gamma}{d} + 4 \frac{v_T^2}{d^2} \frac{\Gamma^2}{d^2}. \qquad (139)$$

Thus we calculated the contribution to (136) from the interval d around one particular resonance. It remains now to average the v_T^2 and a_{12}^2 parameters over all the possible resonances. Since γ's in a_{12} are uncorrelated random variables $\langle a_{12}^2 \rangle = 2\Gamma_{(-)}^n \Gamma_{(+)}^n$. Using the Γ/d smallness, we shall retain in (138) *only the on-resonance contribution.* Thus

$$\langle \Delta_T^2 \rangle \approx 32 \frac{\Gamma_{n(-)}}{d} \frac{\Gamma_{n(+)}}{d} \frac{\langle v_T^2 \rangle}{d^2} \frac{d}{\Gamma} = 4T_{n(-)}T_{n(+)} \frac{2\pi^2 \langle v_T^2 \rangle}{d^2} \frac{2}{\pi^2 t}. \qquad (140)$$

We see that this crude but simple picture almost exactly reproduces the results of (136). The only marked difference is substitution of $2/\pi^2 \approx 0.2$ factor for the $(0.35 - 0.17 \ln t)$. This difference comes essentially because we took from the start a fixed value d for the inter-resonance distance $(E_1 - E_2)$. The actual distribution of this distance obeys a more complicated two level correlation law (see the correlation function R_2 of [70]), which, apart from Wigner repulsion at very small distances allows for all the possible values between 0 and d. If one allows $(E_1 - E_2)$ to vary in this way, the distances smaller than d will contribute more to the resonance effect (137) thus increasing the value $\langle \Delta_T^2 \rangle$. Indeed, energy integration of (115) with the correlation function (see [71]) gives the analytical result exactly equal to (136).

The main point of the above simple arithmetic is that *only the small* Γ*-vicinity of each resonance contributes* to $\langle \Delta^2 \rangle$. It turns out therefore that in order to compare my theoretical value (136) with experiment and to extract $\langle v_T^2 \rangle$, I ask the experimentalist to make accurate measurements not only on the resonance curve, but also in the whole «empty» interval $d >> \Gamma$ between the resonances. At that I know for sure that all these tedious off-resonance measurements would give null results. I also know that in this way I would decrease the sensitivity of $\langle v_T^2 \rangle$ definition by a factor of d/Γ. In order to compensate this loss the experimentalist has to increase the accuracy in measuring each null effect by, say, increasing the beam flux by a huge factor $(d/\Gamma)^2$. One should also recollect that transmission experiments around the strong s-resonances are impossible, or, at best suffer poor statistics. All this almost devoids energy-averaged calculation *for isolated resonances* of any practical meaning. I want to stress this point because of repeated attempts to compare the energy-averaged quantities in this regime with experimentally observed ones. Even in our joint

paper [71], after reading the above critical comments on energy-averaging, one meets a vague statement that it is still appropriate for ^{165}Ho case where there are no observable p-wave resonances below 100 eV. This statement is again a purely academic one* — if you observe no p-resonances in σ_{tot} this just means that either the p-resonance spacing d in this energy-region is anomalously large or that Γ_p^n are anomalously small. Both facts should be somehow taken into account in the «unbiased» estimates (136) as additional biasing and this would lower its value. Even then it would be necessary to drop out of thus biased estimate (136) the unobservable regions around strong s-resonances. One might still hope to get something from averaging the $(s - d)$ mixture term (116). Seemingly one should get for $\langle \Delta_T^2 (s - d) \rangle$ practically the same value as (136). However here comes another very serious danger of energy-averaging. We had already noticed that the $(-\ln t)$ term in brackets of (136) which dominates in our case of small t appears because unbiased energy-averaging procedure favours the situations when the mixing resonances lie anomalously close to each other ($D_{sp} << d$). But exactly in those situations the denominators of observable β (see (98)) would exhibit strong s-resonance maxima which reduces the resonance enhancement of the numerators practically to zero. Therefore the averaged *observed* quantity β would strongly deviate from the calculated $(\langle \Delta^2 \rangle)^{1/2} / \langle \sigma_{tot} \rangle$ because of the strong correlation of the numerator and denominator. In terms of experimentally measured quantities of the type (21)—(25) this means that experimental measurements would be impossible or give extremely poor statistics in exactly the same energy intervals (near strong s-resonances) which mostly contribute to the calculated values of $\langle \Delta^2 (s - d) \rangle$. Together with the above loss of sensitivity by a factor of Γ / d and the abundance of strong s-wave resonances in experimentally observed spectrum of Ho this just means that Ho measurements might be a waste of time. Conclusions to the same effect concerning the energy-averaged estimates of P-violation observables done by Koonin et al. [72] with the aid of optical model functions were reached by Weidenmüller and Lewenkopf [34] — thus averaged quantity lacks resonance enhancement and *bears no relation to the experimental observable P of eq. (20).*

To finish the matter of energy averaging, I mention the recent publication [73] on FC experiments with 2 MeV polarized neutrons in ^{165}Ho, where the theoretical analysis is done in the spirit of a very simple model of T-violation in direct reactions considered almost 30 years ago by Moldauer [66]. I already

*It is unusual to disagree with one's own publication. The main conception and the analytical part of [71] were finished before the end of 1989. However the final text was written only 4 months later, when I was out of reach in Russia and 2 other co-authors in Arizona and Heidelberg, respectively.

mentioned that actually Moldauer had shown in [52,66] that the contribution to T-violating amplitudes from compound resonance mechanisms is about 3 orders of magnitude larger than from direct interaction ones — the fact, which is quite obvious in terms of resonance enhancement physics (time spent by the particles inside the T-violating nuclear field is much larger for compound processes than for direct ones). Therefore I cannot understand why (apart from its extreme simplicity) the authors of [73] applied the direct reaction analysis to their data. This is especially strange, since this experimental energy range might be the most appropriate place to apply the «big guns» of complicated numerical integration worked out [69,74] by one of the authors of ref. [73].

3. «On-Resonance» Ensemble Averaging. Having thus discussed the drawbacks of «unbiased» energy-averaging in isolated resonance regime $\Gamma << d$, we are coming back to the natural idea discussed in Subsection IV.1, namely, to follow the lines of well-developed statistical approach to «strong» chaos of neutron resonances and consider the ensemble of weak-interaction v_{pi} values, measured in different p-resonances as an ensemble of random numbers obeying the normal distribution law with zero mean and variance $\tilde{v}_p \equiv M = \sqrt{\langle v_p^2 \rangle}$:

$$P(v_p) = \frac{1}{\sqrt{2\pi M^2}} \exp\left(- \frac{v_p^2}{2M^2} \right). \tag{141}$$

Thus any particular value of v_p obtained from one on-resonance measurement is of minor importance and the main interest is shifted to the variances M. If we are able to extract the value of M from a set of on-resonance observations (and we shall see below how intricate this extraction might be), then we can use the scaling trick (see eqs. (6)—(8)) and compare this value with its equivalent $\tilde{v}$ for strong interactions, obtained from a well-established quantity of the spreading width Γ_{spr} of eq. (7). This comparison would give us the scaling constant

$$F = \frac{M}{\tilde{v}}, \tag{142}$$

or, at any rate, an upper bound on it.

Everything seems fine in such a simplified scheme. However, the realistic situation is much more complicated. To begin with, in deriving all the expressions for weak symmetry breaking quantities of the previous Section we retained for simplicity only one resonance in the initial and one in the final channel. In principle all the observables of Sec. III should contain a double sum over all the mixing resonances. Since we consider the on-p-resonance measurements in the isolated-resonance regime, the contributions of all the other p-re-

sonances to the observed effect would be smaller by at any rate a factor of $(d/\Gamma)^2$ and can be discarded. However the other sum still remains, and the correct expression for, say, Δ^P_{tot} at E_p would be:

$$\Delta^P_{\text{tot}}(E_p) = \frac{8\pi}{k^2}\frac{\gamma^n_{pi}}{\Gamma_{pi}}\sum_s \frac{\langle s|V_W|p_i\rangle}{E_p - E_s} \equiv \sum_s A_{is}(v_p)_i ,$$

$$A_{is} = \frac{8\pi}{k^2}\frac{\gamma^n_{pi}\cdot\gamma^n_s}{E_p - E_s}, \qquad (v_p)_i = \langle s|V_W|p_i\rangle. \tag{143}$$

Assuming that all the parameters γ^n_p, γ^n_s and E_s, are known, $\Delta^P_{\text{tot}}(E_{pi})$ is a sum if Gaussian distributed random variables $(v_p)_i$ with fixed coefficients. Since a sum of Gaussian random variables is also a Gaussian random variable $\Delta^P_{\text{tot}}(E_p)$ itself is a Gaussian. However it is not ergodic in the sense of ref. [75]. Ergodicity here means that the statistical ensemble average of an observable (whose behaviour we know theoretically) is equal to the running average of the same observable taken over a set of experimentally observed resonances. For $\Delta^P_{\text{tot}}(E_p)$ to be ergodic, it is necessary that it should be independent of the parameters of the actually investigated resonances. In plain words this means that we should get rid of all the trivial constants known for each particular resonance p_i, and consider the new value whose variance is given by $\langle v^2_p\rangle$. Since all the $(v_p)_i$ in (143) have the same variance, such an ergodic variable in the present case would be

$$\Delta^P_i = \frac{\Delta^P_{\text{tot}}(E_{pi})}{|\sum_s A^2_{is}|^{1/2}}. \tag{144}$$

In the one s-resonance approximation $\Delta^P_i = (v_p)_i$.

Let us now slightly complicate the situation. Before doing this, we shall step back to the original expression (61) for Δ^P_{tot}. In order to simplify the derivation we considered the case of zero-spin target $I = 0$. In this case the total compound-resonance spin J is completely defined by $\mathbf{j} = \mathbf{l} + \mathbf{s}$ of the neutron, and the partial width of the p-resonance admixed to s-one is simply $\Gamma^n_p = \Gamma^n_{p\,1/2}$, where 1/2 is neutron j-value. If, however, we remove the restriction $I = 0$, then the p-resonance partial width would contain two components $\Gamma^n_p = \Gamma^n_{p\,1/2} + \Gamma^n_{p\,3/2}$. In the channel spin representation (see, e.g.,

(111)—(116)) this corresponds to 2 different values (±) of the channel spin c. Since T-invariant interaction conserves c, only the $\Gamma^n_{p\,1/2}$ widths (and corresponding amplitudes $\gamma^n_{p\,1/2}$) would enter the $\Delta^P_{\rm tot}$ expression. However in the majority of cases we know only the total Γ^n_p, while the values $\gamma^n_{p\,1/2}$ and $\gamma^n_{p\,3/2}$ are unknown. Therefore for $I \neq 0$ even the simplest form of on-resonance $\Delta^P_{\rm tot}$ would be

$$\Delta^P_{\rm tot}(E_{pi}) = \frac{8\pi}{k^2}\,\frac{\gamma^n_s}{\Gamma_{pi}\,(E_s - E_{pi})}\,\gamma^n_{p\,1/2}\cdot v_p \equiv B_{pi}\,\gamma^n_{pi}\,v_{pi}\,, \tag{145}$$

i.e., the product of a known constant B_p and the unknown $\hat{\Delta}_p = \gamma^n_{p\,1/2}\,v_p$. Now for different choices of p-resonances $\gamma^n_{p\,1/2}$ behaves as a Gaussian random variable with zero mean and variance $\langle\,\Gamma^n_{p\,1/2}\,\rangle$, which can be easily related to, say, neutron strength function. The p-wave amplitude $\gamma^n_{p\,1/2}$ and the matrix element v_p are independent random variables. Thus we can introduce on-resonance ensemble of ergodic values:

$$\hat{\Delta}_{pi} = \frac{\Delta^P_{\rm tot}\,(E_{pi})}{B_i}\,. \tag{146}$$

This random values are, however, distributed according to the law which governs the distribution of a product of 2 independent Gaussian random variables:

$$P\,(\hat{\Delta}_p) = \frac{1}{\pi\omega}\,K_0\,(\hat{\Delta}_p/\,\omega), \tag{147}$$

where K_0 is MacDonald's function and $\omega^2 = \langle\,\Gamma^n_{p\,1/2}\,\rangle\,\langle\,v^2_p\,\rangle$ defines the variance of $\hat{\Delta}_p$.

In the many-level generalization we have (see (143)):

$$\Delta^P_{\rm tot}\,(E_p) = \gamma^n_{p\,1/2}\sum_s\;B_{ps}(v_p)_s \tag{148}$$

and can introduce the ergodic variable:

$$\hat{\Delta}_i = \frac{\Delta^P_{\rm tot}\,(E_{pi})}{|\sum_s\;B^2_{is}|^{1/2}}\,, \tag{149}$$

which obeys the same distribution law (147).

Observe how the lack of knowledge of only one additional parameter $\gamma^n_{p\,1/2}$ of «standard» nuclear spectroscopy complicates the statistical analysis of WSB and data interpretation — instead of the well known analytic Gaussian shape of (142) for Δ^p_i, we get the much more complicated low (148) for $\hat{\Delta}_i$. One can also be sure that statistical confidence levels of variances, extracted with the help of (148) would be much lower than those obtained using (142).

The case of T-violating FC (eq. (116)) generalized for many levels gives the on-resonance expression:

$$\Delta_T(p) \approx \frac{16\pi}{k^2}\frac{1}{\Gamma_p}\sum_k \left(\gamma^n_{p\,1/2}\,\gamma^n_{pk\,3/2} - \gamma^n_{p\,3/2}\,\gamma^n_{pk\,1/2}\right) \times$$

$$\times \frac{(v_T)_k\,(E_p - E_{pk})\,\Gamma}{(E_p - E_{pk})^2 + \Gamma^2/4}\,. \qquad (150)$$

In a rather optimistic case we may know in this expression the parameters of the p-resonance, where we do the measurements, namely E_p, $\Gamma_p \approx \Gamma_{pk} = \Gamma$, $\gamma^n_{p\,1/2}$ and $\gamma^n_{p\,3/2}$. Since our information about p-resonances in general is very poor, the rest of parameters in (150) are very likely to be unknown. The analysis of this situation in [71] demanded numerical Monte-Carlo simulation for the distribution of distant E_{pk} and allowed one to built two approximate analytical expressions for the distribution of ergodic variable δ_T corresponding to (150). Both of them contain two-fold integrals (see [71]) for details).

This strikingly increasing complexity of distributions with the increase of unknown spectroscopic parameters serves a good lesson for experimentalists. If they want to extract useful information on WSB interaction constants rather than surprise the world with large P-violation effects, then they should try to do a good deal of dull job in «standard» spectroscopy in order to define as many spectroscopic parameters as possible. We shall have to strengthen this statement in the analysis below.

4. Analysis of Realistic Imperfect Experimental On-Resonance Measurements. The distribution analysis of the previous subsection concerned only the statistics for the «theoretical» values of observables arising from the chaotic nature of compound-resonances. However each on-resonance measurement of, say, $\hat{\Delta}_i$ value can be done with finite experimental error σ_i, and the experimental results x_i of the measurement in majority of cases would obey the normal distribution law:

$$P\,(x_i|\hat{\Delta}_i) = \frac{1}{\sqrt{2\pi\,\sigma_i^2}}\exp\left\{-\frac{(x_i - \hat{\Delta}_i)^2}{2\sigma_i^2}\right\}. \qquad (151)$$

Here we introduced the notation of conditional probability $P(a|b)$ of a given b. In our case the measured value $\hat{\Delta}_i$ itself is randomly distributed in accordance with the Gaussian law (141), which we shall denote as $P(\hat{\Delta}_i|M)$. Therefore the connection between the measured value x_i and M will be given by:

$$P(x_i|M) = \int d(\hat{\Delta}_i)\, P(x_i|\hat{\Delta}_i)\, P(\hat{\Delta}_i|M) =$$

$$= \frac{1}{\sqrt{2\pi\,(\sigma_i^2 + M^2)}} \exp\left\{-\frac{x_i^2}{2(\sigma_i^2 + M^2)}\right\}. \qquad (152)$$

For an infinite set of experimental measurements, x_i, with small errors, σ_i, one could plot the curve (152) and extract the M value by applying, say, the least square method. Even in this idealized case the problem of finding the confidence intervals ΔM for M is not clearly defined. However the realistic situation of imperfect measurements is much worse. In practice we might hope to get only few experimental points x_i with accuracy not exceeding a few σ_i. To dramatize the problem even more, consider a case when after years of hard experimental work we shall finally get an upper bound $x_1 \leq \sigma_1$ in the triple-correlation measurements on *La* resonance. What shall we do then in order to connect this upper bound with the corresponding upper bound on M?

Up to now denoting (151), (152) as conditional probabilities might seem to be an unnecessary terminological complication of simple things. But when we start considering the above case of imperfect measurements, only the conditional probability theory allows to solve our problems. Indeed, the exact formulation of the problem is: We have a theoretical expression (152) defining probability of experimental result x_i (with σ_i) for a given M value. We need to «inverse» (152) and find a probability $P(M|x_i)$ of M given an experimental result $x_i(\sigma_i)$. This problem is in principle easily solved by using the well-known Bayes theorem of standard conditional probability (CPr) theory:

$$P(M|x)\cdot P(x) = P(x|M)\cdot P(M) \qquad (153)$$

and putting it into the form:

$$P(M|x) = \frac{P(x|M)\cdot P(M)}{P(x)}. \qquad (154)$$

According to the same standard CPr theory the «unconditioned» probability

$$P(x) = \int P(x|M)\, P(M)\, dM \equiv N(x). \qquad (155)$$

Expressions (153)—(155) are given in any textbook on CPr and accepted by all the mathematicians. However the interpretation of (154) given by Bayes himself makes a special branch of *Bayesian statistics* (BS), which is criticized by the representatives of the more orthodox «frequency» school in mathematical statistics for its «subjectivity» (see an excellent and very brief review of this topic in [76]). Unfortunately BS is practically unknown to physicists. Unfortunately, since every physicist who ever worked with experimental data or with any kind of the above «inverse» problem intuitively felt the necessity of BS or even tried to apply it without realizing that this is BS. Bayes supposed that *before* we do any kind of measurements x of the physical quantity M, we often have some «a priori» knowledge concerning $P(M)$ — e.g., *before* measuring the mass we know that it is positive. Bayes theorem (154) formulates in a mathematically precise way how to combine this «a priori» knowledge with the results x of our measurement in order to obtain the «a posteriori» probability $P(M|x)$. One might associate this «a priori» $P(M)$ with considerations of common sense, which prompts to a physicist that application of orthodox statistical prescriptions to, say, negative experimental x_i obtained in the mass-measurement experiment leads to nonsense — he is sure that mass is positive, and that only poor accuracy of his measurement produced the negative x_i. But without BS the physicist does not know how to get out of this trap. The best solution might be to throw this result away and take a more precise measuring device. But what to do if this is the best at your disposal (and often the only one in the world)? In BS approach you just suppose the «a priori» $P(M) = \theta(M)$ and go ahead through (154), (155), obtaining a sensible upper limit on mass as an «a posteriori» result of your imperfect measurement (see [77], where Philip Anderson describes BS as «the correct way to do inductive reasoning from necessarily imperfect data»). In case when nothing is known «a priori» about M the standard assumption is (see [76]) that $P(M)$ is uniform and constant.

There is a close, but sometimes misleading connection between the Bayesian post probability (BPP) given by (154), and the maximal likelihood method (MLM) described in numerous manuals on statistics for the experimentalists (e.g., [78]). One might characterize MLM as an attempt to use Bayesian statistics without recognizing it. Indeed, the $P(x|M)$ function of (154) is often called «likelihood function» $L(M)$ and MLM says that the best estimate of M is the value M_{max}, which maximizes $P(x|M)$ considered as a function of M. One easily sees from (154) that in case of complete «a priori» ignorance (i.e., $P(M) = \text{const}$) BPP coincides with the likelihood function to within the normalization (155). Therefore the BPP in this case has exactly the same maximum. As to the definition of the confidence, the MLM usually prescribes to assign the errors of M by finding the values of M for which $L(M)$ is reduced

from its maximal value by a factor of exp (– 1/2). This prescription is obviously based on the assumption that $L(M)$ is a Gaussian centered at M_{max}. For this (and *only for this*) assumption the above prescription indeed gives the conventional «one σ» confidence level of 68%. What is even more important, the ratio of confidence intervals ΔM for 99% and 68% confidence levels in this case is only a factor of 2.6, and this is known to everybody. We shall see, however, that for a small number n of independent experimental measurements $L(M)$ is highly non-Gaussian — in terms of BPP this means that ΔM for 99% confidence might be larger than ΔM for 68% by a factor of $10^2 \div 10^5$ (see, e.g., [78])! Therefore for small n the MLM confidence prescription becomes senseless. For this reason the most accurate manuals on MLM warn against the use of this method for small n cases and vaguely state that the actual accuracy of M_{max} definition in MLM should not exceed the characteristic width (whatever it is) of the $L(M)$ function maximum (see, e.g., [80]).

Thus we see that standard MLM coincides with BS only when $P(M) = \text{const}$ and the ensemble of experimental measurements n is large. In all the other cases MLM strongly deviates from BS and should not be applied to data analysis at all.

Since most physicists do not know the ordinary CPr theory (not to mention the BS) I shall briefly mention most dangerous points, where CPr and BS disagree with our «intuitive» expectations based on rudimentary knowledge of the ordinary (non-conditioned) probability in its «frequency» modification.

First of all, the BPP of eq. (154) (as well as *any* conditional probability) for 2 independent measurements *is not* equal to the product of BPP's for each measurement:

$$P(M|x_1x_2) = \frac{P(x_1x_2|M)\,P(m)}{N(x_1, x_2)} \neq P(M|x_1)\,P(M|x_2). \tag{156}$$

Here $N(x_1, x_2) = \int P(x_1, x_2|M)\,P(M)\,dM$.

Thus for n independent on-resonance measurements $x_1, x_2, \ldots x_n \equiv \{x_i\}^n$ we obtain:

$$P(M|\{x_i\}^n) =$$

$$= \frac{\theta(M)}{N(\{x_i\}^n)} \prod_{i=1}^{n} \frac{1}{\sqrt{2\pi(\sigma_i^2 + M^2)}} \exp\left\{-\frac{x_i^2}{2(\sigma_i^2 + M^2)}\right\} \tag{157}$$

with normalization

$$N(\{x_i\}^n) = \int_0^\infty dM \prod_{i=1}^{n} \frac{1}{\sqrt{2\pi(\sigma_i^2 + M^2)}} \exp\left\{-\frac{x_i^2}{2(\sigma_i^2 + M^2)}\right\}. \tag{158}$$

Expressions of this type were used by us [79] for the analysis of TVDB experiments [49,65], which were unfortunately done in the regime of strongly overlapping resonances long before the discovery of resonance enhancement. Our analysis revealed the already mentioned highly non-Gaussian shape of $P(M|x_i^n)$ curves for small n. Therefore in case of [49] with its $n = 2$ we got at confidence level 85% the upper bound on T-violation constant $\xi \leq 4 \cdot 10^{-3}$, which is comparable to $3 \cdot 10^{-3}$ quoted in [49]. However at confidence level 99% our result was $\xi \leq 8.8 \cdot 10^{-2} \approx 0.1$. Mark 2 orders of magnitude difference between confidence levels 85% (not even 68%!) and 99%. Only after combining the $n = 6$ independent observations of [49,65] the BPP curve started approaching Gaussian and allowed us to obtain $\xi \leq 3.5 \cdot 10^{-3}$ at 99% confidence level.

We also observe that for one measurement the $N(x)$ integral of (155) diverges logarithmically at the upper limit M_u *even for infinite accuracy* $\sigma = 0$. This means that a single experimental upper bound (however accurate) would *never* allow you to extract the upper bound of random variable variance M. This is obvious, since observed $x_i \approx 0$ might emerge both in case of $M \approx 0$ and for large M — as an unlucky fluctuation of random variable.

All this was true for $p_{1/2}$ resonances. For $p_{3/2}$ ones, which can't mix with s-resonances, we know «a priori» that $M = 0$. Here the BS results differ drastically from our naive expectations. Since now the «a priori» probability $P(M) = \delta(M)$, we get from (152)—(155):

$$P(M|x, 3/2) = \frac{P(x|0)}{P(x|0)} \delta(M) = \delta(M). \tag{159}$$

The meaning of this purely Bayesian result is also quite simple — if we know *for sure* the exact value of M, before the experiment, this knowledge would not be changed by any further measurements.

The situation becomes much more complicated if we do not distinguish between $p_{1/2}$ and $p_{3/2}$ resonances. Then we can only use their statistical weights and claim that while probing p-resonances at random, one gets spin 1/2 with probabiliy $p = 1/3$ and spin 3/2 with probability $q = 2/3$. If only one measurement is done, we can use the ordinary CPr expression:

$$P(M|x) = \sum_{\beta} P(M|x, \beta) P(\beta) \tag{160}$$

in order to combine the BPP's of (157)—(158) (for $n = 1$) for spin 1/2 and (159) for spin 3/2 with the aid of corresponding probabilities $P(\beta)$ (equal to p or q). However, the trivial $\delta(M)$ arising in (160) from the $J = 3/2$ term of

(159) is not of interest for us. Therefore we can easily subtract it from (160) and consider only the $P\ (M|x\ 1/2)$ term given by (157).

The case of 2 measurements x_1, x_2 is more subtle. Then we should consider different possibilities. With probability A both resonances might be $J = 1/2$; with probability B only one of them is $J = 1/2$, and it is equally possible that this is either x_1 or x_2. Therefore:

$$P\ (M|x_1\ x_2) = A{\cdot}P\ (M|x_1\ x_2,\ 1/2) + B\ [P\ (M|x_1,\ 1/2) + P\ (M|x_2,\ 1/2)]. \quad (161)$$

The coefficients A and B are well known in statistics of Bernoulli trials and are closely related to the binomial distribution coefficients. The general analysis of [81] gives for a case of n measurements:

$$P\ (M|\{x_i\}^n) = \frac{1}{1-q^n}\sum_{r=1}^{n} p^r q^{(n-r)} \sum_{K_r} P\ (M|\{x_i\}_r^{K_r},\ 1/2). \quad (162)$$

Here r denotes the number of $1/2$ resonances which we might hit in our n trials, and coefficients in the first sum give the probabilities of this to happen. However for each given r we need to find all the possible combinations K_r of r particular x_i values $\{x_i\}_r^{K_r}$. For each particular combination $\{x_i\}_r^{K_r}$ the BPP $P\ (M|\{x_i\}_r^{K_r}\ 1/2)$ is given by (157)—(158). The number of K_r increases with increasing $r \le n$ in a factorial way. Therefore trying all the options in the sums of (163) for, say, $n = 30$ takes weeks of fast-speed computer time, while the calculation of each particular $P\ (M|\{x_i\}_r^{K_r}\ 1/2)$ defining the M-distribution for a chosen set of $1/2$ resonances takes only seconds. This is another example of how the lack of elementary spectroscopic information on resonance spins enormously complicates the P-violation analysis. Unfortunately this is not the whole truth. Much worse is the fact that this lack of information on spins makes the results of all P-violation measurements practically meaningless. We shall show below that *without the spin assignment* all the measurements performed on ^{238}U and ^{232}Th in recent 6 years allow only to find *the statistically significant upper bound* $F \le 10^{-6}$ on the strength of P-violating weak interaction in those nuclei. It is just a lucky chance that the purely phenomenological expression used for likelihood function in the analysis of these data produced for ^{238}U the results close to those obtained with the spin assignment.

Before showing this, let us summarize the difference between Bayes method and MLM prescriptions of the orthodox statistics in application to our problem. When resonance spins are known the only principal difference for $J = 1/2$ resonances is that BPP of eq. (157)—(158) are normalized to unity,

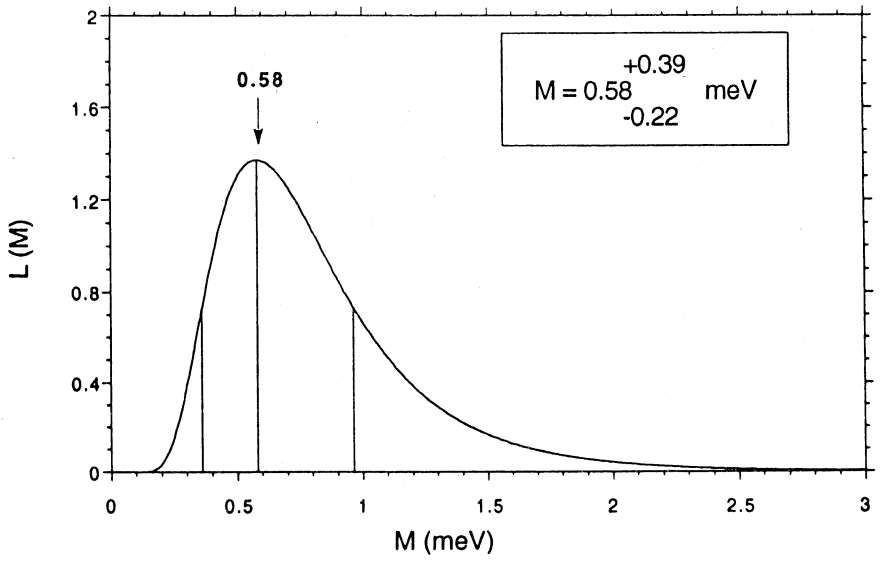

Fig. 3. Likelihood function $L(M)$ for seven $J = 1/2$ p-resonances in ^{238}U based on experimental data of [83] and spin assignment of [84]

while the MLM functions are not. This seemingly insignificant detail leads in case of small ensembles n to quite different results: in case of one measurement the BPP cannot be normalized (and we have seen the deep physical reasons behind it), while standard prescription of the MLM still gives the 68% «confidence level» which is quite meaningless. In case of $n \geq 2$ measurements the BPP curves are normalizable, but the MLM prescription for 68% confidence remains misleading since: a) The exp $(-1/2)$ prescription deviates from actual 68% confidence level; b) The ΔM intervals for confidence levels of 68% and 99% might differ by several orders of magnitude. With increasing n the difference between BS and MLM becomes less marked because $L(M)$ gradually approaches the Gaussian. To illustrate this we show in Fig.3 the $L(M)$ behaviour for seven $p_{(1/2)}$ resonances in ^{238}U based on P-violation measurements of [82,83] and spin assignment of [84] together with «one-σ intervals» of MLM prescription. Mark that even for $n = 7$ the $L(M)$ is still not Gaussian. Therefore the correct definition of 99% confidence would raise the upper limit of M to $M_{up} \approx 1.5$ meV.

In case of $J = 3/2$ the BPP would always give $\delta(M)$ distribution, while MLM will not — see $L(M)$ for nine $3/2$ resonances in ^{238}U of ref. [84] shown in Fig.4. This case shows how misleading the MLM prescriptions might be even

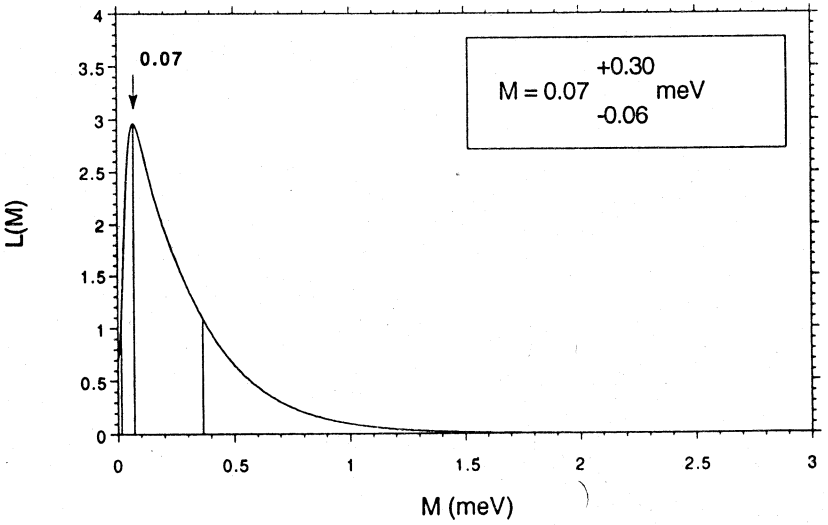

Fig. 4. Likelihood function $L(M)$ for seven $J = 3/2$ p-resonances in ^{238}U based on experimental data of [83] and spin assignment of [84]

for the case of $n = 9$. We all understand that for $3/2$ resonances $L(M)$ results should be compatible with $M = 0$ and that all the extra maxima of $L(M)$ curve should be associated only with poor statistical ensemble (small n). The Bayesian results agree quite well with the above natural expectations — on normalizing the $L(M)$ curve of Fig.4 and looking for 99% confidence level we obtain only the upper bound of $M \leq 1.5$ meV. Definitely this upper bound is a rather poor one, but this reflects the basic fact that $n = 9$ ensemble is still a poor one. Bayesian statistics can't produce miracles and heal this drawback, but it warns that *the positions of L (M) maxima are much less important than the correct definition of their confidence levels.*

In case of no spin assignment the *purely empirical* expression was suggested for $L(M)$ in [82]:

$$L(M) = \prod_{i=1}^{n} \left[\frac{p}{\sqrt{2\pi\,(\sigma_i^2 + M^2)}} \exp\left\{ -\frac{x_i^2}{2\,(\sigma_i^2 + M^2)} \right\} + \right.$$
$$\left. + \frac{q}{\sqrt{2\pi\,\sigma_i^2}} \exp\left\{ -\frac{x_i^2}{2\sigma_i^2} \right\} \right]. \qquad (163)$$

We see that this expression is built in violation of both Bayes statistics (since the $3/2$ term with q coefficient should be δ-shaped — see (159)) and the rule (159) of conditional probability theory (conditional probability of n inde-

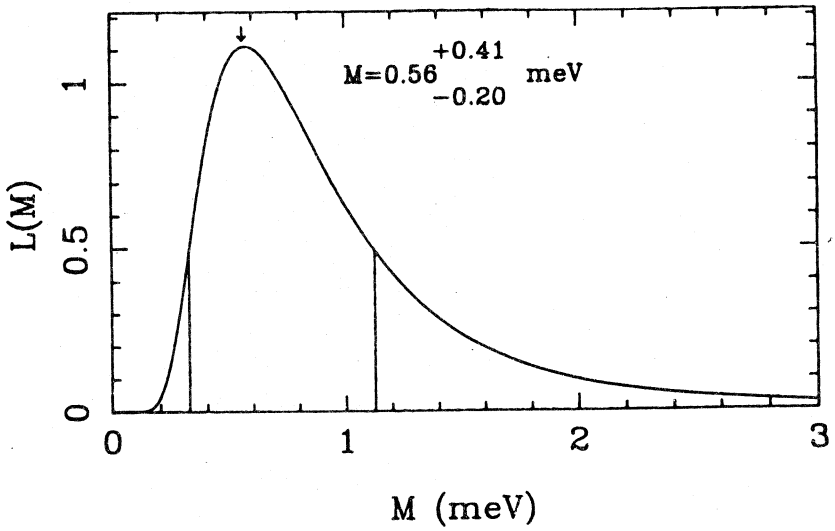

Fig. 5. Likelihood function of ex. (163) for 16 p-resonances in ^{238}U without spin assignment (see [83])

pendent measurements differs from a product of n conditional probabilities). The plot of (163) for 16 resonances measured in ^{238}U as given by [83] is shown in Fig.5. When a similar plot of ref. [82] was first demonstrated at 1989 Alushta School, the response of the experimental audience was: «How do you manage to extract the M values so precisely, when only 6 out of your 17 measured x_i deviate from zero by more than 2σ?» (One should add that now we know that only 3 of those 6 non-zero results are *actually* $J = 1/2$!) This perfectly sound remark aroused my interest to imperfect data statistical analysis and led finally to the above Bayesian results. These results, given by (162), are demonstrated for the case of ^{238}U measurements in Fig.6. Their obvious meaning is (compare with Fig.4) that without spin assignments the extracted value of M is *compatible with zero and gives only the upper bound* $M \leq 3$ *meV at 95% confidence level*, in complete agreement with sound expectations. The oscillations of L (M) curve, likewise in case of Fig.4, result only from the poorness of the statistical ensemble.

The problem now is to understand the striking similarity between the curves of Fig.5 obtained by using the erroneous analysis (163) and Fig.3, whose analysis (besides the above remarks on confidence levels) is correct. The plain answer is — the occurrence of several lucky and unpredictable coincidences.

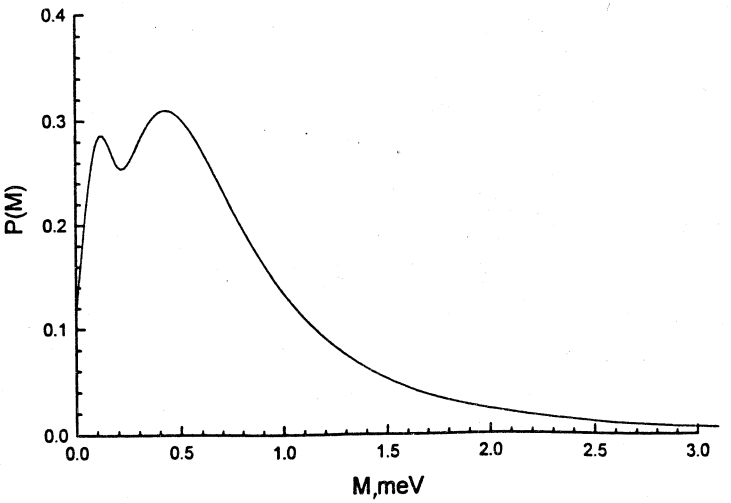

Fig. 6. Bayesian post probability of ex. (162) (normalized to $p = 1/3$) for 16 p-resonances in ^{238}U without spin assignment

Let us compare the phenomenology of (163) with the Bayesian ex. (162). By removing the constant factors $\exp - (x_i^2/ 2\sigma_i^2)$ out of each factor in the product of (163) and presenting (163) as an n-th power of binomial we can simplify this comparison. Now we see that the main difference between (162) and (163) lies in the fact that each term of the binomial expansion in (163) contains an extra weight factor $\exp (x_i^2/ 2\sigma_i^2)$, which exponentially enhances the contribution of each significant deviation $x_i^2/ 2\sigma_i^2$ of the effect from zero. In particular ^{238}U, case a single 63.5 eV resonance with $x_0 \approx 7\sigma_0$ contains an enormous enhancement factor $A_0 = 10^{10}$. Therefore the maximum of this term $M_{\max}^0 = \sqrt{x_0^2 - \sigma_0^2} = 0.65$ meV practically defines the maximum of the whole expression (163). The remaining 4 statistically significant results, whose maxima lie on both sides of M_0, only slightly shift the overall maximum to $0.58^{+0.5}_{-0.2}$ meV of ref. [82]. In order to estimate the influence of those remaining terms, observe that omission of one of the 2σ effects at 57.9 meV in [83] shifted this maximum to $0.56^{+0.4}_{-0.2}$ meV. Naturally, all the abundant zero-effects, mentioned above, produce no influence whatsoever on the L (M) curve of (163).

Thus the phenomenological construction (163), built in violation of conditional probability theory, has a surprising feature of artificial «exponential» selection of the most statistically significant results, or, to put in the other way, exponential suppression of all the null results. Intuitively one might expect that this lucky feature of (163) (quite unexpected by its creators) is a strange but reasonable way to select 1/2 resonances, since we expect that *in average* only those resonances would show *marked* deviations from zero. To a certain extend this is true, but only to a certain extend. Let us come back to our basic expression (152) to understand how sound this selection might be. First of all, we observe that for *any* value of M (that means 1/2 resonances!) the most probable result is $x_i = 0$. ^{238}U case is not an exclusion — 4 out of 7 resonances $J = 1/2$ show zero results. However, the width of the distribution curve (152) depends both on M and σ_i values. Consider first a limiting case of extremely high experimental accuracy $(M/\sigma_i)^2 >> 1$. In this case practically all the non-zero results x_i would come from 1/2 resonances with $M \neq 0$. The «contamination» from 3/2 resonances would be negligible because of small σ values. Therefore in this idealized situation the suppression of null results is perfectly correct and the ex. (163) might be a reasonable approximation of (157).

Consider now the case $(M/\sigma)^2 \simeq 1$. In this case the distributions (152) for $M = 0$ and $M \neq 0$ would come closer to each other and 3/2 resonances would considerably «contaminate» our measurements contributing a lot of non-zero results x_i. However, if we have a very large ensemble of resonance-measurements $n >> 1$ and exponentially select the most significant results, we can still be sure that more $x_i \neq 0$ would come from 1/2 resonances. Mind that for small n ensembles this will not work and a «degree of contamination» coming from 3/2 resonances would randomly vary from ensemble to ensemble.

Finally consider $(M/\sigma_i)^2 << 1$. Then the distributions (152) for $M = 0$ and $M \neq 0$ would practically coincide. Only by taking the unrealistic limit of infinite ensemble $n \to \infty$ plus some kind of selection of largest results one might hope to select the 1/2 contributions.

Coming back to ^{238}U results, we know *only after spin assignment* that $M = 0.56$ meV. Comparing it with σ_i of [82,83] we see that experimental accuracy parameter $(M/\sigma_i)^2$ is more or less evenly distributed between 400 and 0.05. Therefore the chances that non-zero effects come only from 1/2 resonances are roughly «fifty-fifty». Indeed, as we know now, 4 out of 7 non-zero results in U were coming from 3/2 resonances. Therefore the above

coincidence of 2 maxima positions is an unpredictable chance coming essentially from the fact that the main 7σ contribution to (153) *alone* was giving the value M_0^{max} already within σ_0 of the true M-value of [84]. Therefore it would be much simpler and honest to say plainly: «We have reasons to hope that 7σ effect is a $1/2$ resonance one, while with the rest we have no guaranties. So we identify the matrix element of this large effect with the variance M». Obviously, the statistical significance of such a statement if quite unpredictable, but so is the statistical significance of results obtained with the much less transparent ex. (163).

We can also understand now the results of Monte-Carlo simulation [85] of Th case. The authors of [85] considered the ensemble of $n = 7000$ resonances with non-zero effect in case when $(M/\sigma_i)^2$ parameter was distributed in the range from 10^3 to 1. We have already shown above that for such a choice of $(M/\sigma)^2$ the unrealistically large ensemble of 7000 non-zero observations would almost certainly produce the correct results, which was the outcome of [85]. The trouble is that in actual ^{232}Th of [86,87] we have only 7 non-zero effects and do not know in advance the $(M/\sigma_i)^2$ values. Therefore without the spin assignment we cannot even make a clever guess how many non-zero effects arise from «contaminating» $3/2$ resonances and how many null effects come from $1/2$ resonances (in U those were 4 out of 7 resonances with $J = 1/2$).

Therefore in realistic measurements even the correctness of M_{max} derived from (163) would be always unpredictable without spin assignment, not to mention the confidence levels given by (163). This unpredictable character of (163) is mathematically reflected in Bayesian expression (162) and in the results of Fig.6.

5. Sign-Correlation Effect. Returning back to the multilevel ex. (145) for Δ^p_{tot}, we see that the signs of the observed effect should vary randomly from resonance to resonance. This comes from sign-randomness of 3 quantities in it: matrix element $(v_p)_i$, partial amplitudes γ_s^n and γ_p^n, and energy denominators $(E_p - E_s)$.

However the measurements in ^{232}Th (without spin assignment) demonstrated that 7 out of the 7 statistically significant $(x_i \geq 2\sigma_i)$ effects have the same positive sign (see [86,87]). This poses a question — is it a fluctuation or it comes from some systematic effect, which is not included into (143) and which has constant sign. The answer to this question might be best found on the lines of Bayesian statistics (see [77], where Anderson demonstrates how efficient BS is in «null-hypothesis» tests, discarding with notorious «fifth-

force» experiments). However authors of [88] preferred to introduce «ab initio» the constant-sign term in addition to (143). This resulted in constant-sign addition $B\sqrt{1\ \mathrm{eV}/E}$ (%) to the quoted effect $\mathcal{P}$ (see (78), (81)). The magnitude B of this addition was defined in the 2-dimensional MLM analysis, using $L(M)$ of (164) modified by the presence of the B term. The result of this analysis was $B = 8^{+6.2}_{-6.0}$ %, i.e., of the same order of magnitude as the effect $\mathcal{P}$ itself (which ranges between 1% + 10%).

This highly sensational result was taken for its face value as an experimental one by a lot of theorists and experimentalists and produced an avalanche of publications with attempts to explain it theoretically. Since it might take a special review to analyze (and even mention) all of them, I will just classify the main trends in those publications. Some of them concentrated on the analysis of possible sign-correlation between matrix elements $(\nu_p)_i$, completely ignoring the random signs of γ's and $(E_p - E_s)$. Others re-discovered our old statement (see, e.g., [7]) that valence mechanism leads to sign correlation of the P-effects (see ex. (60) for valence part T_{10} of T_1 amplitude), ignoring however that we discarded this mechanism in [7] because it lacks the dynamical enhancement factor $\sqrt{N} \approx 10^3$. Apart stand papers [33,34] which concerned the amplitudes of T_8 type. Since all the diagrams containing the χ wave function (see wavy lines in loops of T_3, T_5–T_9 in Fig.1) describe the motion of valence particle in target mean field, we called them all «the valence mechanism» in [7]. We estimated them with a crude procedure similar to that of eq. (15), (16) and, on discovering that they lack the dynamical enhancement factor $\sqrt{N}$, simply stated this fact in [7]. Weidenmüller in [33] developed a much more elegant technique of principal value integrals evaluation which I borrowed from him in the above estimates of Sec.III.

Practically all the authors concluded that valence mechanism needs extra enhancement of $10^2 + 10^3$ in order to explain the above B-value. Practically nobody mentioned that this extra factor is exactly the same dynamical enhancement which provided for large observed effects in complex nuclei in the first place.

Nobody also questioned the reliability of the above huge B-value, obtained from MLM analysis, whose drawbacks we have just discussed. To those, who do not believe in Bayesian approach, I can suggest to compare the above $B = 8^{+6.2}_{-6.0}$ % value with MLM value $M = 0.07^{+0.30}_{-0.06}$ meV in Fig.4. It is believed by all that the results of Fig.4 should be compatible with $M = 0$. The same must be said about B even by the MLM adepts. So the actual statistical significance of sign correlation effect remains an open question which could be solved, if

really necessary, in terms of Bayesian approach. Since this approach gives only the upper bounds even for M-values without spin assignment, the same will be even more true for B-values. Therefore spin assignment in Th is essential also if one really wants to consider the sign-correlation problem seriously.

V. SUMMARY

Thus we have seen that the enhancements of *all* the symmetry-breaking effects in nuclear reactions on isolated resonances comes essentially from dynamical factor $\tilde{v}/d \sim \sqrt{N}$ and resonance enhancement factor d/Γ, which combine in most optimal situations to the overall factor $\tilde{v}/\Gamma$. For inelastic channels (including TVDB) there might be an additional structural enhancement factor $f \sim (\gamma_1/\gamma_2)$ (see eqs. (73a), (130)). For «elastic channel» observables probed in transmission experiments the situation is more complicated. All of them contain instead of the above f the barrier penetration hindrance factors (kR) or $(kR)^2$ (for FC). However, they also contain an extra resonance enhancement d/Γ (see, e.g., eq. (73b), (73c)) which might almost completely (in case of P-odd correlation) or partially (in case of FC) compensate those hindrance factors.

We have also seen that the «structural (kinematic) enhancement factor» $1/(kR)$, so often used to explain the enhancements for the «elastic channel» P-odd correlations, is merely an artifact of misleading analogy with bound states in theory and of quoting the auxiliary value $\mathcal{P}$ instead of the really observed P in experiment.

Both major enhancements (dynamical and resonance) are quite general results of quantum chaoticity of compound resonances, which increases the complexity N of the compound-resonance wave function and reduces their total widths Γ. This reduction is most efficient in the low-energy region of isolated resonances $\Gamma << d$.

The same chaoticity which produced huge enhancements also necessitates the use of statistical methods for the analysis of observables and their proper connection with strength parameters of the symmetry breaking interactions. This does not lower the reliability of information obtained as compared to simple nucleon-nucleon interaction processes, provided that one obeys certain general rules and uses the correct statistical methods. In theory this boils down to using the methods of random matrix approach, whose reliability was established during half a century in neutron-resonance spectroscopy. In processing the experimental data one should use Bayesian statistics (BS), whose significance is gradually realized by all the physical community.

Both statistical approaches (in theory and experiment) show an important general feature — lack of information on «standard» spectroscopic parameters immediately complicates the analysis and enormously lowers the statistical

significance of the symmetry-breaking observations. BS also strongly vouches for the increase of independent experimental observations rather than their individual accuracy.

In this review I had to concentrate essentially on reaction aspects of symmetry breaking and on proper statistical analysis, paying much less attention to the ultimate aim of on-resonance experiments — analysis of new information on symmetry breaking interaction constants. As mentioned in Introduction, since the creation of Weinberg-Salam electro-weak interaction theory nobody would be surprised by P-violation caused by weak components of nucleon-nucleon interaction. Therefore in P-violation one should try to study the systematic behaviour of F (e.g., its A-dependence). Evèn from this point of view P-violation is only a particular case of symmetry breaking in nuclei. Studies of «strong» symmetry breaking (see Sec.IV.1) are by no means less important — they are only much more advanced. Even in those studies there are still open problems whose solution might be of major importance for P-violation — see Weidenmüller's comments on isospin-violating spreading widths and their implications in [89]. Therefore even more important is to use P-violation as «test sites» for future T-violation «on-resonance» experiments by developing most reliable experimental and theoretical technique.

I have to point that although on-resonance enhancements were continuously predicted for various T-violating observables since 1982, the experimental situation in this field lacks dynamics. Perhaps too much experimental energy is wasted on P-violation, especially on creating and discussing «quasi-sensations». The same applies to FC correlation measurements in almost hopeless Ho. In view of the facts stated in the end of Sec.III the on-resonance TVDB observations seem much more promising than the FC ones in general. I must also repeat that discussion of all the experimentally realistic modifications of TC measurements should be a highest priority. In planning the experimental strategy of T-violation measurements one should especially follow the rule resulting from BS — more independent on-resonance observations even with smaller accuracy. Mind that in the optimistic case of non-zero effect one measurement would only produce a sensation, telling nothing about the interaction constant. In the more probable case of experimental upper-bound observation one point, however accurately measured, would be quite meaningless.

Acknowledgement

I officially acknowledge that this work was supported in part by the Russian Fund of Fundamental Investigations. With much less officiality but much more warmly I express my gratitude to all my co-authors in this field. I am especially grateful to Hans Weidenmüller, whose contribution to this work in many capacities (co-authorship, friendly discussions, hospitality and financial

support during my numerous stays in Heidelberg) is simply impossible to measure.

REFERENCES

1. **Sushkov O., Flambaum V.** — Pis'ma ZhETP, 1980, vol.32, p.377; Proc. of the LNPI 16-th Winter School (Hign Energy Phys.), Leningrad, 1981, p.200.
2. **Bunakov V., Gudkov V.** — Z. Phys. A., 1981, vol.303, p.285; Proc. of the LNPI 16-th Winter School (Nuclear Phys.), Leningrad, 1981, p.32.
3. **Alfimenkov V. et al.** — Pis'ma ZhETP, 1981, vol.34, p.308.
4. **Bunakov V., Gudkov V.** — JETP Letters, 1982, vol.36, p.328; Z. Phys. A, 1982, vol.308, p.363.
5. **Bunakov V.** — Phys. Rev. Lett., 1988, vol.60, p.2250.
6. **Bunakov V., Weidenmüller H.A.** — Phys. Rev. C, 1989, vol.39, p.70.
7. **Bunakov V., Gudkov V.** — Nucl. Phys. A., 1983, vol.401, p.93.
8. **Bunakov V.** — Phys. Lett. B, 1988, vol.207, p.233.
9. **Mitchell G. et al.** — Time-Reversal Invariance and Parity Violation in Neutron Reactions, ed. C.Gould, J.D.Bowman , Yu.P.Popov, World Scientific, Singapore, 1994, p.167.
10. **Mahaux C., Weidemüller H.** — Shell Model Approach to Nuclear Reactions, North Holland, Amsterdam, 1969.
11. **Blin-Stoyle R.** — Fundamental Interactions and the Nucleus, North Holland, Amsterdam, 1973.
12. **Bohr A., Mottelson B.** — Nuclear Structure, vol.1, Benjamin, NY, 1969.
13. **Haas R. et al.** — Phys. Rev., 1959, vol.116, p.1221.
14. **Blin-Stoyle R.** — Phys. Rev., 1960, vol.120, p.181.
15. **Shapiro I.S.** — Sov. Phys. Uspekhi, 1969, vol.11, p.582.
16. **French J. et al.** — Tests of T-Reversal Invariance in Neutron Physics, ed.N.Roberson, C.Gould, J.D.Bowman, World Scientific, Singapore, 1987, p.80.
17. **Lobashov V. et al.** — Pis'ma ZhETP, 1966, vol.3, p.268.
18. **Abov Yu. et al.** — Yad. Fiz., 1965, vol.1, p.4791.
19. **Baz A., Zeldovich Ya., Perelomov A.** — Scattering, Reactions and Decays in Non-relativistic Quantum Mechanics, Nauka, Moscow, 1971.
20. **Alfimenkov V.** — Nucl. Phys. A, 1983, vol.383, p.93.
21. **Stodolsky L.** — Phys. Lett. B, 1971, vol.50, p.352.
22. **Michel F.** — Phys. Rev., 1964, vol.133, p.329.
23. **Karl G., Tadic D.** — Phys. Rev. C., 1977, vol.16, p.1726.
24. **Forte M.** — Fundamental Physics with Reactor Neutrons and Neutrinos, ed. T. von Egidy, Institute of Phys., Bristol, 1978, p.86.
25. **Karmanov V., Lobov G.** — Pis'ma ZhETP, 1969, vol.10, p.332.
26. **Sushkov O., Flambaum V.** — Uspekhi Fiz. Nauk, 1982, vol.196, p.3.
27. **Forte M. et al.** — Phys. Rev. Lett., 1981, vol.45, p.2088.
28. **Kolomensky V. et al.** — Phys. Lett., 1981, vol.107, p.308.
29. **Vanhoy J. et al.** — Z. Phys. A., 1988, vol.333, p.229.
30. **Gould C.** — J. Mod. Phys. A., 1990, vol.5, p.2181.

31. **Bizetti P., Maurenzig P.** — Nuovo Cim. A., 1980, vol.56, p.492.
32. **Baldin A.M. et al.** — Nuclear Reaction Kinematics, Moscow, 1968.
33. **Weidenmüller H.A.** — Group Theory and Special Symmetries in Nuclear Physics, ed. J.Drayer, J.Janecke, World Scientific, Singapore, 1992, p.31.
34. **Lewenkopf C., Weidenmüller H.** — Phys. Rev. C, 1992, vol.46, p.2601.
35. **Mahaux C., Weidenmüller H.** — Phys. Lett., 1966, vol.23, p.100.
36. **Bunakov V.** — Proc. of the II International Seminar on Interaction of Neutron with Nuclei, 26—28, April, 1994, Dubna, Russia, (in press).
37. **Danilyan G.** — Pis'ma ZhETP, 1977, vol.26, p.298; Uspekhi Fiz. Nauk, 1980, vol.131, p.329.
38. **Bunakov V., Gudkov V.** — Tests of T-Reversal Invariance in Neutron Physics, ed. N.Roberson, C.Gold, J.D.Bowman, World Scientific, Singapore, 1987, p.175.
39. **Bunakov V., Gudkov V.** — Z. Phys. A., 1985, vol.321, p.271.
40. **Sailor V.** — Proc. International Conference on Peaceful Use of Atomic Energy, vol.4, United Nations, NY, 1955, p.199.
41. **Lynn J., Pattenden N.** — ibid, p.210.
42. **Bohr A.** — ibid, vol.2, p.220.
43. **Lynn J.** — The Theory of Neutron Resonance Reactions, Clarendon, Oxford, 1968.
44. **Henley E., Jacobsohn B.** — Phys. Rev. Lett., 1966, vol.16, p.708.
45. **Ryndin R.** — Proc. of the LNPI 3rd Winter School, Leningrad, 1968, p.39.
46. **Bunakov V., Gudkov V.** — Proc. of the LNPI 20th Winter School, Leningrad, 1985, p.189.
47. **Henley E., Jackobsohn B.** — Phys. Rev., 1959, vol.113, p.225.
48. **Christenson et al.** — Phys. Rev. Let., 1964, vol.13, p.138.
49. **von Witsch et al.** — Phys. Lett., 1966, vol.22, p.631; Phys. Rev. Lett., 1967, vol.19, p.524; Phys. Rev., 1968, vol.169, p.923.
50. **Ericson T.** — Phys. Lett., 1966, vol.23, p.97.
51. **Pearson J., Richter A.** — Phys. Lett. B., 1975, vol.56, p.112.
52. **Moldauer P.** — Phys. Rev., 1968, vol.165, p.1136.
53. **Boose D. et al.** — Phys. Rev. Lett., 1986, vol.56, p.2012.
54. **Boose D. et al.** — Z. Phys. A, vol.325, p.363.
55. **Stodolsky L.** — Nucl. Phys. B, 1982, vol.197, p.213.
56. **Kabir P.** — Phys. Rev. D, 1982, vol.25, p.2013.
57. **Bunakov V., Gudkov V.** — LNPI preprint No.1236, 1986.
58. **Barabanov A.** — Yad. Fiz., 1986, vol.44, p.1163.
59. **Herczeg P.** — Tests of T-Reversal Invariance in Neutron Physics, ed. N.Roberson, C.Gould, J.D.Bowman , World Scientific, Singapore, 1987, p.24.
60. **Bunakov V., Gudkov V.** — J. Phys. (Paris) C, 1984, vol.3, Suppl., No.3, p.77.
61. **Baryshevsky V., Podgoretsky M.** — JETP, 1964, vol.47, p.1050.
62. **Masuda Y.** — T-Reversal Invariance and P-Violation in Neutron Reactions, ed. C.Gould, J.D.Bowman, Yu.Popov, World Scientific, Singapore, 1994, p.126.
63. **Serebrov A.** — ibid, p.138.
64. **Huffman P. et a.** — ibid, p.151.
65. **Blanke E. et al.** — Phys. Rev. Lett., 1983, vol.51, p.355.
66. **Moldauer P.** — Phys. Lett. B, 1968, vol.26, p.713.
67. **Verbaarschot J. et al.** — Phys. Rep., 1985, vol.129, p.367.

68. **Verbaarschot J. et al.** — Ann. Phys. (NY), 1984, vol.168, p.368.
69. **Davis E.** — Phys. Lett. B, 1989, vol.206, p.197.
70. **Mehta M.** — Random Matrices, Academic, NY, 1967, chap.5.
71. **Bunakov V., Davis E., Weidenmüller H.** — Phys. Rev. C, 1990, vol.42, p.1718.
72. **Koonin S. et al.** — Phys. Rev. Lett., 1992, vol.69, p.1163.
73. **Koster J. et al.** — T-Reversal Invariance and P-Violation in Neutron Reactions, ed. C.Gould, J.D.Bowman, Yu.Popov, World Scientific, Singapore, 1994, p.144.
74. **Davis E., Hartmann U.** — Ann. Phys. (NY), 1991, vol.211, p.334.
75. **French J. et al.** — Phys. Lett. B, 1978, vol.80, p.17.
76. **Barlow R.J.** — Statistics, Wiley, NY, 1989, chap.7.
77. **Anderson P.W.** — Physics Today, January 1992, p.9.
78. **Eadie W.T. et al.** — Statistical Methods in Experimental Physics, North Holland, Amsterdam, 1971.
79. **Bunakov V., Harney H.-L., Richter A.** — Nucl. Phys. A, 1993, vol.560, p.71.
80. **Taupin D.** — Probabilities Data Reduction and Error Analysis in the Physical Sciences, Les Editions de Physique, Paris, 1989.
81. **Bunakov V.** — T-Reversal Invariance and P-Violation in Neutron Reactions, ed. C.Gould, J.D.Bowman, Yu.Popov, World Scientific, Singapore, 1994, p.61.
82. **Bowman J.D. et al.** — Phys. Rev. Lett., 1990, vol.65, p.1721.
83. **Zhu X. et al.** — Phys. Rev. C., 1992, vol.46, p.768.
84. **Corvi F. et al.** — T-Reversal Invariance and P-Violation in Neutron Reactions, ed. C.Gould, J.B.Bowman, Yu.Popov, World Scientific, Singapore, 1994, p.79.
85. **Bowman J.D., Sharapov E.** — ibid, p.69.
86. **Frankle C. et al.** — Phys. Rev. Lett., 1991, vol.46, p.778.
87. **Frankle C. et al.** — Phys. Rev. C, 1992, vol.46, p.778.
88. **Bowman J.B. et al.** — Phys. Rev. Lett., 1992, vol.68, p.780.
89. **Weidenmüller H.A.** — Nucl. Phys. A, 1991, vol.552, p.293c.

«ФИЗИКА ЭЛЕМЕНТАРНЫХ ЧАСТИЦ И АТОМНОГО ЯДРА»
1995, ТОМ 26, ВЫП.2

УДК 539.126.34 + 539.17.01

PIONIC DOUBLE CHARGE EXCHANGE WITHIN QUASIPARTICLE RANDOM PHASE APPROXIMATION

Wiesław A.Kamiński

Institute of Physics, Maria Curie-Sklodowska University, 20-031 Lublin, Poland

The description of the pionic double charge exchange reaction is given within the proton-neutron quasiparticle random approximation. The approach is tested in a case of iron ^{56}Fe, and a fairly good agreement of the calculated quantities with recent data is found. The observed resonance-like behaviour of the energy dependence of the cross section is explained semiquantitatively in terms of two-nucleon process without invoking exotic mechanisms, like dibayrons or multiple quark clusters.

Дано описание реакции двойной перезарядки пионов в рамках протон-нейтронного квазичастичного приближения случайных фаз. Метод апробирован на примере ядра железа ^{56}Fe, и получено довольно хорошее согласие рассчитанных характеристик с современными данными. Наблюдаемое резонансноподобное поведение энергетической зависимости сечения полукачественно объяснено с помощью двухнуклонных процессов без привлечения экзотических механизмов, таких как дибарионы или многокварковые кластеры.

1. INTRODUCTION

Investigations concerning double charge exchange (DCX), both experimental and theoretical ones, have attracted much interest during the last decade. Studies of double charge exchange of pions on nuclei are attractive for many reasons. Since the charge conservation law ensures that at least two nucleons must be involved in pionic DCX on a nucleus, the reaction can be regarded as a promising source of specific information about the short range correlations between bound nucleons. Some authors also hope that the reaction makes it possible to study the expected difference between the neutron and proton densities in nuclei. Depending on the choice of the target nucleus, the DCX process may populate neutron- or proton-rich nuclei far from the stability region [1—4]. It is also possible to obtain information from the reaction about double isobaric analogue states [5,6], double isovector dipole resonances [7,8]

or some exotic states of nuclear matter such as states of three and four neutrons [9,10]. (For a recent competent review of the pionic charge exchange reactions see Ref.11.)

In most theoretical investigations of the DCX reaction in the low energy region one assumes that the process is sequential: If two nucleons are correlated in space, then one can expect that a neutral pion π^0 emitted from the first charge exchange reaction on one nucleon finds a good chance to initiate the second charge changing process on the correlated partner. Further, one expects that the pion interacts during the two step exchange only with valence nucleons and thus the core plays only a passive role. This picture is quite natural for the transitions to the final double analogue state since during such a transition all quantum numbers of nucleons are unchanged except the third component of isospin (change of a neutron into a proton). In a non-analogue transition like the transition to the ground state of $T \neq 1$ nuclei, the core can play an active role due to the antisymmetrization of the total wave function, which allows the core nucleons to participate actively in the reaction [12].

Most of the theoretical approaches in the low pion energy domain are plane wave impulse approximation — PWIA theories. Some of them account for distortion effects (distorted wave impulse approximation — DWIA, coupled channel techniques). The conclusions are not unique and we can find statements about either importance [15—17] or negligence of the distortion [13—14]. Moreover, all calculations of DCX differential cross sections and angular distributions taking into account even simple correlated nuclear wave functions show a fairly satisfactory agreement with data, while theories without such correlations disagree with experiments by an order of magnitude or more. Some authors argue [13,14,18—20], that correlation effects are so important that it is impossible to see other effects such as those of reaction dynamics or the pion distortion unless nucleon-nucleon short range correlations will be accounted properly. It is also not clear what roles play the initial and final state interactions in this context.

From this point of view the nuclear structure involved in the DCX models is a very sensitive aspect of theoretical interpretations of the process. Here one can find pronounced differences ranging from very simple shell model approaches [13,14], through the generalized seniority scheme [21], to very advances *realistic* treatments [22,23]. Of course, the problem of nuclear structure will display its complexity as one deals with heavier nuclei. This is the reason why most existing DCX theoretical treatments concentrate on light nuclei. Recently, Vergados [24] proposed a treatment of the DCX reactions in the context of any shell model in which one separates reaction amplitudes into two parts, one depends on the nuclear wave function and another one is connected with characteristics of the charge changing process between a pion and

a nucleon. It can help in some aspects, but even here one has the problem of explicit construction of the excited states of the intermediate nucleus and the Green functions.

In a series of papers [22,23,25] a new approach to the DCX process in the framework of the proton-neutron quasiparticle random phase approximation (pn-QRPA) was developed. The model utilizes wave functions in large configuration spaces for both protons and neutrons in the initial, intermediate and final nuclei and there is no need for a closure approximation.

The study of the DCX process is especially interesting for the medium-heavy nuclei, for which numerous data exist and therefore this case provides one more subtle test of the theory. Another point is the observation of the *resonance-like* behaviour around the pion energy $T_\pi = 50$ MeV. In contrast to the experimental observations microscopic treatments did not predict a rise of cross sections in this energy domain. Only recently Schepkin proposed a non-nucleon (dibaryon) mechanism [26,27] as a partial explanation of such a behaviour of low-energy cross sections. I am going to show that there is a chance to shed some light on this intriguing behaviour in the framework of an ordinary two-nucleon mechanism.

2. DOUBLE CHARGE EXCHANGE PROCESS

2.1. Brief Description of Chosen Charge Exchange Operators. The formalism of the charge exchange process for the low energy pions was applied to the DCX reactions on calcium [22], germanium [25] and tellurium [23] targets. I shall brifly recapitulate the main features of the theory, however in a more general form than in previous papers.

Within the simplest local πNN interaction Lagrangian known as pseudoscalar coupling, one can construct in the nonrelativistic approximation the effective pion-nucleon Hamiltonian [23,29]

$$h_p(\mathbf{q}) = -\sqrt{2}\, i \frac{f}{m_\pi} \Psi_N^\dagger \boldsymbol{\sigma} \cdot \mathbf{q}\, e^{i\mathbf{q}\cdot\mathbf{x}} \tau_+ \Psi_N , \tag{1}$$

which generates the p-wave pion-nucleon interaction only. In eq. (1) $\boldsymbol{\sigma}$ and τ_+ are Pauli and isospin raising operators, respectively. $\Psi_N^\dagger (\Psi_N)$ are nucleon creation (annihilation) field operators and the momentum transfer is taken to be $\mathbf{q}$.

A possible *s*-wave contribution to the πNN interaction is obtained from phenomenological considerations taking into account a composite meson exchange mechanism [23,29,30]. It has the form

$$h_s(\mathbf{q}) = 4\pi \frac{\lambda_1}{m_\pi} \sqrt{2}\, \Psi_N^\dagger \omega_q \tau_+ \Psi_N \,. \tag{2}$$

In both Hamiltonians the plane wave approximation for pion wave functions was used. The constants f and λ_1 are determined to reproduce the experimental data for nucleon-nucleon and nucleon-pion elastic scattering [29,30]. Of course, in the case of bound nucleons they can, in general, be modified and fitted separately in each DCX reaction of interest. For the purpose of preserving the important features of the model and because of the approximations used in the construction of the charge exchange operators, we will apply these constants with experimentally determined values $f/4\pi = 0.08$ and $\lambda_1 = 0.046$ (Ref. 30 and refs. cited there).

The second quantization procedure applied to the nucleon field allows one to express the interaction Hamiltonians in terms of creation and annihilation operators for the protons ($c_p^\dagger$, c_p) and neutrons ($c_n^\dagger$, c_n) as:

$$h_p(\mathbf{q}) = -\sqrt{2}\, i \frac{f}{m_\pi} \sum_{pn} \left[\int d^3x \psi_p^*(\mathbf{x}) \boldsymbol{\sigma}\cdot\mathbf{q}\, e^{i\mathbf{q}\cdot x}\, \psi(\mathbf{x}) \right] c_p^\dagger c_n \tag{3}$$

and

$$h_s(\mathbf{q}) = 4\pi \frac{\lambda_1}{m_\pi} \sqrt{2}\, \omega_q \sum_{pn} \left[\int d^3x \psi_p(\mathbf{x})^* \psi(\mathbf{x}) \right] c_p^\dagger c_n \,. \tag{4}$$

Here $\psi_a(\mathbf{x})$ is the solution of Schrödinger equation for any average nuclear potential, e.g., harmonic oscillator or Woods — Saxon with $a = p$ or n for protons and neutrons, respectively.

2.2 Transformation to Quasiparticles. Because of the quasiparticle character of the RPA, which we will use to describe the structure of the nuclei involved in the charge changing process one needs to transform expressions (3) and (4) to the Bogoliubov — Valatin quasiprotons ($a_p^\dagger$,a_p) and quasineutrons ($b_n^\dagger$, b_n)

$$a_{pm_p}^\dagger = u_p\, c_{pm_p}^\dagger + v_p\, (-1)^{j_p + m_p} c_{p-m_p} \,, \quad a_{pm_p} = (a_{pm_p}^\dagger)^\dagger, \tag{5}$$

$$b_{nm_n}^\dagger = u_n\, c_{nm_n}^\dagger + v^p\, (-1)^{j_n + m_n} c_{n-m_m} \,, \quad b_{nm_n} = (b_{nm_n}^\dagger)^\dagger, \tag{6}$$

u and v coefficients are related in a well-known way $u_{p(n)}^2 + v_{p(n)}^2 = 1$. After transformations (5)—(6) are performed, the p- and s-wave Hamiltonians have the form:

$$h_p(\mathbf{q}) = -\sqrt{2}\, i \frac{f}{m_\pi} \sum_{pn,\, JM} \mathcal{F}^{JM}_{pn}(\mathbf{q})\, \mathcal{R}^{JM}_{pn}, \tag{7}$$

$$h_s(\mathbf{q}) = -4\pi \frac{\lambda_1}{m_\pi} \sqrt{2}\, \omega_q \sum_{pn} (2j_p + 1)^{1/2}\, \delta_{pn}\, \mathcal{R}^{00}_{pn}. \tag{8}$$

In both eqs. (7) and (8) the transition density operator $\mathcal{R}^{JM}_{pn}$ is given by a formula

$$\mathcal{R}^{JM}_{pn} = u_p v_n C^\dagger(pnJM) + v_p u_n \tilde{C}(pnJM) + u_p u_n D(pnJM) - v_p v_n \tilde{D}^\dagger(pnJM). \tag{9}$$

The proton-neutron pair creation and annihilation operators and additional one-body type operators needed in the construction of operator (9) are defined in the usual way,

$$C^\dagger(pnJM) = \sum_{m_p, m_n} (j_p m_p j_n m_n \mid JM)\, a^\dagger_{pm_p} b^\dagger_{nm_n}, \tag{10}$$

$$C(pnJM) = [C^\dagger(pnJM)]^\dagger, \quad \tilde{C}(pnJM) = (-1)^{J+M} C(pnJ - M), \tag{11}$$

$$D^\dagger(pnJM) = \sum_{m_p m_n} (j_p m_p j_n m_n \mid JM) a^\dagger_{pm_p} (-1)^{j_n + m_n} b_{nm_n}, \tag{12}$$

$$D(pnJM) = [D^\dagger(pnJM)]^\dagger, \quad \tilde{D}(pnJM) = (-1)^{J+M} D(pnJ - M). \tag{13}$$

In eq. (7) we follow Ref. 23 for a definition of the function $\mathcal{F}^{JM}_{pn}$,

$$\mathcal{F}^{JM}_{pn}(\mathbf{q}) = \sum_{(m)} (-1)^{j_n - m_n} (j_p m_p j_n - m_n \mid JM) \left[\int d^3x \psi^*_p(\mathbf{x})\, \boldsymbol{\sigma}\cdot\mathbf{q} e^{i\mathbf{q}\cdot\mathbf{x}} \psi_n(\mathbf{x}) \right]. \tag{14}$$

After some algebra the function $\mathcal{F}^{JM}_{pn}$ can be written in a more compact form

$$\mathcal{F}^{JM}_{pn}(\mathbf{q}) = \sqrt{4\pi}\, \sqrt{6}\, Y^*_{JM}(\Omega_q) G^J_{pn}(q) \tag{15}$$

by setting apart the form factor G^J_{pn}:

$$G^J_{pn}(q) = (-1)^{j_p + j_n} \hat{j}_p \hat{l}_p \hat{j}_p \hat{l}_n \sum_{l''=0} (-1)^{\frac{l_p + l_n - l''}{2}} (l_p 0 l_n 0 \mid l''0)(J010 \mid l''0) \times$$
$$\times R^{l''}_{pn}(q) \begin{Bmatrix} \frac{1}{2} & l_p & j_p \\ \frac{1}{2} & l_n & j_n \\ 1 & l'' & J \end{Bmatrix}. \tag{16}$$

In the above equation the symbol { } is the 9*j*-symbol (Fano) and (1) represents a Clebsh — Gordan coefficient. Further, Y_{JM} denotes the spherical harmonic depending on the solid angle Ω_q. The coefficient $\sqrt{6}$ in eq. (15) comes from the reduced matrix element of the nuclear spin operator $\boldsymbol{\sigma}$. We also used the abbreviation $\hat{j} = \sqrt{2j+1}$ and the corresponding expression for $\hat{l}$. In eq. (16) we introduced the overlap integral $R^{l''}_{pn}$ between radial nuclear wave functions and the radial part of the plane wave pion,

$$R^{l''}_{pn}(q) - \int_0^\infty dr\, r^2 j_{l''}(qr)\, R_{n\,l}{}_{p\,p}(r)\, R_{n\,l}{}_{n\,n}(r). \tag{17}$$

Its explicit form depends on the choice of radial nucleon wave functions $R_{n\,l}{}_{p\,p}$ and $R_{n\,l}{}_{n\,n}$. In the case of harmonic-oscillator wave functions one can find a very compact analytical expression for this integral [23].

3. QRPA MODEL FOR THE DCX REACTION

3.1. DCX Amplitude and Intermediate Excited States. In second order perturbation theory the DCX transition amplitude is given as [23,25,37]

$$F_{if}(\mathbf{k}, \mathbf{k}') =$$

$$= \sum_{mm'} \frac{\langle f, 0^+; \pi^-(\mathbf{k}') \mid \hat{O} \mid mJM \rangle \langle mJM \mid \overline{m'JM} \rangle^* \langle \overline{m'JM} \mid \hat{O} \mid i(\text{G.S.}); \pi^+(\mathbf{k}) \rangle}{D(E_i, E^J_m, E^J_{m'}, \mathbf{q})}. \tag{18}$$

In the above equation $|\, i(\text{G.S.}), \pi^+(\mathbf{k})\rangle$ denotes the ground state of the initial nucleus (A, Z) and an incoming positive pion with momentum $\mathbf{k}$ and the initial energy $(k^2 + m_\pi^2)^{1/2}$. In analogy, $|f, \pi^-(\mathbf{k}')\rangle$ stands for an arbitrary state (ground or excited) of the final nucleus $(A, Z+2)$ and an outgoing negative pion with momenta $\mathbf{k}'$·$\mathbf{q}$ means the momentum transfer. Note that in expression (18) we have assumed that the charge operators are nonrelativistic Hamiltonians (3) and (4). It should be stressed that the denominator in eq. (18) differs in each case of the interaction (3) or (4). The Hamiltonian (3) represents a contribution of pion absorption on nuclear pair. From the general rules the Hamiltonian is known to be a small part of pair absorption at low energies. But in the DCX reaction it can play more important role [55]. The denominator in this case has a simple form $E_i + \omega_k - (E^J_m + E^J_{m'})/2$. The double scattering of a pion by two nucleons within sequential mechanism is caused

by the interaction (4). Of course, the denominator for this channel has no explicit form and one can calculate the nuclear matrix elements of the charge changing operator including the propagator of the intermediate neutral pion. Integration over intermediate pion momentum is understood.

The DCX amplitude (18) contains all terms coming from two different sets of the intermediate states $\{|mJM\rangle\}$ and $\{|\overline{m'JM}\rangle\}$ generated within the proton-neutron quasiparticle random phase approximation (pn — QRPA). In principle, the two sets obtained by QRPA on the initial and on the final nucleus are identical and describe the excited states of the same intermediate nucleus $(A, Z+1)$. But, since both calculations are not exact solutions of the many-body problem, they lead to slightly different solutions $\{|mJM\rangle\}$ and $\{|\overline{m'JM}\rangle\}$ for the intermediate wave functions.

$$|\, mJM\,\rangle = Q^{m\,\dagger}_{JM}\,|\, RPA;\,(A,Z)\rangle \equiv$$

$$\equiv \sum_{(pn)} \left[X^{m}_{(pn)J}\, C^{\dagger}(pnJM) - Y^{m}_{(pn)J}\, \tilde{C}(pnJM) \right] |i;\,(\mathrm{G.S.})\rangle, \tag{19}$$

$$|\,\overline{m'JM}\,\rangle = \overline{Q}^{m'\,\dagger}_{JM}\,|\, RPA;\,(A,Z+2)\rangle \equiv$$

$$\equiv \sum_{(pn)} \left[\overline{X}^{m'}_{(pn)J}\, C^{\dagger}(pnJM) - \overline{Y}^{m'}_{pn)J}\, \tilde{C}(pnJM) \right] |f;\,(\mathrm{G.S.})\rangle. \tag{20}$$

Here $X(\overline{X})$ and $Y(\overline{Y})$ are forward- and backward-going amplitudes, respectively. p and n stand for proton and neutron quasiparticle states (compare eqs. (5) and (6)). As we pointed out states (19) and (20) are mathematically nonequivalent. In particular, the intermediate states belonging to different sets are not orthogonal and this is a reason for involving their overlaps $\langle\, mJ_m\,|\,\overline{m'J_{m'}}\,\rangle$ into sum (18). Some authors applied a similar procedure in double beta decay calculations [35,36]. We also used this scheme in our previous description of the DCX processes on calcium, germanium and tellurium isotopes [22,23,25].

In eq. (18) E_i is the initial energy of the parent (target) nucleus. Usually one can also adopt the average QRPA excitation energies $(E^{J}_{m} + E^{J}_{m'})/2$ in the denominator according to the above-mentioned procedure of accounting for the nonequivalence of the two sets of intermediate states. It is worth emphasizing the fact that the amplitude (18) does not contain the usual closure approximation in which one takes, instead of a sum over states in the odd-odd mass nucleus with their individual energies, some average energy equivalent for all states. In our calculations we use explicitly the intermediate QRPA states,

their structure and the corresponding excitation energies in the denominator of eq. (18). In this respect we are able to find individual contributions coming from the different multipolarities J^π and to estimate the importance of the analogue and nonanalogue routes in the DCX reaction.

3.2. Excited States of the Daughter Nucleus. In Refs. 22 and 23 one can find expressions for the DCX amplitude in the case of ground and analogue state transitions. There are no principal difficulties to obtain more general formulae for transitions to any state of the final $(A, Z+2)$ nucleus. Analogously to what was done above (eqs. (19) and (20)), one can generate such states by the following *Anzatz*:

$$|\nu \mathcal{J}\mathcal{M}\rangle = \overline{Q}^{\nu\dagger}_{\mathcal{J}\mathcal{M}} |RPA; A+2)\rangle \equiv$$

$$\equiv \left\{ \sum_{(pp')} \left[\overline{X}^{\nu}_{pp')\mathcal{J}} A^\dagger(pp'\mathcal{J}\mathcal{M}) - \overline{\mathcal{Y}}^{\nu}_{(pp')\mathcal{J}} \tilde{A}(pp')\mathcal{J}\mathcal{M}) \right] + \right.$$

$$\left. + \sum_{(nn')} \left[\overline{X}^{\nu}_{(nn')\mathcal{J}} B^\dagger(nn'\mathcal{J}\mathcal{M}) - \overline{\mathcal{Y}}^{\nu}_{(nn')\mathcal{J}} \tilde{B}(nn'\mathcal{J}\mathcal{M}) \right] \right\} |f; \text{G.S.}\rangle. \qquad (21)$$

The creation and annihilation pair operators for protons $A^\dagger$, A and neutrons $B^\dagger$, B are defined in full analogy with eq. (10). $\overline{X}^{\nu}$ and $\overline{\mathcal{Y}}^{\nu}$ stand for forward- and backward-going amplitudes. They, as well as other amplitudes, X, Y, $\overline{X}$, $\overline{Y}$, are determined by solving the appropriate QRPA equation of motion for the states in the initial, the intermediate and the final nucleus. Details of the structure of the QRPA equations and their solutions can be found in Refs. 22 and 23.

3.3. Matrix Elements and DCX Cross Section. Using the above expressions for Hamiltonians (3) and (4) and definitions of the intermediate (eqs. (19)—(20)) and final (eq. (21)) states, one can find the following formulae for matrix elements needed to write amplitude (18) in an explicit form:

— matrix element for the s-wave charge changing operator contributing to the transition between the intermediate state $|m'J^\pi M\rangle$ in the nucleus $(A, Z+1)$ and the final state $|\nu \mathcal{J}\mathcal{M}\rangle$ of the daughter nucleus $(A, A+2)$

$$\langle \nu \mathcal{J}\mathcal{M}; \pi^-(\mathbf{k}') | h_s | \overline{m'J^\pi M} \rangle = 4\pi \frac{\lambda_s}{m_\pi} \sqrt{2}\, \omega_k{}' \delta_{J\mathcal{J}} \delta_{M\mathcal{M}} \times$$

$$\times \sum_{p \le p',\, n''} (-1)^{j_p + j_{n''}} \left[\left(\overline{X}^{\nu}_{(pp')\mathcal{J}} \overline{X}^{m'}_{(p'n'')J}\, \overline{u}_p\, \overline{u}_{n''} - \overline{\mathcal{Y}}^{\nu}_{(pp')\mathcal{J}} \overline{Y}^{m'}_{(p'n'')J}\, \overline{v}_p\, \overline{v}_{n''} \right) \delta_{pn''} + \right.$$

$$\left. + (-1)^J \left(\overline{X}^{\nu}_{(pp')\mathcal{J}} \overline{X}^{m'}_{(pn'')J}\, \overline{u}_{p'}\, \overline{u}_{n''} - \overline{\mathcal{Y}}^{\nu}_{(pp')\mathcal{J}} \overline{Y}^{m'}_{(pn'')J}\, \overline{v}_{p'}\, \overline{v}_{n''} \right) \delta_{p'n''} \right]; \qquad (22)$$

— matrix element for the p-wave charge changing operator contributing to the transition between the intermediate state $|\, m'J^{\pi}M\,\rangle$ and the final state $|\, \nu\mathcal{J}\mathcal{M}\rangle$

$$\langle\, \nu\mathcal{J}\mathcal{M};\, \pi^{-}(\mathbf{k}') \,|\, h_p \,|\, \overline{m'J^{\pi}M}\,\rangle =$$

$$= i\frac{f}{m_{\pi}}\sqrt{4\pi}\sqrt{12}\sum_{p\le p',n'',J'M''}\hat{J}\hat{J}''(JMJ''M''\,|\,\mathcal{J}\mathcal{M})\,(-\mathrm{i})^{j_p+j_{p''}+J+J''}\,Y^{*}_{J''}(\Omega_{k'})\times$$

$$\times\left[\begin{Bmatrix} j_{n''} & j_{p'} & J \\ \mathcal{J} & J'' & j_p \end{Bmatrix} G^{J''}_{pn''}(k')\left(\overline{\mathcal{X}}^{\nu}_{(pp')\mathcal{J}}\overline{X}^{m'}_{(p'n'')J}\overline{u}_p\,\overline{u}_{n''} - \overline{\mathcal{Y}}^{\nu}_{(pp')\mathcal{J}}\overline{Y}^{m'}_{(p'n'')J}\overline{v}_p\,\overline{v}_{n''}\right)+\right.$$

$$\left.+(-1)^{\mathcal{J}}\begin{Bmatrix} j_{n''} & j_p & J \\ \mathcal{J} & J'' & j_{p'} \end{Bmatrix} G^{J''}_{p'n''}(k')\left(\overline{\mathcal{X}}^{\nu}_{(pp')\mathcal{J}}\overline{X}^{m'}_{(pn'')J}\overline{u}_{p'}\,\overline{u}_{n''} - \overline{\mathcal{Y}}^{\nu}_{(pp')\mathcal{J}}\overline{Y}^{m'}_{(pn'')J}\overline{v}_{p'}\,\overline{v}_{n''}\right)\right]. \quad (23)$$

Formulae (22)—(23) are written only for proton-proton quasiparticle excitations in the final nucleus. In the complete expressions one has to add analogous terms for neutron-neutron excitations.

Further, we also need two other matrix elements:

— matrix element for the *s*-wave charge changing operator contributing to the transition between the ground state $|\, i;\,(\mathrm{G.S.})\rangle$ of the parent nucleus and the intermediate states $|\, mJ^{\pi}M\,\rangle$

$$\langle\, mJ^{\pi}M \,|\, h_s \,|\, i;\,(\mathrm{G.S.});\,\pi^{+}(\mathbf{k})\rangle =$$

$$= \sqrt{2}\left(4\pi\frac{\lambda_s}{m_{\pi}}\right)\omega_k\delta_{J0}\delta_{M0}\left[\sum_{pn}\delta_{pn}\left(X^{m}_{(pn)J}\,u_p v_n + Y^{m}_{(pn)J}\,v_p u_n\right)\right]; \quad (24)$$

— matrix element for the *p*-wave charge changing operator contributing to the transition between the initial ground state $|\, i;\,(\mathrm{G.S.})\rangle$ of the parent nucleus and the intermediate states $|\, mJ^{\pi}M\,\rangle$

$$\langle\, mJ^{\pi}M \,|\, h_{sp} \,|\, i;\,(\mathrm{G.S.});\,\pi^{+}(\mathbf{k})\rangle =$$

$$= i\sqrt{12}\frac{f}{m_{\pi}}\sqrt{4\pi}\,(-1)^{J}\,Y^{*}_{JM}(\Omega_k)\left[\sum_{pn}G^{J}_{pn}(k)\left(X^{m}_{(pn)J}\,u_p v_n + Y^{m}_{(pn)J}\,v_p u_n\right)\right]. \quad (25)$$

Expressions and definitions (18), (22)—(25) allow one to write down the explicit formula for the DCX amplitudes in the most general case of the transition to any final state $|\, \nu\mathcal{J}\mathcal{M}\rangle$,

$$F_J^s(\mathbf{k},\mathbf{k}') = -\delta_{J\mathcal{J}}\left(4\pi\frac{\lambda_s}{m_\pi}\right)^2 \omega_k\,\omega_{k'} \sum_{m,m'} \frac{\langle mJ^\pi | \overline{m'J^\pi}\rangle}{D(E_i, E_m^J, E_{m'}^J, \mathbf{q})} \times$$

$$\times\left\{\sqrt{2}\sum_{n'',\,p\le p'}(-1)^{j_p+j_{n''}}\left[\left(\overline{X}^{\nu}_{(pp')\mathcal{J}}\overline{X}^{m'}_{(p'n'')J}\,\bar{u}_p\bar{u}_{n''} - \overline{\mathcal{Y}}^{\nu}_{pp'\mathcal{J}}\overline{Y}^{m}_{(p'n''J}\,\bar{v}_p\bar{v}_{b''}\right)\delta_{pn''} + \right.\right.$$

$$+(-1)^J\left(\overline{X}^{\nu}_{(pp')\mathcal{J}}\overline{X}^{m'}_{(pn'')J}\,\bar{u}_{p'}\bar{u}_{n''} - \overline{\mathcal{Y}}^{\nu}_{(pp')\mathcal{J}}\overline{Y}^{m}_{(pn'')}\,\bar{v}_{p'}\bar{v}_{n''}\right)\delta_{p'n''}\Big] +$$

$$\left.\left.+\sum_{p'',\,n\le n'}\left[\begin{pmatrix} p\to n \\ p'\to n' \\ n''\to p'' \end{pmatrix}\right]\right\}\left[\sqrt{2}\,\delta_{J0}\sum_{pn}\hat{j}\,\delta_{pn}\left(X^m_{(pn)J}u_pv_n - Y^m_{(pn)J}v_pu_n\right)\right]. \qquad (26)$$

$$F_J^p(\mathbf{k},\mathbf{k}') = -\left(\frac{f}{m_\pi}\right)^2 \sum_{m,m'} \frac{\langle mJ^\pi | \overline{m'J^\pi}\rangle}{E_i + \omega_k - \dfrac{E_m^J + E_{m'}^J}{2}} \times$$

$$\times \sum_{J''\mathcal{M}} \hat{J}\hat{J}''(-1)^{\mathcal{J}+\mathcal{M}}\{Y_{J''}(\omega_{k'})\otimes Y_{J''}(\Omega_k)\}_{J\mathcal{M}}\left\{\sqrt{12}\sum_{p\le p',\,n''}(-1)^{j_p+j_{p''}}\times\right.$$

$$\times\left[\begin{Bmatrix} j_{n''} & j_{p'} & J \\ \mathcal{J} & J'' & j_p \end{Bmatrix} G^{J''}_{pn''}(k')\left(\overline{X}^{\nu}_{(pp')\mathcal{J}}\overline{X}^{m'}_{(p'n'')J}\bar{u}_p\,\bar{u}_{n''} - \overline{\mathcal{Y}}^{\nu}_{(pp')\mathcal{J}}\overline{Y}^{m'}_{(p'n'')J}\,\bar{v}_p\,\bar{v}_{n''}\right)+\right.$$

$$+(-1)^{\mathcal{J}}\begin{Bmatrix} j_{n''} & j_p & J \\ \mathcal{J} & J'' & j_{p'} \end{Bmatrix} G^{J''}_{p'n''}(k')\left(\overline{X}^{\nu}_{(pp')\mathcal{J}}\overline{X}^{m'}_{(pn'')J}\bar{u}_{p'}\,\bar{u}_{n''} - \overline{\mathcal{Y}}^{\nu}_{(pp')\mathcal{J}}\overline{Y}^{m'}_{(pn'')J}\,\bar{v}_{p'}\,\bar{v}_{n''}\right)\Big] +$$

$$\left.+\sqrt{12}\sum_{p'',\,n\le n'}\left[\begin{pmatrix} p\to n \\ p'\to n' \\ n''\to p'' \end{pmatrix}\right]\right\}\left[\sqrt{12}\sum_{pn} G^J_{(pn)J}\left(X^{m'}_{(pn)J}u_pv_n - Y^{m'}_{(pn)J}v_pu_n\right)\right]. \qquad (27)$$

The full amplitude $F_{if}(\mathbf{k},\mathbf{k}')$ is taken to be a sum of all multipolarities allowed for each part of the charge changing operator. Selection rule steming from angular momentum and parity conservation laws limits the transition caused by *s*-wave operator (4) only to 0^+ intermediate states, whereas *p*-wave operator (3) has nonzero contributions for all the so-called pion-like intermediate states (0^-, 1^+, 2^-, 3^+...). The differential cross section is normalized in such a way that

$$\frac{d\sigma}{d\Omega}(\theta, q) = \left|\frac{1}{4\pi}\sum_{J^\pi}\left[F_J^s(\mathbf{k},\mathbf{k}') + F_J^p(\mathbf{k},\mathbf{k}')\right]\right|^2, \qquad (28)$$

where $\mathbf{q} = \mathbf{k} - \mathbf{k}'$ is the momentum transfer in the DCX process.

As is mentioned above we used throughout the paper the nonrelativistic approximation for the charge changing operator. In general, the relativistic corrections can influence the differential cross section (28). One can expect a negligible role of such terms for the p-wave part of the transition amplitude and a larger contribution to the s-part. The plane wave approximation for pions used in this paper can also be a source of inaccuracies for the cross section. I shall not treat the pion distortions in this paper.

3.4. Ground State DCX Transition. Formulae (26) and (27) represent general expression for the amplitude of the DCX transition into any final state of a daughter nucleus. The DCX transition to the ground state can be simplified to the amplitude [23,27]:

$$F^{s}_{\mathrm{GS}}(\mathbf{k}, \mathbf{k}') = \left(4\pi \frac{\lambda_s}{m_\pi}\right)^2 \omega_k \, \omega_{k'} \sum_{mm'} \frac{\langle m0^+ \mid \overline{m'0^+} \rangle}{D(E_i, E^0_m, E^0_{m'}, \mathbf{q})} \times$$

$$\times \left\{ \left[2\sqrt{2} \sum_{pn} \delta(p, n) \hat{j}_p \left(\bar{X}^{m'}_{(pn)0} \bar{v}_p \bar{u}_n - \bar{Y}^{m'}_{(pn)0} \bar{u}_p \bar{v}_n \right) \right] \times \right.$$

$$\left. \times \left[2\sqrt{2} \sum_{pn} \left(X^{m}_{(pn)0} u_p v_n - Y^{m}_{(pn)0} v_p u_n \right) \right] \right\}. \tag{29}$$

$$F^{p}_{\mathrm{GS}}(\mathbf{k}, \mathbf{k}') = -\left(\frac{f}{m_\pi}\right)^2 \sum_{mm', J} \frac{\langle mJM \mid \overline{m'JM} \rangle}{E_i + \omega_k - \dfrac{E^J_m + E^J_{m'}}{2}} P_J(\cos \theta_{kk'}) \times$$

$$\times \left\{ \left[\sqrt{12} \sum_{pn} (-1)^{j_p + j_n + J} G^{J}_{pn}(k') \left(\bar{X}^{m'}_{(pn)J} \bar{v}_p \bar{u}_n - \bar{Y}^{m'}_{(pn)J} \bar{u}_p \bar{v}_n \right) \right] \times \right.$$

$$\left. \times \left[\sqrt{12} \sum_{pn} G^{J}_{(pn)J}(k) \left(X^{m}_{(pn)J} u_p v_n - Y^{m}_{(pn)J} v_p u_n \right) \right] \right\}. \tag{30}$$

All symbols in the two last equations have been used already. The only new quantity $P_J(\cos \theta_{kk'})$ is Legendre polynomial coming from the reduction of the tensor product of spherical harmonics in eq. (27). We also used the abbreviation $\delta(p, n) = \delta_{\substack{n\,n \\ p\,n}} \delta_{\substack{j\,j \\ p\,n}} \delta_{\substack{l\,l \\ p\,n}}$.

We would like to note that the s-wave part of the transition operator contains only the route in which the neutron occupying some nuclear particle state with defined quantum numbers n, l, j is changed into the proton with exactly the same quantum numbers. These transitions excite the isobaric

analogue state (IAS), if they are coherently superimposed. However, because of the pairing correlations the situation is more complicated and one obtains appreciable transitions through other 0^+ states. In the theory developed here we are able to separate both types of contributions using a method of identification of the IAS transition which, in general, represents the strongest 0^+-transition [23]. We already stressed that the *p*-wave part of the charge changing operator gives a contribution to the DCX amplitude only for the *pion-like* intermediate states and thus causes nonanalogue routes which are sensitive to short-range nucleon-nucleon correlations.

4. EXAMPLE OF THE DCX REACTION ON ^{56}Fe

4.1. Details of the Calculations. As an example of application of the theory I shall discuss the ground transition in iron: $^{25}\mathrm{Fe} \rightarrow {}^{56}\mathrm{Ni}$. This reaction was already studied in the eighties [38,39], but the data base is still very sparse for nonanalogue transitions. For the pion energy of 50 MeV three experimental points of the angular distribution have been measured at PSI for the ground to ground transition as well as to several individual predominantly 0^+ excited states of ^{56}Ni [38]. Some preliminary data also exist at pion energies $T_\pi = 35$ and 61 MeV. Although the data for the ground to ground transition is very limited, one already can conclude the following: The transition exhibits a well pronounced resonance-like behaviour. This means that the cross section at $T_\pi = 50$ MeV is for forward angles by one order of magnitude or more larger than at other energies.

The results presented below are achieved with a model space consisting of $0p_{1/2}$, $0p_{3/2}$, $1s_{1/2}$, $0d_{3/2}$, $0d_{5/2}$, $1p_{1/2}$, $1p_{3/2}$, $0f_{5/2}$ and $0f_{7/2}$. The single particle states used here are calculated with a Coulomb-corrected Woods — Saxon potential. It was assumed that both types of nucleons — protons and neutrons — occupy the same shells and calcium ^{40}Ca was taken as the inactive core. Two-body matrix elements needed for construction of the QRPA matrices were obtained from the realistic nuclear matter *G*-matrix by solving the Bethe — Goldstone equation (see, e.g., Refs. 40 and 41 for more details)

$$G(\omega) = V + \frac{Q}{\omega - H_0} G(\omega) . \tag{31}$$

In the above equation Q is the Pauli projection operator, ω stands for the starting energy and V is taken to be the nucleon-nucleon realistic one-meson exchange Bonn potential [42—44]. H_0 is the unperturbed single particle

Hamiltonian. In the present work we used the harmonic oscillator Hamiltonian. To take into account the effects of the finite nucleus we solve eq. (31) with as small absolute value of the starting energy as -25.0 MeV. This corresponds to an average single particle energy of -12.5 MeV. The oscillator length used is $b = 2.0$ fm.

The two-body matrix elements are obtained for nuclear matter. They are not specialized for a given nucleus. Thus and due to the finite Hilbert space used one has to renormalize them by multiplying with factors slightly different from 1.0: g^n_{pair}, g^p_{pair}, g^{pn}_{pp} and g^{pn}_{ph}. For the ground states of the parent and daughter nuclei one obtains uncorrelated vacuum states by solving the standard BCS equation in the above-mentioned model space. Two renormalization factors g^n_{pair} and g^p_{pair} multiplying the proton and neutron pairing matrix elements $<(aa)0|G|(bb)0>$ are fixed by adjusting the empirical pairing gaps Δ^p_a and Δ^n_a to the lowest quasiparticle energy obtained from the gap equation

$$\Delta^{p(n)}_a = \frac{1}{2} g^{p(n)}_{\text{pair}} \hat{j}_a^{-1} \sum_b \hat{j}_b \Delta_b \left[(\varepsilon_b - \lambda_{p(n)})^2 + \Delta_b^2\right]^{-1/2} <(aa)0|G|(bb)0> . \quad (32)$$

The empirical pairing gaps are deduced according to the recently published prescription of Moeller and Nix [45,46]:

$$\Delta^{\text{even–even}}_{\text{neutron}} = -\frac{1}{8}\left[M(Z,N+2) - 4M(Z,N+1) + 6M(Z,N) - \right.$$

$$\left. - 4M(Z,N-1) + M(Z,N-2)\right] , \quad (33)$$

$$\Delta^{\text{even–even}}_{\text{proton}} = -\frac{1}{8}\left[M(Z+2,N) - 4M(Z+1,N) + 6M(Z,N) - \right.$$

$$\left. - 4M(Z-1,N) + M(Z-2,N)\right] . \quad (34)$$

Expressions (33) and (34) cannot be used for nuclei with a magic number of protons or neutrons. Thus the pairing gap and the corresponding pairing strengths are estimated using the adjacent even-even nucleus. The table contains values of the pairing strengths g^n_{pair} and g^p_{pair} fitted in this way for ^{56}Fe and ^{56}Ni. All the renormalization factors are close to unity. Thus the bare G-matrix elements of the Bonn potential are already reasonably good.

Solutions of the BCS equations with matrix elements fixed in this manner allow one to evaluate the occupation amplitudes u's and v's needed for construction of the QRPA equation of motion. To determine the QRPA matrices fully one must also fix two additional renormalization factors, the strength of the particle-particle g^{pn}_{pp} and the strength of the particle-hole g^{pn}_{ph} interaction. For

Table. Experimental neutron and proton gaps for ^{56}Fe, ^{54}Fe and ^{58}Ni nuclei obtained from eqs. (33) and (34). The last two nuclei are used to estimate the strengths in nickel ^{56}Ni because of its double-magic character. (see text for details). Masses are taken from the mass tables [54]. The pairing strengths g^n_{pair} and g^p_{pair} were fixed to reproduce the experimental gaps

Nucleus	Δ^n_{exp}, MeV	Δ^p_{exp}, Mev	g^n_{pair}	g^p_{pair}
^{56}Fe	1.360	1.570	0.938	0.993
^{54}Fe	—	1.520	—	0.908
^{58}Ni	1.300	—	1.030	—

this purpose we used the isobaric state (IAS) and the Gamow-Teller state in cobalt ^{56}Co which are known to be 3.65 and 10.60 MeV, respectively [47,48]. The QRPA energy of these states depends predominantly on the particle-hole strength and adjustment of them to experimental energies gives $g^{pn}_{ph} = 0.8$. Details of such a procedure are given in Ref. 23. The second factor g^{pn}_{pp} will be treated as a free parameter of the theory and we will discuss all reaction observables as a function of it.

4.2. Results and Discussion. We calculated angular distributions and the energy dependence of the cross section for the DCX ground-ground transitions on ^{56}Fe. Figure 1 shows the angular distribution for the incident pion energy $T_\pi = 50$ MeV. Three curves are presented for three different values of the particle-particle strength g^{pn}_{pp}: 0.8, 1.0 and 1.1. The experimental points are measured at the Paul Scherer Institute by the Tübingen — Karlsruhe group [38]. The angular distribution decreases rapidly as the particle-particle parameter increases. This behaviour is observed in a full range of the g^{pn}_{pp} strength up to the value 1.1. for which the QRPA solution tends to a collapse. A similar behaviour was also observed in other nuclei [22,23,25] and other processes, e.g., the double-beta decay [35,36]. The mechanism for the collapse is connected with increase of the ground-state correlations by enlarging the particle-particle interaction. As a result, the lowest excited QRPA state is pushed down in energy below the ground state. Simultaneously the cross sections drop by factors of 3—10 depending on the scattering angle. The cross section is reduced since increasing g^{pn}_{pp} produces stronger the ground-state correlations. This enlarges the backward-going amplitudes Y's. The terms with Y's in eqs. (29), (30) become large enough to cancel against the terms with the forward-going

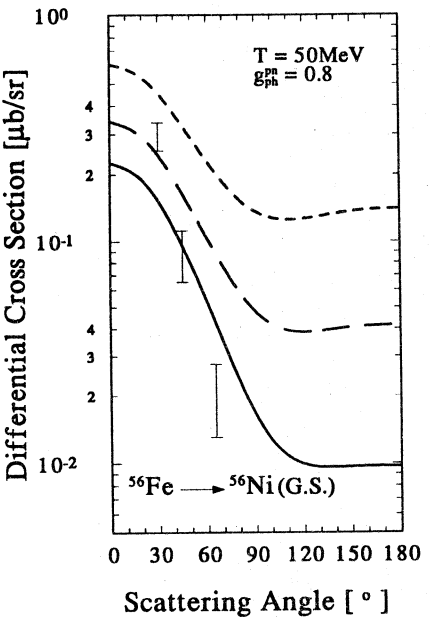

Fig. 1. Angular distribution for the ground state transition on iron ^{56}Fe. The particle-hole strength g_{ph}^{pn} is fixed to reproduce the Gamow — Teller and isobaric analogue state difference in ^{56}Ni. The results for three values of the particle-particle strength are shown: $g_{pp}^{pn} = 0.8$ (short-dashed line), $g_{pp}^{pn} = 1.0$ (long-dashed line) and $g_{pp}^{pn} = 1.1$ (soled line). The experimental data are taken from refs. 38 and 53

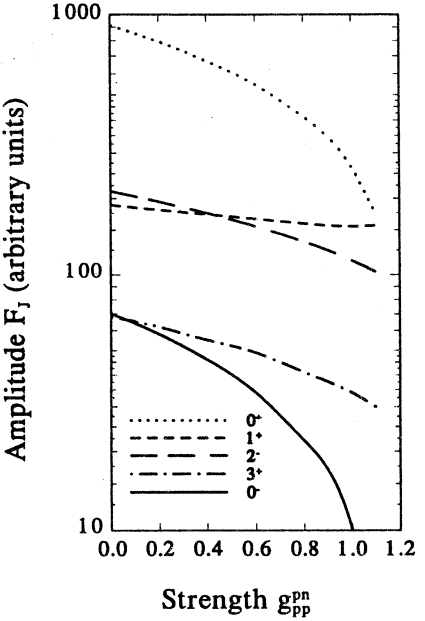

Fig. 2. The most important contributions to the transition amplitude come from the intermediate 0^+ (dotted line), 0^- (solid line), 1^+ (short-dashed line), 2^- (long-dashed line), and 3^+ (dashed-dotted line) states. The results for the pion energy $T_\pi = 50$ MeV are plotted as a function of the particle-particle strength g_{pp}^{pn}. The particle-hole strength is fixed to be 0.8

amplitudes X's. The magnitude of the DCX cross section rapidly diminishes. Comparison of the experimental results and theoretical predictions (fig.1) shows that the physically important domain of g_{pp}^{pn} is the interval 1.0—1.1.

It is interesting to compare the importance of contributions to the total amplitude coming from the different angular momenta. Such contributions for the forward-angle DCX amplitude and for the intermediate states $J^\pi = 0^+, 0^-, 1^+, 2^-$ and 3^+ which are most important, are presented in fig.2. One can notice immediately that a crucial role in pushing the contributions down

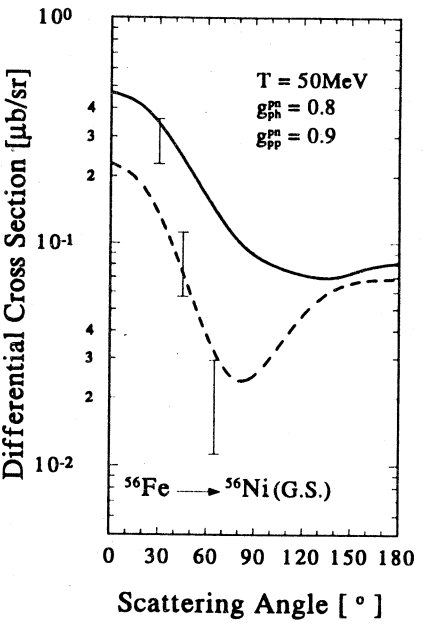

Fig. 3. Angular distributions for two choices of the model space are presented for fixed interaction strengths ($g_{ph}^{pn} = 0.8$, $g_{pp}^{pn} = 0.9$) and the incident pion energy $T_\pi = 50$ MeV. The solid line represents the results of a smaller and the dashed line of a very large model space. The experimental values are from Refs. 38 and 53. (For details see text.)

into agreement with the data is played by the dependence of each partial amplitude on the particle-particle strength g_{pp}^{pn}. The transition through 0^+ states with the biggest contribution from the IAS dominates the total amplitude at law g_{pp}^{pn}. But in the physically interesting interval $g_{pp}^{pn} \geq 1.0$ this amplitude is comparable with the 1^+ and 2^- amplitudes. Thus, all approaches restricted to the intermediate isobaric analogue state are not a good description of the cross sections and other DCX observables because nonanalogue routes play as an important role as transitions through 0^+ states.

We also examine in this paper the influence of the model space on the final results. Additional calculations of angular distributions at the pion energy $T_\pi =$ $= 50$ MeV were performed for a «huge» single particle basis consisting of the states $0s_{1/2}$, $0p_{1/2}$, $0p_{3/2}$, $0d_{3/2}$, $0d_{5/2}$, $1p_{1/2}$, $1p_{3/2}$, $0f_{5/2}$, $0f_{7/2}$, $2s_{1/2}$, $1d_{3/2}$, $1d_{5/2}$, $0g_{7/2}$, $0g_{9/2}$, $2p_{1/2}$, $2p_{3/2}$, $1f_{5/2}$, $1f_{7/2}$, $0h_{11/2}$, $3s_{1/2}$, $2d_{3/2}$, $2d_{5/2}$, $1g_{7/2}$, $1g_{9/2}$ for neutrons and $0s_{1/2}$, $0p_{1/2}$, $0p_{3/2}$, $1s_{1/2}$, $0d_{3/2}$, $0d_{5/2}$, $1p_{1/2}$, $1p_{3/2}$, $0f_{5/2}$, $0f_{7/2}$, $2s_{1/2}$, $1d_{3/2}$, $1d_{5/2}$, $0g_{7/2}$, $0g_{9/2}$, $2p_{1/2}$, $2p_{3/2}$, $1f_{7/2}$ for protons. All these single particle levels are below 5.0 MeV in Woods — Saxon potential and are either bound or quasi-bound. Figure 3 presents the angular distribution for this two choices of the size of the basis for the particle-particle strength $g_{pp}^{pn} = 0.9$. A change of the shape of the angular distribution by increasing the basis is clearly seen. A minimum around the scattering angle $\theta = 70^\circ$ appears, which is also in the agreement with Gibbs' prediction [38]. Compared with the «small» basis, the angular distribution with the large basis is steeper. Absolute values of the

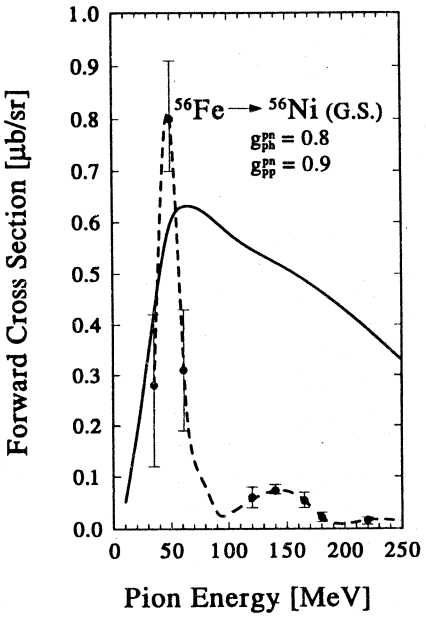

Fig. 4. Energy dependence of the forward-angle (5°) cross section for the ground state transition on iron ^{56}Fe (solid line). The results are obtained for the small basis. Data indicated by error bars are taken from Refs. 38 and 39 (the drawn short-dashed curve is only to guide the eye)

cross section are 2—5 times smaller for the same particle-particle strength g_{pp}^{pn}. This means one obtains agreement with the experiment for smaller values of the particle-particle strength. In this stage of the theory we are not able to separate two effects which influence the lowering of the cross section, i.e., particle-particle correlations manifested by the magnitude of g_{pp}^{pn} and participation of core nucleons in the DCX process (in the «huge» basis all nucleons are involved).

Recently measured ground-ground transition ^{56}Fe on at pion energies $T_\pi = 35$ and 61 MeV [38] together with the earlier data at higher energies from LAMPF [39] allow to systematize the dependence of the DCX cross sections. The experimental observations shown in fig.4 exhibit a resonance-like structure near $T_\pi \approx 50$ MeV.

In a contrast to such an observed behaviour almost all of the theoretical models with a distorted wave as well as with plane wave approximations are not able to predict even roughly this strong energy dependence for the DCX forward-angle cross section. The microscopic calculations give a rather smooth energy behaviour around $T_\pi = 50$ MeV except the predictions of Martemyanow and Schepkin [26,27] who have introduced dibayron resonance «by hand» to explain this dependence. These authors proposed a very narrow dibayron resonance formed in the DCX whose decay into two nucleons is not allowed by selection rules. The condition for building this dibaryon is a large overlap of a pair of nucleons (neutron-neutron or proton-proton) in their relative s-wave with $J^\pi = 0^+$ and $T = 1$. This resonance can appear according to refs. 26 and 27 at distances less than 1 fm between nucleons. Taking the estimation of G.Miller for the 6-quark bag probability to be of the order of a few per cent for all nucleon pairs in a nucleus [49], Martemyanow and Schepkin obtained an energy

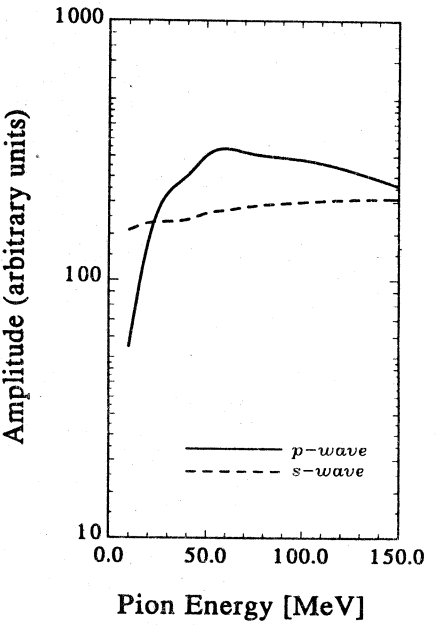

Fig. 5. Energy dependence of the analogue (dashed line) and non-analogue (full line) contributions to the ground state transition amplitude for the scattering angle $\theta = 5°$. The interactions strengths g_{ph}^{pn} and g_{pp}^{pn} are taken to be 0.8 and 1.1, respectively

dependence for the dibaryon mechanism in the double charge exchange reaction which roughly follows the observed behaviour. All such frameworks together with calculations made by Chiang and Zou [50] can be treated as an indication of the importance of quarks in the DCX process.

Presented approach, different in spirit, can also give the gross features of the energy dependence of the DCX. The calculated forward (5°) cross section is shown in fig.4 as a function of the pion energy up to the resonance region*. One can notice that we are able to explain qualitatively within our mechanism the observed experimental behaviour. The curve is not so steep on the high energy side above 60 MeV, but a peak around $T_\pi = 60$ MeV is clearly seen. It is rather obvious that we should look for some effects to reduce the DCX amplitude in the higher energy domain.

A more careful analysis of both *s*- and *p*-wave contributions to the total amplitude at two energies, say 10 and 50 MeV, and at forward angles may supply possible such a mechanism [51]. In fig.5 the dependence of the analogue and nonanalogue amplitude on the incident pion energy is shown. The *s*-wave contribution is almost constant in full domain of the pion energy. A dramatic increase of the nonanalogue amplitude (*p*-wave contribution) is seen up to the energy $T_\pi = 60$ MeV. So this component produces the maximum in the cross section. Because the nonanalogue route (*p*-wave component) depends sensitively on g_{pp}^{pn} [13,14,23] the strong dependence of the amplitude suggests

*Generalization of the model for the Δ-isobar degrees of freedom is possible [37], but we do not intend to discuss such a point in this paper.

that particle-particle correlations are of growing importance as one takes more energetic pions. After maximum is reached both components, *s*- and *p*-wave stay equally important. One clearly needs some additional mechanism for the reduction if the experimental data have to be reproduced. Such a possibility is offered by improving the *s*-wave charge changing operator by taking its relativistic form.

It is worth noting, that Karapiperis and Kobayashi [16] can roughly predict the decrease of the ^{14}C cross section between 50 and 100 MeV. Unfortunately cited calculations were not performed for pion energies lower than 50 MeV. Also Gibbs and co-workers proposed a resonance phenomenon in the pion scattering, which could be seen even more clearly in DCX around the proper energy $T_\pi = 50$ MeV [52]. These approaches — including presented here — point out a possibility of explaining the observed resonance-like behaviour without invoking nonstandard mechanisms. The existing data does not yet discriminate clearly between conventional and more exotic interpretations.

5. FINAL REMARKS

I have investigated the double charge exchange reaction in the framework of the quasi-particle random phase approximation (QRPA). The charge exchange operator was taken in the nonrelativistic form and the plane wave approximation was used for the incident, intermediate and outgoing pions.The approach was applied to the ground state transition on iron ^{56}Fe. The predicted values underestimate the forward-angle cross section and thus the calculated angular distribution is flatter than in the experiment.

Amplitudes and cross sections show smooth dependence on the value of the particle-particle strength g_{pp}^{pn}, which was also observed in earlier calculations of the DCX reaction on calcium [22], germanium [25] and tellurium [23]. A comparison with data allows one to state the physically important values of the strength g_{pp}^{pn} for iron and nickel nuclei lay in the interval 1.0—1.1. One should stress that the choice of the model space influences the calculated quantities. Because of this effect the g_{pp}^{pn} strength is not unique. As larger the basis as smaller is the particle-particle strength. Moreover, in the larger model space we observed a collapse of the QRPA solution for the g_{pp}^{pn} value as small as 0.9 which may suggest a need for inclusion of higher RPA-corrections into the model.

The gross features of the resonance-like shape of the cross section as a function of the pion energy can be reproduced at least semiquantitatively within

the conventional $2N$ mechanism. The prediction is not too good, probably due to approximations made. It has to be seen in the future if the very speculative idea of a dibaryon resonance in the DCX reaction will prevail. Future development of the approach will make it possible to settle more carefully the questions addressed in this talk.

The last but not the least, a sensitivity of the pionic DCX processes to nuclear structure and especially to nucleon-nucleon correlations makes them interesting for the double beta decay. In searches for physics beyond the standard model the last reaction has continually received much attention. Grand unified theories predict the neutrinoless double beta decay if the neutrino is a Majorana particle with rest mass and/or the week right-handed currents exist. Combining both phenomena (DCX and double beta decay) ensures reliable nuclear matrix elements and thus an accurately defined estimate of the nonstandard physics parameters, like the average light neutrino mass, the right-handed week current admixtures and the heavy neutrino mass.

ACKNOWLEDGEMENTS

The author is grateful to all who have contributed to this work. I thankfully acknowledge Profs. Amand Faessler and Heinz Clement for fruitful discussions and suggestions. This work was supported in part by Komitet Badan Naukowych (the State Committee for Scientific Research), Grant No.2 0347 91.01.

REFERENCES

1. **Seth K.K., Nann H., Iversen S., Kaletka M., Hird J.** — Phys. Rev. Lett., 1978, 41, p.1589.
2. **Nann N., Seth K., Iversen S.G., Kaletka M.D., Kaletka D.B., Barlow D.B., Smith D.** — Phys. Lett., 1980, 96B, p.261.
3. **Seth K.K., Iversen S., Nann H., Kaletka M.D., Hird J., Thiessen H.A.** — Phys. Rev. Lett., 1979, 43, p.1574; ibid 1980, 45, p.147.
4. **Gilman R., Fortune H.T., Bland L.C., Kiziah R.R., Moore C.F., Seidel P.A., Morris C.L., Cottingame W.B.** — Phys. Rev., 1984, C30, p.958.
5. **Seidel P.A., Kiziah R.R., Brown M.K., Moore C.F., Morris C.L., Baer H., Greene S.J., Burleson G.R., Cottingame W.B., Bland C.L., Gilman R., Fortune H.T.** — Phys. Rev. Lett., 1983, 50, p.1106.
6. **Baer H.W., Burman R.L., Leitch M.J., Morris C.L., Wright D.W., Rokni S.H., Comfort J.R.** — Phys. Rev., 1988, C37, p.902.
7. **Mordechai S., Auerbach N., Burlein M., Fortune H.T., Greene S.J., Moore C.F., Morris C.L., O'Donnell J.M., Rawoool M.W., Silk J.D., Watson D.L., Yoo S.H., Zumbro J.D.** — Phys. Rev. Lett., 1988, 61, p.531.

8. **Mordechai S., Fortune H.T., O'Donnell J.M., Liu G., Burlein M., Wuosmaa A.H., Greene S., Morris C.L., Auerbach N., Yoo S.H., More C.F.** — Phys. Rev., 1990, C 41 , p.202.
9. **Sperinde J., Fredrickson D., Hinkins R., Perez-Mendez V., Smith B.** — Phys. Lett., 1970, 32B, p.185.
10. **Ungar J.E., McKeown R.D., Geesman D.F., Holt R.J., Specht J.R., Stephenson K.E., Zeidman B., Morris C.L.** — Phys. Lett., 1984, 144B, p.333.
11. **Clement H.** — Prog. Pat. Nucl. Phys., 1992, 29, p.175.
12. **Oset E., Strottman D., Brown G.E.** — Phys. Lett., 1978, 73B, p.393.
13. **Bleszynski E., Bleszynski M., Glauber R.J.** — Phys. Rev. Lett., 1988, 60, p.1483.
14. **Auerbach A., Gibbs W.R., Ginocchio J.N., Kaufmann W.B.** — Phys. Rev., 1988, C 38, p.1277.
15. **Karapiperis T., Kobayashi M.** — Phys. Rev. Lett., 1985, 54, p.1230.
16. **Karapiperis T., Kobayashi M.** — Ann. Phys. (N.Y.), 1987, 177, p.1.
17. **Seth K.K.** — Nucl. Phys., 1988, A478, p.591c.
18. **Johnson M.B., Siciliano E.R., Saraffin H.** — Phys. Lett., 1990, 243B, p.18.
19. **Gibbs W.R., Kaufmann W.B., Siegel P.B.** — In: Proc. LAMPF Workshop on Pion Double Charge Exchange, Los Alamos, edited by H.W.Baer and M.J.Leich, Los Alamos National Laboratory Report No. LA-010550-C, 1985, p.90.
20. **Siciliano S.E., Johnson M.B., Saraffin H.** — Ann. Phys. (N.Y.), 1990, 203, p.1.
21. **Ginocchio J.N.** — Phys. Rev., 1989, C40, p.2168.
22. **Kaminski W.A., Faessler A.** — Phys. Lett., 1990, 244B, p.155.
23. **Kaminski W.A., Faessler A.** — Nucl. Phys., 1991, A529, p.605.
24. **Vergados J.D.** — Phys. Rev., 1991, C44, p.276.
25. **Kaminski W.A., Faessler A.** — J. Phys. G (Nucl. Part. Phys.), 1991, 17, p.1665.
26. **Martemyanov B.V., Schepkin M.G.** — JETP Lett., 1991, 53, p.776.
27. **Bilger R., Broermann B., Clement H., Emmrich R., Fohl K., Heitlinger K., Joram C., Kluge W., Moll M., Reule D., Schepkin M., Wagner G.J., Wieser R., Abela R., Foroughi F., Renker D.** — In: Proc. International Nuclear Physics Conference, Wiesbaden, 1992;
Bilger R., Clement H., Fohl K., Heitlinger K., Joram C., Kluge W., Schepkin M., Wagner G.J., Wieser R., Abela R., Foroughi F., Renker D. — Z. f. Phys. A (short notes), to be published.
28. **Civitarese O., Faessler A., Kaminski W.A.** — J. Phys. G. (Nucl. Part. Phys.), 1991, 17, p.1407.
29. **Erickson T., Weise W.** — Pions and Nuclei (Clarendon, Oxford, 1988).
30. **Koltun D.S., Reitan A.** — Phys. Rev., 1966, 141, p.141.
31. **Serot D., Walecka J.D.** — Adv. Phys., 1986, 16, p.1.
32. **Blunden P.G., McCorquodale P.** — Phys. Rev., 1988, C38, p.1861.
33. **Hong Jung, Beck F., Miller G.A.** — Phys. Rev. Lett., 1989, 62, p.2357.
34. **Marcos S., Lopez-Quelle M., van Gizi N.** — Phys. Lett., 1991, 257B, p.5.
35. **Civitarese O., Faessler A., Tomoda T.** — Phys. Lett., 1987, 194B, p.11.
36. **Muto K., Klapdor H.V.** — Phys. Lett., 1988, 201B, p.420.
37. **Kaminski W.A.** — Double Charge Exchange Reaction with Low-Energy Pions, Maria Curie-Sklodowska Univesrity Press, Lublin, 1991, (in Polish).

38. **Bilger R., Barnett B.M., Clement H., Krell S., Wagner G.J., Jaki J., Joram C., Kirchner T., Kluge W., Metzler M., Wieser R., Renker D.** — Phys. Lett., 1991, 269B, p.247.
39. **Seidl P.A. et al.** — Phys. Rev., 1990, C42, p.1929 and cited here.
40. **deShalit A., Feschbach H.** — Theoretical Nuclear Physics, vol.1, John Wiley&Sons, New York, 1974.
41. **Mahaux C., Weidenmüller H.A.** — Ann. Rev. Part. Phys., 1979, 29, p.1.
42. **Holinde K.** — Phys. Rep., 1981, 68, p.121.
43. **Machleidt R., Holinde K., Elster C.** — Phys. Rep., 1987, 149, p.1.
44. **Machleidt R.** — Adv. Nucl. Phys., 1989, 19, p.189.
45. **Madland D.G., Nix J.R.** — Nucl. Phys., 1988, A476, p.1.
46. **Moeller P., Nix J.R.** — Nucl. Phys., 1992, A 536, p.20.
47. **Becchetti F.D., Dehnhard D., Dzubay T.G.** — Nucl. Phys., 1971, A168, p.151, **Caldwell T., Nathan O., Hansen O., Bork H.** — Nucl. Phys., 1973, A202, p.225.
48. **Nuclear Data Sheets,** 1986, 48, p.251 and refs. cited here.
49. **Miller G.A.** — Phys. Rev., 1984, B53, p.2008.
50. **Chiang H.-C., Zou B.-S.** — Nucl. Phys., 1989, A 496, p.739.
51. **Kaminski W.A., Chocyk D.,** to be published.
52. **Gibbs W.R., Kauffmann W.B., Dedondez J.P.** — Phys. Lett., 1989, 231B, p.6.
53. **Clement H.,** private communication.
54. **Wapstra A.H., Audi G.** — Nucl. Phys., 1985, A432, p.1.
55. **Koltun D.S., Singham M.K.** — Phys. Rev., 1989, C 39, p.704.

«ФИЗИКА ЭЛЕМЕНТАРНЫХ ЧАСТИЦ И АТОМНОГО ЯДРА»
1995, ТОМ 26, ВЫП. 2

УДК 539.16

О СМЕШИВАНИИ ВОЛНОВЫХ ФУНКЦИЙ ОСНОВНЫХ И ВРАЩАТЕЛЬНЫХ СОСТОЯНИЙ ПОЛОС ДЕФОРМИРОВАННЫХ ЯДЕР
Часть 1

Б.С.Джелепов
С.-Петербургский государственный университет,
Радиевый институт им.В.Г.Хлопина, Санкт-Петербург
Н.Н.Жуковский
Радиевый институт им.В.Г.Хлопина, Санкт-Петербург
С.А.Шестопалова
ВНИИ метрологии им.Д.М.Менделеева, Санкт-Петербург

Рассмотрено смешивание волновых функций во вращательных состояниях деформированных ядер. Представлены амплитуды волновых функций для 254 вращательных полос, рассчитанные различными авторами. В дальнейшем предполагается провести обсуждение и сравнение собранной информации с экспериментальными данными.

The mixing of the wave functions in rotational bands of deformed nuclei has been considered. Wave function amplitudes for 254 rotational bands calculated by different authors were collected. The collected information will be compared with the experimental data and discussed in the subsequent paper.

ВВЕДЕНИЕ

Если у какого-нибудь ядра имеются два уровня с одинаковыми квантовыми характеристиками J^{π}, то в волновых функциях этих уровней содержатся примеси: в волновой функции первого уровня содержится примесь второго, а в волновой функции второго уровня — примесь первого. Эти примеси приводят как бы к взаимодействию уровней — к их отталкиванию друг от друга.

Смешивание волновых функций также влияет на вероятности β- и γ-переходов между ядерными состояниями; от деталей смешивания зависят правила Алаги, широко применяемые при конструировании схем распада радиоактивных нуклидов, расчетах отношений матричных элементов переходов и т.п.

Для того чтобы рассчитать вероятности переходов, нужно знать волновые функции состояний, между которыми они происходят, и операторы, вызывающие переходы.

Уровень знания о волновых функциях пока не высок. Приходится искать приближенные выражения — создавать ядерные модели. Начиная с 1953 г. для описания свойств деформированных ядер теоретики пользуются почти исключительно моделью Нильссона, в которую вводят различные уточнения и дополнения. Мы не ставим задачу оценки целесообразности этих уточнений.

В предлагаемом обзоре представлена коллекция результатов расчетов амплитуд (главной и максимальной примесной) смешивания волновых функций для трех нижних уровней ротационных полос нечетных деформированных ядер с $A = 151 \div 187$ по всем вариантам нильссоновской модели. Мы не критикуем ни одну работу; взаимную критику нужно искать в оригинальных расчетных работах. Мы не исключили ни одного результата, кроме первичных авторских оценок, уточненных в последующих работах тех же авторов. Всем расчетам мы придавали одинаковый вес.

Приступая к составлению коллекции мы были готовы к тому, что результаты, полученные авторами в разных вариантах модели Нильссона, будут сильно отличаться друг от друга. К нашему удивлению, этого не произошло (этот вопрос будет рассмотрен в будущей публикации). Мы имеем дело с достаточно «компактным» материалом.

Здесь делаются две попытки.

1. Выявить группу (или группы) ядер, в которых можно либо пренебречь смешиванием волновых функций, либо ограничиться введением такой малой расчетной поправки, которая почти не сказывается на вероятностях β- и γ-переходов.

2. Выявить группы ядер, в которых смешивание волновых функций в каких-то уровнях очень сильное; обычно оно связано с близким расположением уровней с одинаковыми J^π. Эти случаи требуют пересмотра правил Алаги и ревизии всех расчетов, которые используют значения квантового числа K; в ряде случаев это равносильно требованию пересмотра схем распада.

РЕЗУЛЬТАТЫ РАСЧЕТОВ СМЕШИВАНИЯ ВОЛНОВЫХ ФУНКЦИЙ СОСТОЯНИЙ НЕЧЕТНЫХ ДЕФОРМИРОВАННЫХ ЯДЕР С $A = 151 \div 187$

К началу 1994 г. в области атомных масс $A = 151 \div 189$ было идентифицировано 220 ядер с нечетными A (табл. Ледерера и NDS до 1 января 1994 г.). Для многих из этих ядер известны только периоды полураспада и энергии нескольких γ-линий, но неизвестны J^π и неясно, деформированы ли

эти ядра или нет. Расчеты смешивания для таких ядер не производились. Расчеты начинаются, когда выяснены квантовые характеристики JK^{π} нескольких уровней. Объединение их во вращательные полосы и приписка им нильссоновских характеристик $JK^{\pi}[Nn_{Z}\Lambda]$ обычно предшествуют расчетам смешивания.

К настоящему времени нам известны 44 нечетных деформированных ядра с $A = 151 \div 187$, в которых расчеты смешивания выполнены для 254 полос [1—38]. Результаты расчетов амплитуд главного и максимального примесного компонентов волновых функций для трех самых нижних уровней вращательных полос представлены в таблице. Обозначения в таблице следующие: J^{π} — квантовая характеристика уровня, $K^{\pi}[Nn_{Z}\Lambda]$ — нильссоновские характеристики, E^{*}— энергия, $a_{\text{гл}}$ — амплитуда главного компонента волновой функции (совпадающего с $K^{\pi}[Nn_{Z}\Lambda]$), $a_{\text{Мпр}}$ — амплитуда максимальной примеси (эта примесь может иметь любое $K < J$), характеристика $R = |a_{\text{Мпр}}/a_{\text{гл}}|$.

Из таблицы можно сделать следующий вывод: расчеты показали, что волновые функции ядерных уровней являются многокомпонентными с весьма различными соотношениями амплитуд.

Около 14% уровней имеют вторую по величине амплитуду меньше 5% от главной амплитуды; в конкурирующих β- и γ-переходах между такими уровнями можно ожидать хорошего соблюдения правил Алаги. С другой стороны, у 35% уровней вторая по величине амплитуда составляет более 30% от главной амплитуды; разброс в определениях этих больших примесных амплитуд пока очень велик.

Для того, чтобы при анализе отношений матричных элементов конкурирующих β- или γ-переходов можно было бы правильно учесть смешивание, необходимо значительно улучшить информацию о нем: либо уточнить расчеты амплитуд, либо найти закономерности в их появлении; в большинстве случаев очень большие амплитуды — это либо сингулярное кориолисово смешивание, либо ошибки в схемах распада.

Детальный анализ уровней смешивания R предполагается сделать в будущей публикации.

Авторы опасаются, что они имеют не все расчеты амплитуд, которые могли быть напечатаны в изданиях с малыми тиражами, в институтских сборниках и т.п. Авторы были бы рады получить эти расчеты, чтобы учесть их в дальнейших обсуждениях. Сообщения просим присылать по адресу: Россия 196233, С.-Петербург, пр.Космонавтов, 92, кв.76, С.А.Шестопаловой.

Таблица. Амплитуды $a_{гл}$ и $a_{Мпр}$ и характеристики R для трех нижних уровней вращательных полос нечетных деформированных ядер с $A = 151–183$

Номер полосы	$K^{\pi}[Nn_Z\Lambda]$	[ссылка]	J^{π}	E^*, кэВ	$a_{гл}$	$a_{Мпр}$	$100 \cdot R$
			^{151}Sm				
1	$3/2^-$ [532]	[1]	$3/2^-$	4,8	0,989	0,096	9,71
			$5/2^-$	0,0	0,792	0,595	75,1
			$7/2^-$	65,8	0,733	0,569	77,6
2	$3/2^-$ [521]		$3/2^-$	104,8	0,855	0,448	50,6
			$5/2^-$	69,7	0,777	0,590	75,9
			$7/2^-$	209,0	0,783	0,449	57,3
3	$1/2^-$ [530]		$1/2^-$	285,0	0,999	0,047	4,70
			$3/2^-$	315,3	0,883	–0,457	51,7
			$5/2^-$	302,6	0,789	–0,565	71,6
4	$1/2^+$ [400]		$1/2^+$	502,3	0,862	0,507	58,8
			$3/2^+$	521,2	0,949	0,242	25,5
			$5/2^+$	632,1	0,920	0,296	32,2
5	$1/2^+$ [600]		$1/2^+$	355,7	0,862	–0,507	58,8
			$3/2^+$	663,1	0,940	0,263	28,0
			$5/2^+$	1167,8	0,796	0,566	71,4
6	$3/2^+$ [402]		$3/2^+$	306,8	0,853	–0,475	55,7
			$5/2^+$	395,6	0,966	0,241	24,9
			$7/2^+$	514,0	0,951	0,293	30,8
7	$3/2^+$ [651]		$3/2^+$	345,0	0,844	0,496	58,8
			$5/2^+$	445,7	0,677	–0,543	66,5
			$7/2^+$	524,0	0,819	0,500	61,0
			^{153}Eu				
8	$5/2^-$ [532]	[2]	$5/2^-$	97,4	0,987	0,156	15,8
			$7/2^-$	151,6	0,957	0,230	24,0
			$9/2^-$	235,3	0,927	0,282	30,4
9	$3/2^-$ [411]		$3/2^+$	103,2	0,999	0,036	3,60
			$5/2^+$	172,9	0,993	0,077	7,75
			$7/2^+$	269,7	0,989	–0,090	9,10
10	$5/2^+$ [413]		$5/2^+$	0	0,997	0,064	6,42
			$7/2^+$	83,4	0,983	0,147	14,9
			$9/2^+$	193,0	0,967	0,210	21,7

Номер полосы	$K^{\pi}[Nn_Z\Lambda]$	[ссылка]	J^{π}	E^*, кэВ	$a_{гл}$	$a_{Мпр}$	$100{\cdot}R$
				^{155}Eu			
11	5/ 2⁻ [532]	[2]	5/ 2⁻	104,3	0,991	0,134	13,5
			7/ 2⁻	169,0	0,968	0,198	20,4
			9/ 2⁻	254,7	0,945	0,246	26,0
12	3/ 2⁺ [411]		3/ 2⁺	245,8	0,999	0,038	3,80
			5/ 2⁺	307,4	0,996	0,073	7,33
			7/ 2⁺	391,5	0,993	0,078	7,85
13	5/ 2⁺ [413]		5/ 2⁺	0	0,998	0,046	4,61
			7/ 2⁺	78,6	0,993	0,071	7,15
			9/ 2⁺	179,2	0,988	0,101	10,2
				^{153}Gd			
14	3/ 2⁻ [532]	[3]	3/ 2⁻	129	0,994	–0,076	7,65
			5/ 2⁻	110	0,593	0,720	121,4
			7/ 2⁻	216	0,628	0,671	106,8
15	3/ 2⁻ [521]		3/ 2⁻	0	0,985	0,167	16,9
			5/ 2⁻	42	0,886	0,266	30,0
			7/ 2⁻	93	0,851	0,305	35,8
16	1/ 2⁻ [530]		1/ 2⁻	315	0,990	–0,136	13,7
			3/ 2⁻	362	0,939	0,288	30,7
			5/ 2⁻	449	0,870	–0,280	33,1
17	1/ 2⁻ [521]		1/ 2⁻	436	0,991	0,136	13,7
			3/ 2⁻	(496)	0,954	–0,284	29,8
			5/ 2⁻	549	0,916	0,257	28,1
18	1/ 2⁺ [400]		1/ 2⁺	328	1,000	0,001	0,10
			3/ 2⁺	412	0,992	–0,126	12,7
			5/ 2⁺	504	0,979	–0,203	20,7
19	1/ 2⁺ [660]		1/ 2⁺	484	1,000	–0,001	0,10
			5/ 2⁺	184	0,702	0,655	93,3
20	3/ 2⁺ [402]		3/ 2⁺	212	0,992	–0,126	12,7
			5/ 2⁺	304	0,979	0,203	20,7
			7/ 2⁺	491	0,966	0,257	26,6
21	3/ 2⁺ [651]		3/ 2⁺	316	0,934	0,359	38,4
			7/ 2⁺	290	0,759	0,565	74,4
				^{155}Gd			
22	5/ 2⁻ [523]	[4]	5/ 2⁻	321,36	0,812	0,577	71,1
			7/ 2⁻	393	0,738	0,661	89,6

Номер полосы	$K^{\pi}[Nn_Z\Lambda]$	[ссылка]	J^{π}	E^*, кэВ	$a_{гл}$	$a_{Мпр}$	$100{\cdot}R$
			$9/2^-$	485	0,684	0,706	103,2
23	$3/2^-$ [532]		$3/2^-$	287,004	0,995	0,086	8,64
			$5/2^-$	321,381	0,797	–0,577	72,4
			$7/2^-$		0,696	–0,648	93,1
24	$3/2^-$ [521]		$3/2^-$	0	0,997	0,081	8,64
			$5/2^-$	60,02	0,987	0,141	14,3
		[4]	$7/2^-$	146,07	0,971	0,207	21,3
25	$1/2^-$ [521]		$1/2^-$	559,29	0,998	0,066	6,61
			$3/2^-$	614,78	0,992	0,110	11,1
			$5/2^-$	658,97	0,982	0,160	16,3
26	$1/2^-$ [530]		$1/2^-$	423,2	0,998	–0,066	6,61
			$3/2^-$	450,60	0,987	–0,114	11,5
			$5/2^-$	488,64	0,962	–0,172	17,9
27	$1/2^+$ [400]	[5]	$1/2^+$	367,60	0,965	0,263	27,2
			$3/2^+$	427,21	0,992	0,114	11,5
			$5/2^+$	488,69	0,932	0,238	25,5
		[6]	$1/2^+$	367,60	0,952	0,306	32,1
			$3/2^+$	427,21	0,972	0,178	18,3
			$5/2^+$	488,69	0,878	–0,318	56,2
		[7]	$1/2^+$	367,60	–0,994	0,106	10,7
			$3/2^+$	427,21	–0,735	–0,664	90,3
			$5/2^+$	488,69	–0,998	–0,059	5,91
28	$1/2^+$ [660]	[5]	$1/2^+$	(371,6)	0,965	0,263	26,3
			$3/2^+$	(847,4)	0,982	0,144	14,7
			$5/2^+$	(604,1)	–0,831	–0,413	49,8
		[6]	$1/2^+$	(371,6)	0,952	–0,306	32,1
			$3/2^+$	(847,4)	0,974	0,642	65,9
			$5/2^+$	(604,1)	0,880	0,459	52,2
29	$3/2^+$ [402]	[7]	$3/2^+$	268,57	0,932	0,344	36,9
			$5/2^+$	326,04	–0,724	–0,604	83,4
			$7/2^+$	350,36	0,928	0,269	29,0
		[6]	$3/2^+$	268,57	0,838	–0,520	62,0
			$5/2^+$	326,04	0,688	0,435	63,2
			$7/2^+$	350,36	0,771	–0,525	68,1
30	$3/2^+$ [651]	[8]	$3/2^+$	105,308	0,974	0,211	21,7
			$5/2^+$	86,545	0,703	0,590	83,9

Номер полосы	$K^{\pi}[Nn_z\Lambda]$	[ссылка]	J^{π}	E^*, кэВ	$a_{гл}$	$a_{Мпр}$	$100{\cdot}R$
		[8]	$7/2^+$	117,990	0,682	0,693	101,6
		[7]	$3/2^+$	105,308	0,921	0,359	39,0
			$5/2^+$	86,545	0,807	0,423	52,4
			$7/2^+$	117,990	0,817	0,513	62,8
31	$5/2^+[642]$	[5]	$5/2^+$	266,648	–0,723	–0,639	88,4
			$7/2^+$	350,436	–0,488	–0,847	173,6
			$9/2^+$	446,1	–0,760	–0,524	68,9
		[7]	$5/2^+$	266,648	–0,867	0,476	54,9
			$7/2^+$	350,436	–0,832	0,412	49,5
			$9/2^+$	446,1	0,742	–0,654	88,1
		[8]	$5/2^+$	266,648	–0,777	0,367	47,2
			$7/2^+$	350,436	0,693	0,682	98,4
			$9/2^+$	446,1	0,515	0,676	131,3
				^{159}Gd			
32	$5/2^-[523]$	[10]	$5/2^-$	146,4	0,966	–0,258	26,7
			$7/2^-$	227,5	0,928	–0,366	39,4
			$9/2^-$	330	0,892	–0,437	49,0
33	$5/2^-[512]$		$5/2^-$	872,7	0,995	–0,102	10,25
			$7/2^-$	948,5	0,987	–0,160	16,2
			$9/2^-$	1044	0,976	–0,216	22,1
34	$3/2^-[521]$		$3/2^-$	0	1,000	–0,015	1,50
			$5/2^-$	50,7	0,960	0,260	27,1
			$7/2^-$	121,9	0,916	0,372	40,6
35	$1/2^-[521]$		$1/2^-$	507,7	1,000	0	0
			$3/2^-$	558,2	1,000	0,015	1,50
			$5/2^-$	589	1,000	0,025	2,50
				^{155}Tb			
36	$5/2^-[532]$	[2]	$5/2^-$	226,9	0,990	0,138	13,9
			$7/2^-$	250,0	0,851	0,494	58,0
			$9/2^-$	317,1	0,787	0,572	72,7
37	$3/2^+[411]$		$3/2^+$	0	0,998	0,054	5,41
			$5/2^+$	65,5	0,986	0,118	12,0
			$7/2^+$	155,8	0,975	0,175	17,9
38	$5/2^+[413]$		$5/2^+$	271,1	0,999	–0,034	3,40
			$7/2^+$	334,8	0,817	0,570	69,8
			$9/2^+$	452,6	0,785	0,608	77,4

Номер полосы	$K^{\pi}[Nn_z\Lambda]$	[ссылка]	J^{π}	E^*, кэВ	$a_{гл}$	$a_{Мпр}$	$100{\cdot}R$
			^{157}Tb				
39	7/ 2⁻ [523]	[9]	7/ 2⁻	571,7	0,890	–0,440	49,4
			9/ 2⁻	709,1	0,848	–0,489	57,7
			11/ 2⁻	868,6	0,827	–0,471	56,9
40	5/ 2⁻ [532]		5/ 2⁻	326,4	0,990	0,136	13,7
			7/ 2⁻	357,7	0,871	0,456	52,3
			9/ 2⁻	425,9	0,824	0,541	65,4
		[2]	5/ 2⁻	326,4	0,996	0,086	8,63
			7/ 2⁻	357,8	0,889	0,442	49,7
			9/ 2⁻	425,9	0,845	0,514	60,8
41	3/ 2⁺ [411]		3/ 2⁺	0	0,999	0,032	3,20
			5/ 2⁺	60,6	0,996	0,056	5,62
			7/ 2⁺	143,8	0,993	0,072	7,25
42	5/ 2⁺ [413]		5/ 2⁺	327,7	0,997	0,054	5,42
			7/ 2⁺	407,9	0,981	0,159	16,2
			9/ 2⁺	513,8	0,964	0,224	23,2
			^{155}Dy				
43	5/ 2⁻ [523]	[12]	5/ 2⁻	136,3	0,717	0,598	83,4
			7/ 2⁻	224,4	– 0,661	0,713	107,9
44	3/ 2⁻ [532]		3/ 2⁻	202	0,994	0,088	8,85
			5/ 2⁻	325	0,736	0,205	27,8
45	3/ 2⁻ [521]		3/ 2⁻	0	0,986	0,168	17,0
			5/ 2⁻	39,4	0,903	0,273	30,2
			7/ 2⁻	86,7	0,812	0,384	47,3
46	1/ 2⁻ [530]		1/ 2⁻	382	1,000	0	0,00
			3/ 2⁻	449	0,979	–0,165	16,8
			5/ 2⁻	(703)	0,941	–0,229	24,3
47	1/ 2⁺ [660]		1/ 2⁺	(320)	1,000	0	0,00
48	3/ 2⁺ [651]		3/ 2⁺	569	0,837	0,547	65,3
			^{157}Dy				
49	3/ 2⁻ [521]	[11]	3/ 2⁻	0	0,992	0,127	12,8
			5/ 2⁻	61,2	0,971	0,209	21,5
			7/ 2⁻	147,7	0,955	0,243	25,4
50	1/ 2⁺ [660]	[12]	1/ 2⁺	308	1,000	0	0,00
51	3/ 2⁺ [651]		3/ 2⁺	234,5	0,972	0,235	24,2
			5/ 2⁺	188,1	0,740	0,453	61,2

Номер полосы	$K^{\pi}[Nn_Z\Lambda]$	[ссылка]	J^{π}	E^*, кэВ	$a_{гл}$	$a_{Мпр}$	$100{\cdot}R$
		[12]	$7/2^+$	211,2	0,724	0,645	89,1
		11	$3/2^+$	234,5	0,819	0,537	65,6
			$5/2^+$	188,1	0,776	0,320	41,2
			$7/2^+$	211,2	0,745	0,627	84,2
			^{159}Dy				
52	$1/2^+$ [660]	[12]	$1/2^+$	(564)	1,000	0	0,00
53	$3/2^+$ [402]		$3/2^+$	(541)	0,995	0,096	9,65
54	$3/2^+$ [651]		$3/2^+$	618	0,986	0,163	16,5
55	$5/2^+$ [642]		$5/2^+$	177,6	0,954	0,290	30,4
			$7/2^+$	209,0	0,914	0,377	41,2
			$9/2^+$	239,6	0,847	0,463	54,7
			^{161}Dy				
56	$1/2^+$ [400]	[14]	$1/2^+$	774	0,726	0,688	94,8
57	$1/2^+$ [660]		$1/2^+$	608	0,726	–0,688	94,8
		[12]	$1/2^+$	608	1,000	0	0
58	$3/2^+$ [402]	[14]	$3/2^+$	551	0,948	–0,312	32,9
59	$3/2^+$ [651]		$3/2^+$	679	0,695	–0,568	81,7
		[12]	$3/2^+$	679	0,998	–0,060	6,01
60	$5/2^+$ [642]		$5/2^+$	0	0,990	0,118	11,9
			$7/2^+$	43,8	0,970	0,174	17,9
			$9/2^+$	100,4	0,945	0,224	23,7
		[8]	$5/2^+$	0	0,983	0,181	18,4
			$7/2^+$	43,8	0,950	0,255	26,8
			$9/2^+$	100,4	0,912	0,321	35,2
		[13]	$5/2^+$	0	0,983	–0,156	15,9
			$7/2^+$	43,8	0,958	–0,222	23,2
			$9/2^+$	100,4	0,926	–0,282	30,8
		[14]	$5/2^+$	0	0,989	0,147	14,9
			$7/2^+$	43,8	0,958	0,206	21,5
			$9/2^+$	100,4	0,919	0,268	29,2
			^{163}Dy				
61	$7/2^-$ [514]	[10]	$7/2^-$	1448	0,998	– 0,058	5,81
			$9/2^-$	1549	0,995	– 0,087	8,74
			$11/2^-$	(1673)	0,992	– 0,113	11,4
62	$5/2^-$ [523]		$5/2^-$	0	0,998	0,055	5,51
			$7/2^-$	73,44	0,994	0,084	8,45

Номер полосы	$K^{\pi}[Nn_Z\Lambda]$	[ссылка]	J^{π}	E^*, кэВ	$a_{гл}$	$a_{Мпр}$	$100{\cdot}R$
		[10]	$9/2^-$	167,34	0,990	0,108	10,9
		[16]	$5/2^-$	0	0,997	0,093	9,33
			$7/2^-$	73,44	0,992	0,089	8,97
			$9/2^-$	167,34	0,986	0,116	11,8
63	$5/2^-$ [512]	[10]	$5/2^-$	711,47	0,975	–0,221	22,7
			$7/2^-$	801,31	0,942	–0,332	35,2
			$9/2^-$	918,0	0,903	–0,424	47,0
		[16]	$5/2^-$	711,47	0,992	–0,126	12,7
			$7/2^-$	801,31	0,982	–0,179	18,2
			$9/2^-$	918,0	0,971	–0,227	23,4
64	$3/2^-$ [521]	[10]	$3/2^-$	421,84	0,927	0,374	40,3
			$5/2^-$	475,39	0,946	0,237	25,0
			$7/2^-$	553,02	0,852	0,416	48,8
		[16]	$3/2^-$	421,84	0,994	0,083	8,35
			$5/2^-$	475,39	0,917	0,369	40,2
			$7/2^-$	553,02	0,971	0,186	19,1
65	$3/2^-$ [512]	[10]	$3/2^-$	1795	0,999	–0,027	2,70
			$5/2^-$	1856	0,998	–0,044	4,41
			$7/2^-$	1936	0,997	–0,061	6,12
66	$1/2^-$ [521]	[10]	$1/2^-$	351,15	1,000	–0,014	1,40
			$3/2^-$	389,75	0,927	–0,374	40,3
			$5/2^-$	427,68	0,970	–0,232	23,9
		16	$1/2^-$	351,15	0,999	0,045	4,50
			$3/2^-$	389,75	0,993	–0,088	8,86
			$5/2^-$	427,68	0,919	–0,360	39,2
67	$1/2^-$ [510]	[10]	$1/2^-$	1159	1,000	0,014	1,40
			$3/2^-$	1199	0,999	0,028	2,80
			$5/2^-$	1262	0,999	0,038	3,80
		[16]	$1/2^-$	1159	0,951	0,308	32,9
			$3/2^-$	1199	0,963	0,263	27,3
			$5/2^-$	1262	0,858	0,508	59,2
68	$1/2^+$ [400]		$1/2^+$	737,6	0,787	0,617	78,4
			$3/2^+$	766,2	0,798	0,562	70,4
			$5/2^+$	915,7	0,672	–0,434	64,6
69	$1/2^+$ [660]		$1/2^+$	884,3	0,787	–0,617	2,16
			$3/2^+$	1084,2	0,696	–0,593	85,2

Номер полосы	$K^{\pi}[Nn_z\Lambda]$	[ссылка]	J^{π}	E^*, кэВ	$a_{гл}$	$a_{Мпр}$	$100{\cdot}R$
			$5/2^+$	781,1	0,780	0,510	65,4
70	$3/2^+[402]$		$3/2^+$	859,3	0,961	0,212	22,1
			$5/2^+$	949,3	0,867	–0,495	57,1
71	$3/2^+[651]$	[16]	$3/2^+$	935,1	0,770	–0,440	57,1
			$5/2^+$	1129	0,851	0,461	54,2
72	$5/2^+[642]$		$5/2^+$	250,9	0,990	0,134	13,5
			$7/2^+$	285,6	0,997	0,253	25,4
			$9/2^+$	336,5	0,907	0,343	37,8
				^{161}Ho			
73	$7/2^-[523]$	[17]	$7/2^-$	0	0,989	0,144	14,6
			$9/2^-$	99,63	0,972	0,210	21,6
			$11/2^-$	221,95	0,952	0,263	27,6
				^{159}Er			
74	$11/2^-[505]$		$11/2^-$	428,8	0,999	0,054	5,40
			$13/2^-$	(624)	0,997	0,079	7,92
			$15/2^-$	848	0,980	0,111	11,3
75	$7/2^-[514]$		$7/2^-$	566,7	0,921	–0,361	39,2
			$9/2^-$	(731)	0,679	–0,277	40,8
			$11/2^-$	(932)	0,774	–0,355	45,9
76	$5/2^-[523]$		$5/2^-$	220,2	0,985	0,124	12,6
			$7/2^-$	307,0	0,888	0,377	42,4
		[18]	$9/2^-$	(372)	0,820	0,442	53,9
77	$3/2^-[521]$		$3/2^-$	0	0,997	0,076	7,62
			$5/2^-$	59,2	0,982	0,119	12,1
			$7/2^-$	144,1	0,956	0,196	20,5
78	$1/2^+[400]$		$1/2^+$	(725)	1,000	–0,010	1,00
			$3/2^+$	(788)	0,998	–0,055	5,51
79	$3/2^+[402]$		$3/2^+$	348,1	0,998	0,055	5,51
			$5/2^+$	(439)	0,996	0,092	9,24
			$7/2^+$	(566)	0,993	0,121	12,2
80	$5/2^+[642]$		$5/2^+$	88,7	0,507	0,663	130,8
		[15]	$7/2^+$	120,2	0,697	0,658	94,4
			$9/2^+$	0	0,477	0,631	132,3
				^{161}Er			
81	$11/2^-[505]$	[18]	$11/2^-$	396,4	0,997	0,083	8,32
			$13/2^-$	578,5	0,993	0,122	12,3

Номер полосы	$K^{\pi}[Nn_z\Lambda]$	[ссылка]	J^{π}	E^*, кэВ	$a_{гл}$	$a_{Мпр}$	$100{\cdot}R$
			$15/2^-$	782,6	0,988	0,153	15,5
82	$5/2^-$ [523]		$5/2^-$	172,0	0,980	–0,161	16,4
			$7/2^-$	266,5	0,944	–0,247	26,2
			$9/2^-$	383,5	0,901	–0,329	36,5
83	$5/2^-$ [512]		$5/2^-$	843	0,996	–0,082	8,23
			$7/2^-$	(947)	0,719	0,502	69,8
			$9/2^-$	(1096)	0,811	–0,497	61,3
84	$3/2^-$ [532]	[18]	$3/2^-$	724,8	0,994	0,084	8,45
			$5/2^-$	(807)	0,981	0,115	11,7
			$7/2^-$	(910)	0,829	–0,470	56,7
85	$3/2^-$ [521]		$3/2^-$	0	0,998	0,063	6,31
			$5/2^-$	59,5	0,978	0,161	16,5
			$7/2^-$	143,9	0,950	0,247	26,0
86	$1/2^+$ [400]		$1/2^+$	481	1,000	–0,009	0,90
			$3/2^+$	(529)	0,974	–0,224	23,0
			$5/2^+$	(599)	0,936	–0,348	37,2
87	$1/2^+$ [660]	[18]	$1/2^+$	751,0	1,000	0,009	0,90
			$3/2^+$	1109,5	0,983	–0,186	18,9
		[19]	$1/2^+$	751,0	1,000	0	0
			$3/2^+$	1109,5	0,984	–0,178	18,1
88	$3/2^+$ [402]	[18]	$3/2^+$	463,2	0,974	0,224	23,0
			$5/2^+$	496,3	0,937	0,348	37,1
			$7/2^+$	590,0	0,913	0,389	42,6
89	$3/2^+$ [651]		$3/2^+$	391	0,983	0,186	18,9
		[19]	$3/2^+$	391	–0,984	–0,178	18,1
			$5/2^+$	447,6	0,601	0,588	97,8
			$7/2^+$	656,3	–0,767	0,546	71,2
90	$5/2^+$ [642]		$5/2^+$	193,4	–0,793	–0,561	70,7
			$7/2^+$	207,6	–0,806	–0,566	70,2
			$9/2^+$	567,1	–0,639	0,668	105,0
		[13]	$5/2^+$	193,4	0,824	–0,453	55,0
			$7/2^+$	207,6	0,815	–0,470	57,7
			$9/2^+$	567,1	0,674	–0,519	77,0
		[18]	$5/2^+$	193,4	0,824	–0,408	49,5
				^{163}Er			
91	$11/2^-$ [505]	[18]	$11/2^-$	443,8	0,999	0,043	4,30

Номер полосы	$K^{\pi}[Nn_z\Lambda]$	[ссылка]	J^{π}	E^*, кэВ	$a_{гл}$	$a_{Мпр}$	$100 \cdot R$
		[18]	13/ 2⁻	614,6	0,998	0,064	6,41
			15/ 2⁻	808,5	0,997	0,081	8,12
92	5/ 2⁻ [523]	[18]	5/ 2⁻	0	0,993	0,102	10,3
			7/ 2⁻	83,96	0,980	0,162	16,5
			9/ 2⁻	190,02	0,964	0,216	22,4
		[10]	5/ 2⁻	0	0,983	0,178	18,1
			7/ 2⁻	83,96	0,963	0,257	26,7
			9/ 2⁻	190,02	0,934	0,327	35,0
93	5/ 2⁻ [512]	[18]	5/ 2⁻	609	0,994	–0,102	10,3
			7/ 2⁻	699	0,986	–0,147	14,9
			9/ 2⁻	806	0,979	–0,174	17,8
		[10]	5/ 2⁻	609	0,981	–0,171	17,4
			7/ 2⁻	699	0,947	–0,252	26,6
			9/ 2⁻	806	0,886	–0,338	38,1
94	3/ 2⁻ [521]	[18]	3/ 2⁻	104,32	0,996	0,087	8,73
			5/ 2⁻	164,43	0,980	0,133	13,6
			7/ 2⁻	249,55	0,954	0,181	19,0
		[10]	3/ 2⁻	104,32	0,994	0,101	10,2
			5/ 2⁻	164,43	0,948	0,178	18,8
			7/ 2⁻	249,55	0,889	0,269	30,3
95	1/ 2⁻ [530]	[18]	1/ 2⁻	216,4	1,000	–0,022	2,20
			3/ 2⁻	866,9	0,994	–0,086	8,65
			5/ 2⁻	874,1	0,986	–0,137	13,9
		[10]	1/ 2⁻	216,4	1,000	0,029	2,90
			3/ 2⁻	866,9	0,993	0,098	9,87
			5/ 2⁻	874,1	0,978	0,178	18,2
96	1/ 2⁻ [521]	[18]	1/ 2⁻	345,64	0,999	–0,036	3,60
			3/ 2⁻	404,00	0,996	–0,074	7,43
			5/ 2⁻	439,57	0,992	–0,104	10,5
		[10]	1/ 2⁻	345,64	0,999	–0,030	3,00
			3/ 2⁻	404,00	0,996	–0,061	6,12
			5/ 2⁻	439,57	0,989	0,090	9,10
97	1/ 2⁻ [510]	[18]	1/ 2⁻	1075	0,999	0,036	3,60
			3/ 2⁻	1098	0,997	–0,075	7,52
			5/ 2⁻	1183	0,994	0,106	10,7
		[10]	1/ 2⁻	1075	1,000	0,030	3,00

Номер полосы	$K^{\pi}[Nn_Z\Lambda]$	[ссылка]	J^{π}	E^*, кэВ	$a_{гл}$	$a_{Мпр}$	$100{\cdot}R$
		[10]	$3/2^-$	1098	0,998	0,060	6,01
			$5/2^-$	1183	0,995	0,088	8,84
98	$1/2^+$ [400]	[18]	$1/2^+$	540,56	1,000	–0,013	1,30
99	$1/2^+$ [660]	[19]	$1/2^+$	882,8	1,000	0	0,00
			$3/2^+$	1219,5	0,983	–0,157	16,0
100	$3/2^+$ [402]	[18]	$3/2^+$	735,3	0,928	–0,373	40,2
101	$3/2^+$ [651]	[19]	$3/2^+$	619,36	–0,988	–0,157	15,9
			$5/2^+$	664,83	–0,813	–0,479	58,9
			$7/2^+$	(647,0)	–0,860	0,350	40,7
		[18]	$3/2^+$	619,36	0,965	0,260	26,9
102	$5/2^+$ [642]	[18]	$5/2^+$	69,219	0,954	0,284	29,8
			$7/2^+$	91,552	0,912	0,358	39,2
			$9/2^+$	102,346	0,822	0,451	54,9
		[19]	$5/2^+$	69,219	–0,940	–0,330	35,1
			$7/2^+$	91,552	–0,893	–0,401	44,9
			$9/2^+$	120,346	–0,814	–0,483	59,3
			^{165}Er				
103	$7/2^-$ [514]	[10]	$7/2^-$	1177	0,980	–0,178	18,2
			$9/2^-$	1285	0,993	–0,095	9,57
			$11/2^-$	(1419)	0,949	–0,227	23,9
104	$5/2^-$ [523]		$5/2^-$	0	0,996	0,088	8,83
			$7/2^-$	77,254	0,989	0,128	12,9
			$9/2^-$	175,86	0,980	0,161	16,4
105	$5/2^-$ [512]		$5/2^-$	477,76	0,941	–0,325	34,5
			$7/2^-$	573	0,799	–0,523	65,5
			$9/2^-$	684	0,682	–0,632	92,7
106	$3/2^-$ [521]		$3/2^-$	242,935	0,990	0,100	10,1
			$5/2^-$	297,366	0,903	0,310	34,3
			$7/2^-$	372,76	0,811	0,509	62,8
107	$3/2^-$ [512]		$3/2^-$	1474	0,999	–0,038	3,80
			$5/2^-$	1539	0,997	–0,060	6,02
			$7/2^-$	1631	0,995	–0,087	8,74
108	$1/2^-$ [530]		$1/2^-$	(1003)	1,000	0,018	1,80
			$3/2^-$	1039	0,995	–0,091	9,15
			$5/2^-$	1063	0,977	–0,163	16,7
109	$1/2^-$ [521]		$1/2^-$	297,37	1,000	–0,021	2,10

Номер полосы	$K^{\pi}[Nn_z\Lambda]$	[ссылка]	J^{π}	E^*, кэВ	$a_{гл}$	$a_{Мпр}$	$100{\cdot}R$
		[10]	3/ 2⁻	356,52	0,993	0,104	10,5
			5/ 2⁻	384,32	0,965	0,210	21,8
110	1/ 2⁻ [510]		1/ 2⁻	920,5	1,000	0,021	2,10
			3/ 2⁻	962,0	0,998	0,040	4,01
			5/ 2⁻	1024	0,989	–0,131	13,2
111	1/ 2⁺ [400]	[16]	1/ 2⁺	507,4	1,000	0,000	0,00
			3/ 2⁺	589,9	0,935	–0,336	35,9
			1/ 2⁺	507,4	1,000	0,000	0,00
			3/ 2⁺	589,9	0,961	–0,177	18,4
112	1/ 2⁺ [660]		1/ 2⁺	746,0	1,000	0,000	0,00
			3/ 2⁺	(963)	0,826	0,531	64,3
		[19]	1/ 2⁺	746,0	1,000	0,000	0,00
			3/ 2⁺	(963)	0,990	–0,141	14,2
113	3/ 2⁺ [651]		3/ 2⁺	534,55	–0,990	–0,141	14,2
			5/ 2⁺	(564)	–0,880	–0,412	46,8
			7/ 2⁺	(680)	–0,757	0,610	80,6
114	5/ 2⁺ [642]		5/ 2⁺	47,156	–0,970	–0,238	24,5
			7/ 2⁺	66,76	–0,920	–0,314	34,1
			9/ 2⁺	97,955	–0,874	–0,385	44,1
		[16]	5/ 2⁺	47,156	0,972	–0,205	21,1
			7/ 2⁺	66,76	0,903	–0,301	33,3
			9/ 2⁺	97,955	0,854	–0,360	42,2
				^{167}Er			
115	7/ 2⁻ [514]	[10]	7/ 2⁻	1049	0,982	–0,171	17,4
			9/ 2⁻	1173	0,960	–0,250	26,0
			11/ 2⁻	(1323)	0,936	–0,310	33,1
116	5/ 2⁻ [523]		5/ 2⁻	667,903	0,987	0,156	15,8
			7/ 2⁻	745,25	0,960	0,216	22,5
			9/ 2⁻	845,77	0,930	0,255	27,4
117	5/ 2⁻ [512]		5/ 2⁻	346,55	0,991	0,128	12,9
			7/ 2⁻	430,03	0,965	0,194	20,1
			9/ 2⁻	535,80	0,951	0,271	28,5
118	3/ 2⁻ [521]		3/ 2⁻	752,70	0,983	0,154	15,7
			5/ 2⁻	812,49	0,906	0,334	36,9
			7/ 2⁻	894,47	0,857	0,366	42,7
119	3/ 2⁻ [512]		3/ 2⁻	1489,39	0,994	0,102	10,3

Номер полосы	$K^{\pi}[Nn_z\Lambda]$	[ссылка]	J^{π}	E^*, кэВ	$a_{гл}$	$a_{Мпр}$	$100{\cdot}R$
		[10]	$5/2^-$	1440	0,980	0,179	18,3
			$7/2^-$	1526	0,967	0,229	23,7
120	$1/2^-$ [530]		$1/2^-$	(1344)	1,000	0,013	1,30
			$3/2^-$	1377	0,989	0,102	10,3
			$5/2^-$	1426	0,968	0,183	18,9
121	$1/2^-$ [512]		$1/2^-$	207,80	1,000	–0,026	2,60
			$3/2^-$	264,87	0,997	–0,052	5,22
			$5/2^-$	281,57	0,993	–0,077	7,75
122	$1/2^-$ [510]		$1/2^-$	763,48	1,000	0,026	2,60
			$3/2^-$	801,65	0,987	–0,154	15,6
			$5/2^-$	856,9	0,939	–0,326	34,7
123	$1/2^+$ [660]	[21]	$1/2^+$	1819	1,000	0,000	0,00
			$3/2^+$	2088	0,993	–0,117	11,8
124	$3/2^+$ [651]		$3/2^+$	(1490)	0,993	–0,116	11,7
			$5/2^+$	1514	0,904	0,413	45,7
125	$5/2^+$ [642]		$5/2^+$	810,49	0,993	0,113	11,4
			$7/2^+$	873,41	0,978	0,173	17,7
			$9/2^+$	932,96	0,955	0,231	24,2
		[14]	$5/2^+$	810,49	0,981	0,189	19,3
			$9/2^+$	932,96	0,877	0,388	44,2
		[22]	$5/2^+$	810,49	0,955	0,104	10,9
			$5/2^+$	810,49	0,6997	0,6538	93,4
126	$7/2^+$ [633]	[8]	$7/2^+$	0	0,988	0,151	15,3
			$9/2^+$	79,32	0,968	0,217	22,4
			$11/2^+$	177,96	0,946	0,269	28,4
		[14]	$7/2^+$	0	0,995	0,097	9,75
			$9/2^+$	79,32	0,977	0,156	16,0
			$11/2^+$	177,96	0,959	0,219	22,8
			$7/2^+$	0	0,991	0,130	13,1
			$9/2^+$	79,32	0,961	0,201	20,9
			$11/2^+$	177,96	0,934	0,271	29,0
		[21]	$7/2^+$	0	0,993	0,116	11,7
			$9/2^+$	79,32	0,977	0,170	17,4
			$11/2^+$	177,96	0,960	0,213	22,2
		[22]	$7/2^+$	0	0,9929	0,1170	11,8
			$9/2^+$	79,32	0,9746	0,1732	17,8

Номер полосы	$K^{\pi}[Nn_Z\Lambda]$	[ссылка]	J^{π}	E^*, кэВ	$a_{гл}$	$a_{Мпр}$	$100{\cdot}R$
		[22]	$11/2^+$	177,96	0,9548	0,2185	22,9
127	$9/2^+$ [624]	[14]	$9/2^+$	1253	0,978	–0,186	19,0
			$11/2^+$	1382	0,951	–0,233	24,5
			$13/2^+$	1530	0,912	–0,277	30,4
		[21]	$9/2^+$	1253	0,987	–0,151	15,3
			$11/2^+$	1382	0,972	–0,204	21,0
			$13/2^+$	1530	0,958	– 0,236	24,6
			$9/2^+$	1253	0,991	–0,119	12,0
			$11/2^+$	1382	0,980	–0,160	16,3
			$13/2^+$	1530	0,968	–0,183	18,9
			^{169}Er				
128	$7/2^-$ [514]	[10]	$7/2^-$	922	0,614	0,562	91,5
			$9/2^-$	930	0,637	0,662	103,9
			$11/2^-$	1051	0,569	0,679	119,3
129	$5/2^-$ [523]		$5/2^-$	853,0	0,978	–0,204	20,9
			$7/2^-$	942,1	0,848	–0,449	52,9
			$9/2^-$	1052	0,741	–0,580	78,3
130	$5/2^-$ [512]		$5/2^-$	92,0	0,989	0,113	11,4
			$7/2^-$	176,7	0,983	0,149	15,2
			$9/2^-$	285,1	0,961	0,196	20,4
131	$3/2^-$ [521]		$3/2^-$	714,6	0,995	–0,099	9,95
			$5/2^-$	769,6	0,961	0,205	21,3
			$7/2^-$	850	0,733	0,648	88,4
132	$3/2^-$ [512]		$3/2^-$	1081,6	0,999	–0,048	4,80
			$5/2^-$	1144,6	0,996	–0,076	7,63
			$7/2^-$	1230	0,991	–0,113	11,4
133	$1/2^-$ [521]		$1/2^-$	0	0,999	–0,035	3,50
			$3/2^-$	64,55	0,996	–0,074	7,43
			$5/2^-$	74,6	0,986	–0,111	11,3
134	$1/2^-$ [510]		$1/2^-$	562,0	0,999	–0,035	3,50
			$3/2^-$	599,3	0,992	0,098	9,88
			$5/2^-$	654,0	0,981	0,160	16,3
			^{161}Tm				
135	$7/2^-$ [523]	[23]	$7/2^-$	78,2	0,973	0,228	23,4
			$9/2^-$	149,1	0,907	0,294	32,4
136	$5/2^-$ [532]		$5/2^-$	709,6	0,989	–0,037	3,74

Номер полосы	$K^{\pi}[Nn_Z\Lambda]$	[ссылка]	J^{π}	E^*, кэВ	$a_{гл}$	$a_{Мпр}$	$100{\cdot}R$
137	$1/2^-$ [541]	[23]	$1/2^-$	367,2	1,000	0,000	0,00
			$3/2^-$	376,6	0,920	0,390	42,4
			$5/2^-$	465,8	0,881	0,470	53,3
138	$1/2^+$ [411]		$1/2^+$	7,5	1,000	0	0,00
			$3/2^+$	22,7	0,999	0,042	4,20
			$5/2^+$	166,9	0,993	0,104	10,5
139	$3/2^+$ [411]		$3/2^+$	338,0	0,999	–0,041	4,10
			$5/2^+$	433,4	0,988	–0,109	11,0
140	$5/2^+$ [402]		$5/2^+$	18,9	0,995	0,094	9,45
			$7/2^+$	159,1	0,983	0,146	14,8
141	$7/2^+$ [404]		$7/2^+$	0	0,995	0,089	8,94
			$9/2^+$	161,8	0,988	0,132	13,4
			^{163}Tm				
142	$7/2^-$ [523]	[24]	$7/2^-$	86,91	0,991	0,136	13,7
			$9/2^-$	174,57	0,958	0,210	21,9
			$11/2^-$	290,00	0,930	0,278	29,9
143	$1/2^-$ [541]		$1/2^-$	217,14	1,000	–0,011	1,10
			$3/2^-$	326,22	0,991	–0,131	13,2
			$5/2^-$	253,4	0,984	–0,177	18,0
144	$1/2^+$ [411]		$1/2^+$	0	1,000	0,008	0,80
			$3/2^+$	13,517	0,999	0,037	3,70
			$5/2^+$	144,392	0,774	–0,630	81,4
145	$3/2^+$ [411]		$3/2^+$	366,36	0,999	–0,037	3,70
			$5/2^+$	449,20	0,978	–0,181	18,5
			$7/2^+$	559,20	0,959	–0,267	27,8
146	$5/2^+$ [402]		$5/2^+$	136,7	0,755	0,191	25,3
			$7/2^+$	258,4	0,956	0,257	26,9
			$9/2^+$	(356)	0,867	0,355	40,9
147	$7/2^+$ [404]		$7/2^+$	23,28	0,997	0,068	6,82
			$9/2^+$	164,68	0,992	0,106	10,7
			$11/2^+$	331,07	0,986	0,143	14,5
			^{165}Tm				
148	$9/2^-$ [514]	[24]	$9/2^-$	834,4	0,980	–0,183	18,7
			$11/2^-$	972,6	0,962	–0,232	24,1
			$13/2^-$	(1231)	0,945	–0,251	26,6
149	$7/2^-$ [523]		$7/2^-$	160,47	0,991	0,136	13,7

Номер полосы	$K^{\pi}[Nn_z\Lambda]$	[ссылка]	J^{π}	E^*, кэВ	$a_{гл}$	$a_{Мпр}$	$100{\cdot}R$
			$9/2^-$	252,44	0,961	0,195	20,3
			$11/2^-$	370,2	0,935	0,240	25,7
150	$1/2^-[541]$		$1/2^-$	158,20	1,000	0,009	0,90
			$3/2^-$	275,53	0,958	0,296	30,9
			$5/2^-$	181,72	0,953	0,302	31,7
151	$1/2^+[411]$		$1/2^+$	0	1,000	0,008	0,80
			$3/2^+$	11,50	0,999	0,032	3,20
			$5/2^+$	129,52	0,997	0,072	7,22
152	$3/2^+[411]$	[24]	$3/2^+$	416,06	0,999	–0,032	3,20
			$5/2^+$	491,23	0,959	–0,273	28,5
			$7/2^+$	592,25	0,922	–0,378	41,0
153	$5/2^+[402]$		$5/2^+$	315,54	0,962	0,271	28,2
			$7/2^+$	419,79	0,925	0,376	40,6
			$9/2^+$	552,06	0,891	0,425	47,7
154	$7/2^+[404]$		$7/2^+$	80,37	0,999	0,039	3,90
			$9/2^+$	210,59	0,997	0,060	6,02
			$11/2^+$	366,9	0,995	0,080	8,04
				^{167}Tm			
155	$9/2^-[514]$		$9/2^-$	929,77	0,983	–0,172	17,5
			$11/2^-$	1044,09	0,966	–0,220	22,8
			$13/2^-$	(1303)	0,952	–0,239	25,1
156	$7/2^-[523]$		$7/2^-$	292,9	0,991	0,135	13,6
			$9/2^-$	383,8	0,964	0,194	20,1
			$11/2^-$	496,7	0,939	0,244	26,0
157	$3/2^-[532]$		$3/2^-$	852,9	0,986	–0,166	16,8
			$5/2^-$	882,2	0,979	–0,202	20,6
		[24]	$7/2^-$	935,4	0,935	–0,354	37,9
158	$1/2^-[541]$		$1/2^-$	171,7	1,000	0,007	0,70
			$3/2^-$	187,8	0,979	0,202	20,6
			$5/2^-$	282,4	0,986	0,167	16,9
159	$1/2^+[411]$		$1/2^+$	0	1,000	0,006	0,60
			$3/2^+$	10,48	1,000	0,024	2,40
			$5/2^+$	116,66	0,998	0,049	4,91
160	$3/2^+[411]$		$3/2^+$	471,01	0,997	0,024	2,41
			$5/2^+$	522,34	0,707	0,705	99,7
			$7/2^+$	602,09	0,715	0,696	97,3

Номер полосы	$K^{\pi}[Nn_z\Lambda]$	[ссылка]	J^{π}	E^*, кэВ	$a_{\text{гл}}$	$a_{\text{Мпр}}$	$100 \cdot R$
161	$5/2^+$ [402]	[24]	$5/2^+$	557,90	0,709	–0,704	99,3
			$7/2^+$	657,87	0,717	–0,695	96,9
			$9/2^+$	780,53	0,720	–0,689	95,7
162	$7/2^+$ [404]		$7/2^+$	179,56	0,999	0,027	2,70
			$9/2^+$	296,28	0,999	0,042	4,20
			$11/2^+$	436,13	0,998	0,054	5,41
			^{163}Yb				
163	$5/2^-$ [523]	[25]	$5/2^-$	53,6	0,807	0,573	71,0
			$7/2^-$	132,9	0,749	0,629	84,0
			$9/2^-$	234,6	0,695	0,660	95,0
164	$5/2^-$ [512]		$5/2^-$	(854)	0,991	–0,099	10,0
			$7/2^-$	(971)	0,979	–0,148	15,1
			$9/2^-$	(1114)	0,945	0,202	21,4
165	$3/2^-$ [521]		$3/2^-$	0	0,997	0,080	8,02
			$5/2^-$	72	0,801	–0,579	72,3
			$7/2^-$	(160)	0,741	–0,633	85,4
166	$1/2^-$ [521]		$1/2^-$	(609)	1,000	0,000	0,00
			$3/2^-$	(646)	0,932	0,354	38,0
			$5/2^-$	(687)	0,821	0,448	54,6
			^{165}Yb				
167	$5/2^-$ [523]	[25]	$5/2^-$	0	0,991	0,108	10,9
			$7/2^-$	87,51	0,974	0,168	17,2
			$9/2^-$	197,4	0,960	0,227	23,6
168	$5/2^-$ [512]		$5/2^-$	400,8	0,972	–0,232	23,9
			$7/2^-$	(537)	0,883	–0,337	38,2
169	$3/2^-$ [521]		$3/2^-$	120,69	0,997	0,060	6,02
			$5/2^-$	174,23	0,962	0,232	24,1
			$7/2^-$	264,64	0,922	0,313	33,9
170	$1/2^-$ [521]		$1/2^-$	324,44	1,000	0,018	1,80
			$3/2^-$	391,66	0,998	0,045	4,51
			$5/2^-$	427,60	0,996	0,072	7,23
171	$3/2^+$ [651]		$3/2^+$	533,2	0,970	0,244	25,1
172	$5/2^+$ [642]		$5/2^+$	(130)	0,915	0,369	40,3
			$7/2^+$	132,33	0,872	0,406	46,6
			$9/2^+$	126,74	0,749	0,494	66,0

Номер полосы	$K^{\pi}[Nn_z\Lambda]$	[ссылка]	J^{π}	E^*, кэВ	$a_{гл}$	$a_{Мпр}$	$100 \cdot R$
			^{167}Yb				
173	11/ 2⁻ [505]	[25]	11/ 2⁻	571,52	0,996	0,097	9,74
			13/ 2⁻	726,4	0,980	0,141	14,4
			15/ 2⁻	901,0	0,964	0,177	18,4
174	7/ 2⁻ [514]		7/ 2⁻	(612)	0,979	–0,182	18,6
			9/ 2⁻	(743)	0,956	–0,251	26,2
175	5/ 2⁻ [523]		5/ 2⁻	0	0,996	–0,076	7,63
			7/ 2⁻	76,68	0,986	–0,216	21,9
			9/ 2⁻	178,87	0,973	–0,150	15,4
176	5/ 2⁻ [512]		5/ 2⁻	213,18	0,715	–0,691	96,6
			7/ 2⁻	308,44	0,603	–0,561	93,0
			9/ 2⁻	(541)	0,666	0,206	30,9
177	3/ 2⁻ [521]		3/ 2⁻	179,77	0,992	–0,117	11,8
			5/ 2⁻	239,18	0,716	–0,083	11,6
			7/ 2⁻	317,51	0,700	0,111	15,9
178	1/ 2⁻ [521]		1/ 2⁻	188,74	1,000	–0,017	1,70
			3/ 2⁻	258,56	0,992	0,118	11,9
			5/ 2⁻	278,24	0,993	0,334	93,6
179	3/ 2⁺ [651]		3/ 2⁺	(570)	0,961	0,194	20,2
			5/ 2⁺	(603)	0,949	0,455	47,9
180	5/ 2⁺ [642]		5/ 2⁺	29,66	0,960	0,272	28,3
			7/ 2⁺	33,91	0,885	0,338	38,2
			9/ 2⁺	58,54	0,830	0,403	48,5
181	7/ 2⁺ [633]		7/ 2⁺	430,8	0,940	–0,237	25,2
			9/ 2⁺	(534)	0,857	–0,396	46,2
			^{169}Yb				
182	7/ 2⁻ [514]	[25]	7/ 2⁻	960,4	0,989	–0,133	13,4
			9/ 2⁻	1078,1	0,977	–0,186	19,0
			11/ 2⁻	(1242)	0,962	–0,228	23,7
		[26]	7/ 2⁻	960,4	0,989	–0,140	14,2
			9/ 2⁻	1078,1	0,975	–0,200	20,5
183	5/ 2⁻ [523]	[25]	5/ 2⁻	569,830	0,984	0,155	15,7
			7/ 2⁻	647,836	0,958	0,218	22,8
			9/ 2⁻	748,956	0,932	0,261	28,0
		[26]	5/ 2⁻	569,830	0,989	0,129	13,0
			7/ 2⁻	647,836	0,970	0,175	18,0

Номер полосы	$K^{\pi}[Nn_Z\Lambda]$	[ссылка]	J^{π}	E^*, кэВ	$a_{гл}$	$a_{Мпр}$	$100{\cdot}R$
		[26]	$9/2^-$	748,956	0,952	0,200	21,0
		[10]	$5/2^-$	569,830	0,989	0,146	14,8
			$7/2^-$	647,836	0,976	0,209	20,6
			$9/2^-$	748,955	0,964	0,249	25,8
184	$5/2^-$ [512]	[25]	$5/2^-$	191,214	0,997	0,081	8,12
			$7/2^-$	278,597	0,990	0,125	12,6
			$9/2^-$	389,527	0,982	0,166	16,9
		[26]	$5/2^-$	191,214	0,996	0,084	8,43
			$7/2^-$	278,597	0,998	0,127	12,7
			$9/2^-$	389,527	0,980	0,166	17,1
		[10]	$5/2^-$	191,214	0,993	0,116	11,7
			$7/2^-$	278,597	0,979	0,181	18,5
			$9/2^-$	389,527	0,967	0,247	25,5
185	$3/2^-$ [521]	[25]	$3/2^-$	659,627	0,992	–0,061	6,15
			$5/2^-$	722,278	0,963	–0,158	16,4
			$7/2^-$	807,056	0,935	–0,219	23,4
		[26]	$3/2^-$	659,627	0,996	–0,073	7,33
			$5/2^-$	722,278	0,979	–0,130	13,3
			$7/2^-$	807,056	0,959	–0,172	17,9
		[10]	$3/2^-$	659,627	0,999	0,049	4,90
			$5/2^-$	722,278	0,979	–0,148	15,1
			$7/2^-$	807,056	0,954	–0,216	22,6
				^{169}Yb			
186	$1/2^-$ [521]	[25]	$1/2^-$	24,199	1,000	–0,018	1,80
			$3/2^-$	86,918	0,998	0,038	3,81
			$5/2^-$	99,240	0,995	–0,060	6,03
		[26]	$1/2^-$	24,199	0,999	–0,031	3,10
			$3/2^-$	86,918	0,998	0,064	6,41
			$5/2^-$	99,240	0,995	–0,091	9,15
		[10]	$1/2^-$	24,199	1,000	–0,022	2,20
			$3/2^-$	86,918	0,999	–0,045	4,50
			$5/2^-$	99,240	0,998	–0,064	6,41
187	$1/2^-$ [510]	[25]	$1/2^-$	813,3	1,000	0,018	1,80
			$3/2^-$	851,4	0,996	0,081	8,13
			$5/2^-$	911,7	0,991	0,118	11,9
		[10]	$1/2^-$	813,3	1,000	0,022	2,20

Номер полосы	$K^{\pi}[Nn_z\Lambda]$	[ссылка]	J^{π}	E^*, кэВ	$a_{гл}$	$a_{Мпр}$	$100{\cdot}R$
		[10]	$3/2^-$	851,4	0,998	–0,050	5,01
			$5/2^-$	911,7	0,995	–0,078	7,84
188	$3/2^+$ [651]	[25]	$3/2^+$	719,91	0,973	0,232	23,8
			$5/2^+$	761,84	0,594	–0,630	106,1
			$7/2^+$	832,05	0,676	–0,658	97,3
		[26]	$3/2^+$	719,91	0,975	0,220	22,6
			$5/2^+$	761,84	0,782	–0,558	71,3
			$7/2^+$	832,05	0,751	–0,584	77,7
189	$5/2^+$ [642]	[25]	$5/2^+$	590,687	0,767	0,579	75,5
			$7/2^+$	647,286	0,732	0,636	86,9
			$9/2^+$	707,18	0,798	–0,535	67,0
		[26]	$5/2^+$	590,687	0,743	0,541	72,8
			$7/2^+$	647,286	0,799	0,575	72,0
			$9/2^+$	707,18	0,748	–0,604	80,7
190	$7/2^+$ [633]	[25]	$7/2^+$	0	0,986	0,164	16,6
			$9/2^+$	70,882	0,961	0,235	24,4
			$11/2^+$	161,651	0,937	0,285	30,4
		[26]	$7/2^+$	0	0,993	0,119	12,0
			$9/2^+$	70,882	0,965	0,197	20,4
			$11/2^+$	161,651	0,939	0,273	29,1
		[27]	$7/2^+$	0	0,978	0,204	20,9
			$9/2^+$	70,882	0,945	0,289	30,6
			$11/2^+$	161,651	0,912	0,350	38,4
191	$9/2^+$ [624]	[25]	$9/2^+$	1177	0,983	–0,154	15,7
			$11/2^+$	(1325)	0,841	–0,259	30,8
				^{171}Yb			
192	$7/2^-$ [514]	[25]	$7/2^-$	835,062	0,987	0,160	16,2
			$9/2^-$	948,341	0,970	0,239	24,6
			$11/2^-$	(1076)	0,949	0,307	32,3
		[10]	$7/2^-$	835,062	0,999	–0,031	3,10
			$9/2^-$	948,341	0,999	–0,045	4,50
			$11/2^-$	(1076)	0,998	–0,058	5,81
193	$7/2^-$ [503]	[25]	$7/2^-$	1377,5	0,999	–0,048	4,80
			$9/2^-$	(1497)	0,996	–0,072	7,23
194	$5/2^-$ [523]		$5/2^-$	958,158	0,928	0,363	39,1
			$7/2^-$	1024,582	0,843	0,504	59,8

Номер полосы	$K^{\pi}[Nn_z\Lambda]$	[ссылка]	J^{π}	E^*, кэВ	$a_{гл}$	$a_{Мпр}$	$100{\cdot}R$
		[25]	9/ 2⁻	1127,062	0,723	0,631	87,3
195	5/ 2⁻ [512]	[25]	5/ 2⁻	122,42	0,999	0,039	3,90
			7/ 2⁻	208,01	0,997	0,060	6,02
			9/ 2⁻	317,30	0,993	0,079	7,96
		[10]	5/ 2⁻	122,42	0,996	0,081	8,13
			7/ 2⁻	208,01	0,985	0,126	12,8
			9/ 2⁻	317,30	0,984	0,158	16,1
196	3/ 2⁻ [521]	[25]	3/ 2⁻	902,27	0,994	–0,099	9,96
			5/ 2⁻	958,41	0,912	–0,367	40,2
			7/ 2⁻	1024,39	0,837	–0,505	60,3
		[10]	3/ 2⁻	902,27	0,994	0,104	10,5
			5/ 2⁻	958,41	0,976	0,201	20,6
			7/ 2⁻	1024,39	0,941	0,313	33,3
197	1/ 2⁻ [521]	[25]	1/ 2⁻	0	1,000	–0,008	0,80
			3/ 2⁻	66,73	0,999	–0,026	2,60
			5/ 2⁻	75,89	0,998	–0,042	4,21
		[10]	1/ 2⁻	0	1,000	–0,015	1,50
			3/ 2⁻	66,73	0,999	–0,032	3,20
			5/ 2⁻	75,89	0,998	–0,046	4,61
198	1/ 2⁻ [510]	[10]	1/ 2⁻	954,2	1,000	0,015	1,50
			3/ 2⁻	990,9	0,994	–0,105	10,6
			5/ 2⁻	1052	0,978	–0,202	20,6
		[25]	1/ 2⁻	954,2	1,000	0,008	0,80
			3/ 2⁻	990,9	0,995	0,099	9,95
			5/ 2⁻	1052	0,984	0,173	17,6
199	3/ 2⁺ [651]	[25]	3/ 2⁺	(1132)	0,989	0,147	14,9
			5/ 2⁺	(1206)	0,833	–0,392	47,1
			7/ 2⁺	(1363)	0,824	–0,499	60,6
200	5/ 2⁺ [642]	[25]	5/ 2⁺	895,3	0,918	0,388	42,3
			7/ 2⁺	920,7	0,852	0,496	58,2
			9/ 2⁺	987,3	0,958	0,562	94,0
		[28]	5/ 2⁺	895,3	0,9643	0,2523	26,2
			7/ 2⁺	920,7	0,9196	0,3538	38,5
			9/ 2⁺	987,3	0,6235	0,5664	90,8
201	7/ 2⁺ [633]	[25]	7/ 2⁺	95,272	0,989	0,143	14,5
			9/ 2⁺	167,658	0,965	0,207	21,4

Номер полосы	$K^{\pi}[Nn_z\Lambda]$	[ссылка]	J^{π}	E^*, кэВ	$a_{гл}$	$a_{Мпр}$	$100{\cdot}R$
		[25]	$11/2^+$	259,066	0,940	0,257	27,3
		[8]	$7/2^+$	95,272	0,989	0,148	15,0
			$9/2^+$	167,658	0,969	0,214	22,1
			$11/2^+$	259,066	0,948	0,264	27,8
		[28]	$7/2^+$	95,272	0,9881	0,1520	15,4
			$9/2^+$	167,658	0,9630	0,2199	22,8
			$11/2^+$	259,066	0,9377	0,2715	28,9
202	$9/2^+$ [624	[25]	$9/2^+$	935,232	0,813	–0,470	57,8
			$11/2^+$	(1144,4)	0,733	0,426	58,1
		[28]	$9/2^+$	935,232	0,8104	–0,4918	60,7
			$11/2^+$	(1144,4)	0,6400	0,5639	88,1
			$13/2^+$	1407	0,8770	–0,2912	33,2
				^{173}Yb			
203	$7/2^-$ [514]		$7/2^-$	636,07	0,995	0,092	9,25
			$9/2^-$	749,1	0,990	0,136	13,7
			$11/2^-$	866	0,982	0,173	17,6
204	$5/2^-$ [523]		$5/2^-$	(975)	0,998	0,055	5,51
			$7/2^-$	1060	0,991	–0,092	9,28
			$9/2^-$	1172,5	0,982	–0,136	13,85
205	$5/2^-$ [512]		$5/2^-$	0	0,999	0,042	4,20
			$7/2^-$	78,650	0,997	0,064	6,42
			$9/2^-$	178,347	0,994	0,084	8,45
206	$3/2^-$ [521]		$3/2^-$	1232,5	0,999	0,050	8,45
			$5/2^-$	1287,5	0,995	0,074	7,44
		[25]	$7/2^-$	1362,4	0,988	0,105	10,6
207	$3/2^-$ [512]		$3/2^-$	1340,9	1,000	–0,025	2,50
			$5/2^-$	1406,1	0,999	–0,035	3,50
			$7/2^-$	1493,5	0,996	–0,059	5,92
208	$1/2^-$ [521]		$1/2^-$	398,9	1,000	–0,012	1,20
			$3/2^-$	461,5	1,000	0,024	2,40
			$5/2^-$	482,0	0,999	–0,035	3,50
209	$1/2^-$ [510]		$1/2^-$	1032,5	1,000	0,012	1,20
			$3/2^-$	1074,5	0,998	–0,050	5,01
			$5/2^-$	1121,6	0,996	–0,074	7,43
210	$7/2^+$ [633]		$7/2^+$	350,740	0,996	0,167	16,8
			$9/2^+$	412,917	0,949	0,235	24,8

Номер полосы	$K^{\pi}[Nn_z\Lambda]$	[ссылка]	J^{π}	E^*, кэВ	$a_{гл}$	$a_{Мпр}$	$100{\cdot}R$
		[25]	$11/2^+$	497,0	0,917	0,284	31,0
				^{169}Lu			
211	$9/2^-$ [514]	[29]	$9/2^-$	439,0	0,880	0,469	53,3
			$11/2^-$	546,0	0,819	0,558	68,1
			$13/2^-$	683,2	0,779	0,606	77,8
212	$7/2^-$ [523]		$7/2^-$	493,0	0,994	0,108	10,9
213	$1/2^-$ [541]		$1/2^-$	29,0	0,999	–0,034	3,40
			$3/2^-$	152,5	0,990	0,120	12,1
			$5/2^-$	38,1	0,981	0,168	17,1
				^{177}Lu			
214	$9/2^-$ [514]	[30]	$9/2^-$	150	0,999	0,044	4,40
			$11/2^-$	289	0,997	0,067	6,72
			$13/2^-$	451	0,995	0,086	8,64
215	$3/2^-$ [532]		$3/2^-$	1322	0,972	–0,232	23,9
			$5/2^-$	1395	0,976	–0,210	21,5
216	$1/2^-$ [541]		$1/2^-$	795	1,000	0,005	0,50
			$3/2^-$	952	0,972	0,233	24,0
			$5/2^-$	762	0,978	0,210	21,5
217	$1/2^+$ [411]		$1/2^+$	570	1,000	0,003	0,30
			$3/2^+$	574	1,000	0,006	0,60
			$5/2^+$	709	1,000	0,010	1,00
218	$5/2^+$ [402]		$5/2^+$	186,7	1,000	0,006	0,60
			$7/2^+$	289,0	1,000	0,009	0,90
			$9/2^+$	415,1	1,000	0,012	1,20
219	$7/2^+$ [404]		$7/2^+$	0	1,000	0,019	1,90
			$9/2^+$	123,5	1,000	0,028	2,80
			$11/2^+$	289,0	0,999	0,036	3,60
				^{177}Hf			
220	$7/2^-$ [514]	[31]	$7/2^-$	0	0,999	0,033	3,30
			$9/2^-$	113,6	0,998	0,050	5,01
			$11/2^-$	249,7	0,996	0,064	6,43
		[13]	$7/2^-$	0	0,998	0,055	5,51
			$9/2^-$	113,6	0,994	0,079	7,95
			$11/2^-$	249,7	0,990	0,102	10,3
221	$9/2^+$ [624]	[31]	$9/2^+$	321,3	0,982	0,189	19,2
			$11/2^+$	426,7	0,949	0,257	27,1

Номер полосы	$K^{\pi}[Nn_z\Lambda]$	[ссылка]	J^{π}	E^*, кэВ	$a_{гл}$	$a_{Мпр}$	$100{\cdot}R$
		[31]	$13/2^+$	550,2	0,920	0,303	32,9
		[13]	$9/2^+$	321,3	0,970	0,199	20,5
			$11/2^+$	426,7	0,949	0,277	29,2
			$13/2^+$	550,2	0,920	0,332	36,1
			^{179}Hf				
222	$9/2^+$ [624]	[8]	$9/2^+$	0	0,989	0,143	14,5
			$11/2^+$	122,790	0,972	0,206	21,2
			$13/2^+$	268,416	0,953	0,255	26,8
223	$9/2^+$ [624]	[32]	$9/2^+$	0	0,9798	0,1966	20,1
			$11/2^+$	122,790	0,9535	0,2789	29,25
			$13/2^+$	268,416	0,9262	0,3402	36,7
			^{175}Ta				
224	$1/2^-$ [541]	[33]	$1/2^-$	68,9	0,9978	–0,0667	6,60
			$3/2^-$	218,5	0,9551	0,2242	23,5
			$5/2^-$	51,5	0,9695	0,2010	20,7
			^{179}W				
225	$7/2^-$ [514]	[34]	$7/2^-$	0	1,00	–0,07	7,0
			$9/2^-$	120	0,99	–0,10	10,1
226	$5/2^-$ [512]		$5/2^-$	430	–1,00	0,00	0,00
			$7/2^-$	532	–1,00	–0,07	7,00
			$9/2^-$	(662)	–0,99	–0,10	10,1
227	$1/2^-$ [521]		$1/2^-$	222	1,00	–0,04	4,00
			$3/2^-$	305	1,00	–0,09	9,00
			$5/2^-$	318	0,99	–0,12	12,1
228	$7/2^+$ [633]	[35]	$7/2^+$	477,96	–0,953	0,086	9,02
			$9/2^+$	(649,9)	–0,699	–0,551	78,8
			$11/2^+$	(817,5)	–0,582	0,608	105,4
229	$9/2^+$ [624]		$9/2^+$	308,97	0,827	0,529	64,0
			$11/2^+$	372,83	0,757	0,590	77,9
			$13/2^+$	468,67	0,694	0,614	88,5
			^{181}W				
230	$7/2^-$ [514]	[36]	$7/2^-$	409,23	0,972	–0,217	22,3
			$9/2^-$	528,6	0,961	–0,234	24,3
			$11/2^-$	674,9	0,953	–0,231	24,2
			$7/2^-$	409,23	0,928	–0,367	39,5
			$9/2^-$	528,6	0,868	–0,481	55,4

Номер полосы	$K^{\pi}[Nn_z\Lambda]$	[ссылка]	J^{π}	E^*, кэВ	$a_{гл}$	$a_{Мпр}$	$100 \cdot R$
		[36]	$11/2^-$	674,9	0,820	–0,547	66,7
		[34]	$7/2^-$	409,23	0,81	–0,58	71,6
			$9/2^-$	528,6	0,67	–0,72	107,5
231	$7/2^-$ [503]	[36]	$7/2^-$	661,3	0,995	–0,099	9,95
			$9/2^-$	804,4	0,989	–0,147	14,9
			$11/2^-$	974,7	0,981	–0,186	19,0
			$7/2^-$	661,3	0,980	–0,197	20,1
			$9/2^-$	804,4	0,960	–0,276	28,7
			$11/2^-$	974,7	0,941	–0,332	35,3
232	$5/2^-$ [512]	[36]	$5/2^-$	365,5	1,000	0,014	1,40
			$7/2^-$	475,4	0,971	0,216	22,2
			$9/2^-$	609,0	0,961	0,234	24,3
		[34]	$5/2^-$	365,5	–1,00	0,00	0,00
			$7/2^-$	475,4	–0,79	–0,59	74,7
			$9/2^-$	609,0	–0,64	–0,74	115,6
		[36]	$5/2^-$	365,5	1,00	0,029	2,90
			$7/2^-$	475,5	0,908	0,370	40,7
			$9/2^-$	609,0	0,830	0,491	59,2
233	$3/2^-$ [512]	[34]	$3/2^-$	726	–1,00	0,05	5,0
			$5/2^-$	807	–1,00	0,07	7,0
			$7/2^-$	937	–0,99	0,13	13,1
234	$1/2^-$ [521]	[34]	$1/2^-$	385	0,99	–0,16	16,2
			$3/2^-$	450	0,95	–0,30	31,6
			$5/2^-$	488	0,85	–0,53	62,3
235	$1/2^-$ [510]		$1/2^-$	458	–0,99	–0,16	16,2
			$3/2^-$	529	–0,99	–0,15	15,1
			$5/2^-$	560	–0,85	–0,52	61,2
236	$7/2^+$ [633]	[36]	$7/2^+$	953,6	0,923	0,360	39,0
			$9/2^+$	993,3	0,772	0,495	64,1
			$11/2^+$	1095,4	0,707	0,540	76,4
237	$9/2^+$ [624]		$9/2^+$	0	0,983	0,181	18,4
			$11/2^+$	113,3	0,953	0,257	27,0
			$13/2^+$	251,1	0,923	0,314	34,0
				^{183}W			
238	$7/2^-$ [514]	[34]	$7/2^-$	1072	–0,99	–0,17	17,2
			$9/2^-$	1219	–0,98	–0,20	20,4

Номер полосы	$K^{\pi}[Nn_z\Lambda]$	[ссылка]	J^{π}	E^*, кэВ	$a_{гл}$	$a_{Мпр}$	$100{\cdot}R$
239	7/ 2⁻ [503]	[34]	7/ 2⁻	453	1,00	0,05	5,0
			9/ 2⁻	595	1,00	0,08	8,0
240	5/ 2⁻ [512]		5/ 2⁻	906	1,00	0,00	0,00
			7/ 2⁻	1002	0,98	–0,17	17,3
			9/ 2⁻	1128	0,98	0,20	20,4
241	3/ 2⁻ [512]		3/ 2⁻	209	–0,99	0,15	15,1
			5/ 2⁻	296	+0,98	–0,20	20,5
			7/ 2⁻	412	–0,96	0,26	27,1
242	1/ 2⁻ [521]		1/ 2⁻	936	1,00	0,02	2,0
			3/ 2⁻	1029	1,00	–0,04	4,0
			5/ 2⁻	1056	–1,00	–0,06	6,0
243	1/ 2⁻ [510]		1/ 2⁻	0	–1,00	0,02	2,0
			3/ 2⁻	47	–0,99	–0,15	15,1
			5/ 2⁻	99	0,98	0,20	20,4
				^{185}W			
244	7/ 2⁻ [514]	[34]	7/ 2⁻	1058	–0,98	–0,19	19,4
			9/ 2⁻	1219	–0,98	–0,20	20,4
245	7/ 2⁻ [503]		7/ 2⁻	244	1,00	0,05	5,0
			9/ 2⁻	391	0,99	0,08	8,08
246	5/ 2⁻ [512]		5/ 2⁻	888	1,00	0,00	0,00
			7/ 2⁻	986	0,98	–0,19	19,4
			9/ 2⁻	1118	0,98	–0,20	20,4
247	3/ 2⁻ [512]		3/ 2⁻	0	–0,99	–0,16	16,2
			5/ 2⁻	66	0,91	0,42	46,1
			7/ 2⁻	174	0,91	0,42	46,1
248	1/ 2⁻ [521]		1/ 2⁻	1008	1,00	0,02	2,0
			3/ 2⁻	1106	1,00	0,04	4,0
			5/ 2⁻	1118	1,00	0,07	7,0
				^{187}W			
249	7/ 2⁻ [503]	[34]	7/ 2⁻	351	1,00	0,00	0,00
			9/ 2⁻	(482)	0,95	–0,33	34,7
250	3/ 2⁻ [512]		3/ 2⁻	0	–0,99	–0,16	16,2
			5/ 2⁻	77	–0,97	–0,23	23,7
			7/ 2⁻	(186)	–0,95	–0,30	31,6
				^{177}Re			
251	1/ 2⁻ [541]	37	1/ 2⁻		1,000	0,00	0,00

Номер полосы	$K^{\pi}[Nn_Z\Lambda]$	[ссылка]	J^{π}	E^*, кэВ	$a_{гл}$	$a_{Мпр}$	$100{\cdot}R$
		[37]	$3/2^-$	184,2	0,981	0,019	1,94
			$5/2^-$	0	0,924	0,026	2,81
				^{177}Re			
252	$1/2^-$ [541]	37	$1/2^-$		1,000	0,00	0,00
			$3/2^-$	206,6	0,931	0,069	7,41
			$5/2^-$		0,939	0,060	6,39
				^{177}Re			
253	$1/2^-$ [541]	37	$1/2^-$	432,4	1,000	0	0,00
			$3/2^-$	599,5	0,700	0,300	42,9
			$5/2^-$	356,7	0,861	0,137	15,9
				^{177}Re			
254	$11/2^+$ [615]	38	$11/2^+$	275,7	0,916	0,394	43,0
			$13/2^+$	414,1	0,856	0,493	57,6
			$15/2^+$	618,0	0,809	0,549	67,9

Работа выполнена при финансовой поддержке Российского фонда фундаментальных исследований (грант 93-02-3803).

СПИСОК ЛИТЕРАТУРЫ

1. **Vandenput G., van Assche P.H.M., Jacobs L. et al.** — Phys.Rev., 1986, vol. C33, No.4, p.1141.
2. **Аликов Б.А., Бадалов Н.Н., Ваврыщук Я. и др.** — Препринт ОИЯИ Р4-87-917, Дубна, 1987.
3. **Аликов Б.А., Ваврыщук Я., Лизурей Г.И. и др.** — Препринт ОИЯИ 6-84-121, Дубна, 1984.
4. **Kanestrom I., Tjom P.O.** — Nucl.Phys., 1970, vol. A145, p.461.
5. **Lovhoiden G., Widdington J.C., Hagemann A. et al.** — Nucl. Phys., 1970, vol. A148, p.656.
6. **Meyer R.A., Gunnink R., Lederer C.M., Browne E.** — Phys.Rev., 1976, vol. C13, p.2466.
7. **Borgreen J., Lovhoiden G., Waddington J.C.** — Nucl.Phys., 1969, vol. A131, p.241.
8. **Basnat M.I., Pyatov N.I., Chernej M.I.** — Physica Scripta, 1972, vol.6, No. 5, 6, p.227.
9. **Винтер Г., Зодан Х., Каун К. и др.** — ЭЧАЯ, 1973, т. 4, вып. 4, с.895.
10. **Kanestrom I., Tjom P.O.** — Nucl.Phys., 1969, vol. A138, p.177.
11. **Klamra W., Hjorth S.A., Boutet J., Andre C., Barneoud D.** — Nucl.Phys., 1973, vol. A199, p.81.

12. **Аликов Б.А., Громов К.Я., Муминов Т.М. и др.** — Изв. АН СССР, сер.физ., 1980, т.44, № 1, с.103.
13. **Базнат М.И., Пятов Н.И., Черней М.И.** — ЭЧАЯ, 1973, т.4, вып.4, с.941.
14. **Hjorth S.A., Johnson A., Ehrling G.** — Nucl.Phys., 1972, vol. A184, p.113.
15. **Громов К.Я., Зиберт Х.-У., Калинников В.Г. и др.** — ЭЧАЯ, 1975, т.6, вып. 4, с.971.
16. **Шаронов И.А.** — Кандидатская диссертация, Дубна, 1989, с.84.
17. **Renfelt K.-G., Johnson A., Hjorth S.A.** — Nucl.Phys., 1970, vol. A156, p.529.
18. **Аликов Б.А., Бадалов Х.И., Лизурей Г.И. и др.** — Препринт ОИЯИ Р6-84-207, Дубна, 1984.
19. **Hjorth S.A., Ryde H., Hagemann K.A. et al.** — Nucl.Phys., 1970, vol. A144, p.513.
20. **Шаронов И.А., Аликов Б.А., Караджов Д. и др.** — Препринт ОИЯИ Р4-86-36, Дубна, 1986.
21. **Kanestrom I., Lovhoiden G.** — Nucl.Phys., 1971, vol. A160, p.665.
22. **Oshima M., Muhara E., Ishii M. et al.** — Nucl.Phys., 1985, vol. A436, p.518.
23. **Адам И., Аликов Б.А., Бадалов Х.Н. и др.** — Тезисы докладов 35 Совещания по ядерной спектроскопии и структуре атомного ядра, Л.; Наука, 1985, с.113.
24. **Адам И., Аликов Б.А., Бадалов Х.Н. и др.** — Изв. АН СССР, сер.физ., 1985, т.49, № 5, с.867.
25. **Адам И., Аликов Б.А., Бадалов Х.Н. и др.** — Препринт ОИЯИ, Р4-88-934, Дубна, 1988.
26. **Бонч-Осмоловская Н.А., Морозов В.А., Худайбердиев Э.Н.** — Изв. АН СССР, сер.физ., 1988, т.52, № 1, с.53.
27. **Selin E., Hjorth S.A., Ryde H.** — Physica Scripta, 1970, vol.2, No.4,5, p.181.
28. **Lindblad Th., Ryde H., Barneoud D.** — Nucl.Phys., 1972, vol. A193, p.155.
29. **Foin C., Barneoud D., Hjorth S.A., Bethoux R.** — Nucl.Phys., 1973, vol. A199, p.129.
30. **Бонч-Осмоловская Н.А.** — Изв. АН СССР, сер.физ., 1991, т.55, № 5, с.850.
31. **Аликов Б.А., Бонч-Осмоловская Н.А., Нестеренко В.О.** — Изв. РАН, сер.физ., 1992, т.56, № 11, с.43.
32. **Thorsteinsen T.F., Lovhoiden G., Vaagen J.S. et al.** — Nucl.Phys., 1981, vol.A363, p.205.
33. **Foin C., Lindblad Th., Skanberg B., Ryde H.** — Nucl.Phys., 1972, vol. A195, p.465.
34. **Casten R.F., Kleinheinz P., Daly P.J., Elbek B.** — Mat.Fys.Medd.Dan.Vid.Selsk., 1972, vol. 38, No.13.
35. **Lindblad Th., Ryde H., Kleinheinz P.** — Nucl.Phys., 1973, vol. A201, p.369.
36. **Lindblad Th., Ryde H., Kleinheinz P.** — Nucl.Phys., 1973, vol.210, p.253.
37. **Leigh J.R., Newton J.O., Ellis L.A. et al.** — Nucl.Phys., 1972, vol. A183, p.177.
38. **Sodan H., Fromm W.D., Funke L. et al.** — Nucl.Phys., 1975, vol. A237, p.333.

«ФИЗИКА ЭЛЕМЕНТАРНЫХ ЧАСТИЦ И АТОМНОГО ЯДРА»
1995, ТОМ 26, ВЫП.2

УДК 532.142/143

МАКРОСКОПИЧЕСКАЯ МОДЕЛЬ МАГНИТНЫХ РЕЗОНАНСОВ В СФЕРИЧЕСКИХ ЯДРАХ

С.И.Баструков, И.В.Молодцова

Объединенный институт ядерных исследований, Дубна

Дан обзор квантово-макроскопической коллективной ядерной модели, интерпретирующей магнитные резонансы как проявление крутильных упругих колебаний сферического ядра. Представлены основные предсказания модели для энергий, переходных токовых плотностей, суммарных вероятностей возбуждения, магнитных осцилляторных сил, столкновительных ширин, полученных в зависимости от мультипольного порядка возбуждения, атомного номера и массового числа. Приведены расчеты сечений возбуждения $M\lambda$-резонансов в (e, e')-рассеянии в плосковолновом приближении и в приближении искаженных волн. Приводится систематическое сравнение теоретических предсказаний модели с экспериментальными данными по возбуждению магнитных резонансов в реакции неупругого рассеяния электронов на сферических ядрах.

The quantum-macroscopic nuclear model is outlined interpreting the magnetic resonances in terms of torsional elastic vibrations of a spherical nucleus. The basic predictions of this model are summarized for energies, transition current densities, total excitation probability, magnetic oscillator strength and spread width derived as functions of a multipole degree, atomic and mass numbers. The PWBA and DWBA computed cross section are presented for $M\lambda$ resonances excited by means of (e, e')-scattering. Strong emphasis is placed on a comparison of theoretical predictions with experimental data on magnetic resonances with $\lambda \geq 2$ excited by means of electrons inelastically scattered on spherical nuclei.

1. ВВЕДЕНИЕ

Теоретические исследования коллективных возбуждений атомных ядер методами макроскопической физики сплошных сред направлены в конечном итоге на построение адекватной динамической теории ядерного вещества. Тот факт, что многие интегральные характеристики основного состояния и коллективных возбуждений ядра, такие как энергия связи, центро-

иды энергий резонансов, суммарные вероятности возбуждения, столкновительные ширины, плавно меняются с ростом массового числа, указывает на крайне важную роль «размерного эффекта» — зависимости указанных характеристических параметров от радиуса ядра и его формы. Изучение ядерного отклика в рамках коллективных моделей, основанных на конкретных предположениях о макроскопических свойствах ядерной материи, как раз имеет целью установить эти «размерные» закономерности. Рассматривая ядро как макрочастицу сплошной среды и сравнивая теоретически предсказываемые зависимости, скажем, энергий и вероятностей от массового числа с экспериментом, можно судить о том, насколько адекватно используемая модель континуума отражает свойства реальной ядерной материи.

Как известно, первоначальное изучение ядерной динамики строилось на основе представлений о ядре как о капле несжимаемой заряженной невязкой жидкости. Однако накопленная к настоящему времени экспериментальная информация позволяет с уверенностью утверждать, что жидкостная концепция ядерного вещества не может быть признана удовлетворительной по целому ряду причин. Мы приведем лишь несколько аргументов, иллюстрирующих это утверждение, с целью подчеркнуть, что физическая интерпретация *магнитного* коллективного отклика ядра в терминах теории сплошных сред с необходимостью приводит к заключению о том, что ядерная материя обладает свойствами, присущими упругому континууму, а не жидкости.

Вначале кратко остановимся на принципиальных предположениях, составляющих основу ядерной модели жидкой капли. Согласно используемому в этой модели феноменологическому описанию ядерных свойств, предполагается, что деструктивный эффект сил кулоновского отталкивания стабилизируется ядерными силами притяжения, моделируемыми силами поверхностного натяжения. В качестве уравнений, управляющих как равновесием, так и динамическим откликом ядра, принимаются классические уравнения идеальной жидкости (уравнение непрерывности и уравнение Эйлера). Немедленным следствием эвристической гипотезы о сходстве поведения ядерной материи и поведения невязкой жидкости является то, что модель капли допускает только сферическую равновесную форму ядра. Уже это обстоятельство свидетельствует о неадекватности жидкостной гипотезы, поскольку она не отражает накопленных знаний о равновесной форме ядер. Столь же явное расхождение с экспериментальными данными имеет место и для предсказываемых капельной моделью динамических свойств ядра.

Основные принципы гидродинамического описания коллективных движений нуклонов накладывают существенные ограничения на характер коллективных возбуждений ядра, допуская существование в ядерном спектре только одной коллективной ветви возбуждений, связанной с поверхностными колебаниями ядра. Поверхностные коллективные моды идентифици-

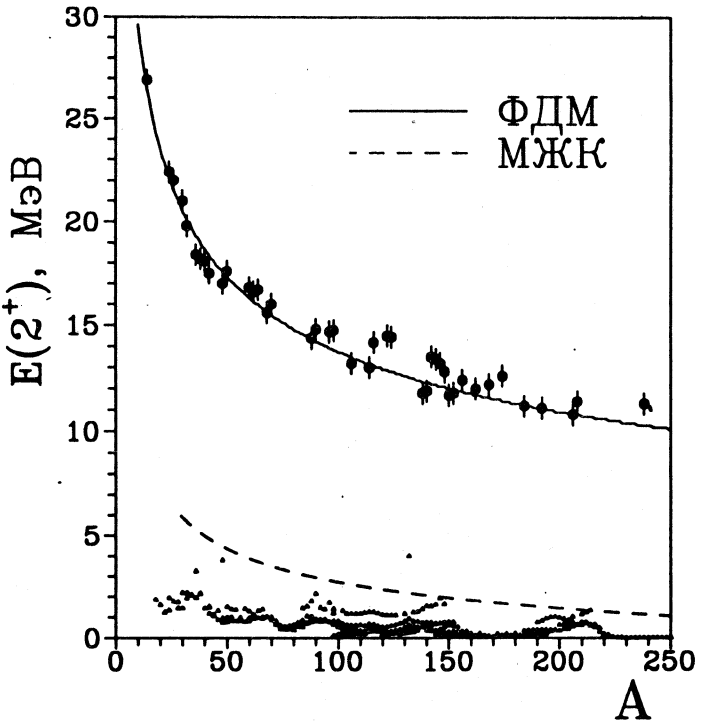

Рис. 1. Экспериментальные данные по энергиям E (2^+) квадрупольных возбуждений в зависимости от массового числа A ядра: ▲ — энергии нижайших 2^+-состояний; ● — центроиды энергий изоскалярных электрических резонансов. Теоретический расчет в рамках флюид-динамической модели — сплошная линия; пунктирная линия — предсказания модели жидкой капли

руются как возбуждения электрического типа, поскольку эти возбужденные состояния характеризуются отличными от нуля значениями электрических мультипольных моментов. Из классической электродинамики сплошных сред известно, что внешнее электромагнитное возмущение заряженной несжимаемой капли может вызвать лишь гармонические искажения ее равновесной сферической формы: $R(t) = R(1 + \alpha_{\lambda\mu}(t)\, Y_{\lambda\mu}(\hat{\mathbf{r}}))$, обусловленные возбуждением колебаний плотности электрического тока $\mathbf{j}(\mathbf{r}, t) = (eZ/A)n_0\delta\mathbf{V}(\mathbf{r}, t)$ с безвихревым полем скорости: $\delta\mathbf{V}(\mathbf{r}, t) = \nabla r^{\lambda} Y_{\lambda\mu}(\hat{\mathbf{r}})\dot{\alpha}_{\lambda}(t)$;

здесь n — плотность числа частиц, $Y_{\lambda\mu}(\hat{\mathbf{r}})$ — сферическая функция мультипольного порядка λ и $\alpha_\lambda(t)$ — амплитуда коллективных колебаний. Теоретическая оценка энергии, например, квадрупольной поверхностной моды ядра, полученная на основе капельной модели со стандартным набором параметров массовой формулы, оказывается приблизительно в 1,5—2 раза выше наблюдаемых энергий нижайших 2^+-возбуждений сферических ядер, подверженных сильному влиянию оболочечной структуры, и в 3—4 раза ниже положения центроидов энергий гигантских квадрупольных резонансов (см. рис.1). Столь явное разногласие с экспериментом говорит о необходимости пересмотра жидкостных представлений о ядерной материи. Следует также отметить, что в капельной модели никак не учитывается квантовая специфика ферми-распределения нуклонов в основном состоянии.

Пожалуй, наиболее существенный недостаток жидкостной трактовки ядерного вещества состоит в принципиальной невозможности описания магнитного отклика ядра, в то время как существование магнитных коллективных мод в спектрах многих ядер является твердо установленным фактом [1—5]. Действительно, состояния магнитного типа оказываются за пределами гидродинамического описания, поскольку переходы капли заряженной идеальной жидкости из равновесного в возбужденные состояния с отличным от нуля магнитным мультипольным моментом не реализуются. В последнем можно убедиться, подставляя приведенное выше выражение для тока в определение ядерного магнитного мультипольного момента порядка λ [6—9]:

$$\mathcal{M}(M\lambda, \mu) = \frac{-1}{c\,(\lambda+1)} \int \mathbf{j}\cdot[\mathbf{r}\times\nabla]\, r^\lambda Y_{\lambda\mu}(\hat{\mathbf{r}})\, d\tau. \qquad (1.1)$$

Легко проверить, что такая подстановка тождественно обращает (1.1) в ноль (см. также [6], с.22). Поскольку осцилляции потенциального потока являются единственно допустимым видом собственных колебаний несжимаемой невязкой жидкости, то из приведенных рассуждений немедленно следует, что стандартная капельная модель в принципе не содержит возможности описания магнитных коллективных мод.

На несостоятельность жидкокапельного подхода к описанию магнитных возбуждений ядра, несколько с иных позиций, обратили внимание Хольцварт и Эккарт, которые в короткой, но крайне содержательной заметке [10] предположили, что коллективный магнитный квадрупольный отклик сферического ядра можно рассматривать как проявление поперечных (мультипольности $\lambda = 2$) колебаний потока нуклонов. Рассмотренное в [10] локальное поле скорости в сферической системе координат с фиксирован-

ной полярной осью z имеет вид: $\delta V_x = -yz\dot{\alpha}$, $\delta V_y = xz\dot{\alpha}$, $\delta V_z = 0$, где α представляет собой геометрически бесконечно малый угол закручивания коллективного потока нуклонов вокруг оси z. В однородно заряженной сферической макрочастице, моделирующей ядро, выделенное направление (в данном случае направление полярной оси), вокруг которого происходят колебания возбуждаемого соленоидального электрического тока, может определяться только направлением проникающего внутрь ядра электромагнитного поля, порождаемого, например, рассеиваемой заряженной частицей. Нетрудно проверить, что такой тип вращательных колебаний приводит к отличному от нуля квадрупольному магнитному моменту ядра в возбужденном состоянии. Геометрическая картина таких колебаний изображена в левой части рис.1: верхнее и нижнее полушария совершают в противофазе осесимметричные сдвиговые осцилляции, выразительно названные авторами этой модели «ядерным твистом» [10—14]. Данный механизм «намагничивания» четно-четного ядра (т.е. переход из основного в возбужденное состояние с отличным от нуля магнитным моментом) обусловлен объемными соленоидальными колебаниями макроскопической плотности тока. Подчеркнем, что возбуждение крутильных колебаний не приводит к флуктуациям массовой плотности, т.е. они могут иметь место в несжимаемом континууме. Эти колебания описываются в терминах осцилляций соленоидального поля смещений сплошной среды.

Из классической теории сплошных сред известно, что способность поддерживать незатухающие, равно как продольные, так и поперечные, колебания является атрибутом идеально-упругой среды [15,16], но не невязкой жидкости. В последней, при ненулевой равновесной температуре, могут распространяться лишь звуковые, существенно продольные колебания [16,17]. Поперечные сдвиговые колебания в конечной сферической массе сплошного вещества, называемые крутильными, являются, пожалуй, главным отличительным признаком того, что данное вещество является упругой средой. В капле идеальной жидкости возбуждение сдвиговых осцилляций невозможно, поскольку уравнения гидродинамики не предусматривают возникновения анизотропии в распределении напряжений при возмущении равновесного состояния. Придерживаясь трактовки $M2$-резонанса как проявления крутильных колебаний [10—14] квадрупольной симметрии, его экспериментальное детектирование с точки зрения физики сплошных сред можно рассматривать как прямое доказательство упругости ядерного вещества.

В работах [18—21] эти соображения легли в основу описания магнитного ядерного отклика в модели упругого шара. В качестве уравнения, управляющего коллективной динамикой нуклонов, было использовано урав-

нение Ламэ* — основное уравнение колебаний классического идеально упругого вещества [16]. То, что адекватное континуальное описание (в переменных теории сплошных сред: плотности, полей скорости, смещений, напряжений и т.д.) коллективных колебаний нуклонов при возбуждении ядерных мультипольных резонансов может быть дано не в рамках классической гидродинамики, а на основании уравнений, способных отразить особенности упругоподобного поведения ферми-вещества, впервые было показано в работах Берча [24,25], посвященных анализу систематики энергий изоскалярных электрических гигантских резонансов в ядрах. Аргументы, выдвинутые в [24,25], послужили стимулом к разработке квантово-макроскопической теории сплошной ядерной среды, получившей название «ядерной флюид-динамики». В настоящее время эта теория продолжает развиваться и рассматривается как наиболее адекватная модель ядерного ферми-вещества**. В рамках данной континуальной модели ядерной материи удается строго, с точки зрения математической физики, показать, что существование магнитных изоскалярных резонансов является следствием фермиевского движения нуклонов и связанной с ним динамической деформации поверхности Ферми, определяющей квантовую природу восстанавливающей силы поперечных колебаний ядра. В современной теории сплошных сред уравнения рассматриваемой в данном обзоре модели известны как уравнения тринадцатимоментного приближения [26], основанного на квантовом кинетическом уравнении (см., например, [25,27—30], где дается вывод этих уравнений и микроскопическое обоснование ядерной флюид-динамики). Описание коллективных ядерных движений, основанное на квантовом кинетическом уравнении, приведено в работах [31—34].

В настоящем обзоре мы представляем коллективную модель изоскалярных магнитных резонансов, следуя работам [35—40]. В этих статьях развита обобщенная на случай произвольной мультипольности флюид-

*Проблема собственных колебаний упругого шара на основе уравнения Ламэ была рассмотрена в конце прошлого столетия Ламбом [22]. Согласно Ламбу, собственные моды упругих колебаний шара характеризуются двумя ветвями. Первая — ветвь сфероидальных колебаний — связана с гармоническими деформациями формы шара. Данный тип движений во многом аналогичен колебаниям капли жидкости. Вторая — ветвь крутильных колебаний — связана с возникновением сдвиговых внутриобъемных деформаций. Современное изложение этой проблемы дано в [23]. С точки зрения данной классификации изоскалярные электрические резонансы описываются в терминах сфероидальных колебаний ядра, магнитные резонансы ассоциируются с возбуждением крутильных колебаний.

**Общепринятый теперь термин «ядерная флюид-динамика» используется главным образом для того, чтобы подчеркнуть отличие современного существенно квантово-макроскопического подхода к описанию коллективных возбуждений ядра, основанного на концепции упругоподобного нуклонного ферми-континуума, от ранней «ядерной гидродинамики», предполагающей классическую жидкостную трактовку сплошной ядерной среды.

динамическая модель магнитных резонансов и откорректированы предсказания для высокомультипольной дипольной моды и квадрупольного магнитного резонанса, сделанные в [10—14]. Мы также во многом опираемся на выводы работ, посвященных изучению магнитных возбуждений тяжелых сферических ядер, выполненных как в рамках макроскопических [18—21, 29,41—46], так и микроскопических [31,47—56] методов теоретического описания коллективного магнитного отклика сферических ядер. Современное состояние экспериментальной физики магнитных возбуждений достаточно полно отражено в обзоре Рамана, Фагга и Хикса [5]. В данном обзоре мы уделяем особое внимание обсуждению вопросов практического выявления крутильного отклика сферических ядер из данных по сечениям неупругого рассеяния электронов с возбуждением магнитных резонансов.

Мы придерживаемся следующего плана изложения.

В разд.2 сформулированы физические принципы, составляющие основу квантовой концепции упругости ядерного вещества и вариационный метод решения проблемы нормальных ядерных колебаний, проявлением которых являются изоскалярные мультипольные резонансы. В частности, показано, что уравнения ядерной флюид-динамики в длинноволновом пределе допускают два типа решений. Первое (полоидальное) решение соответствует сфероидальным колебаниям, связанным с электрическими изоскалярными резонансами. Второе (тороидальное) соответствует крутильным колебаниям, ответственным за магнитные изоскалярные резонансы. Таким образом, подчеркивается, что изоскалярные $E\lambda$- и $M\lambda$-резонансы могут быть описаны в рамках единого подхода.

Механизм длинноволновых крутильных колебаний подробно обсуждается в разд.3, где также представлен аналитический вывод выражений для мультипольного энергетического спектра и вероятностей возбуждения твистовых резонансов. Здесь же проведено сравнение предсказаний модели с данными дармштадтского и массачусетского линейных ускорителей по интегральным характеристикам магнитного квадрупольного резонанса в сферических ядрах.

Раздел 4 посвящен теоретическому описанию процесса неупругого рассеяния электронов на сферических ядрах. Мы приводим аналитически полученные формулы для коллективных переходных токовых плотностей и магнитных формфакторов твистовых резонансов. Представлены результаты численных расчетов сечений (e, e')-рассеяния в борновском приближении искаженных волн. На основе полученных переходных токовых плотностей даны оценки суммарных приведенных вероятностей возбуждения $M\lambda$, $T = 0$ резонансов и вычислены их осцилляторные силы. Предсказания сравниваются с данными DALINAC для сечений возбуждения $M2$-резонанса в ^{140}Ce.

Анализ высокоэнергетического дипольного магнитного отклика сферических ядер сделан в разд.5. Мы приводим оценки положения центроида

энергий, вероятности и сечения возбуждения высоколежащей 1^+-моды в зависимости от атомного номера и массового числа ядра. Предсказания сравниваются с данными линейного ускорителя электронов в Бейтсе (Bates LINAC) по выявлению этой моды в сечении неупругого рассеяния электронов на ^{208}Pb.

В разд.6 описывается флюид-динамическая модель затухания локальных вращательных колебаний на основе концепции вязкости ядерного вещества, введенной при анализе процесса деления. Приводятся аналитическая зависимость столкновительных ширин $M\lambda$, $T = 0$ резонансов от массового числа и мультипольности возбуждения.

В заключении обсуждаются представленные в обзоре результаты и основные выводы ядерного флюид-динамического подхода, касающиеся аспектов макроскопической трактовки магнитных резонансов.

2. ВАРИАЦИОННЫЙ МЕТОД ФЛЮИД-ДИНАМИЧЕСКОГО ОПИСАНИЯ КОЛЛЕКТИВНЫХ ДВИЖЕНИЙ НУКЛОНОВ

Современное понимание квантово-макроскопических особенностей коллективного ядерного отклика было достигнуто благодаря многоплановым исследованиям, выполненным в последние годы в рамках широко признанных и взаимно дополняющих методов ядерной флюид-динамики, изложению которых посвящены обзоры [25,29—31,57—62] и монографии [9,28], где исчерпывающим образом изложены физические принципы ядерной флюид-динамики и отражены работы, опубликованные до начала текущего десятилетия.

2.1. Уравнения ядерной флюид-динамики. Конструктивное утверждение ядерной флюид-динамики состоит в том, что адекватное макроскопическое описание коллективных движений нуклонов может быть дано в терминах тринадцати локальных переменных теории сплошных сред — плотности распределения массы ρ (**r**, t), трех компонент средней скорости возбуждаемого потока V_i (**r**, t) и девяти компонент симметричного тензора упругих напряжений P_{ij} (**r**, t), динамика которых подчиняется следующей замкнутой системе уравнений [35]:

$$\frac{d\rho}{dt} + \rho \frac{\partial V_k}{\partial x_k} = 0, \tag{2.1}$$

$$\rho \frac{dV_i}{dt} + \frac{\partial P_{ik}}{\partial x_k} + \rho \frac{\partial U}{\partial x_i} = 0, \tag{2.2}$$

$$\frac{dP_{ij}}{dt} + P_{ik} \frac{\partial V_j}{\partial x_k} + P_{jk} \frac{\partial V_i}{\partial x_k} + P_{ij} \frac{\partial V_k}{\partial x_k} = 0, \tag{2.3}$$

где d/dt — полная (субстанциональная) производная и n — плотность числа частиц. Здесь и далее по повторяющимся индексам подразумевается суммирование. Первое из уравнений — (2.1) представляет собой хорошо известное уравнение непрерывности. Уравнение (2.2) описывает движение потока ядерного вещества. Коллективные возбуждения ядра классифицируются по типу возмущаемого поля средней скорости движения нуклонов. U обозначает плотность внутренней энергии ядра, отнесенную к массе нуклона. Уравнение (2.3) контролирует динамику внутренних напряжений. Недиагональная структура тензора упругих напряжений подразумевает возможность того, что внешние возмущения могут вызывать коллективный отклик ферми-системы нуклонов, сопровождаемый анизотропными искажениями в распределении внутренних напряжений в объеме ядра. Это может иметь место либо в упругой среде, либо в вязкой жидкости. В идеальной (невязкой) жидкости процесс распространения возмущений происходит без разрушения равновесного изотропного состояния. Введение в описание коллективной ядерной динамики уравнения (2.3) фактически означает отождествление поведения сплошной ядерной материи с поведением идеально упругого вещества, характерным динамическим свойством которого является способность поддерживать незатухающие как продольные, так и поперечные колебания, поскольку, как показано в [23], уравнения (2.1)—(2.3) могут быть точно приведены к основным уравнениям линейной теории упругости (точнее говоря, уравнениям, управляющим колебаниями идеально упругого вещества). Данное обстоятельство является одной из главных причин того, что в ядерной флюид-динамике коллективный отклик нуклонов интерпретируется в терминах колебаний упругого континуума. Интересно отметить, что излагаемый в данном обзоре метод позволяет получить в аналитической форме спектр собственных мод длинноволновых упругих сфероидальных и крутильных колебаний шара, в то время как канонический метод теории упругости, основанный на уравнении Ламэ, не позволяет однозначным образом решить эту проблему [23].

Как было отмечено во введении, принципиальная возможность возбуждения в сферическом объеме несжимаемой ядерной материи поперечных сдвиговых колебаний является следствием того, что ядро представляет собой существенно квантовую ферми-систему частиц, распределенных по одночастичным орбитам среднего поля в соответствии с принципом Паули. В приводимых ниже построениях флюид-динамической модели квантовая природа ядерной среды отражена в том, что параметры основного состояния сферического ядра радиуса $R = r_0 A^{1/3}$ фм рассчитываются в приближении Томаса — Ферми для вырожденной по спину и изоспину ферми-системы нуклонов [14,18,24,27,35]. При моделировании ядра

сферической макрочастицей сплошного несжимаемого ферми-вещества обычно принимают, что масса и заряд однородно распределены в объеме ядра, а распределение напряжений, вследствие сферической симметрии, изотропно и описывается тензором второго ранга: $P_{ik}^{eq} = P_0\delta_{ik}$. Следует отметить, что предположение о возможности описания упругих свойств ядра в терминах тензора напряжений второго ранга является в значительной степени эвристическим. В «методе моментов», развитом Михайловым и Бальбуцевым с коллегами [29], описание ядерной динамики строится с использованием тензоров напряжений высших рангов (до пятого включительно).

2.2. Гамильтониан нормальных колебаний. Рассмотрим линейные колебания ядра, пренебрегая при этом флуктуациями плотности, т.е. полагая, что ядерная среда несжимаема. Линеаризованные уравнения движения, описывающие малые отклонения ядра от состояния равновесия, имеют вид:

$$\frac{\partial \delta V_k}{\partial x_k} = 0, \tag{2.4}$$

$$\rho_0 \frac{\partial \delta V_i}{\partial t} + \frac{\partial \delta P_{ik}}{\partial x_k} + \rho_0 \frac{\partial \delta U}{\partial x_i} = 0, \tag{2.5}$$

$$\frac{\partial \delta P_{ij}}{\partial t} + P_0 \left(\frac{\partial \delta V_i}{\partial x_j} + \frac{\partial \delta V_j}{\partial x_i} \right) + \delta_{ij} \left(\delta V_k \frac{\partial P_0}{\partial x_k} \right) = 0. \tag{2.6}$$

Собственные частоты колебаний могут быть получены на основе вариационного принципа, фактически представляющего собой современную формулировку «метода нормальных координат» Рэлея [22,63]. Исходным пунктом метода является уравнение энергетического баланса, которое получается умножением уравнения (2.5) на δV_i с последующим интегрированием по объему ядра:

$$\frac{\partial}{\partial t} \int_v \frac{1}{2} \rho_0 \delta V^2 d\tau - \int_v \delta P_{ij} \frac{\partial \delta V_i}{\partial x_j} d\tau + \oint_s [\rho_0 \delta U \delta V_i + \delta P_{ij} \delta V_j]_s \, d\sigma_i = 0. \tag{2.7}$$

Это уравнение контролирует сохранение энергии в процессе колебаний. Разделим, далее, пространственную и временную зависимости мультипольных флуктуаций потенциала и скорости:

$$\delta U(\mathbf{r}, t) = \phi^{\lambda}(\mathbf{r})\, \alpha_{\lambda}(t), \qquad \delta V_i(\mathbf{r}, t) = a_i^{\lambda}(\mathbf{r})\, \dot{\alpha}_{\lambda}(t). \tag{2.8}$$

Здесь $a_i^{\lambda}(\mathbf{r})$ — компоненты поля мгновенных смещений, и $\alpha_{\lambda}(t)$ рассматривается ниже как амплитуда (нормальная координата) в соответствии с трактовкой коллективных ядерных колебаний, данной Бором и

Моттельсоном [7]. Учитывая выражение для флуктуации скорости (2.8), из уравнения (2.6) находим, что флуктуация тензора напряжений выражается бесследовым симметричным тензором вида

$$\delta P_{ij}(\mathbf{r}, t) = -\left[P_0 \left(\frac{\partial a_i^\lambda}{\partial x_j} + \frac{\partial a_j^\lambda}{\partial x_i} \right) + \delta_{ij} \left(a_k^\lambda \frac{\partial P_0}{\partial x_k} \right) \right] \alpha_\lambda. \tag{2.9}$$

Подставляя (2.8) и (2.9) в (2.7), можно убедиться, что уравнение энергетического баланса (2.7) сводится к осцилляторному гамильтониану (энергия линейных колебаний):

$$H = \frac{B_\lambda \dot{\alpha}_\lambda^2}{2} + \frac{C_\lambda \alpha_\lambda^2}{2}, \tag{2.10}$$

который является интегралом коллективного ядерного движения. Из описанной процедуры вывода коллективного гамильтониана ядра следует, что массовый параметр B_λ и параметр жесткости C_λ определяются соотношениями [68]:

$$B = \int_V \rho_0 a_i^\lambda a_i^\lambda \, d\tau, \tag{2.11}$$

$$C = \frac{1}{2} \int_V P_0 \left(\frac{\partial a_i^\lambda}{\partial x_j} + \frac{\partial a_j^\lambda}{\partial x_i} \right)^2 d\tau +$$

$$+ \oint_S \left[P_S \left(\frac{\partial a_i^\lambda}{\partial x_j} + \frac{\partial a_j^\lambda}{\partial x_i} \right) a_j^\lambda - \left(\rho_0 \phi^\lambda - a_j^\lambda \frac{\partial P_0}{\partial x_j} \right) a_i^\lambda \right] d\sigma_i. \tag{2.12}$$

Таким образом, проблема нахождения собственных частот ядерных колебаний сводится к вычислению флуктуаций скорости (или, что то же самое, поля мгновенных смещений) и флуктуаций потенциала. Равновесные значения плотности ρ_0, внутриобъемного P_0 и поверхностного P_S давлений рассматриваются как главные параметры модели, отражающие специфику ядерной структуры. Так, в обобщенном методе Томаса — Ферми эти параметры вычисляются в приближении локальной плотности с использованием сил Скирма или Гони.

В работе [27] данный вариационный подход был использован при вычислении собственных энергий электрических изоскалярных резонансов. Для оценки объемного давления использовалось ферми-газовое приближение. Поверхность при этом считалась свободной от напряжений: $P_S = 0$. Предполагалось также, что благодаря несжимаемости и свойству насыщения ядерных сил флуктуациями плотности внутренней энергии можно пренебречь: $\delta U = 0$. В этом приближении уравнения (2.4)—(2.6) сводятся к

стандартному волновому уравнению для флуктуаций скорости δV_i (равно как и для флуктуаций напряжений δP_{ij}). Последнее, в свою очередь, сводится к уравнению Гельмгольца:

$$\Delta\delta\mathbf{V} + k^2\delta\mathbf{V} = 0, \tag{2.13}$$

если зависимость от времени основных динамических переменных коллективного движения нуклонов полагать гармонической. Многочисленные расчеты, выполненные в рамках ядерной флюид-динамики, показывают, что наблюдаемые энергии гигантских резонансов хорошо воспроизводятся на основе предположения о возбуждении длинноволновых ($k \to 0$) колебаний. В приближении длинноволновых колебаний уравнение (2.13), записанное в терминах поля мгновенных смещений, переходит в векторное уравнение Лапласа, дополненное (в силу несжимаемости) условием соленоидальности:

$$\Delta\mathbf{a}^{\lambda} = 0, \qquad \operatorname{div}\mathbf{a}^{\lambda} = 0. \tag{2.14}$$

Это уравнение имеет только два независимых, регулярных в нуле решения — полоидальное и тороидальное [63,64], обладающие противоположными пространственными четностями. Последнее свойство позволяет связать электрический и магнитный изоскалярные отклики ядра с типом возбуждаемого поля смещений.

2.3. Собственные сфероидальные колебания ядра: электрические изоскалярные резонансы. В ядерной флюид-динамике электрические резонансы интерпретируются в терминах сфероидальных колебаний ядра. Таким колебаниям соответствует полоидальное решение векторного уравнения Лапласа [63]:

$$\mathbf{a}(\mathbf{r}) = \operatorname{rot}\operatorname{rot}\mathbf{r}\, r^{\lambda}Y_{\lambda\mu}(\hat{\mathbf{r}}) = (\lambda + 1)\,\nabla r^{\lambda}Y_{\lambda\mu}(\hat{\mathbf{r}}). \tag{2.15}$$

Энергетический спектр изоскалярных электрических мультипольных резонансов, впервые полученный Никсом и Сирком в работе [27] (см. также [58, 62, 65—67]), дается выражением

$$E\,(E\lambda,\ T = 0) = \hbar\omega_F\left[\frac{2}{5}\,(2\lambda + 1)\,(\lambda - 1)\right]^{1/2}, \tag{2.16}$$

ω_F — основная частота коллективных колебаний сферической ферми-системы нуклонов:

$$\omega_F = \frac{v_F}{R} = \frac{\hbar}{2mr_0^2}\,(9\pi)^{1/3}\,A^{-1/3}, \tag{2.17}$$

v_F обозначена граничная скорость Ферми. Сплошная линия, изображенная на рис.1, воспроизводит результат вычислений, выполненных в [27] на

основе (2.16). Как подчеркивается в [27], формула (2.16) с трехпроцентной точностью воспроизводит наблюдаемые энергии квадрупольных электрических изоскалярных резонансов. Столь выразительное согласие теоретического предсказания энергии сильно коллективизированного отклика ядра, каковым является гигантский изоскалярный квадрупольный резонанс, указывает на то, что его формирование в значительной мере определяется свойством квантовой упругости ядерного вещества. Принимая это во внимание, в следующих разделах, посвященных магнитному изоскалярному отклику, мы придерживаемся тех же приближений и физических предположений.

Физическое содержание понятия упругости ядерной материи проясняют следующие аргументы. Рассматривая основное состояние ядра как насыщенную по спину и изоспину конечную ферми-систему нуклонов, можно отметить, что равновесный тензор изотропных напряжений (давление) изображается в импульсном пространстве ферми-сферой, радиус которой фиксирован граничной скоростью Ферми v_F, поскольку равновесное давление в ферми-системе задается уравнением $P_0 = \frac{\rho_0 v_F^2}{5}$. Имея в виду эту картину, флуктуации напряжений δP_{ij}, вводимые конструктивно при линеаризации уравнений (2.1)—(2.3) с помощью замены

$$P_{ij} \to P_0 \delta_{ij} + \delta P_{ij} \tag{2.18}$$

(совместно с подстановками $\rho \to \rho_0 + \delta\rho$ и $V_i \to V_i^0 + \delta V_i$, причем $\delta\rho = 0$ в силу несжимаемости и $V_i^0 = 0$, т.к. в основном состоянии предполагается отсутствие потоков), трактуются как квадрупольные искажения ферми-сферы. Такая интерпретация обусловлена тем, что тензор флуктуаций напряжений δP_{ij} обладает теми же свойствами симметрии, что и тензор квадрупольного момента (в частности, шпур этого тензора равен нулю). При возмущении основного состояния ядра, что в импульсном пространстве соответствует возмущению узловой структуры орбит одночастичного ферми-движения, заполняющих ферми-сферу, возникает обратная когерентная реакция нуклонных орбит, стремящаяся вернуть искаженную ферми-сферу в равновесное сферически-симметричное состояние. В координатном пространстве ядерного объема искажения ферми-сферы проявляются как сдвиговые анизотропные напряжения, локальное распределение которых описывается тензором (2.9). Таким образом, восстанавливающая сила упругих деформаций $F = G_\lambda \alpha_\lambda$ есть сила, возвращающая ферми-сфере равновесную сферически-симметричную форму, а распределению внутренних напряжений — равновесный изот-

ропный вид. Представленные рассуждения иллюстрируют квантовое происхождение ядерной упругости, которая, как подчеркивается в [28], не столько связана со спецификой оболочечной ядерной структуры, сколько является следствием более общих причин — фермиевского движения нуклонов и динамической деформации поверхности Ферми.

3. КОЛЛЕКТИВНАЯ МОДЕЛЬ КРУТИЛЬНОГО МАГНИТНОГО ОТКЛИКА ЯДРА

Изоскалярные магнитные коллективные моды в ядерной флюид-динамике связываются с возбуждением чисто вихревого поля смещений и описываются вторым из двух независимых решений векторного уравнения Лапласа (2.14). Найденное в [35] регулярное в нуле решение последнего, называемое тороидальным полем [63], имеет вид

$$\mathbf{a}_\lambda(\mathbf{r}) = \mathrm{rot}\,\mathbf{r}\, r^\lambda Y_{\lambda\mu}(\hat{\mathbf{r}}). \tag{3.1}$$

Поле (3.1) отвечает возбуждению дифференциально-вращательных осцилляций коллективного потока нуклонов. Как было показано в разд.2, уравнения классической гидродинамики, принятые за основу в стандартной модели жидкой капли, не имеют решений, соответствующих такого рода коллективным возбуждениям ядра. В работе [23] математически строго доказано, что уравнения ядерной флюид-динамики (2.4)—(2.6) могут быть сведены к уравнению для идеально упругой сплошной среды. В связи с этим естественным образом ядерной материи приписываются физические качества, присущие упругому континууму. Магнитные твистовые резонансы являются одним из наиболее характерных проявлений этого фундаментального свойства.

В ротационном характере коллективных крутильных колебаний можно убедиться, представив поле скорости $\delta\mathbf{V}$ в хорошо знакомом из классической механики виде

$$\delta\mathbf{V} = [\mathbf{r} \times \boldsymbol{\Omega}], \tag{3.2}$$

где

$$\boldsymbol{\Omega} = -\nabla r^\lambda Y_{\lambda\mu}(\hat{\mathbf{r}})\,\dot{\alpha}_\lambda$$

есть поле угловой скорости вращательных движений, которое, как ясно видно, является локальной векторной функцией. Коллективная амплитуда α_λ в геометрическом смысле представляет собой бесконечно малый азимутальный угол закручивания коллективного потока нуклонов вокруг оси, направление которой, например, при возбуждении ядра неупруго рас-

сеянными электронами, задается направлением поперечной (тороидальной) компоненты проникающего в ядро электромагнитного поля, индуцируемого потоком электронов. Как мы видим, флюид-динамическая модель расширяет представления о вращательных коллективных степенях свободы ядра. Рассматриваемые коллективные колебания потока нуклонов носят характер дифференциального (а не жесткого, твердотельного) вращения, что, как было подчеркнуто выше, может происходить только благодаря упругим свойствам ядерной ферми-среды.

3.1. Собственные моды крутильных ядерных колебаний и энергетический спектр $M\lambda$, $T = 0$ резонансов. Массовый параметр B_λ и параметр жесткости C_λ крутильных колебаний ядра вычисляются на основе тех же выражений (2.11) и (2.13), что и параметры электрических резонансов, что само по себе показывает общность флюид-динамического метода описания обоих типов резонансов. Подставляя (3.1) в (2.11), получаем следующее выражение для инерционного параметра:

$$B_\lambda = M \frac{\lambda\,(\lambda + 1)}{2\lambda + 1} \langle\, r^{2\lambda} \,\rangle. \tag{3.3}$$

Коэффициент крутильной жесткости, вычисленный в приближении Томаса — Ферми из соотношения (2.13), равен

$$C_\lambda = M \frac{\langle\, v^2 \,\rangle}{3} \lambda\,(\lambda^2 - 1) \langle\, r^{2\lambda - 2} \,\rangle, \tag{3.4}$$

где $M = mA$ — масса ядра, $\langle\, v^2 \,\rangle$ — средняя скорость ферми-движения нуклонов (в приближении ферми-газа $\langle\, v^2 \,\rangle = \frac{3}{5} v_F^2$) и $\langle\, r^\lambda \,\rangle$ — радиальный момент порядка λ. В дальнейших расчетах мы используем фермиевскую аппроксимацию плотности распределения частиц

$$n_0(r) = n(0)\,[1 + \exp\,\{(r - R)/a\}]^{-1}. \tag{3.5}$$

Детали вычислений интегралов, определяющих массовый параметр и параметр жесткости, вынесены в приложение 1.

Из мультипольной зависимости параметра крутильной жесткости (3.3) следует, что несжимаемое ядро не допускает дипольных длинноволновых крутильных колебаний: частота дипольной моды обращается в ноль. Нетрудно проверить, что возбуждение дипольного тороидального поля смещений приводит к твердотельному вращению ядра как целого без изменения его внутреннего состояния. Действительно, в случае $\lambda = 1$ компоненты поля скорости имеют вид: $\delta V_x = \Omega y$, $\delta V_y = -\Omega x$, $\delta V_z = 0$, что соответствует распределению поля скорости при твердотельном вращении ядра с уг-

Таблица 1. Теоретическая зависимость центроидов энергий и приведенных вероятностей возбуждения изоскалярных магнитных резонансов в сферических ядрах от массового числа и атомного номера

$M\lambda$	$E(M\lambda) = k_\lambda A^{-1/3}$, МэВ	$\sum B(M\lambda)\uparrow = \gamma_\lambda Z^2 A^{(2\lambda-4)/3}$, μ^2 фм$^{2\lambda-2}$
$M2$	$45\,A^{-1/3}$ МэВ	$0{,}7\,Z^2\,\mu^2$ фм^2
$M3$	$70\,A^{-1/3}$ МэВ	$2{,}3\,Z^2 A^{2/3}\,\mu^2$ фм^4
$M4$	$95\,A^{-1/3}$ МэВ	$5{,}9\,Z^2 A^{4/3}\,\mu^2$ фм^6

ловой частотой вращения $\Omega = \dot{\alpha}_\lambda$. Возбуждение дипольного поля дает вклад только в кинетическую энергию коллективного гамильтониана (2.10), тогда как потенциальная энергия вместе с коэффициентом крутильной жесткости обращается в ноль. Вспоминая из механики основную формулу для кинетической энергии вращения $T_{вр} = \frac{1}{2} J\Omega^2$, видим, что массовый коэффициент есть просто момент инерции ядра: $B_\lambda = J_\lambda$. Легко убедиться, что при $\lambda = 1$ вычисленный массовый коэффициент точно совпадает с моментом инерции твердого шара: $J_1 = (2/5)\,MR^2$.

В ядерной флюид-динамике энергии мультипольных колебаний $E_\lambda = \hbar\omega_\lambda$ отождествляются с центроидами энергий коллективных возбуждений (в данном случае изоскалярных резонансов). Полный мультипольный спектр энергий $E(M\lambda, T = 0) = \hbar\sqrt{C_\lambda / B_\lambda}$ магнитных резонансов, трактуемых в терминах собственных мод длинноволновых крутильных колебаний сферического ядра, имеет вид [38,39]:

$$E(M\lambda, T = 0) = \hbar\left[\frac{\langle v^2\rangle}{3}(2\lambda + 1)(\lambda - 1)\frac{\langle r^{2\lambda-2}\rangle}{\langle r^{2\lambda}\rangle}\right]^{1/2}. \qquad (3.6)$$

В приближении резкого края это выражение преобразуется к следующему*:

$$E(M\lambda, T = 0) = \hbar\omega_F\left[\frac{1}{5}(2\lambda + 3)(\lambda - 1)\right]^{1/2}. \qquad (3.7)$$

*В приближении резкого края массовый параметр (момент инерции крутильных колебаний) и параметр крутильной жесткости, соответственно, равны [35]: $R_\lambda = 3M\frac{\lambda(\lambda+1)}{(2\lambda+1)(2\lambda+3)}R^{2\lambda}$ и $C_\lambda = \frac{3}{5}Mv_F^2\frac{\lambda(\lambda^2-1)}{(2\lambda+1)}R^{2\lambda-2}$.

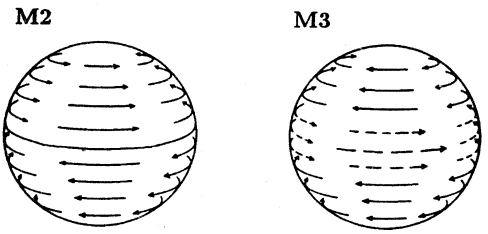

Рис. 2. Геометрическая картина магнитных квадрупольного (слева) и октупольного (справа) твистовых откликов сферического ядра

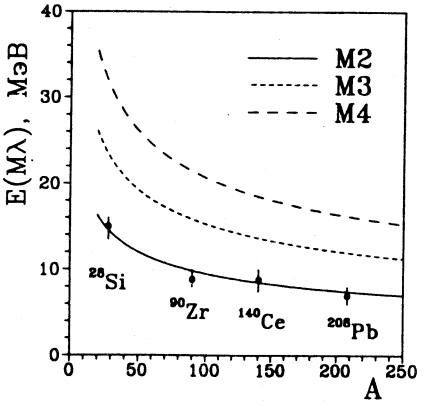

Рис. 3. Теоретические оценки положения центроидов энергий изоскалярных магнитных квадрупольных резонансов в зависимости от массового числа (линии). Символы — данные DALINAC [3,4]

Приближенные оценки центроидов энергий мультипольных твистовых резонансов в зависимости от массового числа приведены в табл.1. Эти оценки получены при значении параметра ядерного радиуса $r_0 = 1{,}3$ фм. Модель предсказывает, что изоскалярный магнитный квадрупольный резонанс занимает энергетически нижайшее положение. Этот факт является следствием предположения о длинноволновом характере возбуждаемых колебаний, в которые вовлекается вся масса сферического ядра. Как уже отмечалось, квадрупольное возбуждение ассоциируется с крутильными колебаниями, при которых полушария сферического ядра осциллируют в противофазе, как показано в левой части рис.2. В правой части рисунка изображено распределение смещений, характеризующее октупольный магнитный отклик.

Накопленная к настоящему времени экспериментальная информация о магнитных резонансах с $\lambda \geq 2$ не столь богата по сравнению с информацией об электрических. На рис.3 приведены предсказываемые ядерной флюид-динамикой центроиды энергий $M\lambda$, $T = 0$ резонансов в зависимости от массового числа. Судя по литературе [5], наиболее надежными являются данные Дармштадтского линейного ускорителя (DALINAC), полученные при изучении сечений неупругого рассеяния под углом $\theta = 165°$ электронов с энергией 20—100 МэВ на ядрах ^{28}Si, ^{90}Zr, ^{140}Ce и ^{208}Pb [1,3,4]. Согласно Рихтеру, сила $M2$-коллективных возбуждений сферических ядер локализо-

вана в области энергий, центроид которой хорошо аппроксимируется следующей зависимостью от массового числа [3,69]:

$$E_{exp} \sim 44\, A^{-1/3}\ \text{МэВ}. \qquad (3.8)$$

Такая зависимость, как отмечалось выше, свидетельствует об объемном характере магнитных возбуждений. Как видно из табл.2, экспериментальная систематика энергий $M2$-резонансов [5] в сферических ядрах находится в неплохом согласии с предсказаниями ядерной флюид-динамики положений центроидов энергий твистовых коллективных возбуждений. Приведенные численные оценки получены при значениях параметра радиуса $r_0 = 1{,}2$–$1{,}3$ фм и параметра диффузности $a = 0{,}55$–$0{,}6$ фм. Разброс в теоретических значениях приведенных в табл.2 характеристических параметров резонансов обусловлен вариацией этих параметров в указанных пределах.

Таблица 2. Теоретические предсказания положения центроидов энергий, приведенных вероятностей возбуждения и столкновительных ширин изоскалярных магнитных твистовых резонансов в сферических ядрах. Экспериментальные данные DALINAC

Элемент	E ($M2$), МэВ		$\sum B$ ($M2$)↑, μ^2 фм^2		Γ ($M2$)↑, МэВ
	Теория	Эксперимент	Теория	Эксперимент	Теория
^{28}Si	11—13	13—16	230 ± 20	340 ± 20	1,5 ± 0,5
^{90}Zr	8—10	8—10	1300 ± 300	1620	1,0 ± 0,3
^{140}Ce	7,5—9	7,5—10	3100 ± 300	6000 ± 600	0,8 ± 0,3
^{208}Pb	6,5—8	6—8,5	5300 ± 300	8500 ± 750	0,6 ± 0,2

Необходимо также отметить, что выводы данной модели совпадают с результатами, полученными в рамках метода моментов функции Вигнера, в том случае, если ограничиться при описании тензорами деформаций второго ранга [29]. Одна из важных особенностей метода моментов состоит в том, что частоты колебаний за рамками длинноволнового приближения рассчитываются путем самосогласованного включения высокомультипольных деформаций равновесного ферми-распределения, описывающихся тензорами деформаций высших рангов. Следствия данного эффекта при описании резонансов высших мультипольностей $\lambda \geq 3$ подробно обсуждаются в обзорах [29,61].

Важный вывод ядерной флюид-динамики состоит в том, что гигантские резонансы формируются когерентными колебаниями всех нуклонов в полном ядерном объеме, т.е. носят объемный, а не поверхностный характер. При возбуждении поверхностных колебаний в коллективное движение вовлекается только периферийная часть нуклонов. В работе [67] показано, что степень коллективности поверхностных возбуждений ниже, чем объемных. Об объемном характере гигантских возбуждений свидетельствует также $A^{1/3}$-зависимость центроида энергии резонанса от массового числа [28]. Влияние диффузности ядерного края на энергии коллективных возбуждений продемонстрировано в [62,70]. Расчет с реалистическим распределением плотности уменьшает значения энергий по сравнению с их значениями, вычисленными в приближении резкого края ядра [28].

Исследование зависимости энергии твистового резонанса от температуры показало [71], что с ростом последней от 0 до 5 МэВ центроиды энергий твистовых резонансов сдвигаются в высокоэнергетическую область не более чем на 1—2%.

Говоря об общих тенденциях в относительном положении центроидов энергий магнитных и электрических изоскалярных резонансов в спектре сферического ядра, следует оценить отношение

$$\frac{E\,(M\lambda,\ T=0)}{E\,(E\lambda,\ T=0)} = \frac{(2\lambda+3)}{2\,(2\lambda+1)} < 1, \qquad \lambda \geq 2. \tag{3.9}$$

Из (3.9) следует, что центроиды энергий магнитных изоскалярных резонансов мультипольности $\lambda \geq 2$ в энергетическом спектре расположены ниже центроидов энергий электрических изоскалярных резонансов той же мультипольности. Это условие также выполняется и для дипольных изоскалярных резонансов, в предположении о несжимаемости ядерного вещества. В расчетах [18,29,39,72,73], выполненных в рамках различных методов ядерной флюид-динамики, изоскалярный дипольный электрический резонанс связывается с возбуждением в объеме ядра полоидальных токовых колебаний тороидоподобной структуры. Положение центроида этого резонанса характеризуется оценкой 50—70 $A^{-1/3}$ МэВ. Экспериментальная систематика энергий дипольного магнитного резонанса хорошо аппроксимируется оценкой 41 $A^{-1/3}$ МэВ.

3.2. Суммарная вероятность возбуждения $M\lambda$, $T = 0$ твистовых мод. Излагаемый макроскопический подход позволяет сделать вполне конкретные выводы о степени коллективности магнитных возбуждений резонансов, мерой которой служит приведенная вероятность возбуждения. Эта характеристика может быть определена как среднее по времени от квадрата модуля магнитного мультипольного момента:

$$B\,(M\lambda) = \begin{pmatrix} \hat{J}_f \\ \overline{\times} \\ J_i \end{pmatrix}^2 \langle |\mathcal{M}\,(M\lambda,\, t)|^2 \rangle_t \,. \qquad (3.10)$$

Здесь J_i и J_f — полный момент ядра в начальном и конечном состояниях соответственно, $\hat{J} = \sqrt{2\lambda + 1}$. Определение магнитного момента через флуктуации электрического тока дано во введении. Здесь и далее мы приводим результаты вычислений в системе с фиксированной полярной осью.

Мы рассматриваем отклик ядра на возмущение, которое не затрагивает спиновых степеней свободы и не снимает изоспинового вырождения в ферми-системе нуклонов. Подчеркнем, что изучаемые ротационные флуктуации поля скорости происходят при постоянной плотности распределения заряда $n_e = (eZ/A)\, n_0$ и массы $\rho_0 = mn_0$. В рамках таких предположений коллективные осцилляции нуклонов когерентно соотнесены с колебаниями соленоидального электрического тока, пространственное распределение которого характеризуется плотностью*

$$\mathbf{j}_\lambda\,(\mathbf{r},\, t) = \frac{eZ}{A}\, n_0\, \mathrm{rot}\, \mathbf{r}\, r^\lambda Y_{\lambda 0}(\hat{\mathbf{r}})\, \dot{\alpha}_\lambda\,(t), \qquad (3.11)$$

где $\alpha_\lambda(t) = \alpha_\lambda^0\, e^{i\omega_\lambda t}$ и α_λ^0 — амплитуда нулевых колебаний, которая, согласно Бору и Моттельсону, дается выражением [7]:

$$\alpha_\lambda^0 \equiv \langle |\alpha_\lambda(t)|^2 \rangle_t^{1/2} = \left[\frac{\hbar}{2B_\lambda\, \omega_\lambda} \right]^{1/2}. \qquad (3.12)$$

С учетом сказанного, приведенная вероятность возбуждения $M\lambda$, $T = 0$ твистовой моды определяется следующим выражением:

$$B\,(M\lambda) = \gamma_\lambda\, Z^2\, A^{(2\lambda-4)/3}\, \mu^2\, \text{фм}^{2\lambda-2}, \qquad (3.13)$$

где

$$\gamma_\lambda = \frac{3}{4\pi}\, \frac{\lambda\,(2\lambda+1)}{(\lambda+1)} \left[\frac{(\lambda-1)}{5\,(2\lambda+3)} \right]^{1/2} (9\pi)^{1/3}\, r_0^{2\lambda-2}.$$

*Сравнивая формулу (3.11) с хорошо известным из классической электродинамики [74,75] выражением тока намагничивания

$$\mathbf{j}(\mathbf{r},\, t) = c\ \mathrm{rot}\ \mathbf{M}(\mathbf{r},\, t),$$

находим

$$\mathbf{M}(\mathbf{r},\, t) = \frac{eZ}{cA}\, n_0\, \mathbf{r}\, r^\lambda Y_{\lambda 0}(\hat{\mathbf{r}}) \dot{\alpha}_\lambda(t).$$

Таким образом, дифференциально-вращательные колебания ядра сопровождаются осцилляциями соленоидального тока намагничивания.

Эта формула получена в приближении резкого края ядра, которое позволяет выделить явную зависимость $B\,(M\lambda)$ от атомного номера и массового числа.

Приведенные рассуждения показывают, что переходы ядра в возбужденные состояния с отличным от нуля магнитным мультипольным моментом могут быть вызваны возбуждением коллективных ротационных колебаний потока нуклонов. Усредненный по времени магнитный мультипольный момент, обусловленный такими колебаниями с частотой ω_λ, дается выражением

$$\mathcal{M}(M\lambda) = \frac{Z}{A}\sqrt{\frac{\lambda}{\lambda+1}}\,\frac{2B_\lambda\,\omega_\lambda}{\hbar}\,\alpha_\lambda^0\left(\frac{e\hbar}{2mc}\right), \qquad \lambda \geq 2. \tag{3.14}$$

Суммарные вероятности $M\lambda$, $T = 0$ резонансов в зависимости от атомного номера и массового числа, вычисленные по формуле (3.13), приведены в табл.1. Если ограничиться приближением резкого края, можно отметить, что в аналитические выражения для энергии (3.7) и вероятности возбуждения (3.13) входит единственный параметр — константа ядерного радиуса r_0, дающая некоторый разброс в численных оценках этих величин. Отметим следующую внутримодельную корреляцию между положениями центроидов энергий и величинами приведенных вероятностей и значением параметра r_0. С увеличением r_0 энергия магнитной твистовой моды произвольной мультипольности уменьшается пропорционально r_0^2, а суммарная приведенная вероятность растет как $r_0^{2\lambda-2}$.

Вопрос о сравнении полученных в данной коллективной модели приведенных вероятностей возбуждения $M\lambda$, $T = 0$ резонансов с экспериментальными данными требует специальных комментариев. Реальные измерения показывают, что магнитная мультипольная сила расфрагментирована по довольно большому числу состояний. Например, по данным работы [69] в ядре ^{90}Zr сила $M2$-коллективных возбуждений распределена между 34 состояниями в области энергий 8 ÷ 10 МэВ; центр локализации силы находится при энергии ~ 9 МэВ. Экспериментальной интегральной характеристикой интенсивности возбуждения резонанса является суммарная вероятность $M\lambda$-переходов: $\sum B_{\text{exp}}(M\lambda)$. Согласно общепринятой в макроскопических теориях точке зрения, именно с этой величиной следует сравнивать теоретические оценки вероятности возбуждения изучаемой коллективной моды. Такое сравнение приведено в табл.2 для сферических ядер, в спектрах которых впервые был идентифицирован магнитный квадрупольный резонанс.

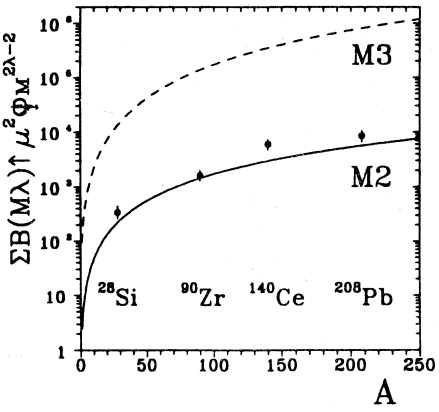

Рис. 4. Рассчитанные в рамках флюид-динамической модели суммарные приведенные вероятности изоскалярных квадрупольного и октупольного магнитных резонансов как функции массового числа. Символы — данные DALINAC [3,4]

На рис.4 изображены суммарные приведенные вероятности $M2$- и $M3$-твистовых возбуждений как функции массового числа. Зависимость атомного номера от массового числа параметризовалась известной эмпирической формулой [76]:

$$Z = \frac{A}{2 + 0{,}015\, A^{2/3}}, \qquad (3.15)$$

которая хорошо описывает ядра, расположенные вдоль дорожки β-стабильности. Символами нанесены данные DALINAC, представленные в обзорных докладах Рихтера [1,3,4]. Видно, что теоретические предсказания для абсолютных значений $B\,(M\lambda)$, выводимые из рассматриваемой коллективной флюид-динамической модели, находятся в неплохом качественном согласии с экспериментальными. Одной из причин недостатка предсказываемой магнитной силы, как это следует из табл.2, по сравнению с экспериментальными данными являются, как мы полагаем, упрощенные предположения о ядерной структуре. Действительно, в представленной модели индивидуальность каждого ядра специфицируется лишь его атомным и массовым числами, и не учитываются особенности оболочечной структуры. Последнее обстоятельство является, естественно, слишком сильным упрощением. Тем не менее, как видно из рис.4, модель качественно правильно передает наблюдаемую зависимость $B\,(M2)$-фактора от массового числа.

В данном разделе мы привели оценки суммарных вероятностей возбуждения магнитных коллективных мод, полученные безотносительно к тому, какой пробной заряженной частицей индуцированы соленоидальные колебания электрического тока внутри ядра. Вычисленная вероятность является количественной мерой интенсивности изоскалярного резонанса, обусловленного когерентными колебаниями в фазе протонов и нейтронов. Поэтому вероятность (3.13) следует трактовать как приведенную вероятность кол-

лективного отклика ядра, возбуждаемого поперечной (тороидной) компонентой электромагнитного поля. В следующем разделе рассматривается теория возбуждения $M\lambda$, $T = 0$ твистовых мод в реакции неупругого рассеяния электронов.

4. ВОЗБУЖДЕНИЕ КРУТИЛЬНЫХ $M\lambda, T = 0$ МОД В РЕАКЦИИ НЕУПРУГОГО РАССЕЯНИЯ ЭЛЕКТРОНОВ

Эксперименты по рассеянию электронов на ядрах служат источником наиболее достоверных данных о равновесных и динамических ядерных свойствах. Как известно, электрические гигантские изоскалярные резонансы (с $\lambda \geq 2$) были открыты именно в экспериментах по неупругому рассеянию электронов. Более того, практически вся накопленная к настоящему времени информации по $E\lambda$, $T = 0$ резонансам была получена из анализа сечений (e, e')-реакции. Поскольку ядерная флюид-динамика интерпретирует магнитные твистовые резонансы на основе тех же самых физических принципов, что и электрические, то, как нам представляется, (e, e')-реакция должна быть столь же эффективным средством возбуждения данной коллективной ветви ядерного спектра. Примечательно, что первая последовательная теория (e, e')-рассеяния с возбуждением изоскалярных коллективных состояний электрического типа, развитая Тасси [78], была также основана на макроскопической (капельной) модели ядерной структуры. Предсказываемые этой моделью сечения (e, e')-реакции по форме удовлетворительно согласуются с экспериментом, что свидетельствует о корректности предположений относительно типа коллективных движений нуклонов, индуцируемых налетающими электронами (продольных конвекционных колебаний тока с потенциальным полем скорости). Что же касается теории магнитного (e, e')-рассеяния (с возбуждением магнитных коллективных мод), то сколько-нибудь последовательный макроскопический подход, основанный на коллективной модели ядра, насколько нам известно, не обсуждался в литературе.

В данном разделе представлен, следуя [40], один из возможных вариантов теории магнитного мультипольного ядерного отклика в неупругом рассеянии электронов, основанный на коллективной флюид-динамической модели, рассматривающей ядро как сферическую макрочастицу насыщенного по спину и изоспину упругоподобного несжимаемого ферми-континуума. Под вырождением по спину подразумевается, что суммарный магнитный момент основного состояния четно-четного сферического ядра равен нулю. Рассматриваемый механизм «намагничивания» ядра неупруго рассеянными электронами (т.е. перехода из основного в возбужденное состояние с отличным от нуля магнитным моментом) несет в себе исключительно

классическое, с точки зрения электродинамики сплошных сред, содержание. Как видно из представленной выше математической трактовки магнитных мультипольных резонансов, колебания плотности электрического тока описываются в терминах поля скорости. Используемое классическое представление плотности тока не связано явным образом с квантово-механическим его определением и, как следствие этого, с квантово-механическим оператором магнитного мультипольного момента (последний, как известно, в одночастичной модели представляется суммой операторов, явно зависящих от орбитального и спинового моментов нуклонов). В этой связи уместно подчеркнуть, что оставаясь в рамках макроскопического описания коллективной динамики нуклонов, было бы непоследовательно пытаться проинтерпретировать рассмотренный механизм в концептуальных терминах микроскопической одночастичной модели оболочек (т.е. говорить о спиновой или орбитальной природе переходов). Цель, которую преследует макроскопическое описание коллективного ядерного отклика, состоит, как мы уже отмечали во введении, в поиске адекватной динамической теории сплошной ядерной среды. Основная направленность нашего изучения нацелена на выявление в ядерном отклике динамических свойств, присущих упругой сплошной среде, и сопоставление результатов с хорошо известными исследованиями, выполненными на основе представлений о ядре, как о капле однородно заряженной несжимаемой жидкости.

Необходимо подчеркнуть, что к настоящему моменту имеется довольно обширная литература по микроскопическому анализу механизмов возбуждения магнитных коллективных состояний в реакции неупругого рассеяния электронов (см., например [12, 51—53, 79,80]). Основное внимание в этих исследованиях уделено дипольным и квадрупольным коллективным магнитным возбуждениям. Микроскопические особенности возбуждения в (e, e')-рассеянии магнитных состояний высокой мультипольности в тяжелых ядрах обсуждаются в работе [54], в легких ядрах — в [80]. Судя по литературе, главным объектом изучения магнитного отклика деформированных ядер является дипольная ножничная мода (см. [81—89], а также приведенные там ссылки). Теоретическому изучению распределения $M2$- и $M3$-силы отклика деформированных ядер посвящены работы [91,92], выполненные в рамках микроскопической квазичастично-фононной модели ядерных коллективных возбуждений [77].

Основная цель формулируемого нами подхода состоит в том, чтобы дополнить перечисленные выше исследования и выяснить качественные закономерности зависимости интегральных параметров магнитных твистовых резонансов, извлекаемых экспериментально из анализа (e, e')-реакции, от атомного номера, массового числа и мультипольности возбуждаемой моды.

4.1. Краткий обзор теории электронного рассеяния. Для полноты изложения мы начнем с краткого обзора известных формул теории рассе-

яния неполяризованных электронов на неориентированной мишени. Выражение для дифференциального сечения (e, e')-реакции в борновском приближении плоских волн имеет вид [93—95]:

$$\frac{d\sigma}{d\Omega} = \sigma_M f_{\text{rec}} \left\{ \left(\frac{q_\lambda}{q} \right)^2 |S^L(q)|^2 + \left[\frac{1}{2} \left(\frac{q_\lambda}{q} \right)^2 + \text{tg}^2 \frac{\theta}{2} \right] |S^T(q)|^2 \right\}. \qquad (4.1)$$

Здесь $\sigma_M = \left[\frac{Z \alpha \hbar c \cos \theta/2}{2E \sin^2 \theta/2} \right]^2$ — моттовское сечение рассеяния для единичного заряда, $f_{\text{rec}} = \left[1 + \frac{2E \sin^2 \theta/2}{Mc^2} \right]^{-1}$ — фактор отдачи, E — энергия налетающего электрона, M — масса ядра-мишени, θ — угол рассеяния. Переданный импульс $q = \sqrt{q_\lambda^2 + \omega^2}$, $q_\lambda = 2\sqrt{EE_0}/\hbar c \sin \theta/2$, $\hbar\omega = E - E_0$ — энергия возбуждения ядра. Ядерная структура проявляется в сечении рассеяния через продольный и поперечный формфактор. Продольный (кулоновский) формфактор $|S^L(q)|^2 = \sum_\lambda |F_\lambda^C(q)|^2$ содержит всю информацию о пространственном распределении зарядовой плотности ядра, трансверсальный формфактор $S^T(q)$ связан с переходной токовой плотностью и является суммой формфакторов электрических и магнитных мультипольных переходов:

$$|S^T(q)|^2 = \sum_\lambda \{ |F_\lambda^E(q)|^2 + |F_\lambda^M(q)|^2 \}.$$

При рассеянии назад возбуждаются только токовые поперечные колебания нуклонов. Поэтому измерение сечений рассеяния электронов на угол $\theta = 180°$ является наиболее информативным в плане изучения состояний магнитного типа.

Магнитный формфактор $F_\lambda^M(q)$ связан с переходной токовой плотностью $J_{\lambda,\lambda}(r)$ преобразованием Фурье — Бесселя [95]:

$$F_\lambda^M(q) = \frac{\sqrt{4\pi}}{Z} \frac{\hat{J}_f}{\hat{J}_i} \int_0^\infty J_{\lambda,\lambda}(r)\, j_\lambda(qr) r^2 dr, \qquad (4.2)$$

$j_\lambda(qr)$ — функция Бесселя ранга λ, J_i и J_f — полный момент ядра в начальном и конечном состояниях соответственно, $\hat{J} = \sqrt{2\lambda + 1}$.

Главным и единственным элементом борновского формализма, содержащим информацию о ядерной структуре, являются переходные зарядовые

и токовые плотности. Рассчитываемые в ядерной флюид-динамике характеристики возбуждений несут в себе существенно коллективное содержание. Поэтому сравнение предсказываемых переходных токовых плотностей, формфакторов и вероятностей возбуждения магнитных твистовых резонансов целесообразно проводить только с интегральными характеристическими параметрами, должным образом просуммированным по параметрам реально наблюдаемых состояний.

4.2. Переходная токовая плотность и формфактор $M\lambda$, $T = 0$ резонансов. Для анализа процесса электронного рассеяния удобнее воспользоваться несколько иным, эквивалентным (4.2), представлением решения векторного уравнения Лапласа, описывающим длинноволновые мультипольные крутильные колебания сферического ядра (см., например, [96], с.188):

$$\mathbf{a}_\lambda(\mathbf{r}) = -\,\mathrm{i} r^\lambda \mathbf{Y}^0_{\lambda,\lambda 1}(\hat{\mathbf{r}}), \quad \mathbf{a}^*_\lambda(\mathbf{r}) = \mathrm{i} r^\lambda [\mathbf{Y}^0_{\lambda,\lambda 1}(\hat{\mathbf{r}})]^* = \mathbf{a}_\lambda(\mathbf{r}), \tag{4.3}$$

где $\mathbf{Y}^\mu_{\lambda\lambda' 1}(\hat{\mathbf{r}})$ — векторные сферические гармоники, обладающие следующими свойствами:

$$\int [\mathbf{Y}^\mu_{\lambda_1\lambda_2 1}(\hat{\mathbf{r}})]^* \cdot \mathbf{Y}^{\mu'}_{\lambda'_1\lambda'_2 1}(\hat{\mathbf{r}}) d\hat{\mathbf{r}} = \delta_{\mu\mu'} \delta_{\lambda_1\lambda'_1} \delta_{\lambda_2\lambda'_2}, \tag{4.4}$$

$$[\mathbf{Y}^\mu_{\lambda_1\lambda_2 1}(\hat{\mathbf{r}})]^* = (-)^{\lambda_1+\lambda_2+\mu+1} \mathbf{Y}^{-\mu}_{\lambda_2\lambda_1 1}(\hat{\mathbf{r}}). \tag{4.5}$$

Распределение соленоидального электрического тока в ядре, индуцируемого налетающим электроном, в данном подходе описывается классическим выражением

$$\mathbf{j}_\lambda(\mathbf{r}, t) = n_e \delta\, \mathbf{V}_\lambda(\mathbf{r}, t) = n_e \mathbf{a}_\lambda(\mathbf{r})\, \dot{\alpha}_\lambda(t). \tag{4.6}$$

Коллективная переходная токовая плотность магнитного крутильного отклика мультипольности λ в системе с фиксированной полярной осью выражается формулой

$$J_{\lambda,\lambda'}(r) = \left\langle \left| \frac{\mathrm{i}}{ec} \int \mathbf{j}_\lambda(\mathbf{r}, t) \cdot \mathbf{Y}^0_{\lambda\lambda' 1}(\hat{\mathbf{r}}) d\hat{\mathbf{r}} \right|^2 \right\rangle^{1/2}_t = N_\lambda n_e(r) r^\lambda,$$

$$N_\lambda = \frac{\alpha^0_\lambda \omega_\lambda}{ec} = \sqrt{\frac{\hbar\omega_\lambda}{2e^2c^2B_\lambda}}. \tag{4.7}$$

Здесь, как и ранее, $\langle \ldots \rangle_t$ означает усреднение по времени.

На рис.5 приведены вычисленные для ядра ^{90}Zr переходные токовые плотности (4.7), соответствующие возбуждению магнитных резонансных мод различной мультипольности. Из этого рисунка, в частности, следует, что коллективный магнитный отклик ядра носит объемный характер. С рос-

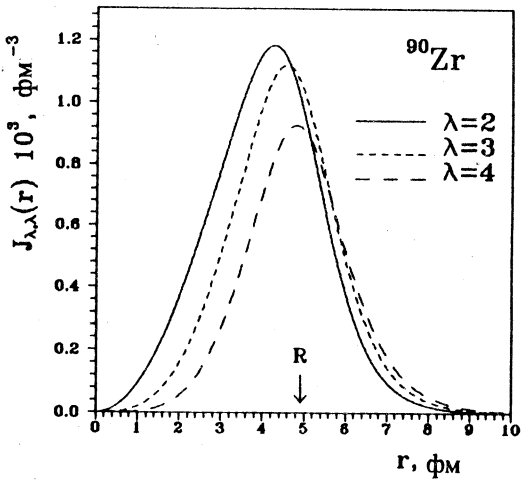

Рис. 5. Коллективные переходные токовые плотности для магнитных квадрупольного, октупольного и гексадекапольного изоскалярных резонансов в ^{90}Zr. Расчет выполнен с реалистическим распределением плотности числа частиц

том мультипольности максимум функции $J_{\lambda,\lambda}$ смещается в сторону поверхности ядра.

Явное выражение для коллективного магнитного мультипольного формфактора возбуждений, связанных с длинноволновыми дифференциально-вращательными колебаниями потока, в плосковолновом борновском приближении имеет вид

$$|F_\lambda^M(q)|^2 = \frac{4\pi}{Z^2}(2\lambda+1)N_\lambda^2\left|\int_0^\infty n_e r^{\lambda+2} j_\lambda(qr)dr\right|^2. \qquad (4.8)$$

В приближении резкого края данный интеграл может быть вычислен аналитически [36,38]:

$$|F_\lambda^M(q)|^2 = \frac{4\pi n_e^2}{Z^2}R^{2(\lambda+3)}(2\lambda+1)N_\lambda^2\left[\frac{(2\lambda+1)j_\lambda(qR)-qRj_{\lambda-1}(qR)}{q^2R^2}\right]^2. \qquad (4.9)$$

Вычисленные здесь переходные токовые плотности и формфакторы характеризуют вызванные налетающим электроном длинноволновые коллективные колебания нуклонов, приводящие к возбужденным состояниям с отличными от нуля магнитными мультипольными моментами, и содержат информацию о макроскопическом распределении потока нуклонов. Как мы уже отмечали, оставаясь в рамках изложенной выше флюид-динамической модели магнитных возбуждений, строго говоря, не представляется возможным количественно выявить роль спинового вклада в формирование $M2$-резонанса, поскольку макроскопическая плотность электрического тока не разделяется на конвекционную и спиновую компоненты, как то предписывает микроскопический подход. Более того, изложенная трактовка $M\lambda$-ядер-

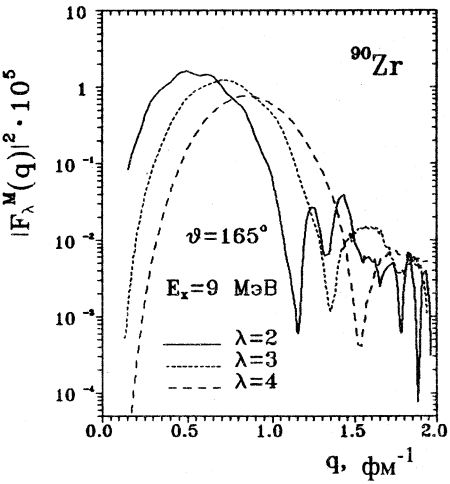

Рис. 6. Коллективные формфакторы магнитных изоскалярных резонансов, возбуждаемых в реакции неупругого рассеяния электронов под углом 165° на ядре ^{90}Zr, как функции переданного импульса q. Расчет выполнен в приближении искаженных волн

ного отклика не затрагивает вопроса о распределении силы магнитного отклика по изоспиновым каналам. Ясно, что проблема доминантности спинового и конвекционного вкладов в $M\lambda$, $T=0$ отклик ядра находится в компетенции микроскопической теории коллективных ядерных возбуждений, основанной на оболочечной картине ядерной структуры. Обсуждению этих проблем посвящены работы [12,48,50,53,56,69], в которых 2^- коллективный отлик сферического ядра анализировался с микроскопической точки зрения. В [31,89] отмечается, что магнитный твистовый отклик по своей макроскопической динамической природе коллективных ядерных движений аналогичен изовекторной 1^+-ножничной моде в деформированных ядрах.

Результаты наших расчетов для магнитных формфакторов, полученные в приближении искаженных волн, для ядра ^{90}Zr представлены на рис.6—8. При фиксированном угле рассеяния варьировалась энергия налетающих частиц так, чтобы переданный импульс мог меняться, но возбуждался бы при этом определенный уровень с энергией, соответствующей центру локализации твистового магнитного резонанса. На рис.6 изображены коллективные магнитные формфакторы $|F_\lambda^M(q)|^2$ мультипольности $\lambda=2,3,4$ в зависимости от переданного импульса, вычисленные при угле рассеяния $\theta=165°$. Область малых переданных импульсов ($q<0{,}5$ фм$^{-1}$) является наиболее предпочтительной для регистрации $M2$-резонанса по сравнению с резонансными модами высших мультипольностей [36]. Примечательным является тот факт, что в области $q\approx 1$ фм$^{-1}$, где гексадекапольный формфактор имеет первый максимум, квадрупольный отклик минимален. Похожая картина наблюдается и в области второго максимума функции $|F_4^M(q)|^2$.

Рис.7 дает представление о виде $|F_2^M(q)|^2$ в зависимости от угла рассеяния θ электронов с первоначальной энергией $E=40$, 80, 120 и 200 МэВ; с рос-

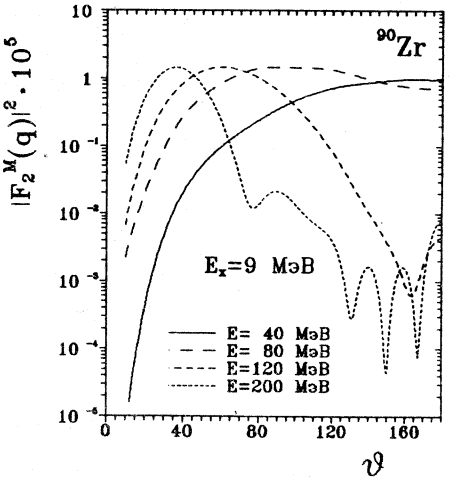

Рис.7. Зависимость коллективного формфактора для квадрупольного магнитного резонанса от угла рассеяния электронов θ. Расчет выполнен в приближении искаженных волн для ^{90}Zr при указанных значениях энергии налетающих электронов E

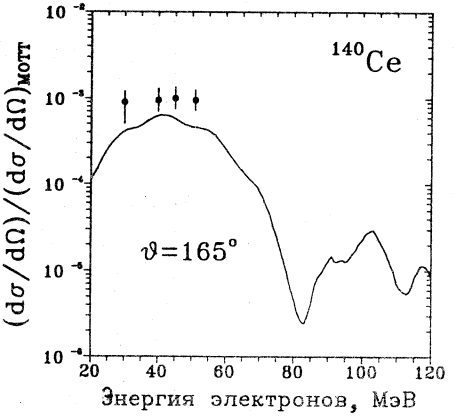

Рис. 8. Измеренные на линейном ускорителе электронов в Дармштадте [1] сечения возбуждения магнитного квадрупольного резонанса в ^{140}Ce (символы). Линия — теоретический расчет на основе флюид-динамической модели твистового отклика

том энергии налетающего электрона E дифракционный минимум смещается в сторону меньших углов. Из наших расчетов следует, что 1) магнитные резонансы более высокой мультипольности возбуждаются с заметно меньшей интенсивностью и 2) в тяжелых ядрах ожидается более заметное проявление твистового эффекта, чем в легких.

На рис.9 символами представлены данные дармштадтского линейного ускорителя электронов по интегральным сечениям (e, e')-рассеяния на ядре ^{140}Ce для всех $M2$-состояний в интервале энергий 7,5÷10,0 МэВ при угле рассеяния 165° и энергиях налетающих электронов от 30 до 55 МэВ. Анализ данной реакции с точки зрения микроскопической теории ядерной структуры дан в работе [51]. На этом рисунке мы также приводим теоретические сечения возбуждения твистового квадрупольного резонанса,

вычисленные в рамках PWBA и DWBA. Как видно, экспериментальный и теоретический формфакторы, рассчитанные на основе данной коллективной модели, имеют весьма похожую форму. Следуя логике, общепринятой в изложении выводов коллективных моделей, можно отметить, что качественное совпадение по форме теоретического формфактора (который несет в себе информацию о пространственном распределении возбуждаемого тока) и экспериментально свидетельствует о корректности предсказываемого характера коллективных колебаний.

В теории электровозбуждения приведенная вероятность $B(M\lambda)$ перехода ядра в состояние с магнитным моментом мультипольного порядка λ определяется интегралом от переходной токовой плотности $J_{\lambda,\lambda}(r)$ согласно соотношению

$$B(M\lambda) = \frac{\lambda}{\lambda+1}\left[\frac{\hat{J}_f}{J_i}\int_0^\infty eJ_{\lambda,\lambda}(r)r^{\lambda+2}dr\right]^2 = \frac{\lambda}{(\lambda+1)}\frac{2B_\lambda\omega_\lambda}{\hbar}\left(\frac{Z}{A}\right)^2 \mu^2 \text{фм}^{2\lambda-2}. \quad (4.10)$$

Как можно легко убедиться, это выражение точно совпадает с полученным выше соотношением (3.13). Сопоставление приведенной вероятности возбуждения $M\lambda$, $T=0$ твистового резонанса с измеряемой в эксперименте суммарной приведенной вероятностью $\sum B(M\lambda)$ переходов представлено на рис.4. который мы обсуждали в предыдущем разделе. Здесь мы лишь добавим, что в длинноволновом пределе формфактор $F_\lambda^M(q)$ выражается через приведенную вероятность возбуждения $B(M\lambda)$:

$$|F_\lambda^M(q)|^2 = \frac{4\pi}{e^2Z^2}\frac{q^2}{[(2\lambda+1)!!]^2}\frac{\lambda+1}{\lambda}B(M\lambda). \quad (4.11)$$

Из теории электронного рассеяния известно, что применимость длинноволнового приближения ($qR << 1$, где R — радиус ядра) оправдана лишь при сравнительно малых энергиях E налетающего электрона. Однако в экспериментах это условие, как правило, не реализуется. Так, например, при неупругом рассеянии электронов на ^{90}Zr на угол $\theta = 165°$, $qR = 1$ для $E = 26$ МэВ. В этом случае $|F_\lambda^M(q)|^2$ уже не пропорционален величине $B(M\lambda)$, а определяется индивидуальными особенностями переходной токовой плотности возбуждаемого состояния. Поэтому при расчете формфакторов необходимо пользоваться непосредственно формулой (4.2).

Интегральной мерой степени коллективности ядерного отклика является правило сумм. Правила сумм для магнитных возбуждений рассмотрены в работах [72, 96—99]. В макроскопическом подходе аналогом правила сумм является осцилляторная сила возбуждения [7]. Согласно нашим

вычислениям магнитная осцилляторная сила $M\lambda$ изоскалярного крутильного отклика дается оценкой

$$S(M\lambda) = \sum E(M\lambda)B(M\lambda) = \beta_\lambda Z^2 A^{(2\lambda-5)/3} \text{ МэВ}\cdot \mu^2 \text{ фм}^{2\lambda-2}, \qquad (4.12)$$

где $\beta_2 = 30$, $\beta_3 = 160$, $\beta_4 = 560$.

5. ВЫСОКОЭНЕРГЕТИЧЕСКИЙ ДИПОЛЬНЫЙ МАГНИТНЫЙ ОТКЛИК СФЕРИЧЕСКОГО ЯДРА

Как мы уже отмечали, дипольная твистовая мода требует специального рассмотрения. Главная причина отсутствия этой моды в представленном выше спектре магнитных твистовых резонансов (3.6) связана с предположением о том, что внешнее возмущение индуцирует только длинноволновые вращательные осцилляции потока частиц. В этом приближении не удается описать хорошо установленный магнитный дипольный резонанс, энергетический центроид которого дается оценкой $41A^{1/3}$ МэВ [5]. Однако, как показано в [100], вне рамок этого ограничения уравнения ядерной флюид-динамики допускают решение, описывающее сдвиговые колебания, которые соответствуют коллективной высокоэнергетической $M1$, $T = 0$ моде, возможность существования которой обсуждается в [2].

Вернемся к уравнению (2.13). После подстановки в него (2.8) находим, что поле смещений подчиняется векторному уравнению Гельмгольца:

$$\Delta\, \mathbf{a}(\mathbf{r}) + k^2 \mathbf{a}(\mathbf{r}) = 0. \qquad (5.1)$$

Регулярное в нуле решение последнего уравнения, соответствующее крутильным колебаниям ядра,

$$\mathbf{a}(\mathbf{r},t) = j_1(kr)\mathbf{Y}^0_{111}(\hat{\mathbf{r}}), \qquad (5.2)$$

где $k = \omega/c_t$ — волновой вектор и $c_t = \sqrt{P_F/\rho_0} = v_F/\sqrt{5}$ — скорость распространения поперечных осесимметричных крутильных колебаний в сферическом ядре. Частота ω этих колебаний может быть однозначно определена из граничного условия, которое требует отсутствия сдвигов на поверхности сферического ядра: $n_k \delta P_{ik} = 0$, где n_k — единичный вектор нормали к поверхности ядра. Явное выражение этого условия имеет вид

$$\delta P_{r\phi} = 0 \to \frac{da_\phi}{dr} - \frac{a_\phi}{r} = 0. \qquad (5.3)$$

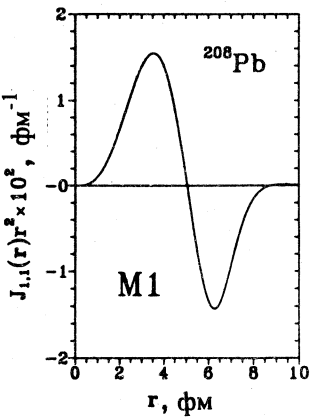

Рис. 9. Переходная токовая плотность (умноженная на r^2) для высокоэнергетического $M1$, $T=0$ твистового резонанса в ядре ^{208}Pb, предсказываемого ядерной флюид-динамикой

Условие (5.3) приводит к следующему дисперсионному уравнению:

$$z\frac{dj_\lambda(z)}{dz}=j_\lambda(z),\quad z_{\lambda i}=k_{\lambda i}R. \tag{5.4}$$

Численные значения корней этого уравнения для $1\le\lambda\le5$ приведены в табл.3. Собственные частоты крутильных колебаний определяются выражением $\omega_{\lambda i}=\frac{\hbar\omega_F}{\sqrt{5}}z_{\lambda i}$. Энергия нижайшего дипольного твистового изоскалярного отклика оценивается величиной (при $r_0=1{,}1$ фм)

$$E(M1,T=0)=\hbar\omega_{11}=\frac{\hbar^2(9\pi)^{1/3}}{\sqrt{20}mr_0^2}z_{11}A^{-1/3}=135\ A^{-1/3}\ \text{МэВ}. \tag{5.5}$$

Предположение о длинноволновом характере колебаний скорости потока нуклонов ядра является критичным лишь для дипольного отклика, поскольку просто его исключает (энергия дипольного колебания равна нулю). Что же касается $M\lambda(\lambda\ge2)$-резонансов, то энергии, вычисленные в длинноволновом приближении, практически точно совпадают с энергиями, полученными из уравнения Гельмгольца (5.1) с граничным условием свободной от напряжений поверхности ядра, которое выражено дисперсионным уравнением (5.4). Тот факт, что энергия высокоэнергетического 1^+, $T=0$ резонанса может быть вычислена только за рамками длинноволнового приближения продемонстрирован в работе [46].

К настоящему моменту известен единственный эксперимент, выполненный Вудвордом и Петерсоном на линейном ускорителе Массачусетского университета [2] на ядре ^{280}Pb с целью поиска магнитной дипольной силы в области энергий от 19 до 25 МэВ, незадолго до того предсказанной в микроскопических расчетах [89]. В этом эксперименте измерено сечение неупругого рассеяния электронов с энергией 60 МэВ на угол 180° и обнаружен пик при энергии 24 МэВ с шириной порядка 1,5 МэВ и абсолютной величиной сечения $d\sigma/d\Omega=(50\pm20)$ нб/ср.

С целью сопоставления предсказаний ядерной флюид-динамики для высокоэнергетического дипольного изоскалярного резонанса с данными, приведенными в [2], ниже мы представляем результаты вычислений сум-

Таблица 3. Корни $z_{\lambda i}$ дисперсионного уравнения для определения частот возбуждения изоскалярных состояний магнитного типа

i	$\lambda = 1$	$\lambda = 2$	$\lambda = 3$	$\lambda = 4$	$\lambda = 5$
1	5,7635	2,5011	3,8647	5,0946	6,2658
2	9,0950	7,1360	8,4449	9,7125	10,9506
3	12,3229	10,5146	11,8817	13,2187	14,5108

марной приведенной вероятности и поперечного сечения возбуждения этой моды. В макроскопическом представлении переходная токовая плотность магнитного дипольного возбуждения дается выражением

$$J_{1,1}(r) = \left\langle \left| \frac{1}{ec} \int \mathbf{j}(\mathbf{r},t) \cdot \mathbf{Y}^0_{111}(\hat{\mathbf{r}}) d\,\hat{\mathbf{r}} \right|^2 \right\rangle_t^{1/2} = N_1 n_e(r)\, j_1(k_1 r), \qquad (5.6)$$

где константа N_1 зависит от энергии возбуждения следующим образом: $N_1 = \frac{E(M1)}{e\hbar c}\,\alpha_0$. Коллективная амплитуда нормальных токовых колебаний определяется, согласно [7], выражением $\alpha_0 \equiv \langle |\alpha(t)|^2 \rangle_t^{1/2} = \frac{\hbar}{\sqrt{2B_1 E(M1)}}$. Как и ранее, символ $\langle \ldots \rangle_t$ означает усреднение по времени, и B_1 — массовый параметр, равный

$$B_1 = \int \rho_0 \mathbf{a}_1^2 d\tau = \frac{3mA}{8\pi} [j_1^2(k_1 r) - j_0(k_1 r) j_2(k_1 r)]. \qquad (5.7)$$

Приведенная на рис.9 переходная токовая плотность иллюстрирует объемный характер рассматриваемых коллективных поперечных колебаний потока нуклонов.

В борновском приближении магнитный формфактор $F_1\,M(q)$ выражается через переходную токовую плотность $J_{1,1}(r)$:

$$F_1^M(q) = \frac{\sqrt{12\pi}}{Z} \int J_{1,1}(r)\, j_1(qr) r^2 dr = \frac{\sqrt{12\pi}}{Z} N_1 \int j_1(k_1 r)\, j_1(qr) r^2 dr. \qquad (5.8)$$

На рис.10 мы приводим дифференциальные сечения возбуждения 1^+, $T = 0$ твистовой моды ^{208}Pb в в реакции неупругого рассеяния электронов с энергией $E_e = 60$ МэВ на угол 180°, рассчитанные как в DWBA-,так и в PWBA-приближении.

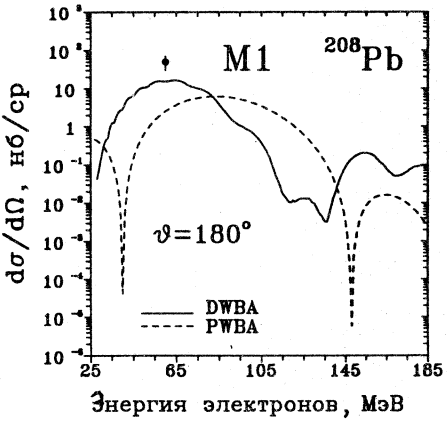

Рис. 10. Предсказываемое на основе флюид-динамической модели сечение возбуждения высокоэнергетического $M1$, $T=0$ твистового резонанса в ядре ^{208}Pb. Расчеты выполнены как в рамках плосковолнового борновского приближения (PWBA), так и в приближении искаженных волн (DWBA). Экспериментальная точка — результат измерения сечения неупругого рассеяния электронов на 180° при энергии налетающих электронов 60 МэВ. Данные линейного ускорителя электронов в Бейтсе (Bates LINAC) [2]

Таблица 4. Теоретические предсказания для $M1, T=0$ твистовой моды в ^{208}Pb и экспериментальные данные [2] по возбуждению магнитного дипольного резонанса в реакции неупругого рассеяния электронов с энергией 60 МэВ на угол 180°

^{208}Pb	Теория	Эксперимент
$E(M1)$, МэВ	22,9	24,0
$B(M1)$, μ^2	2,0	—
$d\sigma/d\Omega$, нб/ср	15,0	50±20

Суммарная вероятность возбуждения $B(M1)$ для $M1$, $T=0$ моды ядерного кручения, вычисленная в зависимости от атомного номера ядра и его массового числа, дается выражением

$$B(M1)=\frac{3e^2}{2}\left[\int J_{1,1}(r)r^3dr\right]^2\approx 1{,}0\cdot 10^{-2}\,Z^2A^{-2/3}\mu^2. \qquad (5.9)$$

Представленные в данном разделе результаты позволяют сделать следующее резюме. Ядерная флюид-динамика предсказывает высокоэнергетическую $M1$, $T=0$ моду, локализацию силы которой следует ожидать в районе 20—25 МэВ. В работах [10,18—21,42] приводятся для области локализации центроида энергии высокоэнергетического $M1$, $T=0$ резонанса оценки в интервале $E(M1, T=0)=21\div 27$ МэВ. Результаты наших расчетов и данные обсуждаемого эксперимента суммированы в табл.4.

6. ШИРИНЫ МАГНИТНЫХ ТВИСТОВЫХ МОД

Релаксация коллективных ядерных возбуждений в последние годы является предметом интенсивного изучения в ядерной флюид-динамике [28,33,101,102]. Микроскопическое происхождение рассматриваемого в данном разделе механизма затухания коллективного ядерного движения связывается с двухчастичными столкновениями нуклонов, приводящими, в конечном итоге, к вязкости ядерного вещества. Анализ затухания коллективных ядерных движений, связанных с изоскалярными электрическими резонансами с $\lambda \geq 2$, показал, что роль отдельной диссипации (затухание Ландау) менее значительна по сравнению с ролью двухтельной диссипации [102]. В теории сплошных сред двухчастичная диссипация макроскопически описывается тензором вязких напряжений. Эффект сдвиговой вязкости имеет объемное происхождение и характеризуется коэффициентом динамической вязкости μ, который в наших вычислениях рассматривается как параметр. Однако, как показано в [27], этот коэффициент может быть извлечен из данных по кинетической энергии фрагментов деления тяжелых ядер. Численная оценка коэффициента μ составляет [103]:

$$\mu = (0{,}03 \pm 0{,}01)\ \text{ТП}, \quad 1\text{ТП} = 0{,}948\hbar\ \text{фм}^{-3},$$

где ТП означает терапуаз. В нижеприводимых расчетах мы также используем кинематический коэффициент вязкости, не зависящий от плотности и определяемый соотношением $\nu = \mu/\rho_0$, где ρ_0 — равновесная плотность ядерного вещества. Подчеркнем, что при фиксированном значении коэффициента динамической вязкости наши вычисления перестают зависеть от каких-либо свободных параметров. Наиболее последовательное изложение механизма двухтельной диссипации представлено в недавней серии работ, указанных в [33], где, в частности, получены оценки коэффициента вязкости на основе развитого авторами кинетического подхода (см. также [104,105]). Микроскопические теории релаксации ядерных возбуждений изложены в [31,77,106,107]. В данном разделе дается макроскопический расчет столкновительных ширин магнитных твистовых резонансов согласно [37].

6.1. Уравнения диссипативной ядерной флюид-динамики. Макроскопическое описание затухания коллективных колебаний нуклонов основано на введении диссипативной функции Рэлея F, которая определяется как скорость потери полной энергии коллективных колебаний и представляется в виде (см., например, уравнение (3.8) в [108]):

$$\frac{d}{dt} H(\alpha_\lambda, \dot{\alpha}_\lambda) = F(\dot{\alpha}_\lambda), \tag{6.1}$$

где H — гамильтониан собственных нормальных колебаний (2.10), а диссипативная функция связана с коэффициентом трения D соотношением $F = \dot{\alpha}_\lambda^2 D_\lambda$. В лагранжевой трактовке уравнение диссипативной ядерной флюид-динамики имеет вид

$$\frac{d}{dt}\frac{\partial L}{\partial \dot{a}_\lambda} - \frac{\partial L}{\partial a_\lambda} + \frac{\partial F}{\partial \dot{a}_\lambda} = 0, \tag{6.2}$$

где L — лагранжиан нормальных крутильных колебаний

$$L = \frac{B_\lambda (\dot{\alpha}^\lambda)^2}{2} - \frac{C_\lambda (\alpha^\lambda)^2}{2}. \tag{6.3}$$

Массовый параметр B_λ и параметр крутильной жесткости C_λ определены в разд.3 формулами (3.3) и (3.4) соответственно. Подстановка (6.1) и (6.3) в (6.2) приводит к хорошо известному уравнению затухающих линейных колебаний:

$$B_\lambda \ddot{\alpha}_\lambda + 2D_\lambda \dot{\alpha}_\lambda + C_\lambda \alpha_\lambda = 0, \tag{6.4}$$

откуда следует, что собственная частота ω_λ и коэффициент затухания крутильных колебаний γ_λ равны

$$\omega_\lambda = (C_\lambda / B_\lambda)^{1/2}, \quad \gamma_\lambda = D_\lambda / B_\lambda. \tag{6.5}$$

Коэффициент трения D_λ определяется интегралом

$$D_\lambda = \frac{\nu}{2} \int \rho_0 \left(\frac{\partial a_i^\lambda}{\partial x_j} + \frac{\partial a_j^\lambda}{\partial x_i} \right)^2 d\tau, \tag{6.6}$$

структура которого, как видно, совпадает со структурой коэффициента жесткости. С учетом диффузности ядерной поверхности вычисления коэффициента трения сдвиговых колебаний дают

$$D_\lambda = M\nu \langle r^{2\lambda-2} \rangle \lambda(\lambda^2 - 1), \tag{6.7}$$

где M — масса ядра. Результат вычислений в приближении резкого края приводится ниже.

6.2. Столкновительные ширины магнитных резонансов. Согласно теории линейных ядерных колебаний, энергии $E(M\lambda)$ и столкновительные ширины $\Gamma(M\lambda)$ ядерных изоскалярных резонансов в рассматриваемом подходе определяются соотношениями [27]:

$$E(M\lambda) = \hbar\omega_\lambda, \quad \Gamma(M\lambda) = \hbar\,\gamma_\lambda. \tag{6.8}$$

Подставляя сюда (6.7), получаем следующее выражение для столкновительной ширины $M\lambda$, $T = 0$ твистового резонанса:

$$\Gamma(M\lambda) = \hbar\nu\,(2\lambda+1)(\lambda-1)\,\frac{\langle r^{2\lambda-2}\rangle}{\langle r^{2\lambda}\rangle}. \qquad (6.9)$$

В приближении резкого края формула (6.9) приобретает вид

$$\Gamma(M\lambda) \approx 6{,}0(2\lambda+3)(\lambda-1)\,A^{-2/3}\ \text{МэВ}. \qquad (6.10)$$

Таким образом, мы находим, что механизм двухтельной диссипации энергии приводит к тому, что ширины магнитных резонансов спадают с ростом массового числа по закону $A^{-2/3}$. С увеличением мультипольности возбуждения ширина резонанса растет пропорционально множителю $(2\lambda+3)(\lambda-1)$. Численные оценки ширины квадрупольного магнитного изоскалярного резонанса в некоторых сферических ядрах приведены в табл.2. Эти оценки получены при вышеприведенных значениях параметров фермиевского распределения для плотности.

Обратив внимание на то, что энергия и ширина имеют сходную мультипольную зависимость, можем представить выражение (6.10) в виде

$$\Gamma(M\lambda) = \frac{5\nu}{\hbar v_F^2}\,[E(M\lambda)]^2\ \text{МэВ}^{-1}. \qquad (6.11)$$

Как следует из (6.11), столкновительная ширина магнитного резонанса данной мультипольности пропорциональна квадрату энергии возбуждения. Аналогичная зависимость столкновительной ширины от массового числа имеет место и для электрических изоскалярных резонансов [27,28,33]. Аналитическая зависимость ширины электрических изоскалярных резонансов от мультипольного порядка λ в наших расчетах имеет вид

$$\Gamma(E\lambda) = \frac{5\nu}{\hbar v_F^2}\,[E(E\lambda)]^2, \qquad (6.12)$$

где $E(E\lambda)$ дается формулой Никса — Сирка (2.16). Сравнивая выражения для ширин (6.11) и (6.12), находим

$$\frac{\Gamma(M\lambda)}{\Gamma(E\lambda)} = \frac{1}{2}\,\frac{(2\lambda+3)}{(2\lambda+1)} < 1, \quad \lambda \geq 2, \qquad (6.13)$$

т.е. ширина магнитного изоскалярного резонанса данной мультипольности $\lambda \geq 2$ всегда больше ширины электрического изоскалярного резонанса той же мультипольности.

Представленные оценки носят предсказательный характер, поскольку в настоящее время отсутствует какая-либо экспериментальная информация о ширинах магнитных резонансов. Наши предсказания довольно хорошо согласуются с результатами работ [28,33], где приведены оценки на параметры релаксации трансверсальных ядерных колебаний. В частности, предсказанный в [28] $A^{-2/3}$-закон спадания ширин трансверсальных коллективных мод

с ростом массового числа, воспроизводится в рассмотренном нами случае магнитных резонансов с $\lambda \geq 2$.

7. ЗАКЛЮЧЕНИЕ

В настоящее время коллективные магнитные возбуждения ядер являются предметом активных исследований, которые стимулируются экспериментами, проводимыми в Дармштадте (DALINAC), Москве, Штутгарте, Массачусетсе (Bates LINAC) и других центрах. В этой связи представляется своевременным представить обзор теоретических исследований, выполненных в рамках макроскопической теории коллективных ядерных возбуждений.

Одна из целей данного обзора состояла в конструктивном аналитическом представлении полного набора измеряемых интегральных характеристических параметров изоскалярных магнитных мультипольных резонансов: положений центроидов энергий, суммарных вероятностей возбуждения, столкновительных ширин и сечений возбуждения в реакции неупругого рассеяния электронов. Указанные величины представляются в виде степенных функций атомного номера, массового числа и мультипольного порядка возбуждения. Это делает модель открытой для экспериментальной проверки ее предсказаний. Тот факт, что изложенная теория предсказывает значения основных интегральных характеристических параметров для $M2$ коллективной моды, находящиеся в качественном согласии с имеющимися экспериментальными данными, указывает на адекватность развитой макроскопической трактовки наблюдаемого квадрупольного резонанса.

В изложенной коллективной модели магнитные изоскалярные резонансы интерпретируются в терминах крутильных колебаний ядра, рассматриваемого как сферическая макрочастица ядерной ферми-среды. Этим подчеркивается, что ядерная материя обладает свойствами упругого континуума, причем физическая природа упругости ядерного вещества имеет существенно квантовое происхождение, поскольку является следствием фермиевского движения нуклонов и связанной с ним динамической деформации поверхности Ферми. В этой связи уместно добавить, что проблема упругости ядерного вещества является предметом активного изучения в теории ядерных движений большой амплитуды [110,111]. Можно надеяться, что конкретность представленных в обзоре результатов окажется полезной при выборе направления планируемых экспериментов, которые позволят установить, насколько достоверными являются представления об упругоподобном поведении ядерной материи.

В заключение мы хотели бы поблагодарить В.В.Гудкова, В.М.Шилова, А.В.Сушкова за плодотворное сотрудничество, а также выразить призна-

тельность В.О.Нестеренко, И.Н.Михайлову, М.Ди Торо, Е.Б.Бальбуцеву, А.И.Вдовину, Дж.Петерсону, Р.Хилтону, Л.А.Малову, Б.С.Ишханову, С.Раману, Дж.Провиденсия, Э.Х.Юлдашбаевой, П.Рингу, Ж.Либеру, В.В.Воронову, Н.Г.Гончаровой, М.Браку, А.Г.Магнеру и Н.Ло Юдечи за полезные дискуссии по затронутым вопросам.

Работа выполнена при поддержке Российского фонда фундаментальных исследований (грант 94-02-04615) и Европейского Физического Общества (грант INTAS-93-151).

ПРИЛОЖЕНИЕ I

Вычисление интегралов, фигурирующих в тексте, удобнее проводить в системе с фиксированной полярной осью. В этом случае сферические компоненты тороидального поля мгновенных смещений a_i, соответствующего крутильным колебаниям сферического ядра, имеют вид

$$a_r = 0, \quad a_\theta = 0, \quad a_\phi = A_\lambda r^\lambda (1-\mu^2)^{1/2} \frac{dP_\lambda(\mu)}{d\mu}, \qquad (\text{П.1.1})$$

где $\mu = \cos\theta$, $P_\lambda(\mu)$ — полиномы Лежандра.

Компоненты тензора упругих напряжений, возникающих при крутильных колебаниях, даются соотношениями

$$\frac{\partial a_1}{\partial x_1} = \frac{\partial a_r}{\partial r} = 0,$$

$$\frac{\partial a_2}{\partial x_2} = -\frac{(1-\mu^2)^{1/2}}{r}\frac{\partial a_\theta}{\partial \mu} + \frac{a_r}{r} = 0,$$

$$\frac{\partial a_3}{\partial x_3} = \frac{1}{r(1-\mu^2)^{1/2}}\frac{\partial a_\phi}{\partial \phi} + \frac{a_r}{r} + \frac{a_\theta}{r}\frac{\mu}{(1-\mu^2)^{1/2}} = 0,$$

$$\frac{\partial a_1}{\partial x_2} = -\frac{(1-\mu^2)^{1/2}}{r}\frac{\partial a_\theta}{\partial \mu} - \frac{a_\theta}{r} = 0,$$

$$\frac{\partial a_2}{\partial x_1} = \frac{\partial a_\theta}{\partial r} = 0,$$

$$\frac{\partial a_1}{\partial x_3}=\frac{1}{r(1-\mu^2)^{1/2}}\frac{\partial a_r}{\partial \phi}-\frac{a_\phi}{r}=-A_\lambda r^{\lambda-1}(1-\mu^2)^{1/2}\frac{dP_\lambda(\mu)}{d\mu},$$

$$\frac{\partial a_3}{\partial x_1}=\frac{\partial a_\phi}{\partial r}=A_\lambda \lambda r^{\lambda-1}(1-\mu^2)^{1/2}\frac{dP_\lambda(\mu)}{d\mu},$$

$$\frac{\partial a_2}{\partial x_3}=-\frac{1}{r}\frac{\partial a_\theta}{\partial \mu}-\frac{a_\phi}{r}\frac{\mu}{(1-\mu^2)^{1/2}}=-A_\lambda r^{\lambda-1}\mu\frac{dP_\lambda(\mu)}{d\mu},$$

$$\frac{\partial a_3}{\partial x_2}=-\frac{(1-\mu^2)^{1/2}}{r}\frac{\partial a_\phi}{\partial \mu}=-A_\lambda r^{\lambda-1}\left[\mu\frac{dP_\lambda(\mu)}{d\mu}-\lambda(\lambda+1)P_\lambda(\mu)\right].$$

В вычислениях используются следующие основные интегралы:

$$\int_{-1}^{+1}P_\lambda^2(\mu)d\mu=\frac{2}{(2\lambda+1)},$$

$$\int_{-1}^{+1}(1-\mu^2)\left(\frac{dP_\lambda(\mu)}{d\mu}\right)^2 d\mu=\frac{2\lambda(\lambda+1)}{(2\lambda+1)},$$

$$\int_{-1}^{+1}\mu P_\lambda(\mu)\frac{dP_\lambda(\mu)}{d\mu}d\mu=\frac{2\lambda}{(2\lambda+1)},$$

$$\int_{-1}^{+1}\left(\mu\frac{dP_\lambda(\mu)}{d\mu}\right)^2 d\mu=\frac{\lambda(\lambda+1)(2\lambda-1)}{(2\lambda+1)},$$

два последних получены с использованием рекуррентных соотношений для полиномов Лежандра.

Вышеприведенные формулы позволяют значительно облегчить громоздкие вычисления интегралов, содержащих тензор упругих напряжений. В частности,

$$\frac{1}{2}\int_v F(r)\left(\frac{\partial a_i^\lambda}{\partial x_j}+\frac{\partial a_j^\lambda}{\partial x_i}\right)^2 d\tau=4\pi A_\lambda^2\lambda(\lambda-1)(\lambda+1)\int_0^R F(r)r^{2\lambda}dr, \quad (\text{П.1.2})$$

где $F(r)$ — произвольная функция от r.

СПИСОК ЛИТЕРАТУРЫ

1. **Richter A.** — Lecture Notes in Physics, 1979, vol.108, p.19; Prog. Part. Nucl. Phys., 1984, vol.13, p.1; Nucl. Phys., 1989, vol.A507, p.99.
2. **Woodward C., Peterson G.A.** — Phys. Rev., 1979, vol.C20, p.2437.
3. **Richter A.** — Proc. Dubna Int. School on Nucl. Structure, D4-80-385, Dubna, 1980.
4. **Hicks R.S., Huffman R.L., Lindgren R.A. et al.** — Phys. Rev., 1982, vol. C26, p.920.
5. **Raman S., Fagg L.W., Hicks R.** — In: Electric and Magnetic Giant Resonances. World Scientific, Singapore, 1991, ch.4, p.355.
6. **Rowe D.J.** — Nuclear Collective Motion: Models and Theory. Methuen, London, 1970.
7. **Bohr A., Mottelson B.** — Nuclear Structure. Benjamin, New York, 1970.
8. **Соловьев В.Г.** — Теория сложных ядер. М.: Наука, 1974.
9. **Ring P., Schuck P.** — The Nuclear Many-Body Problem. Springer, Berlin, 1978.
10. **Holzwarth G., Eckart G.** — Z.Phys., 1977, vol.A283, p.219; Nucl. Phys. A, 1979, vol.325, p.1.
11. **Eckart G., Holzwarth G., Da Providencia J.P.** — Nucl. Phys. A, 1981, vol.364, p.1.
12. **Schwesinger B., Pingel K., Holzwarth G.** — Nucl. Phys., 1982, vol.A341, p.1.
13. **da Providencia J.P., Holzwarth G.** — Nucl. Phys., 1983, vol.A398, p.59.
14. **Holzwarth G.** — Density Functional Methods in Physics. (Ed. R.M.Dreizler, J.P. da Providencia). Plenum Publishing Corporation, 1985, p.381.
15. **Ландау Л.Д., Лифшиц Е.М.** — Теория упругости. М.: Наука, 1986.
16. **Морс Ф., Фешбах Г.** — Методы математической физики. М.: Наука, 1986, т.2.
17. **Ландау Л.Д., Лифшиц Е.М.** — Гидродинамика. М.: Наука, 1988.
18. **Семенко С.Ф.** — ЯФ, 1975, т.21, с.977; ЯФ, 1981, т.26, с.274; ЯФ, 1981, т.34, с.356; ЯФ, 1984, т.39, с.351.
19. **Wong C.Y., Azziz A.** — Phys. Rev., 1981, vol.C24, p.2290; Phys. Rev., 1982, vol.C25, p.2777.
20. **Hasse R.W., Ghosh G., Winter J., Lumbrozo A.** — Phys. Rev., 1982, vol.C25, p.2771.
21. **Баструков С.И., Гудков В.В., Деак Ф., Сушков А.В.** — Краткие сообщения ОИЯИ, 1990, №45[6], с.51.
22. **Ламб Н.** — Гидродинамика: Пер. с англ. М.: Гостехиздат, 1947.
23. **Bastrukov S.I.** — Phys. Rev., 1994, vol.E49, p.3166.
24. **Bertsch G.F.** — Ann. Phys., 1974, vol.86, p.138; Nucl. Phys., 1975, vol.A249, p.253.
25. **Bertsch G.F.** — Les Houches 1977, Session XXX (ed. by R.Balian et. al.) vol.1, North-Holland, Amsterdam, 1978, p.175.
26. **Климонтович Ю.Л.** — Статистическая физика. М.: Наука, 1982.
27. **Nix J.R., Sierk A.J.** — Phys. Rev., 1980, vol.C21, p.396.
28. **Коломиец В.М.** — Приближение локальной плотности в атомной и ядерной физике. Киев: Наукова думка, 1990.
29. **Бальбуцев Е.Б., Михайлов И.Н.** — Коллективная ядерная динамика (под ред. Р.В.Джолоса). Л.: Наука, 1990, с.3.
30. **Коломиец В.М.** — Коллективная ядерная динамика (под ред. Р.В.Джолоса). Л.: Наука, 1990, с.67.

31. **Wambach J.** — Rep. Prog. Phys., 1988, vol.51, p.989.
32. **Speth J., Wambach J.** — In: Electric and Magnetic Giant Resonances. World Scientific, Singapore, 1991, ch.1, p.3.
33. **Коломиец В.М., Магнер А.Г., Плюйко В.А.** — ЯФ, 1992, т.55, с.45; ЯФ, 1993, т.56, с.110; Z.Phys., 1993, vol.A345, p.131; ibid p.137.
34. **Abrosimov V., Di Toro M., Strutinsky V.** — Nucl. Phys., 1993, vol.A562, p.41.
35. **Bastrukov S.I., Gudkov V.V.** — Z. Phys., 1992, vol.A341, p.395.
36. **Bastrukov S.I., Molodtsova I.V.** — Europhys. Lett., 1993, vol.22(2), p.85.
37. **Баструков С.И., Молодцова И.В., Шилов В.М.** —Изв. РАН., сер. физ., 1993, т.57(10), с.148; Int. J. Mod. Phys., 1993, vol.E2, p.731.
38. **Баструков С.И., Молодцова И.В., Шилов В.М.** — Препринт ОИЯИ Р4-94-68, Дубна, 1994; ЯФ, 1995, т.58(6), с.6.
39. **Bastrukov S.I., Misicu S., Sushkov A.V.** — Nucl. Phys., 1993, vol.A562, p.191.
40. **Bastrukov S.I., Molodtsova I.V., Shilov V.M.** — Physica Scripta, 1995, vol.51, p.54.
41. **Денисов В.Ю.** — ЯФ, 1985, т.42, с.351.
42. **da Providencia J.P.** — J. Physique Coll., 1984, vol.C6, p.333; J. Phys., 1987, vol.G13, p.783; Nucl. Phys., 1988, vol.A489, p.190.
43. **Balbutsev E.B., Mikhailov I.N.** — J. Phys., 1988, vol.G14, p.245.
44. **Бальбуцев Е.Б., Молодцова И.В., Пиперова Й.** — ЯФ, 1991, т.53, с.670.
45. **Баструков С.И., Бальбуцев Е.Б., Молодцова И.В. и др.** — ЯФ, 1991, т.54, с.927.
46. **Бальбуцев Е.Б., Баструков С.И., Михайлов И.Н. и др.** — ЯФ, 1989, т.50, с.1264.
47. **Ponomarev V.Yu., Soloviev V.G., Stoyanov Ch., Vdovin A.I.** — Nucl. Phys., 1979, vol.A323, p.446.
48. **Cha D., Schwesinger B., Wambach J., Speth J.** — Nucl. Phys., 1984, vol.A430, p.321; Phys. Rev., 1984, vol.C29, p.636.
49. **Schwesinger B.** — Phys. Rev., 1984, vol.C29, p.1475.
50. **Dumitrescu T.S., Suzuki T.** — Nucl. Phys., 1984, vol.A423, p.277.
51. **Ponomarev V.Yu., Shilov V.M., Voronov V.V., Vdovin A.I.** — Phys. Lett., 1980, vol.B97, p.131.
52. **Вдовин А.И., Пономарев В.Ю., Шилов В.М.** — ЯФ, 1985, т.41, с.79.
53. **Ponomarev V.Yu.** — J. Phys., 1984, vol.G10, p.L177.
54. **Пономарев В.Ю.** — ЯФ, 1985, т.41, с.79.
55. **Kamerdzhiev S.P., Tkachev V.N.** — Phys. Lett., 1984, 142B, p.225; Изв. АН СССР, 1988, т.52, с.874; Z. Phys., 1989, vol.A334, p.19.
56. **Vdovin A.** — New Trends in Nuclear Physics. Proc. III Kiev Int. School on Nucl. Phys., Kiev, 1992, p.145.
57. **Саперштейн Е.Е., Фаянс С.А., Ходель В.А.** — ЭЧАЯ, 1978, т.9, с.221.
58. **Stringari S.** — Ann. Phys., 1983, vol.151, p.35.
59. **Lipparini E., Stringari S.** — Phys. Rep., 1989, vol.174, p.105.
60. **Cleissl P., Brack M., Meyer J., Quentin P.** — Ann. Phys., 1990, vol.197, p.205.
61. **Бальбуцев Е.Б.** — ЭЧАЯ, 1991, т.22, вып.2, с.333.
62. **Ди Торо М.** — ЭЧАЯ, 1991, т.22, вып.2, с.385.
63. **Chandrasekhar S.** — Hydrodynamic and Hydromagnetic Stability. Clarendon, Oxford, 1961.

64. **Elsasser W.M.** — Phys. Rev., 1946, vol.70, p.202; Rev. Mod. Phys., 1950, vol.22, p.1.
65. **da Providencia J.P.** — Portugal Phys., 1987, vol.18, p.7.
66. **Di Toro M., Russo G.** — Z.Phys., 1988, vol.A331, p.381.
67. **Bastrukov S.I., Maruhn J.A.** — Z. Phys., 1990, vol.A337, p.139.
68. **Баструков С.И., Молодцова И.В., Юлдашбаева Э.Х.** — ЯФ, 1994, т.57, №7, с.1245.
69. **Meuer D., Frey R., Hoffmann D.H.H. et al.** — Nucl. Phys., 1980, vol.A349, p.309.
70. **Bastrukov S.I., Sushkov A.V.** — J. Phys., 1992, vol.G18, p.L37.
71. **da Providencia J.P.** — J. Phys., 1986, vol.G12, p.23.
72. **Mikhailov I.N., Briancon Ch.** — Nuclear Shape and Nuclear Structure at Low Excitation Energies. NATO ASI SERIES B, 1991, vol.289, p.271.
73. **Bastrukov S.I.** — New Trends in Nuclear Physics. Proc. III Kiev Int. School on Nucl. Phys., Kiev, 1992, p.262.
74. **Тамм И.Е.** — Основы теории электричества. М.: Наука, 1989.
75. **Ландау Л.Д., Лифшиц Е.М.** — Электродинамика сплошных сред. М.: Наука, 1992.
76. **Valantin L.** — Physique Subatomique. Hermann, Paris, 1982.
77. **Соловьев В.Г.** — Теория атомного ядра. Квазичастицы и фононы. М.: Наука, 1989.
78. **Tassie L.J.** — Austr. J. Phys., 1956, vol.9, p.407.
79. **Семенко С.Ф.** — Препринт ФИАН №76, М., 1986.
80. **Гончарова Н.Г.** — ЭЧАЯ, 1992, т.23, с.1715.
81. **Lo Iudeci N., Palumbo F.** — Phys. Rev. Lett., 1978, vol.41, p.1532; Nucl. Phys., 1979, vol.A326, p.193.
82. **Zilges A. et al.** — Nucl. Phys., 1994, vol. A577, p.191c.
83. **Lo Iudeci N., Richter A.** — Phys. Lett., 1989, vol.B228, p.291.
84. **Heil R.D., Pitz H.H., Kneissl U. et al.** — Nucl. Phys., 1988, vol.A476, p.39.
85. **Hilton R.R.** — Ann. Phys., 1992, vol.214, p.258.
86. **De Coster C.**–Thesis of Gent University, Gent, 1991.
87. **Otsuka T.** — Nucl. Phys., 1990, vol.A507, p.129c.
88. **Zawisha D., Speth J.** — Phys. Lett., 1988, vol.B211, p.247; Phys. Lett., 1989, vol.B219, p.529; Phys. Lett., 1990, vol.B252, p.4.
89. **Speth J., Wambach J., Klemt V., Krewald S.** — Phys. Lett., 1976, vol.B63, p.257.
90. **Ishkhanov B.S., Kapitonov I.M., Shirokov E.V., Ugaste A.Yu.** — IV Int. Conf. on Selected Topics in Nuclear Structure. Abstracts. JINR, Dubna, 1994.
91. **Нестеренко В.О.** — Сообщения ОИЯИ, Р4-12513, Дубна, 1979.
92. **Соловьев В.Г., Ширикова Н.Ю.** — ЯФ, 1992, т.55, с.2359; Nucl. Phys., 1992, vol.A542, p.410.
93. **Donnelly T.W., Waleska J.D.** — Ann. Rev. Nucl. Sci., 1975, vol.25, p.329.
94. **Lee H.C.** — Preprint of Chalk River Nucl. Lab., AECL-4839, Chalk River, Ontario, 1975.
95. **Heisenberg J., Blok H.P.** — Ann. Rev. Nucl. Part. Sci., 1983, vol.33, p.569.
96. **Варшалович Д.А., Москалев А.Н., Херсонский В.К.** — Квантовая теория углового момента. Л.: Наука, 1975.
97. **Kurath D.** — Phys. Rev., 1963, vol.130, p.1525.

98. **Traini M.** — Phys. Rev. Lett., 1978, vol.41, p.1535.
99. **Orlandini G., Traini M.** — Rep. Prog. Phys., 1991, vol.54, p.257.
100. **Bastrukov S.I., Bonasera A., Di Toro M., Sushkov A.V.** — Z. Phys., 1991, vol.A338, p.455.
101. **Kiderlen D., Hoffmann H., Ivanyuk F.A.** — Nuclk. Phys., 1992, vol.A550, p.473.
102. **Fiolhais C.** — Ann. Phys., 1986, vol.171, p.186.
103. **Blocki J., Boneh Y., Nix J.R. et al.** — Ann. Phys., 1977, vol.113, p.330.
104. **Bonasera A., Di Toro M., Gulminelli F.** — Phys. Rev., 1990, vol.C42, p.966.
105. **Ayik S., Boilley D.** — Phys. Lett., 1992, vol.B276, p.263.
106. **Mikhailov I.N., Piperova J., Di Toro M., Smerzi A.** — Nucl. Phys., 1994, vol. A575, p.269.
107. **Урин М.Г.** — Релаксация ядерных возбуждений. М.: Энергоатомиздат, 1990.
108. **Hasse R.W.** — Ann. Phys., 1975, vol.93, p.68; Rep. Prog. Phys., 1978, vol.41, p.1027.
109. **De Coster C., Heyde K., Richter A.** — Nucl. Phys., 1992, vol.A542, p.375.
110. **Swiatecki W.J.** — Nucl. Phys., 1988, vol.A488, p.375c.
111. **Bastrukov S.I., Molodtsova I.V., Gudkov V.V.** — Collective Nuclear Dynamics. Proc. IV Kiev Int. School on Nuclear Phys., Kiev, 1994, p.328.

«ФИЗИКА ЭЛЕМЕНТАРНЫХ ЧАСТИЦ И АТОМНОГО ЯДРА»
1995, ТОМ 26, ВЫП.2

УДК 530.145 + 539.19

GAUSSIAN EQUIVALENT REPRESENTATION OF FUNCTIONAL INTEGRALS IN QUANTUM PHYSICS

G.V.Efimov

Joint Institute for Nuclear Research, Dubna, 141980, Russia

G.Ganbold

Joint Institute for Nuclear Research, Dubna, 141980, Russia
and Institute of Physics and Technology, Ulaanbaatar, Mongolia

A new method is proposed for systematic approximate calculations of a large class of non-Gaussian functional integrals beyond the region of perturbative expansion. This method provides a good accuracy of the lowest approximation, obtained in a simple way, which represents a generalization of the variational estimation if the functionals are real. In contrast to the variational approach, this method is applicable to complex functionals and theories with ultraviolet divergencies. Higher-order corrections to the lowest approximation are evaluated by a regular scheme. This method is applied to different problems of theoretical physics: the polaron problem in solid states, the phase-transition phenomenon in quantum field models and the investigation of wave transmission in randomly distributed media.

Предложен новый, непертурбативный метод систематического вычисления широкого класса функциональных интегралов, применяемых в квантовой физике. Метод обеспечивает хорошую точность в низшем приближении, получаемом несложным путем. В случае вещественных функционалов оно представляет собой обобщение вариационного принципа. Предлагаемый метод выгодно отличается от вариационных подходов применимостью для комплексных функционалов и в теориях с расходимостями. Поправки высших порядков к низшему приближению вычисляются по регулярной схеме. Метод применен к ряду задач из различных областей теоретической физики: теории полярона в физике твердого тела, изучению фазового перехода в скалярной модели φ^4 в теории поля и к исследованию распространения волн в стохастических средах.

INTRODUCTION

In modern theoretical physics the formulation of quantum theory relying on the original classical system is mainly distinguished in two mutually complementary ways. One of them is the method of canonical quantization (CQ),

where the field dynamic variables are considered as operators satisfying certain commutation relations and defined on a Hilbert space of states. Many papers have been devoted to CQ and for history and details we refer readers to [1,2].

The second formalism of quantization is Feynman's method of path integrals (PI) [3,4]. The basic idea of the Feynman formulation of PI is that the quantum motion of a particle is considered as the sum of all quantum transitions along all possible classical trajectories with amplitudes proportional to

$$A\,[\mathbf{x}] \propto \exp\left(i \frac{S\,[\mathbf{x}]}{\hbar} \right),$$

where $S\,[\mathbf{x}]$ is the classic action taken on a given trajectory $\mathbf{x}$. The total transition amplitude is supposed to be proportional to the integral

$$A \propto \int_{\Gamma} \delta \mathbf{r} \exp\left\{ \frac{i}{\hbar} S\,(t, \mathbf{x}) \right\}, \tag{1}$$

where the classical action

$$S\,(t, \mathbf{r}) = \int_0^t d\tau \left\{ \frac{m^2}{2} |\dot{\mathbf{r}}(\tau)|^2 - V\,[\mathbf{r}(\tau)] \right\} \tag{2}$$

is taken along the given path $\mathbf{r}(\tau)$. Integration in (1) is performed over the space Γ of all possible «path-trajectories» $\mathbf{r}(\tau)$ with $0 < \tau < t$ for which $\mathbf{r}(0) = \mathbf{x}_0$ and $\mathbf{r}(t) = \mathbf{x}$. This representation attracts much attention because it is close to the classical theory, having both the physical clarity and the fine compact mathematical formulation. These advantages stimulated applications of PI to various problems in quantum physics [4].

From a technical point of view, the PI formalism of quantization represents an essential attempt to go out beyond the perturbation expansion and becomes effective for describing systems with infinite numbers of degrees of freedom.

In mathematics Wiener [5] was the first to introduce in 1920, the conception of PI to describe Brownian motion. Dirac first suggested a representation of a particle propagator in terms very close to PI techniques [6]. The systematic development of quantum mechanics (QM) within the PI approach belongs to Feynman.

In quantum physics, Feynman [3] formulated non-relativistic QM on the language of PI (in other words, the functional or continual integrals) and showed that this approach is completely equivalent to the solution of the Schrödinger equation. One of the main reasons for the popularity of «path integrals» is the understanding that classical mechanics becomes an approximation of QM in Feynman's formulation if one applies the method of «stationary phases» to the latter. At the classic limit $\hbar \to 0$ the leading contribution to PI is given by

the stationary points of the phase function $S(t, \mathbf{r})$ in (1), which is the solution of Newton's classical equation of motion.

In 1949 Feynman used the functional integral (FI) for construction of covariant QED (the Feynman diagrams) [4]. After that, acknowledging the dignity of this new approach, Kac (1951) suggested a FI of Wiener's type for representation of the evolution operator in Euclidean space [7].

Path integration has come a long way since the 1950s. Probably the most famous early application of FI in statistical physics was to the **polaron** (a nonrelativistic electron «dressed» by the surrounding quanta of lattice vibrations in ionic crystals). In polaron theory, FI not only helps to formulate the answer qualitatively, but also remains the best way to calculate the answer more exactly than other methods. It is a tractable field theory; the benefits obtained from using FI are entirely analogous to those gotten in quantum field theory (QFT). But contrary to the polaron problem, all steps for QFT are more difficult because of the divergences, the vector character of the fields and also gauge problems.

A number of investigators [8,9] independently came to the formulation of QFT in terms of FI considering variational estimations for Green functions.

A relatively simple way to represent the Green function of a quantized field within FI was suggested in [10], where the equivalence of FI over bosonic fields to the averaging over vacuum states of these fields is proved.

A new understanding of FI occured in [11,12], where the evolution operator of the model $P(\varphi)_2$ in Euclidean metrics was represented in FI form as follows

$$\exp\{-\beta H\} = \int d\sigma_0 \exp\{-\int dx : P(\varphi) :\},$$

$$d\sigma_0 = C\,\delta\varphi \exp\left\{\frac{1}{2}\int dx\,[(\nabla\varphi)^2 + m^2\varphi^2]\right\}, \qquad (3)$$

where $d\sigma_0$ is a Gaussian measure of integration, generated by the action $S_0(\varphi) = \frac{1}{2}\int dx\,[(\nabla\varphi)^2 + m^2\varphi^2]$ of a free bosonic field and $\int dx : P(\varphi) :$ introduced for a certain renormalization of the classic interaction $\int dx\, P(\varphi)$. This definition of FI in (3) which allows the removal of interaction divergences coming from low-order «tadpole-type» diagrams is the essentially new and important feature of construction by Glimm and Jaffe.

Next important step in the application of FI in QFT was made in the quantization of Yang-Mills fields. A consequent scheme of quantization for a massless Yang-Mills field was constructed in 1967 by Faddeev, Popov [13] and De Witt [14] within the PI approach. FI turned out to be the shortest and most convenient method for constructing the Feynman rules for perturbation expansion in gauge field theories. This method played an important role in the

investigations of Slavnov [15], Taylor [16], Lee and Zinn-Justin [17], t'Hooft and Weltman [18]. In these papers a generalized Ward-Takakhashi identity was obtained, various methods of invariant regularization were developed and a procedure renormalizing the perturbation series was built. Within FI there has also been an attempt made to construct a quantum theory of gravitation [19].

In the 1970s, techniques based on the original ideas of Peak and Inomata [20], and Duru and Kleinert [21] for solving certain non-Gaussian FIs occuring in QM have attracted much attention. Standard examples of QM considered in this approach are defined by using Bessel- and Legendre-type diffusion processes, other than the Wiener process often used on these subjects. These results do not require the machinery of stochastic analysis and can be treated in a quick, transparent way. A development of this method is assumed in [22], where certain non-Gaussian integrals with potentials like $\sim 1/r^2$ or of the Morse-type have been derived rigorously by using techniques of changing dimension and time in FIs.

Excellent monographs and review papers have been devoted to FI in quantum theory [13], [23—29].

Although many points concerning the correct mathematical definition and practical calculation of FIs still remain open, it becomes clear that the description of a quantum system within the FI method is as convenient as using linear operators acting on vectors of Hilbert space within the method of CQ.

We summarize the above, stressing in particular that:

— the FI is a *convenient conception for the qualitative consideration* of quantum theories owing to the simplicity of using the WKB approximation, the evident relativistic covariance of the fomulation and the ease with which some specific constraints can be taken into account (e.g., introduction of «ghosts» in Yang-Mills theory);

— the FI can serve as a *practical tool for the quantitative estimation* of characteristics of quantum systems because of the possibilities of reducing some dynamical variables by exact integration (e.g., in the polaron problem), changing space/time (for the inverse-square potential in QM) and the convenience of computer calculations for imaginary-time sum over paths [32], etc.

In the present paper we consider mostly the second aspect of the application of FIs in quantum physics.

1. APPROXIMATE METHODS FOR CALCULATING FUNCTIONAL INTEGRALS

A great number of problems of modern physics can be formulated in terms of the FI approach. These problems have a common feature: their solution can be obtained in the form of a functional integral, which is defined on the

Gaussian measure. The most general form of a typical functional integral can be written as follows:

$$Z(g) = C_0 \int \delta\varphi \exp\left\{ -\frac{1}{2} (\varphi D_0^{-1} \varphi) + gW[\varphi] \right\}, \tag{4}$$

where

$$(\varphi D_0^{-1} \varphi) = \int_\Gamma dx \int_\Gamma dy \, (\varphi(x) \, D_0^{-1}(x, y) \, \varphi(y))$$

and $\Gamma \in R^d$ $(d = 1, 2, \ldots)$. The Gaussian functional measure

$$d\sigma_0 = C_0 \, \delta\varphi \exp\left\{ -\frac{1}{2} (\varphi D_0^{-1} \varphi) \right\} \tag{5}$$

is defined by a Green function $D_0(x, y)$ corresponding to a differential operator $D_0^{-1}(x, y)$ with appropriate boundary conditions. The normalization constant C_0 is chosen in such a way that

$$\int d\sigma_0 = 1 \quad \text{or,} \quad Z(0) = 1.$$

In the standard nonrelativistic quantum mechanics the interaction functional W is usually defined by a potential $gU(\varphi)$:

$$W[\varphi] = g \int_\Gamma dx U(\varphi(x)), \tag{6}$$

where the coupling constant g is real. In other and more interesting cases (for example, polaron, bound states in QFT, stochastic processes, etc.) the interaction functional $W[\varphi]$ usually represents more complicated dependence on $\varphi(x)$.

Up to now exact calculations of functional integrals of this type are known [30] only for a quite limited class of interaction functionals: for quadratic forms of interaction leading to the pure Gaussian integral and very limited numbers of potentials (Coulomb potential and some others), for which the path integral can be reduced to the Gaussian integral after a definite change of variables. For others various approximate methods should be applied.

The contemporary progress in the computer hardwares and effective softwares for the numerical simulation technique enables one to obtain numerical calculations of (4) with sufficient accuracy although the practical implementation of this approach is very laborious. Besides, direct numerical (lattice) simulation is bound up with the difficulties of the continuous limit in lattice discretization and limited computer resources.

The development of analytical methods is very important because only analytical methods permit us to investigate qualitative features of quantum physical systems and indicate effective ways for improvement of numerical algorithms. Much efforts have been devoted to construct analytic methods for calculating the characteristics of quantum system within the FI formalism.

Among numerous approximate analytical FI methods we can list the following popular approaches: the standard perturbation expansion over g, the quasi-classic WKB approximation, the $1/N$ expansion, the instanton approximation and the variational methods (e.g., the Gaussian effective potential and space time transformation).

However, these methods have some limitations. For example, the WKB method cannot be used to study high-order quantum effects, the $1/N$ expansion gives a low convergence of the approximation series at real space-dimension numbers $N = 3$.

The standard perturbative method usually provides the perturbation series

$$Z(g) = \sum_{n=0}^{\infty} g^n Z_n$$

having the practical sense for a weak interaction $g << 1$ when only a few of the lowest terms Z_n is enough for getting $Z(g)$ with an acceptable accuracy. In addition, the calculation of Z_n for large n really is not more a simple task.

If the FI (4) is real, then the problems of such kind are studied by means of variational methods, which are popular due to their clear physical meaning and relatively simple calculations. However, the variational technique does not provide a regular prescription for choosing the trial functionals and it also does not allow one to control the accuracy of the estimation. Moreover, there is a class of problems (most of the QFT models with ultraviolet (UV) divergencies, complex and nonhermitean functionals, and so on), where the variational methods cannot be applied at all because the Jensen inequality no longer holds for these nonreal actions.

Our goal is to develop a universal method to calculate this path integral for any and especially large g. Sometimes it is possible to hear an opinion that in the strong coupling regime $g \to \infty$ the integral of the type (4) loses its Gaussian character and another non-Gaussian measure should be introduced. For example, it can be like this

$$d\sigma = C\, \delta\varphi \exp\{-\int_{\Gamma} dx\, \varphi^4(x)\}.$$

We want to claim that it is not true in the case of integrals of the type (4), where

- the highest derivative of the differential operator $D_0^{-1}(x, y)$ is 2ν, i.e. $D_0^{-1}(x, y) \sim \partial^{2\nu}$ for $\nu \geq 1$;
- the interaction functional $W[\varphi]$ depends only on $\varphi(x)$ and does not contain derivatives like $\partial\varphi(x)$.

Really, let us bring semiqualitative arguments. Let $f_n(x)$ is an orthonormal system of eigenfunctions of the operator D_0^{-1}:

$$D_0^{-1} f_n(x) = \frac{1}{D_n} f_n(x),$$

$$(f_n, f_m) = \int_\Gamma dx\, f_n(x)\, f_m(x) = \delta_{nm}. \tag{7}$$

The eigennumbers D_n satisfy the following asymptotics

$$D_n = O\left(\frac{1}{n^{2\nu}}\right) \quad \text{for} \quad n \to \infty.$$

Let us introduce the representation

$$\varphi(x) = \sum_n f_n(x) \sqrt{D_n}\, u_n, \tag{8}$$

where $\{u_n, (n = 0, 1, \ldots)\}$ are a new denumerate set of variables. We have

$$(\varphi D_0^{-1} \varphi) = \sum_n |u_n|^2,$$

$$Z(g) = C_0 \int \prod_n du_n \exp\left\{-\frac{1}{2}\sum_n |u_n|^2 + gW[\varphi]\right\}.$$

We expand $\varphi(x)$ as follows

$$\varphi(x) = \phi_N(x) + \phi_{>N}(x),$$

$$\phi_N(x) = \sum_{n<N} f_n(x) \sqrt{D_n}\, u_n, \tag{9}$$

$$\phi_{>N}(x) = \sum_{n>N} f_n(x) \sqrt{D_n}\, u_n \sim \sum_{n>N} \frac{f_n(x)}{n^\nu} u_n = O\left(\frac{1}{N^\nu}\right),$$

where N is a large number. Then we have

$$d\sigma = C_0 \prod_n du_n \exp\left\{-\frac{1}{2}\sum_n |u_n|^2\right\} = d\sigma_N\, d\sigma_{>N},$$

$$d\sigma_N = C_N \prod_{n<N} du_n \exp\left\{-\frac{1}{2}\sum_{n<N} |u_n|^2\right\},$$

$$d\sigma_{>N} = C_{>N} \prod_{n>N} du_n \exp\left\{-\frac{1}{2}\sum_{n>N} |u_n|^2\right\},$$

$$\int d\sigma_N = \int d\sigma_{>N} = 1.$$

The interaction functional can be represented as follows

$$W[\varphi] = g\int_\Gamma dx U(\phi_N(x)) + O\left(\frac{1}{N^\nu}\right). \tag{10}$$

Thus the functional integral under consideration can be approximated

$$Z(g) \sim Z_N(g) = \int d\sigma_N \exp\{gW[\phi_N]\} \tag{11}$$

and

$$Z(g) = \lim_{N\to\infty} Z_N(g).$$

One can see that the existence of this limit does not depend on the value of the coupling constant g and for any large g there exists a number $N(g)$ so that

$$Z(g) = Z_N(g) + O\left(\frac{1}{g}\right), \tag{12}$$

i.e., the functional measure can be considered as a Gaussian measure.

As a result we can conclude that the path integrals of the type (4) for any g can be considered as functional integrals over a Gaussian measure. Thus we can expect that there exists a representation of the initial functional integral (4)

$$Z(g) = C_g \int \delta\varphi \exp\left\{-\frac{1}{2}(\varphi D_g^{-1}\varphi) + W_g[\varphi]\right\} \tag{13}$$

with another C_g, D_g^{-1} and $W_g[\varphi]$, for which the main contributions from the interaction functional $gW[\varphi]$ should be accumulated in the operator D_g^{-1} and the perturbation corrections over the new interaction $W_g[\varphi]$ should be small. Our problem is to find this representation.

For this aim we shall use the idea that *the normal ordering of the Hamiltonian means essentially that the main quantum contributions to the ground state or vacuum of the system are taken into account.*

In the language of the FI it means that the conception of normal ordering with respect to a given Gaussian measure should be formulated and next problem is to represent the functional integral (4) in the form (13), where

- the Gaussian measure is defined by the operator D_g^{-1},
- the interaction functional $W_g[\varphi]$ is written in the normal form with respect to the Gaussian measure with D_g^{-1} and it does not contain quadratic terms over φ, i.e. $W_g[\varphi] = O(\varphi^4)$ for $\varphi \to 0$.

This representation we shall call the Gaussian equivalent representation of functional integrals. In section 2 all definitions will be formulated.

This method will be applied to the following problems:

- investigation of the behaviour of the polaron in ionic crystals in quantum statistics,
- phase transitions and phase restructure in quantum field models,
- propagation of waves in a stochastic medium with stochastically distributed centres in radiophysics.

2. GAUSSIAN EQUIVALENT REPRESENTATION OF FUNCTIONAL INTEGRALS

The main content of this Section is the development of the method of **Gaussian equivalent representation** (GER) of FIs and its application to the investigation of the ground state (vacuum) of various QFT and QM models in order to study nonperturbative phenomena such as the strong coupling regime, phase structure and phase transitions.

The GER method is a type of generalization of the variational technique, but in contrast to the latter, it is efficient for QFT models with UV divergencies and to theories with nonhermitean and nonlocal actions (stochastic and dissipative processes), where variational methods cannot be used.

This method is characterized by a high accuracy of the lowest approximation, which can be obtained by simple and rapid calculations. It gives a regular prescription for calculation of higher order corrections to the lowest approximation and can be considered as the next step in the development of approximate calculation methods.

2.1. General Formalism. Considering many theoretical problems in statistical physics [33], quantum field theory and mathematical physics one

deals with a class of functional integrals defined on a Gaussian measure. We shall consider functional integrals of the general type (4) as follows

$$Z_\Gamma(g) = C_0 \int \delta\varphi \exp\left\{ -\frac{1}{2}(\varphi D_0^{-1}\varphi) + gW_0[\varphi] \right\} =$$

$$= \int d\sigma_0 \exp\{gW_0[\varphi]\}. \tag{14}$$

Here we have introduced the following notation for the Gaussian measure

$$d\sigma_0 = C_0\, \delta\varphi \exp\left\{ -\frac{1}{2}(\varphi D_0^{-1}\varphi) \right\} =$$

$$= \frac{1}{\sqrt{\det D_0}} \prod_x d\varphi(x) \exp\left\{ -\frac{1}{2} \int\int_\Gamma dx\, dy\, \varphi(x)\, D_0^{-1}(x, y)\, \varphi(y) \right\}. \tag{15}$$

The Gaussian measure is normalized in such a way that $\int d\sigma_0 \cdot 1 = 1$. The integration in (14) is performed over functions $\varphi(x)$ defined on a region $\Gamma \subseteq \mathbf{R}^d$ ($d = 1, 2, \ldots$). Usually the region Γ is chosen as a multidimensional box: $\Gamma = \{x : a_j \le x_j \le b_j,\ (j = 1, \ldots, d)\}$.

A differential operator $D_0^{-1}(x, y)$ is defined on functions $\varphi(x)$ with appropriate boundary conditions. For example, the operator

$$D_0^{-1}(x, y) = \left(-\frac{\partial^2}{\partial x^2} + m_0^2 \right) \delta(x - y) \tag{16}$$

acts on functions satisfying some periodic boundary conditions. The corresponding Green function $D_0(x, y)$ satisfies the equation

$$\int_\Gamma dy\, D_0^{-1}(x, y)\, D_0(y, z) = \delta(x - z)$$

and ensures definite boundary conditions.

The parameter g is a coupling constant. The interaction functional $W_0[\varphi]$ can be written in a general form

$$W_0[\varphi] = \int d\mu_a\, e^{i(a\varphi)}, \tag{17}$$

where we have introduced the notation

$$(a\varphi) = \int_\Gamma dy\, a(y)\, \varphi(y),$$

and $d\mu_a$ is a functional measure. For example, for a potential having a Fourier transfrom one can write

$$W_0[\varphi] = \int_\Gamma dx U[\varphi(x)] = \int_\Gamma dx \int \frac{dk}{2\pi} \tilde{U}(k) \exp\{i \int_\Gamma dy\, k\varphi(y)\, \delta(x-y)\}.$$

FI in representation (14) is well defined as a perturbation expansion over the coupling constant g. Thus, physically acceptable results can be obtained only in the weak coupling regime $g << 1$. In this case the Gaussian measure $d\sigma_0$ (15) gives the main contribution in FI and corrections can be calculated by using a perturbation expansion.

The task is to give a representation of this integral in the strong coupling regime [34]. Our idea is that the FI beyond the perturbation regime remains of the Gaussian type but with another Green function in the measure. In other words, we want to obtain a representation in which all main contributions of strong interaction are concentrated in the measure.

Let us perform the following transformations of the integral (14):

$$\varphi(x) \to \varphi(x) + b(x),$$
$$D_0^{-1}(x, y) \to D^{-1}(x, y), \tag{18}$$

where $b(x)$ is an arbitrary function and $D(x, y)$ is an appropriate Green function of the differential operator D^{-1}:

$$\int_\Gamma dy\, D^{-1}(x, y)\, D(y, z) = \delta(x - z)$$

providing the same boundary conditions.

Transformations (18) represent in a certain sense a functional analogue of standard canonical transformations made in the Hamiltonian formalism. The functional integral (14) takes the form

$$Z_\Gamma(g) = \sqrt{\det \frac{D}{D_0}} \exp\left\{-\frac{1}{2}(bD_0^{-1}b)\right\} \cdot \int d\sigma \exp\{gW_1[\varphi, b, D]\}, \tag{19}$$

where

$$d\sigma = C\, \delta\varphi \exp\left\{-\frac{1}{2}(\varphi D^{-1}\varphi)\right\},$$
$$dW_1[\varphi, b, D] = gW[\varphi + b] - (bD_0^{-1}\varphi) - \frac{1}{2}(\varphi [D_0^{-1} - D^{-1}]\, \varphi), \tag{20}$$

with the normalization condition $\int d\sigma \cdot 1 = 1$.

The tadpole Feynman diagrams give the main quantum contributions into background energy of the system under consideration or, in other words, into the formation of the background state or vacuum. The mathematical problem is to take them into account correctly. In the quantum theory the main divergences given by tadpole vacuum diagrams are efficiently eliminated out of consideration if the normal- ordered product of operators is introduced into the interaction Hamiltonian. Following this, the interaction functional in (19) should be written in the normal-ordered form. Thus we should introduce in W_1 the concept of the normal product according to the given Gaussian measure $d\sigma$. It can be done in the following way

$$: e^{i(a\varphi)} : = e^{i(a\varphi)} e^{\frac{1}{2}(aDa)}. \tag{21}$$

This definition leads to the following relations

$$\int d\sigma : e^{i(a\varphi)} : = 1, \qquad \int d\sigma : \varphi(x_1) \ldots \varphi(x_n) : = 0.$$

After these transformations the functional in the integrand can be rewritten

$$gW_1 = g \int d\mu_a \, e^{i(ab) - \frac{1}{2}(aDa)} : e_2^{i(a\varphi)} : +$$

$$+ \left[g \int d\mu_a \, e^{i(ab) - \frac{1}{2}(aDa)} - \frac{1}{2} ([D_0^{-1} - D^{-1}] D) \right] +$$

$$+ \left[ig \int d\mu_a \, e^{i(ab) - \frac{1}{2}(aDa)} (a\varphi) - (bD_0^{-1}\varphi) \right] -$$

$$- \frac{1}{2} : \left[g \int d\mu_a \, e^{i(ab) - \frac{1}{2}(aDa)} (a\varphi)^2 + (\varphi [D_0^{-1} - D^{-1}] \varphi) \right] : \tag{22}$$

where $e_2^z = e^z - 1 - z - \frac{z^2}{2}$.

Now we introduce the concept of the «correct form» of the action in the FI. We demand that the linear and quadratic terms on the integration variables $\varphi(x)$ should be absent in the interaction functional W_1 in (22). This requirement is argued in the same way. The system under consideration should be near its equilibrium point so that any linear terms on the variable $\varphi(x)$ must be absent. The quadratic configurations $\sim \varphi^2$ determine the Gaussian oscillator character of the equilibrium point and all of them are concentrated in the Gaussian measure $d\sigma$ only. Therefore, they should not appear in the interaction functional and

$$W_I \sim \varphi^3 \quad \text{for} \quad \varphi \to 0.$$

Thus the «correct form» requirement is satisfied if the following equations are held

$$g \int d\mu_a \, ia(x) \, e^{i(ab) - \frac{1}{2}(aDa)} - \int_\Gamma dy \, D_0^{-1}(x, y) \, b(y) = 0,$$

$$g \int d\mu_a \, a(x) \, a(y) \, e^{i(ab) - \frac{1}{2}(aDa)} + D_0^{-1}(x, y) - D^{-1}(x, y) = 0. \tag{23}$$

These equations provide the removal of the linear and quadratic terms from the interaction functional. Let us introduce the following functional and its correlation functions:

$$\hat{W}[b] = \int d\mu_a \exp\left\{ i(ab) - \frac{1}{2}(aDa) \right\},$$

$$\omega_n(x_1, \ldots, x_n) = \frac{\delta^n}{\delta b(x_1) \cdot \ldots \cdot \delta b(x_n)} \hat{W}[b]. \tag{24}$$

Equations (24) can be written in the form

$$b(x) = g \int_\Gamma dy \, D_0(x, y) \, \omega_1(y),$$

$$D(x_1, x_2) = D_0(x_1, x_2) + g \iint_\Gamma dy_1 \, dy_2 D_0(x_1, y_1) \, \omega_2(y_1, y_2) \, D(y_2, x_2). \tag{25}$$

These equations determine the new Green function $D(x_1, x_2)$ and the function $b(x)$ in (22). Finally the new representation for FI in (14) can be rewritten in the form:

$$Z_\Gamma(g) = \exp\{E_0\} \cdot \int d\sigma \exp\{g W_I[\varphi]\}, \tag{26}$$

where

$$E_0 = \frac{1}{2} \ln \det\left(\frac{D}{D_0}\right) - \frac{1}{2}(bD_0^{-1}b) - \frac{1}{2}([D_0^{-1} - D^{-1}]D) + g\hat{W}[b],$$

$$gW_I[\varphi] = g \int d\mu_a \, e^{i(ab) - \frac{1}{2}(aDa)} : e^{i(a\varphi)}_2 : . \tag{27}$$

The representation of the interaction functional in the normal product form means that

$$\int d\sigma \, W_I[\varphi] = 0.$$

The function E_0 defines the «energy» of the zero approximation. Next corrections to the leading term in (26) can be calculated by using a perturbation expansion over the new interaction functional W_I.

It should be stressed that representations (14) and (26) are equivalent. Therefore the mathematical object $Z_\Gamma(g)$ has at least two different representations (14) and (26). In principle other representations may exist if equation (26) has a more distinct solution. In this case we give preference to the representation in which the perturbation corrections connected with gW or gW_I are minimal for given parameters.

All our transformations are valid for real and complex functions and functionals in the FI.

In the case of real FIs representation (26) leads to the following conclusion. Using Jensen's inequality one can get

$$Z_\Gamma(g) \geq \exp\{E_0\}, \tag{28}$$

so that E_0 defines the lowest estimation for our FI.

On the other hand, one can easily check that (26) defines the minimum of the function E_0. Thus, inequality (28) is the variational estimate of the initial FI. Moreover, representation (26) makes it possible to calculate the perturbation corrections to E_0 by developing the functional integral (26) over W_I.

2.2. The GER Method for Calculating the Partition Function. In this Section we develop the main techniques of the GER method especially for calculating the partition function in QM and QS. In other words, we deal with integrals where the field variable is the coordinate of a particle $\mathbf{r}(t)$ which is parameterized by the one-dimensional parameter t. For simplicity one can choose the symmetrical interval $-T < t < T$. The parameter T is connected with time in QM or the inverse temperature $2T = \beta$ in QS.

The partition function plays an important role in QS. For a wide class of quantum mechanical and quantum statistical problems describing the interaction of a quantum particle with a field or the propagation of waves and quantum particles through a media with random or stochastic admixtures the partition function can be represented in the form of a FI of the following general type

$$Z_T(g) =$$

$$= C_0 \int\limits_{\mathbf{r}(-T)=\mathbf{r}(T)} \delta\mathbf{r} \exp\left\{-\frac{1}{2}\int\limits_{-T}^{T} dt\, \dot{\mathbf{r}}^2(t) + \frac{g}{2}\iint\limits_{-T}^{T} dt\, ds\, V(\mathbf{r}(t) - \mathbf{r}(s);\, t-s)\right\}. \tag{29}$$

The standard normalization is $Z_T(0) = 1$. The integration in (29) is performed over all «paths» in a d-dimensional space satisfying periodic boundary conditions.

The kinetic term in the Gaussian measure can be written in the form

$$\int_{-T}^{T} dt\, \dot{\mathbf{r}}^2(t) = \iint_{-T}^{T} dt\, ds\, \mathbf{r}(t)\, D_0^{-1}(t, s)\, \mathbf{r}(s),$$

$$D_0^{-1}(t, s) = -\frac{\partial^2}{\partial t^2}\, \delta(t - s). \tag{30}$$

The Green function $D_0(t, s)$ corresponding to the differential operator $D_0^{-1}(t, s)$ and satisfying the periodic boundary conditions is

$$D_0(t, s) = -\frac{1}{2}\, |t - s| - \frac{ts}{2T} \xrightarrow{T\to\infty} -\frac{1}{2}\, |t - s|. \tag{31}$$

The Fourier transform of this Green function is

$$\tilde{D}_0(p^2) = \int_{-\infty}^{\infty} dt\, e^{ipt} D_0(t) = \frac{1}{2}\left[\frac{1}{(p + i0)^2} + \frac{1}{(p - i0)^2}\right] \to \frac{1}{p^2}. \tag{32}$$

The parameter g is a coupling constant. In QM and QS, the potentials describing the influence of a field interaction or media on a quantum particle usually have a general form like $V(\mathbf{r} - \mathbf{r}'; t - t')$. So, we will consider this class of potentials further. The potential $V(\mathbf{r}(t) - \mathbf{r}(s); t - s)$ in (29) is assumed to have the Fourier representation

$$V(\mathbf{r}(t) - \mathbf{r}(s); t - s) = \int \frac{d\mathbf{k}}{(2\pi)^d}\, \tilde{V}(\mathbf{k}; t - s)\, e^{i\mathbf{k}\mathbf{R}(t, s)} = \int d\mathcal{K}(\mathbf{k}; t - s)\, e^{i\mathbf{k}\mathbf{R}(t, s)},$$

$$d\mathcal{K}(\mathbf{k}; t - s) = \frac{d\mathbf{k}}{(2\pi)^d}\, \tilde{V}(\mathbf{k}; t - s),$$

$$\mathbf{R}(t, s) = \mathbf{r}(t) - \mathbf{r}(s). \tag{33}$$

Thus the initial FI in (29) can be rewritten as

$$Z_T(g) = \int d\sigma_0 \exp\{gW_0[\mathbf{r}]\}, \tag{34}$$

where

$$d\sigma_0 = C_0\, \delta\mathbf{r} \exp\left\{-\frac{1}{2}\iint_{-T}^{T} dt\, ds\, \mathbf{r}(t)\, D_0^{-1}(t, s)\, \mathbf{r}(s)\right\}, \tag{35}$$

$$gW_0[\mathbf{r}] = \frac{g}{2}\iint_{-T}^{T} dt\, ds \int d\mathcal{K}(\mathbf{k}; t - s)\, e^{i\mathbf{k}\mathbf{R}(t, s)} \tag{36}$$

and the normalization condition is $\int d\sigma_0 \cdot 1 = 1$.

Now we are ready to apply the GER method to this FI. Note that for the potentials $V(\mathbf{r}; t)$ of type (33) having their maximum at $\mathbf{r} = 0$ we do not need to introduce the function $\mathbf{b}(t)$, i.e., $\mathbf{b}(t) = 0$. According to the GER method a new Gaussian measure should be introduced into the integral (34) as follows

$$d\sigma = C\,\delta\mathbf{r}\,\exp\left\{-\frac{1}{2}\iint_{-T}^{T} dt\,ds\;\mathbf{r}(t)\,D^{-1}(t-s)\,\mathbf{r}(s)\right\}. \tag{37}$$

The normalization constant C is $\int d\sigma \cdot 1 = 1$.

Second, we introduce the «normal-ordered» form of the potential (33) in the following way

$$e^{i\mathbf{kR}(t,\,s)} = :e^{i\mathbf{kR}(t,\,s)}: \exp\left[-\mathbf{k}^2 F(t-s)\right], \tag{38}$$

where

$$F(t-s) = D(0) - D(t-s),$$

$$\int d\sigma\, R_i(t, s)\, R_j(t, s) = 2\delta_{ij}\, F(t-s).$$

In particular, the next relations are valid:

$$\int d\sigma :e^{i\mathbf{kR}(t,\,s)}: = 1,$$

$$r_i(t)\, r_j(s) = :r_i(t)\, r_j(s): + \delta_{ij}\, D(t-s), \qquad i, j = 1 \ldots d.$$

The functional $\hat{W}[b]$ in (24) becomes

$$\hat{W}[b] = \frac{1}{2}\iint_{-T}^{T} dt\,ds \int d\mathcal{K}(\mathbf{k};\, t-s)\,\exp\left[-\mathbf{k}^2 F(t-s)\right] e^{i\mathbf{k}(\mathbf{b}(t)\,-\,\mathbf{b}(s))}. \tag{39}$$

Its second correlation function is

$$\frac{\delta^2}{\delta b_i(t)\,\delta b_j(s)}\,\hat{W}[\mathbf{b}]\Big|_{b=0} = -\delta_{ij}\left[\delta(t-s)\int_{-\infty}^{\infty} d\tau\,\Phi(\tau) - \Phi(t-s)\right], \tag{40}$$

where

$$\Phi(\tau) = \frac{1}{d}\int d\mathcal{K}(\mathbf{k};\,\tau)\,\mathbf{k}^2 \exp\left[-\mathbf{k}^2 F(\tau)\right].$$

Equation (26) defining «the correct form» of the interaction functional becomes

$$\tilde{\Sigma}(p^2) = \frac{1}{d}\int_{-\infty}^{\infty} d\tau\,[1-\cos(p\tau)]\int d\mathcal{K}(\mathbf{k};\,\tau)\,\mathbf{k}^2 \exp\left[-\mathbf{k}^2 F(\tau)\right], \tag{41}$$

$$F(\tau) = \int_0^{\infty} \frac{dp}{\pi}\,\frac{1-\cos(p\tau)}{p^2 + g\,\tilde{\Sigma}(p^2)}. \tag{42}$$

Equations (41) and (42) define the Green function $D(\tau)$. For the asymptotic cases of weak ($g \to 0$) and strong ($g \to \infty$) interaction regimes, these equations may admit analytic solutions because one needs only that their behaviour be within the accuracy of the first several leading order terms such as $\sim g, g^2$ or, $\sim 1/g, 1/g^2$. In general, these are not solvable analytically as they are nonlinear integral equations over functionals, but their solutions may be obtained by developing some numerical techniques. For example, the fixed-point method of consequent iterations can be used. Starting from guess function $\tilde{\Sigma}_0(p^2)$ we can calculate the iterations:

$$\tilde{\Sigma}_{n+1}(p^2) = \frac{1}{d} \int_{-\infty}^{\infty} d\tau \, [1 - \cos(p\tau)] \int d\mathcal{K}(k; \tau) \, \mathbf{k}^2 \exp[-\mathbf{k}^2 F_n(\tau)],$$

$$F_{n+1}(\tau) = \int_0^{\infty} \frac{dp}{\pi} \cdot \frac{1 - \cos(p\tau)}{p^2 + g\,\tilde{\Sigma}_n(p^2)}. \tag{43}$$

This procedure can be developed for numerical solutions of (41) and (42). In this case, however, the initial guess functions $F_0(\tau)$ and $\tilde{\Sigma}_0(p^2)$ should be chosen reasonably, i.e., the iteration process (43) has to converge to solutions

$$\tilde{\Sigma}(p^2) = \tilde{\Sigma}_{\infty}(p^2) = \lim_{n\to\infty} \tilde{\Sigma}_n(p^2), \tag{44}$$

$$F(t) = F_{\infty}(t) = \lim_{n\to\infty} F_n(t). \tag{45}$$

For a reasonable choice of guess functions, it is useful to investigate asymptotics of solutions for equations (41) and (42). An example of analytic and numerical solution of (41) and (42) is given in Section 3.3 within the polaron problem.

Substitution of (37)—(42) into (34) and the requirement that the new interaction functional to be written in the «correct form» (see Section 2.1) lead to the new representation of the initial FI

$$Z_T(g) = \exp(-2TE_0(g)) \cdot J_T(g),$$

$$J_T(g) = \int d\sigma \exp\{gW_I[\mathbf{r}]\}, \tag{46}$$

where the interaction functional looks as

$$gW_I[\mathbf{r}] = \frac{g}{2} \iint_{-T}^{T} dt\, ds \int d\mathcal{K}(\mathbf{k}; t - s) \exp[-\mathbf{k}^2 F(t - s)] : e_2^{i\mathbf{k}\mathbf{R}(t, s)} :. \tag{47}$$

The function $E_0(g)$ being «the leading-order energy» or the energy in the zero approximation is

$$E_0(g) = d \int_0^\infty \frac{dp}{2\pi} \left[\ln \frac{\tilde{D}_0(p^2)}{\tilde{D}(p^2)} + p^2 \tilde{D}(p^2) - 1 \right] +$$

$$+ \frac{g}{2} \int_{-\infty}^{\infty} d\tau \int d\mathcal{K}(\mathbf{k}; \tau) \exp [- \mathbf{k}^2 F(\tau)]. \qquad (48)$$

Thus the Gaussian equivalent representation of the initial FI in (34) is defined by (46)—(48). For a given potential $V(\mathbf{r})$ we have a pure mathematical problem to solve (41), (42) and find the Green function $D(t, s)$. Then we can compute the leading-order energy $E_0(g)$ (48) and the highest corrections to it by perturbation calculations over the new interaction functional W_I (47).

Below, in the following sections of this paper, we apply the GER method to different problems of theoretical physics:

- the problem of the polaron in QS,
- the phase transition phenomenon in the QFT model,
- the solution of the wave differential equation.

Each of these subjects reflects a feature of the GER method. High accuracy is reached in calculation of the ground state energy of the d-dimensional Fröhlich polaron. One effective scheme of mass renormalization in the $g\varphi^4_{2,3}$ theory, suggested within the GER method, leads to the correct prediction of the nature of phase transitions in this theory. Finally an estimate of non-Hermitean path integral arising in the theory of wave propagation in media with Gaussian noise is obtained. The reduction of the initial PI to the new representation generates a certain constraint equation determining this state and one should give preference to the representation, that is efficient for solving a given task.

3. THE POLARON PROBLEM

The study of the physical properties of a particle interacting with a quantum medium is common to many branches of physics. A classic example of this kind is the Fröhlich model of the polaron, — an electron moving with the polarization distortion of ions in a crystal. The polaron's popularity as a model is due to its similarity to many field-theoretical constructions where bosons couple linearly to fermions (the meson-nucleon interactions inside nuclei, the «dressing» of quarks in the nonperturbative vacuum of QCD, etc.). The polaron problem is treated most straightforwardly in the FI formalism which allows one to reduce this problem to an effective one-particle task and, leads to new results

not given by other conventional techniques. However, despite its long history and importance, the exact solution of the Fröhlich Hamiltonian is still lacking due to a high nonlocality (in time) and a Coulomb-like singularity in the polaron action. The application of the GER method to the d-dimensional polaron in this chapter results in highly accurate estimations of the main quasi-particle characteristic of the polaron — its ground-state energy.

The polaron problem embraces a wide range of questions concerning the behaviour of the electron of conductance in polar crystals [35—37]. The first field-theoretical formulation of polaron theory was proposed by Fröhlich [38] to describe the interaction of a single band electron with phonons, quanta associated with the longitudinal optical branch of lattice vibrations. Since that time, the Fröhlich polaron model has attracted interest as a testing ground of various nonperturbative methods in quantum physics. One of the main quasi-particle characteristics of the polaron is its ground-state energy (GSE) $E_0(\alpha)$.

Historically, the GSE of the polaron has been investigated in the weak [38], intermediate [39] and strong coupling regimes [40,41] using different methods. The first attempt to build the polaron theory, valid for arbitrary values of α, was made by Feynman [35] within the path integral (PI) formalism using variational estimations. As a result, Feynman's PI approach gives good upper bounds of $E_0(\alpha)$ in the entire range of α in a unified way.

There arises the question, whether the Feynman's estimations of the polaron GSE can be improved by introducing some trial actions, more general than the quadratic action with two variational parameters used in [35]. This question, in particular, has been studied within different variational approaches [42,43]. But giving variational answers, it could not estimate the next corrections to the obtained values.

Traditionally, the polaron problem has been investigated in three-dimensional space ($d=3$) [44,45]. In recent years, however, polaron effects have been observed in low-dimensional systems [46], and certain physical problems have been mapped into a two-dimensional ($d=2$) polaron theory [47]. The possibility that an electron may be trapped on the surface of a dielectric material has attracted much interest [48]. The GSE of the polaron for $d=2$ is discussed in [49,50].

In the Section, we investigate the GSE of the polaron in the case of arbitrary space dimensions ($d>1$) and try not only to improve Feynamn's result, but also to estimate the next corrections that allow one to test the accuracy and reliability of the obtained values.

3.1. Polaron Path Integral in *d* Dimensions. The Fröhlich longitudinal-optical (LO) polaron model for $d=3$ is determined by the Hamiltonian

$$H=\frac{1}{2m}\,\mathbf{p}^2+\hbar\,\omega\sum_{\mathbf{k}}\,a_{\mathbf{k}}^{\dagger}a_{\mathbf{k}}+\frac{1}{\sqrt{\Omega}}\sum_{\mathbf{k}}\,g_{\mathbf{k}}(a_{\mathbf{k}}^{\dagger}\,\mathrm{e}^{-i\,\mathbf{kx}}-a_{k}\,\mathrm{e}^{i\,\mathbf{kx}}), \tag{49}$$

which describes the interaction of an electron (position and momentum vectors **x** and **p**, band mass m) with the phonon field (creation and annihilation operators $a_{\mathbf{k}}^{\dagger}$, $a_{\mathbf{k}}$, quantization volume Ω, Plank constant $\hbar$) associated with a LO branch of lattice vibrations (wave vector **k** and frequency ω) in a polar crystal. The electron-phonon interaction coefficient for coupling with the wave vector **k** in (49) is defined as follows:

$$g_{\mathbf{k}} = \frac{i\hbar\,\omega(\hbar/2m\omega)^{1/4}(4\pi\,\alpha)^{1/2}}{|\mathbf{k}|}, \tag{50}$$

where the dimensionless Fröhlich coupling constant α takes the value $\alpha \sim 1 + 20$ in most of the real ionic crystals (e.g.,$\alpha \simeq 5$ for sodium chloride). In the following, units will be chosen such that $\hbar = m = \omega = 1$.

Until now, no nontrivial solution of $H\Psi_n = E_n\Psi_n$ was known. It has been shown [51] for generalized Fröhlich models that the function $E_0(\alpha)$ has no points of nonanalyticity for an arbitrary $\alpha \geq 0$. Various methods [35,40,52,39] have been used to approximately calculate the spectrum of H, especially to obtain its GSE E_0 for selected (weak, intermediate or strong) regions of α.

To extend the Fröhlich Hamiltonian (49) written for $d = 3$ to arbitrary spatial dimensions $d > 1$, we follow a physical approach [53,54] inspired by the formulation of a lower-dimensional polaron problem obtained from the Fröhlich Hamiltonian of a higher-dimensional system by integrating out one or more dimensions. Following [54] we assume that the form of the Fröhlich Hamiltonian in d-dimensions is the same as in (49) except that now all vectors and operators are d-dimensional and the electron-phonon interaction coefficient $g_{\mathbf{k}}$ is redefined as follows:

$$|g_{\mathbf{k}}|^2 = \frac{\lambda_d^2}{|\mathbf{k}|^{d-1}}, \quad \lambda_d^2 = \Gamma\left(\frac{d-1}{2}\right)2^{d-3/2}\pi^{(d-1)/2}\alpha. \tag{51}$$

Accordingly, we write the FI representation of the free-energy $F(\beta)$ of a polaron with a given temperature $\Theta = 1/\beta$ as follows:

$$\exp(-\beta F) = \mathrm{Tr}\,[\exp(-\beta H)], \tag{52}$$

where the Hamiltonian H in (49) should be written in terms of the coordinates and momenta. The «Trace» $\mathrm{Tr} = \mathrm{Tr}_{el}\mathrm{Tr}_{ph}$ here is assumed to be taken over the whole space of states of the «electron + phonon» system.

It is well known from the famous paper by Feynman [35] that the path integral approach to the polaron has an advantage because the phonon trace Tr_{ph} in (52) can be adequately eliminated and as a consequence, the polaron

problem is reduced to an effective one-particle problem with retarded interaction. The result reads

$$Z_\beta(\alpha) = \exp(-\beta F) = \int_{\mathbf{x}(0)=\mathbf{x}(\beta)} \delta\,\mathbf{x}\,\exp(S[\mathbf{x}]), \tag{53}$$

where the action $S[\mathbf{x}]$ is

$$S[\mathbf{x}] = -\frac{1}{2}\int_0^\beta dt\,\dot{\mathbf{x}}^2(t) + \frac{\lambda_d^2}{8\pi}\iint_0^\beta dtds\,\frac{1}{|\mathbf{x}(t)-\mathbf{x}(s)|}\,\frac{e^{|t-s|}+e^{\beta-|t-s|}}{e^\beta-1}. \tag{54}$$

The free energy $F(\beta)$ tends to the GSE as $\beta \to \infty$ (zero temperature case)

$$E_0 = -\lim_{\beta\to\infty}\frac{1}{\beta}\ln Z_\beta(\alpha). \tag{55}$$

The path integral in (53) is not explicitly solvable due to the non-Gaussian character of S. For its variational estimation for $d = 3$, Feynman proposed [35] a quadratic two-body trial action S_F instead of S:

$$S[\mathbf{x}] \to S_F[\mathbf{x}] = -\frac{1}{2}\int_0^\beta dt\,\dot{\mathbf{x}}^2(t) +$$

$$+\frac{C}{2}\iint_0^\beta dtds[\mathbf{x}(t)-\mathbf{x}(s)]^2\exp\{-\omega|t-s|\}, \tag{56}$$

where constants C and ω are variational parameters. With the trial action S_F one gets an exact solution for path integral in (53). A variation for finding of the absolute minimum of $E_0^F(\alpha) = F_F(\alpha)$ for $\beta \to \infty$ over parameters C and ω leads to a rigorous upper bound of the polaron GSE at arbitrary α, that is Feynman's known result [35].

Here we will show that the application of the GER method improves Feynman's estimation. We consider the polaron GSE in the case of arbitrary space dimension $d > 1$ and start again from the FI in (53)—(54).

For further convenience, to get a symmetrical region over t [56], we change the variable of FI in (53) to

$$\mathbf{x}(t) \to \mathbf{r}(t-T), \quad T = \beta/2 \tag{57}$$

with the electron motion $\mathbf{r}(t)$ embedded in d-dimensional space. Accordingly, the GSE of the Fröhlich polaron $E_0(\alpha)$ (it will hereafter be denoted by $E(\alpha)$) can be defined as follows:

$$E(\alpha) = -\lim_{T\to\infty}\frac{1}{2T}\ln Z_T(\alpha), \tag{58}$$

where a FI is introduced [55]

$$Z_T(\alpha) = C_0 \int\limits_{\mathbf{r}(-T)=\mathbf{r}(T)} \delta\,\mathbf{r} \exp\left\{-\frac{1}{2}(\mathbf{r}D_0^{-1}\mathbf{r}) + \frac{\alpha}{2}\int\limits_{-T}^{T} dtds\, V[\mathbf{r}(t)-\mathbf{r}(s); t-s]\right\},$$

$$C_0 = \sqrt{\det D_0^{-1}}, \quad (\mathbf{r}, D_0^{-1}\mathbf{r}) = \int\limits_{-T}^{T} dtds\, \mathbf{r}(t) D_0^{-1}(t, s)\, \mathbf{r}(s). \tag{59}$$

The standard normalization $E(0) = 0$ in (58) is satisfied under the condition $Z_T(0) = 1$.

The free-electron system is described by the kinetic term $(\mathbf{r}D_0^{-1}\mathbf{r})$, where the differential operator D_0^{-1} and its Green function D_0 are given by (30)—(31) in the previous Section as $T \to \infty$.

The Coulomb-like interaction part, the electron self-interaction, is given by the retarded potential

$$V[\mathbf{R}; t-s] = \frac{\Gamma(d/2 - 1/2)}{4\sqrt{2}\pi^{(d+1)/2}} e^{-|t-s|} \int \frac{d\,\mathbf{k}}{|\mathbf{k}|^{d-1}} \exp(i\,\mathbf{kR}),$$

$$\mathbf{R} = \mathbf{r}(t) - \mathbf{r}(s). \tag{60}$$

with the electron position vector $\mathbf{r}(t)$ embedded into d-dimensions.

The path integral in (59) is not explicitly solvable due to the non-Gaussian character of $V[\mathbf{R}; t-s]$ in (60).

3.2. Bounds for the Polaron Ground-State Energy in d Dimensions. For α not too large, the PI in the initial presentation (59) may be estimated by using a perturbation expansion in α. The problem is to estimate $Z_T(\alpha)$ beyond the weak coupling regime. Accordingly, we can apply the GER method to this problem.

Our key steps will be the same as those in the previous Section. We remember that these are:

(i) *the introduction of new Gaussian measure $d\sigma$ (20) standing for the kinetic part of the FI*, which forms a new representation of the initial FI, and

(ii) *the requirements of the «normal-ordered» and «correct» form of the interaction part of the FI in this representation,* that is reached by introducing constraint equations (41), (42). This scheme results in a new representation of the initial FI: an exponential with the leading term of energy factorized out as a free multiplicand (48) and all the corrections to it are defined by another FI (47).

Performing this scheme and using formulae (41), (42) and (46)—(48), we obtain the new representation (47) of the GSE of optical polaron within the GER method as follows:

$$E(\alpha) = E_0(\alpha) + \Delta E(\alpha), \tag{61}$$

where the function $E_0(\alpha)$ being the «leading-order energy», or the GSE in the zeroth approximation, is (see Eq. (48))

$$E_0(\alpha) = -d\left\{\frac{1}{2\pi}\int_0^\infty dk[\ln(k^2\tilde{D}(k)) - k^2\tilde{D}(k)+1] + \frac{\alpha_d}{3\sqrt{2\pi}}\int_0^\infty dt\,\frac{\exp(-t)}{F^{1/2}(t)}\right\}. \tag{62}$$

The function $F(t)$ in (62) is defined by the equations (see Eqs. (41) and (42))

$$F(t) = \int_{-\infty}^{\infty}\frac{dk}{2\pi}\,\tilde{D}(k)(1-e^{ikt}) = \frac{1}{\pi}\int_0^\infty dk\,\frac{1-\cos(kt)}{k^2+\alpha_d\tilde{\Sigma}(k)}, \tag{63}$$

$$\tilde{\Sigma}(k) = \int_{-\infty}^{\infty} dt\,e^{-ikt}\,\Sigma(t) = \frac{1}{3\sqrt{2\pi}}\int_0^\infty dt\,\exp(-t)\,\frac{1-\cos(kt)}{F^{3/2}(t)}. \tag{64}$$

Here we have introduced the «effective coupling constant»

$$\alpha_d = \alpha\cdot R_d, \quad R_d = \frac{3\sqrt{\pi}\,\Gamma(d/2-1/2)}{2d\,\Gamma(d/2)}. \tag{65}$$

Our leading term (the zero-order approximation) $E_0(\alpha)$ gives an upper bound to the exact GSE of a polaron $E(\alpha)$. Actually, applying the Jensen's inequality to (61) one gets

$$\exp\{-2T\cdot E(\alpha)\} \geq \exp\{-2T\cdot E_0(\alpha)\}. \tag{66}$$

Consequently,

$$E_0(\alpha) \geq E(\alpha). \tag{67}$$

The high-order corrections $\Delta E(\alpha)$ in (61) can be obtained by evaluating the PI

$$\exp\{-2T\cdot\Delta E(\alpha)\} = C\int_{\mathbf{r}(-T)=\mathbf{r}(T)}\delta\mathbf{r}\,\exp\left\{-\frac{1}{2}\iint_{-T}^{T} dtds\,\mathbf{r}(t)D^{-1}(t,s)\,\mathbf{r}(s) + W[\mathbf{r}]\right\}. \tag{68}$$

Here, the interaction functional written in the new representation is

$$W[\mathbf{r}] = \alpha_d\cdot\frac{\Gamma(d/2)d}{6\sqrt{2\pi}^{\,d/2+1}}\iint_{-T}^{T} dtds\,e^{-|t-s|}\times$$

$$\times\int\frac{d\,\mathbf{k}}{|\mathbf{k}|^{d-1}}\exp\{-\mathbf{k}^2F(t-s)\} : e_2^{i\,\mathbf{k}[\mathbf{r}(t)-\mathbf{r}(s)]} :, \tag{69}$$

where $e_2^x = e^x - 1 - x - x^2/2$.

Due to equations (64) and (63) in the new representation, all the quadratic terms in the polaron action functional are concentrated only in the new Gaussian measure $d\sigma$ and do not enter $W[\mathbf{r}]$.

It should be stressed that representation (61) is completely equivalent to the initial representation (58) for asymptotically large $T \to \infty$. The Gaussian equivalent representation (61) gives the origin of various approximations differing from each other in the accuracy of deriving equations (63)—(64).

As a simple approximation of $\tilde{\Sigma}(k)$ obeying the necessary asymptotics, one can take the function:

$$\tilde{\Sigma}(k) = \frac{\mu^2}{\alpha_d} \cdot \frac{k^2}{\xi^2 + k^2}, \tag{70}$$

where μ and ξ are parameters. Then, (62) becomes

$$E_0(\alpha) = -\frac{d}{2}\left[\xi - \lambda + \frac{\mu^2}{2\lambda}\right] - \frac{\alpha_d \lambda^{3/2} d}{3\mu\sqrt{\pi}} \int_0^\infty \frac{dt \exp(-t)}{\sqrt{1 - \exp(-\lambda t) + \lambda t\, \xi^2/\mu^2}},$$

$$\lambda = \sqrt{\mu^2 + \xi^2}. \tag{71}$$

Minimizing the obtained energy over the parameters μ and ξ, one easily finds a variational upper bound in d dimensions. For $d = 3$ ($\alpha_3 = \alpha$) it explicitly reproduces the well-known Feynman's variational upper bound to the polaron GSE [35]:

$$E^F(\alpha) = \min_{\mu} \min_{\xi} E_0(\alpha, d = 3). \tag{72}$$

We stress that the extremal conditions on parameters μ, ξ in (72) are equivalent to a particular choice of the function $\tilde{\Sigma}(k)$ in (70). However, the function in (70) is not an exact solution of (64) and (63). It means, that Feynman's trial quadratic action does not represent entirely the Gaussian part of the polaron action for $d = 3$. Exact numerical solution of equations (64), (63) by the iteration procedure allows us to obtain $E_0(\alpha)$ more exactly, which improves Feynman's result $E^F(\alpha)$ in the entire range of α. The obtained numerical results $E_0(\alpha)$ for $d = 2$ and $d = 3$ as compared with Feynman's variational estimation are displayed in Tables I—VI.

The correction $\Delta E(\alpha)$ should be evaluated from the functional integral in (69) by expanding e^W in (68) in a series

$$\Delta E(\alpha) = \sum_{n=1}^{\infty} \Delta E_n(\alpha) = -\lim_{T\to\infty} \frac{1}{2T} \sum_{n=1}^{\infty} \frac{1}{n!} \int d\sigma \{W[\mathbf{r}]\}^n_{\text{connected}}. \tag{73}$$

We stress that (73) is not a standard perturbation series in the coupling constant α_d as α_d enters into W not only explicitly as a factor, but also implicitly through the function $F(t)$. The first term in (73) with $n = 1$ equals zero due to normal ordering. Nontrivial corrections are given by terms with $n \geq 2$. For the second order correction to $E_0(\alpha)$ we get

$$\Delta E_2(\alpha) = -\alpha_d^2 \cdot \frac{\Gamma(d/2)d^2}{18\pi^{3/2}} \sum_{n=2}^{\infty} Q_n R_n(\alpha), \tag{74}$$

where

$$Q_n = \frac{(2n)!\Gamma(n+1/2)}{16^n (n!)^2 \Gamma(n+d/2)},$$

$$R_n = \iiint_0^{\infty} dadbdc \left\{ e^{-a-c} \frac{[F(a+b)+F(b+c)-F(a+b+c)-F(b)]^{2n}}{[F(a)F(c)]^{n+1/2}} + \right.$$

$$+ e^{-a-2b-c} \frac{[F(a)+F(c)-F(a+b+c)-F(b)]^{2n}}{[F(a+b)F(b+c)]^{n+1/2}} +$$

$$\left. + e^{-a-2b-c} \frac{[F(a+b)+F(b+c)-F(a)-F(c)]^{2n}}{[F(a+b+c)F(b)]^{n+1/2}} \right\}.$$

We stress that expression (74) can further be simplified, but we keep this form for clarity.

Finally, we get the following expression for the GSE of the polaron

$$E^{(2)}(\alpha) = E_0(\alpha) + \Delta E_2(\alpha), \tag{75}$$

which can be evaluated numerically for arbitrary α and different space dimensions d.

Notice that $E_0(\alpha)$ in (62) is of an order of α^i, $(i = 0, 1, 2, \ldots)$ while $\Delta E_2(\alpha)$ in (74) is only of an order of α^j, $(j = 2, 3, \ldots)$.

The theory under consideration has two parameters α and d. In general, all our expressions should depend on both of them. Notice that key expressions in (64) and (63), completely defining the functions $F(t)$ and $\tilde{\Sigma}(k)$, depend only on the effective coupling constant α_d. This means that the following relations

$$F^{[n]}(\alpha_m, t) = F^{[m]}(\alpha_n, t), \quad \tilde{\Sigma}^{[n]}(\alpha_m, k) = \tilde{\Sigma}^{[m]}(\alpha_n, k) \quad n,m > 1 \tag{76}$$

take place, where the numbers of space-dimensions n and m are in square brackets [...]. In the particular case of $d = 2$ and $d = 3$, we found

$$F^{[2]}(\alpha, t) = F^{[3]}\left(\frac{3\pi\alpha}{4}, t\right), \quad \tilde{\Sigma}^{[2]}(\alpha, k) = \tilde{\Sigma}^{[3]}\left(\frac{3\pi\alpha}{4}, k\right). \tag{77}$$

Table I. Comparison of known weak coupling results for the polaron ground state energy $E(\alpha) = \alpha \cdot C_{\omega 1} + \alpha^2 \cdot C_{\omega 2} + O(\alpha^3)$ in two-dimensions

Authors	$C_{\omega 1}$	$C_{\omega 2}$
S.Das Sarma, B.Mason [58]	$-\pi/2$	–0.062
R.Feynman's theory [59]	$-\pi/2$	–0.04569
4th, 6th order pert. theory [59]	$-\pi/2$	–0.06397
O.Hipolito [60]	$-\pi/2$	–0.0245
Present $E_0(\alpha)$	$-\pi/2$	–0.046626
Present $E_0(\alpha) + \Delta E_2$	$-\pi/2$	–0.063974

Table II. Comparison of known weak coupling results for the polaron ground state energy $E(\alpha) = \alpha \cdot C_{\omega 1} + \alpha^2 \cdot C_{\omega 2} + O(\alpha^3)$ in three-dimensions

Authors	$C_{\omega 1}$	$C_{\omega 2}$
S.Das Sarma, B.Mason [58]	–1	–0.016
R.Feynman's theory [59]	–1	–0.012347
J.Röseler [61]	–1	–0.0159196*
T.Lee,... [52]	–1	–0.014
D.Larsen [39]	–1	–0.016
Present $E_0(\alpha)$	–1	–0.012598
Present $E_0(\alpha) + \Delta E_2$	–1	–0.015919

*The exact value

Then, considering (62) one easily finds that this scaling relation is also valid for $\frac{1}{d} E_0(\alpha_d)$. We have

$$E_0^{[2]}(\alpha) = \frac{2}{3} E_0^{[3]}\left(\frac{3\pi\,\alpha}{4}\right). \tag{78}$$

Note that the relation (78) was obtained earlier in [54,50]. But this scaling is not valid beyond E_0 because the interaction functional $W[\mathbf{r}]$ depends not only on α_d, but also on d in a complicated way.

Let us consider the asymptotic limits of spatial dimensions d at fixed finite α. We get

$$\lim_{d\to 1} \alpha_d = \frac{3\alpha}{d-1} \to \infty, \quad \lim_{d\to\infty} \alpha_d = \frac{3\alpha\sqrt{\pi e}}{\sqrt{2}\,d^{3/2}} \to 0. \tag{79}$$

Table III. Comparison of obtained estimations of the coefficient C_s of the polaron ground state energy $E(\alpha) = \alpha^2 \cdot C_s + O(1)$ for $d = 2$ as $\alpha \to \infty$

Authors	C_s
S.Das Sarma, B.Mason [58]	–0.392699
R.Feynman's theory [59]	–0.392699[1]
W.Xiaoguang, ... [59]	–0.4047[2]
O.Hipolito [60]	–0.392699
Present $E_0(\alpha)$	–0.392699
Present $E_0(\alpha) + \Delta E_2$	–0.400538

[1]Estimated in [59]
[2]Adiabatic approximation

Table IV. Comparison of obtained estimations of the coefficient C_s of the polaron ground state energy $E(\alpha) = \alpha^2 \cdot C_s + O(1)$ for $d = 3$ as $\alpha \to \infty$

Authors	C_s
Feynman, Schultz [65]	–0.1061
Pekar (by Miyake) [41]	–0.108504[1]
Miyake [41]	–0.108513[2]
Luttinger, Lu [62]	–0.1066
Marshall, Mills [67]	–0.1078
Sheng, Dow [68]	–0.1065
Adamowski, ... [57]	–0.1085128
Feranchuk, Komarov [69]	–0.1078
Efimov, Ganbold [56]	–0.10843

[1]Estimated in [41]
[2]The exact value

Taking into account (79) we can conclude that as d becomes larger, α_d decreases rapidly and in fact we deal with the effective weak-coupling regime $\alpha_d << 1$ even for α not too small. For example, the second-order corrections $\Delta E_2(\alpha)$ behave as follows:

$$\Delta E_2(\alpha) \underset{d \to \infty}{\to} -\frac{1}{8\pi} \alpha_d^2 \to 0. \tag{80}$$

In other words, our leading-order energy term $E_0(\alpha)$ tends to the exact GSE $E(\alpha)$ as d grows because the role of $\Delta E(\alpha)$ becomes insignificant.

Table V. The obtained estimations of the poralon ground state energy $E_0(\alpha)$ and $E^{(2)}(\alpha)$ for $d=2$ in the intermediate range of α compared with known results obtained in [60,70,58]

α	Feynman*	Hipolito [60]	Huybrecht [70]	Das Sarma [58]	Present	
					E_0	E_0+E_2
0.6364	−1.0198	−1.0266	−1.0201	−1.0405	−1.020	−1.028
1.909	−3.2247	−3.2263	−3.2263	−3.5690	−3.231	−3.250
3.183	−5.9191	−6.0902	−5.9193	−6.9688	−5.928	−6.039
4.450	−9.6935	−9.8723	−9.7154	−11.388	−9.710	−9.871

*Our estimation by Feynman's variational method

Table VI. The obtained estimations of the poralon ground state energy $E_0(\alpha)$ and $E^{(2)}(\alpha)$ for $d=3$ in the intermediate range of α compared with known results obtained in [57,65,64,39]

α	Osc. [57]	Feynman [65]	Smondyrev [64]		Larsen [39]		Present	
	upper	upper	upper	lower	upper	lower	E_0	E_0+E_2
0.5	−0.5	−0.5032	−0.5041	−0.5041	−0.5040	−0.5052	−0.504	−0.5041
1.0	−1.0	−1.0130	1.0167	−1.0175	−1.0160	−1.0270	−1.014	−1.017
1.5	−1.5	−1.5302	—	—	−1.5361	−1.576	−1.532	−1.539
2.0	−2.0	−2.0554	—	—	−2.0640	−2.172	−2.058	−2.071
2.5	−2.5	−2.5894	—	—	−2.5995	−2.872	−2.593	−2.614
3.0	−3.0	−3.1333	−3.1645	−3.2122	−3.1421	—	−3.138	−3.167
4.0	−4.0	−4.2565	—	—	−4.2771	—	−4.265	−4.305
5.0	−5.0	−5.4401	−5.4945	−5.7767	—	—	−5.452	−5.528
7.0	−7.356	−8.1127	−8.0406	−8.8832	—	—	−8.137	−8.255
9.0	−10.72	−11.486	−10.834	−12.654	—	—	−11.54	−11.69
11.0	−14.94	−15.710	−13.905	−17.165	—	—	−15.83	−16.04
20.0	−44.53	−45.283	—	—	—	—	−45.33	−45.99
30.0	−97.58	−98.328	—	—	—	—	−98.52	−99.86
40.0	−171.9	−172.60	—	—	—	—	−173.4	−175.1

3.3. Numerical Results. In this Section, we present numerical values of $E_0(\alpha)$ and $E^{(2)}(\alpha)$ estimated within the GER method and compare them with known results obtained in various (weak, strong and intermediate) ranges of α. Obtained results are given in Tables I-IV.

A. *Weak Coupling Limit.* Among known numerical results, concerning the GSE of the polaron, the more accurate are those obtained for $\alpha \to 0$. Below, we calculate the exact GSE of the d-dimensional polaron for the order α^2 in the

weak coupling limit and compare the accuracy of the obtained results with exact perturbation estimations presented in [52,58,59,49,60,54] for $d=2$ and $d=3$.

For α not too large, the polaron self-energy $E(\alpha)$ has the form

$$E(\alpha)=\alpha\cdot C_{\omega 1}+\alpha^2\cdot C_{\omega 2}+O(\alpha^3). \tag{81}$$

The coefficients $C_{\omega 1}$ and $C_{\omega 2}$ are known with a good accuracy for $d=2$ [54] and $d=3$ [58,54]. In our approach, the coefficient $C_{\omega 1}$ arises only from $E_0(\alpha)$ in (62); whereas the $C_{\omega 2}$, from both $E_0(\alpha)$ and $\Delta E_2(\alpha)$ in (74). We get the coefficients $C_{\omega 1}$ and $C_{\omega 2}$ exactly as follows

$$C_{\omega 1}=-\frac{R_d}{3}d \tag{82}$$

and

$$C_{\omega 2}=-\frac{R_d^2 d}{36}\left(1-\frac{8}{3\pi}\right)-\frac{R_d^2\Gamma(d/2)d^2}{9\pi^{3/2}}\sum_{n=2}^{\infty}\frac{(2n!)\Gamma(n+1/2)}{4^n(n!)^2\Gamma(n+d/2)}B_n,$$

$$B_n=\int_1^{\infty}\int dxdy\,\frac{1}{(x+y)^2}\left[\frac{1}{(x\cdot y)^{n+1/2}}+\frac{1}{(x+y-1)^{n+1/2}}\right]. \tag{83}$$

The behaviour of these coefficients with respect to the space-dimension number d is shown in Fig.1.

For comparison, in Table I we give the known results for $d=2$ as $\alpha\to 0$. One can see from Table I that our $C_{\omega 2}$ obtained only from $E_0(\alpha)$ improves Feynman's estimate about 2 per cent. Adding the next correction calculated from ΔE_2 results in $C_{\omega 2}=-0.063974$ which is in good agreement with the exact value in [54]. Note that ΔE_2 contributes about 40 per cent to the total value of $C_{\omega 2}$.

For three dimensions, obtained results are displayed in Table II together with the known results of the polaron GSE for the weak coupling limit. Our leading term of energy $E_0(\alpha)$ improves the Feynman variational estimation of $C_{\omega 2}$ by 2 per cent. Next correction results in $C_{\omega 2}=-0.015919$ which is in good agreement with the exact value in [54]. Note, for $d=3$ our ΔE_2 contributes about 29 per cent (smaller than for $d=2$) to the total value of $C_{\omega 2}$. Comparing the obtained results for $d=2$ and $d=3$, we conclude that higher-order corrections (the second-order one in our case) coming from $J_T(\alpha)$ are substantially more important for $d=2$ than for $d=3$. In other words, the polaron effect is stronger in low space dimensions (see Eq. (80)). This effect was noted earlier in [54,50].

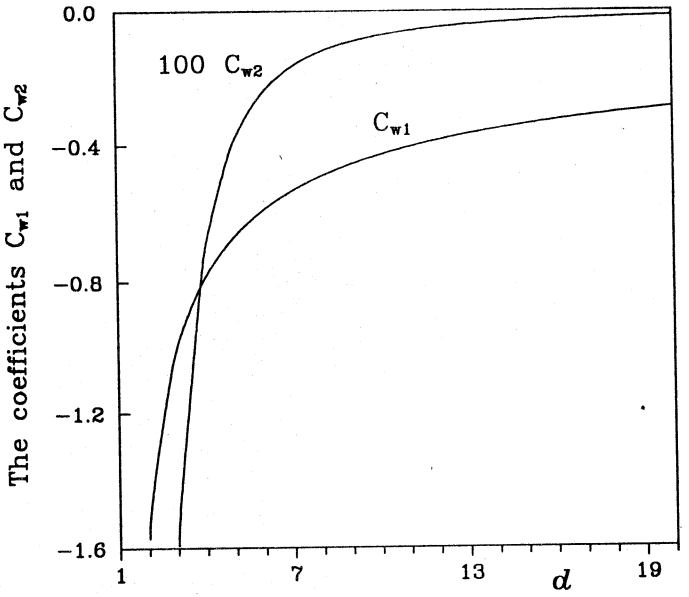

Fig. 1. The behaviour of the coefficients $C_{\omega 1}$ and $C_{\omega 2}$ of the polaron ground state energy $E(\alpha) = \alpha \cdot C_{\omega 1} + \alpha^2 \cdot C_{\omega 2} + O(\alpha^3)$ at the weak coupling limit $\alpha \to 0$ in dependence on the number of space-dimensions d

B. *Strong Coupling Regime.* The GSE of the polaron in the strong electron-phonon coupling regime has been considered in [41,58,59,57,56].

It is well known that at this limit

$$E(\alpha) = \alpha^2 \cdot C_s + O(1). \tag{84}$$

For large α (75) becomes

$$E^{(2)}(\alpha) = -\alpha_d^2 \left\{ \frac{d}{9\pi} + \frac{2\Gamma(d/2)d^2}{9\pi^{3/2}} \cdot \sum_{n=2}^{\infty} \frac{(2n)!\Gamma(n+1/2)}{16^n (n!)^2 n\Gamma(n+d/2)} \right\} + O(1). \tag{85}$$

For comparison, in Table III we give our result with the known results of the polaron GSE for $d = 2$ in the strong coupling regime $\alpha \to \infty$.

For three-dimensions the estimation of the next higher-order corrections for the coefficient C_s was obtained by the authors earlier in [56]:

$$C_s \leq -0.108431. \tag{86}$$

A comparison of the known results for the coefficient C_s for $d = 3$ is displayed in Table IV.

C. *Intermediate Coupling Range.* In the intermediate-coupling regime the main tool for obtaining polaron properties is the variational approach [35,52]. For $d=3$, the Feynman variational method based on a trial oscillator-type action gives an upper bound of the polaron free energy, valid for arbitrary α. Generalizations of the Feynman action for $d=3$ to the arbitrary density function [42] and arbitrary quadratic action [43] have improved this upper bound. In our opinion, the result [43] obtained for $d=3$ is the best variational upper bound in the whole range α. But this variational method does not give the next corrections to this bound. Other numerical methods dealing with this problem [62,63] require specific complicated schemes of calculations which may introduce statistical errors. Estimations of both the upper and lower bounds for the polaron self-energy obtained in [39,64] should be improved.

Considering intermediate values of α, we have derived equations (64) and (63) numerically, by the following iteration scheme:

$$F_{n+1}(t) = \Phi_t[\tilde{\Sigma}_n],$$

$$\tilde{\Sigma}_n(k) = \Omega_k[F_n], \quad n \geq 0, \tag{87}$$

starting from reasonable assumed functions $F_0(t)$ and $\tilde{\Sigma}_0(k)$ (see (70)). Both the series $F_n(t)$ and $\tilde{\Sigma}_n(k)$ turn out to be rapidly convergent and the value of the leading term $E_0(\alpha)$ does not change after $n \geq 6$. The results for $E_0(\alpha)$ and $E^{(2)}(\alpha)$ in two dimensions are presented in Table V.

The values of $E_0(\alpha)$ and $E^{(2)}(\alpha)$ for $d=3$ are given in Table VI (and displayed in Fig.2) in comparison with the known data [39,65,43,64]. Our $E_0(\alpha)$ for $d=3$ coincides with the upper bound obtained in [43] and improves the variational results calculated in [71].

We have made preliminary estimations which indicate that the decreasing series in (73) is alternating. Then one can expect that the third-order correction $\Delta E_3(\alpha)$ may slightly increase the value of $E^{(2)}(\alpha)$ and inclusion of higher-order corrections $\Delta E_{n>2}(\alpha)$ might result in an insignificant oscillation of $E^{(n>2)}(\alpha)$ between $E_0(\alpha)$ and $E^{(2)}(\alpha)$. In other words, the obtained $E^{(2)}(\alpha)$ may be accepted as a lower bound of the ground state energy of the polaron. Note that numerical results obtained in [66] at three points ($\alpha = 1,3,5$) by the method of «partial averaging» lie exactly between our curves for $E_0(\alpha)$ and $E^{(2)}(\alpha)$. Recent exact Monte-Carlo calculations [72] are in good agreement with our results for $d=3$.

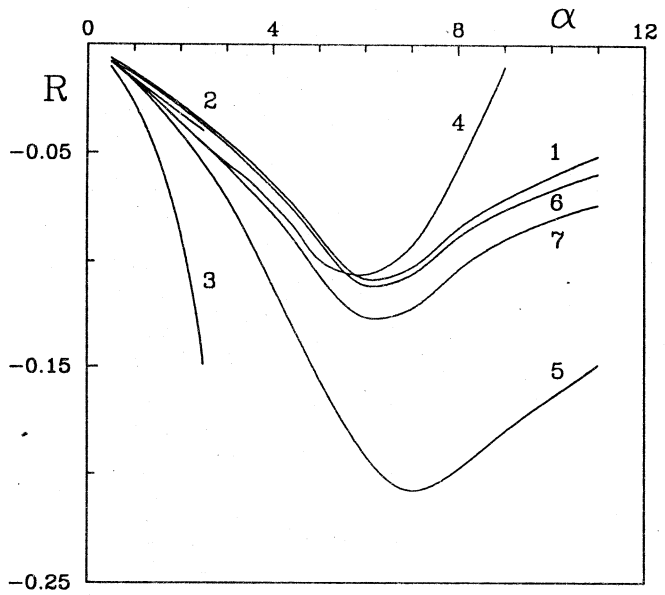

Fig. 2. Some known results of the polaron ground state energy E (in three-dimensional space) displayed as a function of the electron-phonon coupling constant α. For clarity, the ratio $R = (E_* - E_{\text{harm}})/|E_{\text{harm}}$ is shown, where E_* are estimations obtained in [86,52,89,97] and E_{harm} is the «harmonic-oscillator» approximation [86]. In these units the curve for E_{harm} coincides with the abscissa axis. Curves correspond to estimations: 1 — Feynmans's upper; 2/3 — Larsen's upper/lower; 4/5 — Smondyrev's upper/lower; 6 — our $E_0(\alpha)$ and 7 — our $E^{(2)}(\alpha)$

Our results obtained with the proposed method provide a reasonable description of both two- and three-dimensional polarons at an arbitrary coupling α. The consideration could be extended to computing the other characteristics of the polaron, the effective mass and the average number of phonons, as well as to estimating the energy of the polaron in the presence of a magnetic field due to the validity of the proposed method for the complex functionals.

4. CHARACTER OF PHASE TRANSITION IN TWO- AND THREE-DIMENSIONAL φ^4-THEORY

The phenomenon of spontaneous symmetry breaking, or in other words, the vacuum structure rearrangement is an important part of many quantum field

constructions. In this Section, we will investigate this phenomenon within the GER method. The problem, of course, can also be studied within the canonical quantization method. However, the functional representation has an advantage of calculating the whole effective potential (EP) in this theory, which allows one to get more information about phase transitions in the system under consideration.

4.1. Statement of the Problem. The scalar φ^4 theory in two- and three-dimensions has been intensively investigated [73,74] as a simple, but nontrivial example, on which the problem of spontaneous symmetry breaking or, in other words, the phase structure of quantum field models is studied. It has been found [75] that the highest order quantum corrections can give rise to the instability of the classical symmetric vacuum. There are two phases in this system and PT phenomena take place at certain coupling strengths. The most difficult problem here is to determine the order of the PT.

The simplest example, where the vacuum exhibits a nontrivial structure, is the φ_2^4 theory. Many papers [73—76] are devoted to investigation of the nature of PT in this model. We shortly treat some nonperturbative methods that seem to be basic among the investigations on this subject. An original approximation [73] using the Hartree-type renormalization exhibits the first order PT in this theory. A similar result was obtained [77] within the Gaussian EP approach. The dimensionless critical coupling constant, for which the first order phase transition takes place is $G = 1.62$ in both papers. These conclusions disagree with the mathematical theorems [83,84] proving that the second order PT should occur in the φ_2^4 model. There are papers [76—85], where different variational methods have been used for solving this problem and the second order PT has been observed in the region $G \sim 1$. In the previous studies [88,89], we have shown that the critical coupling constant leading to a second order PT cannot exceed the value $G_0 = 1.4392$ and may be found near $G_{crit} \sim 0.53$.

We study this problem using the method of the EP. The absolute minimum of the EP $V(\varphi_0)$ at the point $\varphi_0 = \varphi_c$ determines the true ground state (vacuum) of the theory. If a PT takes place at a certain coupling $g = g_c$, then for $g < g_c$ the system is still in the original unbroken symmetry phase with $\varphi_c = 0$. At reaching $g = g_c$ the origin $\varphi_0 = 0$ is no longer the absolute minimum of $V(\varphi_0)$ and the system goes to a new state with $\varphi_c \neq 0$ corresponding to the lower energy. The first-order PT means that the point $\varphi = 0$ remains local, but is not the absolute minimum of $V(\varphi_0)$. In other words, the first derivative of $V(\varphi_0)$ is zero and the second one is positive at the origin $\varphi_0 = 0$. In the case of the second-order transition, the point $\varphi_0 = 0$ is a local maximum of EP at $g > g_c$. The second

derivative of $V(\varphi_0)$ at $\varphi_0 = 0$ becomes negative. Thus, the coefficient $\alpha(g)$ in the representation of $V(\varphi_0)$ for small φ_0

$$V(\varphi_0) = E(g) + \alpha(g)\cdot \varphi_0^2 + O(\varphi_0^4) \tag{88}$$

plays an important role in determination of the character of phase transition. If $\alpha(g)$ is zero at certain $g = g_c$ and negative for $g > g_c$ up to $g \to \infty$, then one can say that the second-order PT appears here. On the contrary, the positiveness of $\alpha(g)$ for any g excludes the second-order transition. Rigorous calculation of $\alpha(g)$ at an arbitrary coupling constant is a complicated problem. However, we know that at large g, the coefficient $\alpha(g)$ remains negative in case of the second-order PT and is positive if the transition is of the first-order.

We study this problem qualitatively by using the GER method, described in Section 2.1. We will show the possibility of the second order PT in $g\varphi_2^4$ and give an estimation for the corresponding critical coupling constant g_c. For the model $g\varphi_3^4$ our result excludes the occurrence of the second order phase transition.

4.2. Renormalized Lagrangian of the $\varphi^4_{2,3}$-Model. We consider the $g\varphi^4$ scalar field model in two- and three-dimensions. We will use throughout this Section the Euclidean form of the model*. This theory contains ultraviolet divergences, but it is superrenormalizable, i.e., it has only a finite number of divergent Feynman diagrams. In order to remove these divergences we should introduce appropriate counter-terms into the Lagrangian. In this section we consider the superrenormalized scalar field theory with the Lagrangian:

$$L = \frac{1}{2}\varphi(x)[\partial^2 - m^2]\varphi(x) - \frac{g}{4}N_m\{\varphi^4(x)\} - R_m, \tag{89}$$

where we have introduced a «normal-ordered» form of interaction as follows:

$$N_m\{\varphi^4(x)\} = \varphi^4(x) - 6\varphi^2(x)D_m(0) + 3D_m^2(0),$$

$$D_m(x) = \int \frac{d^dk}{(2\pi)^d}\frac{\exp\{ikx\}}{m^2 + k^2}. \tag{90}$$

Here $x \in \Omega$, Ω is a large but finite volume in R^d, $(d = 2,3)$ and m and g are the mass and the self-coupling constants, respectively. In two-dimensions $(d = 2)$ all divergences are only of the «tadpole»-type and are readily removed by

*In the case of the Euclidean metrics a separation of the coordinates into space and time is unimportant, so the accepted notation for the «space-time» is R^d, where d relates to number of space coordinates plus Euclidean (imaginary) time as well.

introducing the normal product N_m of the fields $\varphi(x)$ into (89). In this case $R_m = 0$. In the three-dimensional theory there arise additional divergences which are cancelled by counter-terms

$$R_m = \frac{1}{2} A_m N_m \{\varphi^2(x)\} + \delta E_m, \tag{91}$$

where

$$A_m = 6g^2 \int d^3x D_m^3(x),$$

$$\delta E_m = \frac{3}{4} g^2 \int d^3x D_m^4(x) - \frac{3}{2} g^3 \int \frac{d^3k}{(2\pi)^3} \left\{ \int d^3x e^{ikx} D_m^2(x) \right\}^3. \tag{92}$$

At small g the Lagrangian (89) describes a system invariant with respect to the transformation $\varphi \leftrightarrow -\varphi$. The question is whether this symmetry remains for increasing g.

4.3. Effective Potential in the $\varphi^4_{2,3}$-Theory. The EP is defined as

$$V(\varphi_0) = -\lim_{\Omega \to \infty} \frac{1}{\Omega} \ln I_\Omega(\varphi_0),$$

$$I_\Omega(\varphi) = C_m \int \delta\varphi\, \delta\left\{ \varphi - \frac{1}{\Omega} \int d^dx \varphi(x) \right\} \exp \int_\Omega d^dx L[\varphi(x)], \tag{93}$$

$$C_m = \sqrt{\det\{-\partial^2 + m^2\}}.$$

All integrations are performed in Euclidean metrics.

According to the GER method, we transform the field variable as:

$$\varphi(x) = \phi_0 + b(x) + \phi(x), \tag{94}$$

where the new field variable $\phi(x)$ corresponding to the new mass μ and the function $b(x)$ satisfy the conditions:

$$\int_\Omega d^dx \phi(x) = 0, \quad \int_\Omega d^dx b(x) = 0, \quad b^2(x) = b^2 = \text{const}. \tag{95}$$

Let us go over to the normal ordering in the new fields $\phi(x)$ using the well-known formula [75]

$$N_m\{\exp\{\beta\varphi(x)\}\} = N_\mu \left\{ \exp\left\{ \beta(\phi_0 + b(x) + \phi(x) + \frac{\beta^2}{2} \Delta(m,\mu) \right\} \right\},$$

$$\Delta = \Delta(m,\mu) = D_m(0) - D_\mu(0), \tag{96}$$

$$D_\mu(x) = \int \frac{d^dk}{(2\pi)^d} \frac{\exp\{ikx\}}{\mu^2 + k^2} - \frac{1}{\mu^2 \Omega}.$$

First we substitute (94) and (96) into (93) and perform integration over $d\phi_0$. Then, following the key steps of the GER method, we obtain

$$I_\Omega(\varphi_0) = e^{-\Omega V_0(\varphi_0)} \int d\sigma_\mu \times$$

$$\times \exp\left\{ \int_\Omega d^d x N_\mu \left\{ \frac{g}{4} [\phi^4(x) + 4\phi^3(x)(\varphi_0 + b(x)) + 12\varphi_0 b(x)\phi^2(x)] - \right.\right.$$

$$\left.\left. - \left[\frac{1}{2} A_\mu \phi^2(x) + A_\mu b(x)\phi(x) + \delta E_\mu + \frac{1}{2}(b^2 + \varphi_0^2) A_\mu \right] \right\} \right\},$$

$$\int d\sigma_\mu \cdot 1 = C_\mu \int \delta\phi \exp\left\{ -\frac{1}{2} \int_\Omega d^d x \phi(x)(-\partial^2 + \mu^2)\phi(x) \right\} = 1, \tag{97}$$

where the new counter-terms concentrated in the second square brackets in (97) coincide with (92) if we substitute $m \to \mu$. The leading order term of the EP is obtained as the «cactus»-type part $V_0(\varphi_0)$ of the EP as follows:

$$V_0(\varphi_0) = -\frac{1}{2} \int \frac{d^d k}{(2\pi)^d} \left[\ln\left(1 + \frac{m^2 - \mu^2}{\mu^2 + k^2} \right) - \frac{m^2 - \mu^2}{\mu^2 + k^2} \right] + \frac{m^2}{2}(\varphi_0^2 + b^2) +$$

$$+ \frac{g}{4}(\varphi_0^4 + 6\varphi_0^2 b^2 + b^4 - 6\Delta(\varphi_0^2 + b^2) + 3\Delta^2) +$$

$$+ \frac{\varphi_0^2 + b^2}{2}(A_m - A_\mu) + \left(\delta E_m - \delta E_\mu - \frac{1}{2} A_m \Delta \right). \tag{98}$$

The requirement that the linear term $N_\mu\{\phi\}$ must not arise in the interaction and the quadratic field configurations be concentrated in the Gaussian measure $d\sigma_\mu$ leads to the following constraint equations for the parameters $b(x)$ and μ:

$$b(x)[-m^2 + 3g(\Delta - \varphi_0^2) - gb^2 - A_m + A_\mu] = 0,$$

$$\mu^2 - m^2 + 3g(\Delta - \varphi_0^2 - b^2) - A_m + A_\mu = 0. \tag{99}$$

Thus, we finally obtain the formula for the effective potential

$$V(\varphi_0) = V_0(\varphi_0) + V_{sc}(\varphi_0),$$

$$V_{sc}(\varphi_0) = -\lim_{\Omega \to \infty} \frac{1}{\Omega} \ln J_\Omega(\varphi_0), \tag{100}$$

where the new path integral is introduced:

$$J_\Omega(\varphi_0) = e^{-\Omega V_{sc}(\varphi_0)} =$$

$$= \int d\sigma_\mu \exp\left\{ \int_\Omega d^d x \times N_\mu \left\{ -\frac{g}{4} [\varphi^4(x) + 4\varphi^3(x)(\varphi_0 + b(x)) + \right.\right.$$

$$\left.\left. + 12\varphi_0 b(x)\, \phi^2(x)] - \left[\frac{1}{2} A_\mu \phi^2(x) + A_\mu b(x)\phi(x) + \delta E_\mu + \frac{1}{2}(b^2 + \varphi_0^2) A_\mu \right] \right\} \right\}. \quad (101)$$

Equations (98) and (99)—(101) define completely the EP at an arbitrary coupling g. Below we will investigate the EP in (100), whose parameters $b(x)$ and μ are limited by the constraints (96).

For further consideration, it will be convenient to work in units of m dealing with numerical results. We define

$$\xi = (\mu/m)^{4-d}, \quad \Phi_0^2 = 4\pi m^{2-d}\varphi_0^2 \quad \text{and} \quad B^2 = 4\pi m^{2-d} b^2. \quad (102)$$

4.4. The «Cactus»-Type Potential as the Leading-Order Term of the Effective Potential. In two-dimensions, the «cactus-type» part of the EP becomes as follows

$$V_0(\Phi_0) = \frac{m^2}{8\pi} \{\xi - 1 - \ln \xi + \Phi_0^2 + B^2$$

$$+ \frac{G}{6} [\Phi_0^4 + B^4 + 3\ln^2 \xi + 6(B^2\Phi_0^2 - B^2 \ln \xi - \Phi_0^2 \ln \xi)]\}. \quad (103)$$

We note that the potential (103) is invariant for $\Phi_0 \leftrightarrow B$.

The parameters ξ and B in (103) are limited by the following equations:

$$\begin{cases} B^2(\xi - GB^2) = 0, \\ 2\xi - 2 + 3G(\ln \xi - \Phi_0^2 - B^2) = 0. \end{cases} \quad (104)$$

Let us consider the constraint (104). A pair of «trivial» solutions:

$$B = 0 \quad \text{and} \quad \xi = 1 - \frac{3G}{2}(\ln \xi - \Phi_0^2) \quad (105)$$

can be found for an arbitrary coupling constant G. Since $G > G_0 = 1.4392$ an additional pair of «nontrivial» solutions

$$B = \frac{\xi}{G} \quad \text{and} \quad \xi = -2 + \frac{3G}{2}(\ln \xi - \Phi_0^2) \quad (106)$$

appears here, too. So for $G < G_0$ the only solution to be substituted into (103) is the «trivial» one, but since $G > G_0$ there is an alternative: one can choose

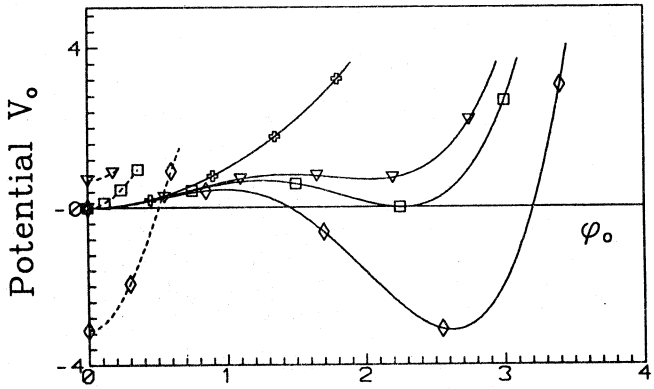

Fig. 3. The Gaussian part $V_0(\Phi_0)$ (in units of $m^2/8\pi$) of the effective potential as a function of Φ_0 for different values of the constant: crosses, $G = 0.5$; triangles, $G = 1.5$; squares, $G = 1.6251$ and rhombs, $G = 2.0$. The dashed lines represent the «nontrivial» branches. The «trivial» branches are denoted by the solid lines

either (105) or (106). We choose the pair obeying the lowest value of $V_0(\Phi_0)$ for certain fixed Φ_0.

All necessary calculations can be performed numerically. The obtained potential $V_0(\Phi_0)$ is plotted in Fig.3. Near the origin $\Phi_0 = 0$ the potential $V_0(\Phi_0)$ is presented by the «nontrivial» branch (if $G > G_0$) $B \neq 0$ as it is situated lower than the «trivial» one. But for larger values of Φ_0 the «trivial» solution $B = 0$ provides the lowest value of the potential. This picture leads to an interesting result. Let us consider the local minima of both branches. For $B = 0$ the minimum point $\Phi_0 = A$ in Fig.3 is given by the equations

$$\begin{cases} B = 0, \\ 2 - 3G \ln \xi + G\Phi_0^2 = 0. \end{cases} \tag{107}$$

On the other hand, the minimum of the «nontrivial» branch $B \neq 0$ is fixed at the origin $\Phi_0 = 0$ for any $G > G_0$ and (104) becomes

$$\begin{cases} \Phi_0 = 0, \\ 2 - 3G \ln \xi + GB^2 = 0. \end{cases} \tag{108}$$

Due to the invariance of the potential $V_0(\Phi_0, B)$ in (103) for $\Phi_0 \leftrightarrow B$ Eqs.(107) and (108) are identical. In other words, the minima of the potential (103) corresponding to different solutions of (104) are equal. The vacuum with $\langle\Phi(x)\rangle = \Phi_0 \neq 0$ is not lower than the initial one located at the point $\langle\Phi(x)\rangle = \Phi_0 = 0$. There is no reason for occurrence of the first order phase transition.

4.5. Non-Gaussian Correction in the φ_2^4-Model. In the previous Section, we derived the expression for the EP consisting of two parts. Considering only the «leading» term $V_0(\varphi_0)$ one can say nothing about the nature of the PT in the theory. To answer this question one should also consider the remaining part $V_{sc}(\varphi_0)$ of the effective potential, defined in (100). In the weak coupling limit one can estimate it expanding the exponential in (97) in perturbative series. But explicit calculation of the non-Gaussian functional integral $J_\Omega(\varphi_0)$ in (97) at arbitrary values of the coupling constant g and φ_0 is a complicated problem. However, we are able to estimate it for infinitesimal values of φ_0 at arbitrary g.

We rewrite (97) in the form correct for infinitesimal φ_0:

$$J_\Omega(\varphi_0) = \int d\sigma_\mu \exp\left\{ -\frac{g}{4}\int_\Omega d^d x N_\mu [\phi^4(x) + 4b(x)\phi^3(x)] + \right.$$

$$\left. + \frac{g^2\varphi_0^2}{2}\left[\int_\Omega d^d x N_\mu (\phi^3(x) + 3b(x)\phi^2(x))\right]^2 \right\}. \qquad (109)$$

This representation can easily be obtained due to the validity of the following transformation in the integrand of (97):

$$\exp(-\varphi_0 W) = \cosh(\varphi_0 W) \simeq \exp\left\{\frac{1}{2}\varphi_o^2 W^2 + O(\varphi_0^4)\right\}$$

for infinitesimal φ_0 and a finite functional W.

Applying to (109) the Jensen's inequality we get upper bound

$$V_{sc}(\varphi_0) \le V_{sc}^{+}(\varphi_0) = -\frac{g^2\varphi_0^2}{2\Omega}\int_\Omega d^d x \int_\Omega d^d y \int d\sigma_\mu \times$$

$$\times \{N_\mu \phi^3(x) N_\mu \phi^3(y) + 9b(x)b(y) N_\mu \phi^2(x) N_\mu \phi^2(y)\}. \qquad (110)$$

It is easy to show that

$$\int d\sigma_\mu N_\mu \phi^3(x) N_\mu \phi^3(y) = 6D_\mu^3(x-y),$$

$$\int d\sigma_\mu N_\mu \phi^2(x) N_\mu \phi^2(y) = 2D_\mu^3(x-y). \tag{111}$$

Then, we rewrite (110) in the form

$$V_{sc}^+(\Phi_0) = -\frac{m^2}{8\pi}\frac{3G^2\Phi_0^2}{2\xi}(Q+3B^2),$$

$$Q = \frac{4\pi \ln 2}{3\sqrt{3}} - 4\int_0^1 \frac{du}{u^2+3}\ln(1-u^2) = 2.3439\ldots. \tag{112}$$

Substituting the parameters ξ and B in either (105) or (106) into (112) one gets the behaviour of $V_{sc}^+(\Phi_0)$ for small values $\Phi_0 \sim 0$. Omitting the details of calculations we write the results

$$V_{sc}^+(\Phi_0) = -\frac{m^2}{8\pi}\left\{-\frac{3Q}{2}G^2\Phi_0^2 + O(\Phi_0^2)\right\} \quad \text{for} \quad G < G_* \tag{113}$$

and

$$V_{sc}^+(\Phi_0) = -\frac{m^2}{8\pi}\left\{-\left[\frac{3QG^2}{2\xi}+\frac{9G}{2}\right]\Phi_0^2 + O(\Phi_0^4)\right\} \quad \text{for} \quad G > G_*,$$

$$3G\ln\xi - \xi - 2 = 0. \tag{114}$$

From (103) we get the following asymptotic behaviour:

$$V_0(\Phi_0) = \frac{m^2}{8\pi}\{\Phi_0^2 + O(\Phi_0^4)\} \tag{115}$$

as $\Phi_0 \to 0$ at any G.

Finally, taking into account (100) we obtain the following behaviour of an upper bound of the EP in the region of small $\Phi_0 \sim 0$:

$$V^+[\Phi_0] = V_0[\Phi_0] + V_{sc}^+[\Phi_0] = \frac{m^2}{8\pi}[\alpha(G)\Phi_0^2 + O(\Phi_0^4)], \tag{116}$$

where

$$\alpha(G) = \begin{cases} \alpha_1(G) = 1 - 3QG^2/2, & G \le 1.6251, \\ \alpha_2(G) = 1 - 3QG^2/(2\xi) - 9G/2, & G > 1.6251, \end{cases}$$

$$3G\ln\xi - \xi - 2 = 0. \tag{117}$$

One can easily check that the coefficient $\alpha_1(G)$ in (117) becomes negative as $G > G_{crit} = 0.5333$ and remains negative for increasing G. But $\alpha_2(G)$ is negative at arbitrary $G > 1.4392$. In our opinion, it indicates an occurrence of the second order PT in the model under consideration.

4.6. Strong Coupling Regime in the φ_3^4-Model. In the three-dimensional case the counter-terms defined by (92) play an important role in the behaviour of the EP in the strong coupling regime. We have

$$D_\mu(x) = \frac{\exp\{-\mu|x|\}}{4\pi|x|}, \quad \Delta = \frac{m}{4\pi}(\xi - 1). \tag{118}$$

Substituting (118) into (99) we get

$$B(x)[2 + 3G(\Phi_0^2 - \xi + 1) + GB^2 + 3G^2 \ln \xi] = 0,$$

$$-2\xi^2 + 2 + 3G(\Phi_0^2 - \xi + 1) + GB^2 + 3G^2 \ln \xi = 0. \tag{119}$$

A non-trivial solution $B \neq 0$ exists only for $0 < \xi < 1$. Let us consider the solution $B = 0$. In the strong coupling regime we obtain

$$\xi = G\sqrt{\frac{3}{2}\ln G} + O(G\sqrt{\ln \ln G}). \tag{120}$$

In other words, the effective coupling constant

$$G_{\text{eff}} = \frac{g}{2\pi\mu} = \frac{G}{\xi} = \sqrt{\frac{2}{3\ln G}}\left\{1 + O\left(\frac{\ln \ln G}{\ln G}\right)\right\} \tag{121}$$

becomes small as $G \to \infty$ and one can successfully develop a perturbation expansion in G_{eff} series for the functional integral (101):

$$V_{\text{sc}}(\varphi_0) = \sum_{n=1}^{\infty} G_{\text{eff}}^n V_{\text{sc}}^{(n)}(\varphi_0). \tag{122}$$

Here $V_{\text{sc}}^{(1)} = 0$ due to normal ordering in the exponential in (101). After some calculations we obtain:

$$V_{\text{sc}}^{(1)}(\varphi_0) = V_{\text{sc}}^{(2)}(\varphi_0) = 0,$$

$$V_{\text{sc}}^{(3)}(\varphi_0) = \frac{m^3}{8\pi}\frac{18C_1}{\xi}G^3\Phi_0^2, \tag{123}$$

where the constant is

$$C_1 = \frac{1}{2\pi^6} \iiint \frac{d^3k d^3p d^3q}{(1+k^2)(1+p^2)(1+q^2)(1+(k+p)^2)(1+(k+q)^2)} =$$

$$= \frac{16}{\pi} \int_0^\infty \frac{du}{1+4u^2} (\arctan u)^2 = 1.7593\ldots .$$

Taking into account the «cactus»-type potential

$$V_0(\Phi_0) = \frac{m^3}{8\pi} \left\{ E_0(G) + \frac{3G}{2} (G \ln \xi - \xi)\Phi_0^2 + O(\Phi_0^4) \right\}, \tag{124}$$

we finally obtain the effective potential

$$V(\Phi_0) = V_0(\Phi_0) + V_{sc}(\Phi_0) = \frac{m^3}{8\pi} \{E(G) + \alpha(G)\cdot\Phi_0^2 + O(\Phi_0^4)\}, \tag{125}$$

where the desired coefficient

$$\alpha(G) = \frac{3G^2}{2} \ln G \left\{ 1 + \frac{\sqrt{96}C_1}{(\ln G)^{3/2}} + O\left(\frac{1}{(\ln G)^{5/2}} \right) \right\}, \tag{126}$$

is positive. This result excludes the second-order phase transitions in the ϕ_3^4 model. It can be accepted as an argument in favour of either existence of the only first-order transition or absence of any PT in the three-dimensional case.

Comparing the results (117) and (126) for $d = 2$ and $d = 3$ we find that the effective mass renormalization is crucial for this problem. In two-dimensions the mass renormalization includes the «tadpole» divergences only and the behaviour of $\alpha(G)$ in (117) indicates a favour of the second-order PT in φ_2^4. For $d = 3$ the mass renormalization contains an additional term of the second perturbative expansion's order which has the opposite sign comparable with a «tadpole» contribution. As a result, the function $\alpha(G)$ in (126) remains positive for all $G > 0$.

5. WAVE PROPAGATION IN RANDOMLY DISTRIBUTED MEDIA

Theoretical investigation of the propagation properties of waves in a randomly distributed environment reflects certain interest due to its many practical applications, including calculation of electronic conductance in crystals [90], wave localization [91] and dumping of signals in the atmosphere or water [92]. A series of different methods has been applied to this problem, among which path integral techniques [93]—[95] reflect considerable interest.

In this Section we investigate wave transmission in a randomly distributed media using the GER method.

5.1. The Green Function of the Wave Equation. The propagation of a wave $u(\mathbf{x})$ (e.g., electromagnetic) in a time-independent environment can be described by the wave equation given in real 3-dimensional space $\mathbf{x} \in R^3$:

$$[\Delta + \omega^2(1 + \varepsilon(\mathbf{x}))]u(\mathbf{x}|\varepsilon) = J(\mathbf{x}), \quad \omega \neq 0. \tag{127}$$

The constant ω is the «dielectric constant» and defines the frequency of unperturbed waves. $J(\mathbf{x})$ is the source function.

The random noise is described by a random stationary field $\varepsilon(\mathbf{x})$, which is assumed to vary stochastically with a certain correlation function $\langle \varepsilon(\mathbf{x})\varepsilon(\mathbf{y})\rangle$. For simplicity we shall consider Gaussian noise

$$\langle \varepsilon(\mathbf{x})\varepsilon(\mathbf{y})\rangle_\varepsilon = \lambda P(\mathbf{x} - \mathbf{y}) =$$

$$= \lambda \exp\left(-\frac{(\mathbf{x}-\mathbf{y})^2}{4l^2}\right) = \lambda \int \frac{d\,\mathbf{k}}{\pi^{3/2}} \exp\left\{-\mathbf{k}^2 + i\,\mathbf{k}\,\frac{\mathbf{x}-\mathbf{y}}{l}\right\}, \tag{128}$$

where the interaction coefficient λ shows the intensity of noise described by the distribution function $P(\mathbf{x} - \mathbf{y})$ with a correlation length l. These two constants define the influence of the Gaussian noise on the propagation of waves in media.

The solution of (127) can be represented in the form

$$u(\mathbf{x}|\varepsilon) = \int d\,\mathbf{y} G(\mathbf{x},\mathbf{y}|\varepsilon) J(\mathbf{y}),$$

where $G(\mathbf{x},\mathbf{y}|\varepsilon)$ is the Green function of wave equation:

$$[\Delta + \omega^2(1 + \varepsilon(\mathbf{x}))]G(\mathbf{x},\mathbf{y}|\varepsilon) = \delta(\mathbf{x} - \mathbf{y}). \tag{129}$$

The problem is to find the solution of (127) and then average it over random fields $\varepsilon(\mathbf{x})$ to find the wave amplitude:

$$u(\mathbf{x}) = \langle u(\mathbf{x}|\varepsilon)\rangle_\varepsilon.$$

For this the Green function should be averaged over random fields $\varepsilon(\mathbf{x})$:

$$G(\mathbf{x} - \mathbf{y}) = \langle G(\mathbf{x},\mathbf{y}|\varepsilon\,\rangle_\varepsilon.$$

Thus we consider this problem solved if the averaged Green function $G(\mathbf{x})$ is found and its asymptotic behaviour for large distances $|\mathbf{x}| \to \infty$ can be calculated.

Let use proceed to solve the equation (129) for the Green function. It is essential that the operator

$$K = \Delta + \omega^2(1 + \varepsilon(\mathbf{x}))$$

is not definitely positive. We shall consider the solution

$$G(\mathbf{x},\mathbf{y}|\varepsilon) = \frac{1}{K + i0}\,\delta(\mathbf{x} - \mathbf{y}),$$

corresponding to the so-called causal Green function. This solution can be written in integral representation like (29) as follows:

$$G(\mathbf{x},\mathbf{y}|\varepsilon) = -\frac{i}{2}\int_0^\infty du\, e^{\frac{i}{2}(K+i0)u}\delta(\mathbf{x} - \mathbf{y}) =$$

$$= -\frac{i}{2}\int_0^\infty du T_\tau \exp\left\{\frac{i}{2}\int_0^u d\tau\left[\left(\frac{\partial}{\partial \mathbf{x}_\tau}\right)^2 + \omega^2(1+\varepsilon(\mathbf{x}_\tau))\right]\right\}\delta(\mathbf{x} - \mathbf{y}).$$

Here we have used the «time-ordering» operator T_τ. Omitting details of calculations we display the results:

$$G(\mathbf{x},\mathbf{y}|\varepsilon) = -\frac{1}{2}\int_0^\infty \frac{du}{(2\pi\, iu)^{3/2}} \exp\left[-\frac{i}{2}\left(\omega^2 u + \frac{(\mathbf{x}-\mathbf{y})^2}{u}\right)\right] I_u(\mathbf{x},\mathbf{y}|\varepsilon),$$

where a FI is introduced:

$$I_u(\mathbf{x},\mathbf{y}|\varepsilon) = \int d\sigma_0 \exp\left\{\frac{i}{2}\omega^2\int_0^u d\tau\varepsilon\left(\mathbf{x}\frac{\tau}{u} + \mathbf{y}\left(1 - \frac{\tau}{u}\right) + \nu(\tau)\right)\right\}, \qquad (130)$$

with the measure defined as

$$d\sigma_0 = C_0\delta\,\nu \exp\left\{\frac{i}{2}\int_0^u d\tau\dot{\nu}^2(\tau)\right\}.$$

The integration in (130) is taken over «paths» ν obeying the condition

$$\nu(0) = \nu(u) = 0.$$

Here the normalization is chosen as

$$\int d\sigma_0 = 1 \quad \text{or,} \quad I_u(\mathbf{x},\mathbf{y}|\varepsilon)|_{\varepsilon=0} = 1.$$

Now we can average the functional $I_u(\mathbf{x},\mathbf{y}|\varepsilon)$ over the random fields $\varepsilon(\mathbf{x})$:

$$I_u(\mathbf{x} - \mathbf{y}) = \langle I_u(\mathbf{x},\mathbf{y}|\varepsilon)\rangle_\varepsilon =$$

$$= \int d\sigma_0 \exp\left\{ -\lambda \frac{\omega^4}{8} \iint_0^u d\tau d\tau' P\left(\mathbf{v}(\tau) - \mathbf{v}(\tau') + (\mathbf{x}-\mathbf{y}) \frac{\tau - \tau'}{u} \right) \right\}.$$

The averaged Green function is

$$G(\mathbf{x}) = -\frac{1}{2} \int_0^\infty \frac{du}{(2\pi i u)^{3/2}} \exp\left[\frac{i}{2} \left(\omega^2 u + \frac{\mathbf{x}^2}{u} \right) \right] I_u(\mathbf{x}),$$

where

$$I_u(\mathbf{x}) = C_0 \int_{\mathbf{v}(0)=\mathbf{v}(u)=0} \delta\mathbf{v} \exp\left\{ \frac{i}{2} \int_0^u d\tau \dot{\mathbf{v}}^2(\tau) - \right.$$

$$\left. - \lambda \frac{\omega^4}{8} \iint_0^u d\tau d\tau' P\left(\mathbf{v}(\tau) - \mathbf{v}(\tau') + \mathbf{x} \frac{\tau - \tau'}{u} \right) \right\}. \tag{131}$$

For further convenience we introduce the following notation:

$$r = |\mathbf{x}|, \quad u = \frac{r}{\omega} z, \quad \beta = r\omega, \quad \tau = \frac{z}{\omega^2} t, \quad \tau' = \frac{z}{\omega^2} s, \quad g = \frac{\lambda z^2}{4}$$

and change the variable of the FI:

$$\mathbf{v}(\tau) = \frac{\sqrt{z}}{\omega} \boldsymbol{\rho}(t).$$

Then we have

$$G(\beta) = -\frac{\omega}{2\sqrt{\beta}} \int_0^\infty \frac{dz}{(2\pi i z)^{3/2}} \exp\left[i \frac{\beta}{2} \left(z + \frac{1}{z} \right) \right] I(\beta, z),$$

where

$$I(\beta, z) = C_0 \int_{\boldsymbol{\rho}(0)=\boldsymbol{\rho}(\beta)} \delta\boldsymbol{\rho} \exp\left\{ \frac{i}{2} \int_0^\beta dt \dot{\boldsymbol{\rho}}^2(t) - \right.$$

$$\left. - \frac{g}{2} \iint_0^\beta dt ds P\left(\frac{\sqrt{z}}{\omega} (\boldsymbol{\rho}(t) - \boldsymbol{\rho}(s)) + \mathbf{n} \frac{t-s}{\omega} \right) \right\}, \tag{132}$$

where

$$\mathbf{n} = \frac{\mathbf{x}}{|\mathbf{x}|}, \quad (\mathbf{nn}) = 1.$$

5.2. Calculation of the FI by the GER Method. In order to apply the GER method to this problem, let us introduce into (132) symmetrical limits by redefining

$$2T = \beta, \quad t \to t - T, \quad s \to s - T, \quad \rho(t) \to \rho(t - T).$$

Then we rewrite (132):

$$I_T(z) = C_0 \int\limits_{\rho(-T)=\rho(T)=0} \delta\rho \exp\left\{ \frac{i}{2} \int\limits_{-T}^{T} dt\, \dot{\rho}^2(t) - \right.$$

$$\left. - \frac{g}{2} \int\int\limits_{-T}^{T} dtds P\left(\frac{\sqrt{z}}{\omega} [\rho(t) - \rho(s)] + \mathbf{n} \frac{t-s}{\omega} \right) \right\}.$$

Let us introduce the operator

$$D_0^{-1}(t-s) = i \frac{\partial^2}{\partial t^2} \delta(t-s).$$

Note that it differs from (30) by the factor $-i$. The Green function $D_0(t,s)$ corresponding to this operator satisfies some periodic conditions and reads

$$D_0(t,s) = -\frac{i}{2} |t-s| - \frac{ts}{2T} \to -\frac{i}{2} |t-s|.$$

Its Fourier transform is

$$\tilde{D}_0(p) = \frac{i}{p^2}.$$

Then we rewrite

$$I_T(z) = C_0 \int\limits_{\rho(-T)=\rho(T)=0} \delta\rho \exp\left\{ -\frac{1}{2} \iint\limits_{-T}^{T} dtds (\rho(t) \mathbf{D}_0^{-1}(t-s) \rho(s)) - gW[\rho] \right\},$$

$$C_0 = (\det \mathbf{D}_0)^{-1/2}.$$

The free «kinetic» term is diagonal:

$$(\rho(t) \mathbf{D}_0^{-1}(t-s)\, \rho(s)) = (\rho_i(t)\, \delta_{ij}\, D_0^{-1}(t-s)\, \rho_j(s)).$$

The interaction is given by

$$gW[\rho] = \frac{g}{2}\iint_{-T}^{T} dtds P\left(\frac{\sqrt{z}}{\omega}(\boldsymbol{\rho}(t)-\boldsymbol{\rho}(s)) + \mathbf{n}\frac{T-s}{\omega}\right) =$$

$$= \frac{g}{2}\iint_{-T}^{T} dtds \int \frac{d\mathbf{k}}{\pi^{3/2}} \exp\left\{-\mathbf{k}^2 + i\frac{\mathbf{k}}{l\omega}(\sqrt{z}\,(\boldsymbol{\rho}(t)-\boldsymbol{\rho}(s)) + \mathbf{n}(t-s))\right\}.$$

We find that the measure $d\mathcal{K}$ of momentum integration now becomes

$$d\mathcal{K}_{\mathbf{n}}(\mathbf{k}, t-s) = \frac{d\mathbf{k}}{\pi^{3/2}} \exp\left\{-\mathbf{k}^2 + \frac{i}{l\omega}(\mathbf{kn})(t-s)\right\}.$$

Following the GER method, we define the new measure

$$d\sigma = C\delta\boldsymbol{\rho} \exp\left\{-\frac{1}{2}\int\int_{-T}^{T} dtds\,(\boldsymbol{\rho}(t)\,\mathbf{D}^{-1}(t-s)\,\boldsymbol{\rho}(s))\right\},$$

where

$$(\boldsymbol{\rho}(t)\,\mathbf{D}^{-1}(t-s)\,\boldsymbol{\rho}(s)) = (\rho_i(t) D_{ij}^{-1}(t-s)\,\rho_j(s)).$$

Notice that, the operator D_{ij}^{-1} has nondiagonal elements owing to the presence of the vector $\mathbf{n}$ in $W[\boldsymbol{\rho}]$.

In the following we will use the notations

$$\int d\sigma \exp\left\{i\frac{\sqrt{z}}{l\omega}\mathbf{k}(\boldsymbol{\rho}(t)-\boldsymbol{\rho}(s))\right\} = \exp\left\{-\frac{z}{(l\omega)^2}(\mathbf{kF}(t-s)\mathbf{k})\right\},$$

$$(\mathbf{kF}(t-s)\mathbf{k}) = (k_i F_{ij}(t-s)k_j),$$

$$\mathbf{F}(t-s) = \mathbf{D}(0) - \mathbf{D}(t-s) = \int_0^{\infty} \frac{dp}{\pi}\,[1-\cos p(t-s)]\,\tilde{\mathbf{D}}(p^2),$$

$$g\hat{W}[\mathbf{b}] = \frac{g}{2}\int_{-T}^{T} dtds \int \frac{d\mathbf{k}}{\pi^{3/2}} \exp\left\{-\left(\mathbf{k}[\mathbf{I} + \frac{z}{(l\omega)^2}\mathbf{F}(t-s)]\mathbf{k}\right)\right\} \times \tag{133}$$

$$\times \exp\left\{i\frac{\sqrt{z}}{\omega l}\mathbf{k}(\mathbf{b}(t)-\mathbf{b}(s)) + i\,\mathbf{kn}\frac{t-s}{\omega l}\right\},$$

$$(|\mathbf{q}\rangle\langle\mathbf{q}|)_{ij} = q_i q_j,$$

$$\Phi(t-s)=\frac{gz^3}{(\omega l)^4}\int\frac{d\,\mathbf{q}}{\pi^{3/2}}\,|\mathbf{q}\rangle\langle\mathbf{q}|\times$$

$$\times\exp\left\{-\left(\mathbf{q}\left[\mathbf{I}+\frac{z}{(l\omega)^2}\,\mathbf{F}(t-s)\right]\mathbf{q}\right)+i\,\mathbf{qn}\,\frac{t-s}{\omega l}\right\}=$$

$$=\mathbf{\Phi}_0(t-s)+|\mathbf{n}\rangle\langle\mathbf{n}|\mathbf{\Phi}_1(t-s),$$

$$\Phi_{ij}(t-s)=\delta_{ij}\cdot\Phi_0(t-s)+n_i n_j\,\Phi_1(t-s).$$

Then we get

$$\omega_{ij}(t-s)=g\,\frac{\delta^2\hat{W}[\mathbf{b}]}{\delta b_i(t)\,\delta b_j(s)}\,|_{\mathbf{b}=0}=-\,[\tilde{\Phi}_{ij}(0)-\Phi_{ij}(t-s)].$$

Following all the steps described in section 2 we finally obtain

$$I_T(z)=\mathrm{e}^{-2TE_0(z)}J_T(z),$$

$$J_T(z)=C\int\delta\rho\,\exp\left\{-\frac{1}{2}\int\limits_{-T}^{T}dtds(\rho\,\mathbf{D}^{-1}\rho)-g:\tilde{W}[\rho]:\right\},\qquad(134)$$

where the leading-order term (or the zeroth approximation of the GER method) is

$$E_0(z)=\frac{3}{2\pi}\int\limits_0^\infty dp\left[\ln\left(1+\frac{i}{p^2}\,\mathbf{\Sigma}(p)\right)\right]-$$

$$-\frac{g}{2}\int\limits_{-\infty}^{\infty}dt\int\frac{d\,\mathbf{q}}{\pi^{3/2}}\exp\left\{-\left(\mathbf{q}\left[\mathbf{I}+\frac{z}{(l\,\omega)^2}\,\mathbf{F}(t)\right]\mathbf{q}\right)+i\,\mathbf{qn}\,\frac{t}{\omega l}\right\}.$$

The interaction functional in the new representation is

$$\tilde{W}[\rho]=-\frac{g}{2}\int\limits_{-T}^{T}dtds\int d\mathcal{K}_{\mathbf{n}}(\mathbf{q},t-s)\times$$

$$\times\exp\left\{-\left(\mathbf{q}\left[\mathbf{I}+\frac{z}{(l\omega)^2}\,\mathbf{F}(t-s)\right]\mathbf{q}\right)+i\,\mathbf{qn}\,\frac{t-s}{\omega l}\right\}:e_2^{\frac{i\sqrt{z}}{l\omega}[\mathbf{q}(\rho(t)-\rho(s))]}:\qquad(135)$$

where $:e_2^z:=e^z-1-z-\frac{z^2}{2}$.

The requirement of the «*correct*» form for the interaction functional is held if we put

$$\tilde{\mathbf{D}}(p) = \tilde{\mathbf{D}}_0(p) + \tilde{\mathbf{D}}_0(p)\boldsymbol{\Sigma}(p)\tilde{\mathbf{D}}_0(p),$$

or

$$\tilde{\mathbf{D}}_0(p) = \frac{\tilde{\mathbf{D}}_0(p)}{\mathbf{I} + \tilde{\mathbf{D}}_0(p)\boldsymbol{\Sigma}(p)} = \frac{i\,\mathbf{I}}{p^2 + i\,\boldsymbol{\Sigma}(p)}.$$

Then (41) and (42) become

$$\boldsymbol{\Sigma}(p) = -\,\tilde{\mathbf{w}}(p) = \int_{-\infty}^{\infty} dt[1 - \cos(pt)]\boldsymbol{\Phi}(t) \tag{136}$$

and

$$\mathbf{F}(t) = i \int_0^{\infty} \frac{dp}{\pi} \frac{1 - \cos p(t)}{p^2 + i\,\boldsymbol{\Sigma}(p)}. \tag{137}$$

5.3. The Green Function for Large Distances. The initial (131) and the new (134) representations are equivalent. The next step is to solve (136) and (137) which allows one to calculate the function $E_0(z)$. The explicit form of the interaction functional (135) allows the highest corrections to be calculated. In principle, these calculations are similar to those in the polaron problem except that now all functionals are complex. Nevertheless, all transformations of the GER method applied here are valid. In the future we plan to solve these equations and investigate the behaviour of the Green function $G(\mathbf{x})$ for different values of the parameters λ and l.

So the main problem is to solve the integral equations (136) and (137). However this represents a laborious task and one can by-pass this difficulty considering the large distance's behaviour of the Green function $G(\beta)$.

We now consider wave propagation for large distances $\beta \to \infty$. Then by analogy with the polaron problem, where the similar asymptotics have been studied, we can expect that the following behaviour of the FI occurs

$$I(\beta, z) \sim \frac{1}{\beta^{0(1)}} \exp\{-\beta E(z; \lambda, \omega l)\}.$$

Consequently,

$$G(\beta) \sim \frac{1}{\beta^{0(1)}} \int_0^{\infty} \frac{dz}{z^{3/2}} \exp\left\{\beta\left[\frac{i}{2}\left(z + \frac{1}{z}\right) - E(z; \lambda, \omega l)\right]\right\} \sim$$

$$\sim \frac{1}{\beta^{0(1)}} \int_0^{\infty} \frac{dz}{z^{3/2}} \exp\{\beta S(z)\}, \tag{138}$$

where

$$S(z) = \frac{i}{2}\left(z + \frac{1}{z}\right) - E(z; \lambda, \omega l).$$

The main contribution to the FI in (138) for large β can be obtained by using the saddle-point method:

$$S(z) = S(z_0) - \frac{1}{2} S''(z_0)(z - z_0)^2 + O(z - z_0)^3,$$

with the conditions

$$S'(z_0) = 0, \quad S''(z_0) > 0.$$

Finally, one gets

$$G(\beta) \sim \frac{1}{\beta^{0(1)}} \exp\{\beta S(z_0)\}.$$

CONCLUSION

We have formulated a regular method for calculating a wide class of functional integrals beyond the region of perturbative expansion. Providing a good accuracy of the lowest approximation, this method has the following advantages compared to the variational approach: the possibility for obtaining higher-order corrections in a regular way and the validity for complex functionals and theories with divergencies.

We have applied this method to different problems of theoretical physics, namely:

(i) the polaron problem in QS,

(ii) the PT phenomenon in the QFT model,

(iii) the solution of the wave's differential equation.

These subjects show the efficiency of the GER method. High accuracy is achieved in calculation of the ground state energy of the d-dimensional polaron. An effective scheme of mass renormalization in the $g\varphi^4_{2,3}$ theory, suggested within the GER method, leads to the correct prediction of the nature of the PT in this theory. At last, an estimation of the nonhermitean path integral for the Green function in the theory of wave propagation in media with a Gaussian distribution is performed.

The developed approach opens up new possibilities for estimating, with high accuracy, the bound states of few-body systems under any potential as well as for investigating static characteristics of the polaron in magnetic fields, when the action of the system is complex and any variational method becomes inapplicable.

ACKNOWLEDGEMENTS

The authors are grateful to Profs. V.K.Fedyanin, H.M.Fried, H.Leschke, L.V.Prokhorov and M.A.Smondyrev for useful discussions.

REFERENCES

1. **Dirac P.A.M.** — The Principles of Quantum Mechanics, Clarendon Press, Oxford, 1930.
2. **Kugo T., Ojima I.** — Phys. Lett., 1978, B73, p.459.
3. **Feynman R.P.** — Rev. Mod. Phys., 1948, 20, p.367.
4. **Feynman R.P.** — Phys. Rev., 1950, 80, p.440; 1951, 84, p.108.
5. **Wiener N.** — Ann. Math., 1920, 22, p.66.
6. **Dirac P.A.M.** — Soviet J. Phys., 1933, 3, p.1.
7. **Kac M.** — In: Proceed. Second Berkeley Symposium on Probability and Statistics, ed. J.Neyman, Univ. Calif. Press, Berkeley, 1951.
8. **S.F.Edwards, Peierls R.E.** — Proceed. Royal Soc., 1954, 224, p.24.
9. **Gelfand I.M., Minlos R.A.** — Soviet Doklady Akad. Nauk, 1954, 97, p.209.
10. **Bogoliubov N.N.** — Soviet Doklady Akad. Nauk, 1954, 99, p.225.
11. **Glimm J., Jaffe A.** — Comm. Math. Phys., 1971, 22, p.253.
12. **Glimm J., Jaffe A.** — Field Theory Models in Statistical Mechanics and QFT, Gordon Breach, N.Y., 1971.
13. **Faddeev L.D., Popov V.N.** — Phys. Lett., 1967, B25, p.29.
14. **De Witt** — Phys. Rev., 1967, 160, p.1113.
15. **Faddeev L.D., Slavnov A.A.** — Gauge Fields, Introduction to Quantum Theory, Benjamin/Cummings, Mass., 1980.
16. **Taylor J.G.** — Nucl. Phys., 1971, B33, p.436.
17. **Lee B.W., Zinn-Justin J.** — Phys. Rev., 1972, D5, p.3137.
18. **t'Hooft G., Veltman M.** — Nucl. Phys., 1972, B44, p.189.
19. **Fradkin E.S., Tyutin I.V.** — Phys. Lett., 1969, B30, p.562; Phys. Rev., 1970, D2, p.2841.
20. **Peak D., Inomata A.** — J. Math. Phys., 1969, 10, p.1422.
21. **Duru I.H., Kleinert H.** — Phys. Lett., 1979, B84, p.185.
22. **Fischer W., Leschke H., Müller P.** — J. Phys., 1992, A25, p.3835.
23. **Antoine E.P., Tirapegui E. (eds.),** Functional Integration. Theory and Application, Plenum Press, N.Y., 1980.
24. **Papadopoulos G.J., Devreese J.T. (eds.),** Path Integrals and Their Applications in Quantum, Statistical and Solid State Physics, Plenum Press, N.Y., 1978.
25. **Bogoliubov N.N., Shirkov D.V.** — An Introduction to the Theory of Quantized Fields, Wiley, N.Y., 1959.
26. **Simon B.** — Functional Integration and Quantum Physics, Academic Press, N.Y., 1979.
27. **Glimm J., Jaffe A.** — Quantum Physics, A Functional Integral Point of View, Springer-Verlag, Berlin, 1981.
28. **Ramond P.** — Field Theory, A Modern Primer, Benjamin/Cummings, Mass., 1981.

29. **Roepstorff G.** — Path Integral Approach to Quantum Physics, Springer Verlag, Berlin 1994.
30. Proceed. Int. Conference «Path Integrals from meV to MeV: Tutzing-92», eds. H.Grabert et. al., World Scientific, Singapore, 1993.
31. **Kleinert H.** — Path Integrals in Quantum Mechanics, Statistics and Polymer Physics, World Scientific, Singapore, 1990.
32. **Albeverio S., Paycha S., Scarlatti S.** — Prog. Phys., 1989. 13, p.230.
33. **Feynman R.P., Hibbs A.R.** — Quantum Mechanics and Path Integrals, McGraw-Hill Book Company, N.Y., 1965.
34. **Efimov G.V., Ganbold G.** — NATO ASI Series, 1991, B225, p.133.
35. **Feynmann R.P.** — Phys. Rev., 1955, 97, p.660.
36. **Devreese J.T., Peeters F.M. (eds.),** Physics of Polarons and Excitons in Polar Semiconductors and Ionic Crystals, Plenum Press, N.Y., 1984.
37. **Mitra T.K., Chatterjee A., Mukhopadhyay S.** — Phys. Rep., 1987, 153, p.91.
38. **Fröhlich H., Peltzer H., Zienau S.** — Philos. Mag., 1950, 41, p.221.
39. **Larsen D.M.** — Phys. Rev., 1968, 172, p.967.
40. **Pekar S.I.,** Untersuchungen über die Elektronentheorie der Kristalle, Akademie-Verlag, Berlin, 1954.
41. **Miyake S.** — Jour. Phys. Soc. Jap., 1975, 38, p.181.
42. **Saitoh M.** — Jour. Phys. Soc. Jap., 1980, 49, p.878.
43. **Adamowski J., Gerlach B., Leschke H.** — In: Functional Integration, Theory and Applications, eds. J.P.Antoine and E.Tirapegui, Plenum, N.Y., 1980.
44. Proceed. Int. Workshop on Variational Calculations in Quantum Field Theory, eds. L.Polley and D.E.L.Pottinger, World Scientific, Singapore, 1987.
45. **Devreese J.T., Peeters F.M. (eds.),** Polarons and Excitons in Polar Semiconductors and Ionic Crystals, Plenum Press, N.Y., 1984.
46. **Horst M., Merkt V., Kottaus J.P.** — Phys. Rev. Lett., 1983, 50, p.754.
47. **Jackson S.A., Platzman P.M.** — Phys. Rev., 1981, B24, p.499.
48. Proceed. IV Int. Conf. on Electronic Properties of 2D-Systems, New Hampshire, August 1981.
49. **Larsen D.M.** — Phys. Rev., 1987, B35, p.4435.
50. **Smondyrev M.A.** — Physica A, 1991, 171, p.191.
51. **Gerlach B., Löwen H.** — Rev. Mod. Phys., 1991, 63, p.63.
52. **Lee T.D., Low F., Pines D.** — Phys. Rev., 1953, 90, p.297.
53. **Das Sarma S.** — Phys. Rev., 1983, B27, p.2590.
54. **Peeters F.M., Xiaoguang Wu, Devreese J.T.** — Phys. Rev., 1986, B33, p.3926.
55. **Ganbold G., Efimov G.V.** — Phys. Rev., 1994, B50, p.3733.
56. **Efimov G.V., Ganbold G.** — phys. stat. sol. (b), 1991, 168, p.165.
57. **Adamowski J., Gerlach B., Leschke H.** — Phys. Lett., 1980, A79, p.249.
58. **Das Sarma S., Mason B.A.** — Ann. Phys., 1985, 163, p.78.
59. **Xiaoguang Wu, Peeters F.M., Devreese J.T.** — Phys. Rev., 1985, B31, p.3420.
60. **Hipolito O.** — Sol. Stat. Commun., 1979, 32, p.515.
61. **Röseler J.** — phys. stat. sol., 1968, 25, p.311.
62. **Luttinger J.M., Lu C.-Y.** — Phys. Rev., 1982, B21, p.4251.
63. **Becker W., Gerlach B., Schliffke H.** — Phys. Rev., 1983, B28, p.5735.
64. **Smondyrev M.A.** — phys. stat. sol.(b), 1989, 155, p.155.

65. **Schultz T.D.** — Phys. Rev., 1959, 116, p.526.
66. **Alexandrou C., Fleischer W., Rosenfelder R.** — Phys. Rev. Lett., 1990, 65, p.2615.
67. **Marshall J.T., Mills L.R.** — Phys. Rev., 1970, B2, p.3143.
68. **Sheng P., Dow L.D.** — Phys. Rev., 1971, B4, p.1343.
69. **Feranchuk I.D., Komarov I.I.** — phys. stat. sol. (b), 1982, 15, p.1965.
70. **Huybrecht W.J.** — Sol. Stat. Commun., 1978, 28, p.95.
71. **Bogoliubov Jr. N.N., Soldatov A.V.** — Mod. Phys. Lett., 1993, B7, p.1773.
72. **Alexandrou C., Rosenfelder R.** — Phys. Rep., 1992, 215, p.1.
73. **Chang S.-J.** — Phys. Rev., 1975, D12, p.1071.
74. **Polley L., Pottinger D. (eds.),** Variational Calculations in Quantum Field Theory, World Scientific, Singapore 1988.
75. **Coleman S., Weinberg E.** — Phys. Rev., 1973, D7, p.1888.
76. **Polley L., Ritschel U.** — Phys. Lett., 1989, B221, p.44.
77. **Stevenson P.M.** — Phys. Rev., 1984, D30, p.1712; 1985, D32, p.1389.
78. **Efimov G.V., Ganbold G.** — Int. J. Mod. Phys., 1990. A5, p.531.
79. **Fukuda R., Kyriakopoulos E.** — Nucl. Phys., 1975, B85, p.354.
80. **Efimov G.V.** — Int. Jour. Mod. Phys., 1989, A4, p.4977.
81. **Jackiw R.** — Phys. Rev., 1984, D9, p.1686.
82. **Efimov G.V., Ganbold G.** — Preprint ICTP-91-30, 1991.
83. **Simon B., Griffiths R.B.** — Comm. Math. Phys., 1973, 33, p.145.
84. **McBryan O.A., Rosen J.** — Comm. Math. Phys., 1979, 51, p.97.
85. **Chang S.-J.** — Phys. Rev., 1976, D13, p.2778; 1977, D16, p.1979.
86. **Drell S.D., Weinstein M., Yankielowicz S.** — Phys. Rev., 1976, D14, p.487.
87. **Funke M., Kaulfuss U., Kummel H.** — Phys. Rev., 1987, D35, p.631.
88. **Efimov G.V., Ganbold G.** — Preprint JINR E2-91-437, Dubna, 1991.
89. **Efimov G.V., Ganbold G.** — Preprint JINR E2-92-176, Dubna, 1992.
90. **Garcia N., Genack A.Z.** — Phys. Rev. Lett., 1991, 66, p.1850.
91. **Bouchaud J.P.** — Europhys. Lett., 1990, 11, p.505.
92. **Flatte S.M., Bernstein D.R., Dashen R.** — Phys. Fluids, 1983, 26, p.1701.
93. **Chow P.L.** — J. Math. Phys., 1972, 13, p.1224.
94. **Codona J.L. et al.** — J. Math. Phys., 1986, 27, p.171.
95. **Dashen R.** — J. Math. Phys., 1979, 20, p.894.

РЕФЕРАТЫ СТАТЕЙ, ОПУБЛИКОВАННЫХ В ВЫПУСКЕ

УДК 539.1.01

Нарушение фундаментальных симметрий в ядерных реакциях. *Бунаков В.Е.* Физика элементарных частиц и атомного ядра, 1995, том 26, вып.2, с.285.

В обзоре приведен теоретический анализ эффектов *P*- и (или) *T*-нарушения в ядерных реакциях. Показано, что всем этим эффектам свойственны два основных механизма усиления. Динамическое усиление, пропорциональное корню из числа компонент волновой функции компаунд-резонанса, знакомо нам еще по теории *P*-нарушения для связанных состояний ядра. Резонансное усиление, пропорциональное времени жизни компаунд-резонанса, является спецификой ядерных реакций в непрерывном спектре системы и не имеет аналогий в теории связанных состояний. Возникающее при этом суммарное усиление эффектов нарушения симметрии достигает 5-6 порядков (в случае *P*-несохранения предсказанные теоретические усиления на 6 порядков неоднократно подтверждены экспериментальными наблюдениями). Показано, что оба механизма усиления являются общим следствием квантовой хаотичности (сложности) структуры резонансов компаунд-ядра. Эта сложность, однако, приводит к необходимости использования статистических методов анализа экспериментально наблюдаемых величин для извлечения из них информации о силовых константах взаимодействий, нарушающих симметрию. Анализ таких статистических методов также приводится в обзоре.

Ил.6. Библиогр.: 89.

УДК 539.126.34+539.17.01

Двойная перезарядка пионов в рамках квазичастичного приближения случайных фаз. *Камински В.А.*Физика элементарных частиц и атомного ядра, 1995, том 26, вып.2, с.362.

Реакция двойной перезарядки пионов описана в рамках протон-нейтронного квазичастичного приближения случайных фаз. Данный метод апробирован на примере ядра железа ^{56}Fe, и получено довольно хорошее согласие рассчитанных характеристик с современными данными. Наблюдаемое резонансноподобное поведение энергетической зависимости сечения полукачественно объяснено с помощью двухнуклонных процессов без привлечения экзотических механизмов, таких как дибарионы или многокварковые кластеры.

Табл.1. Ил.5. Библиогр.: 55.

УДК 539.16

О смешивании волновых функций основных и вращательных состояний полос деформированных ядер. Часть 1. *Джелепов Б.С., Жуковский Н.Н., Шестопалова С.А.* Физика элементарных частиц и атомного ядра, 1995, том 26, вып.2, с.384.

Рассмотрено смешивание волновых функций во вращательных состояниях деформированных ядер. Представлены амплитуды волновых фукнций для 254 вращательных полос, рассчитанные различными авторами. В дальнейшем предполагается провести обсуждение и сравнение собранной информации с экспериментальными данными.

Табл.1. Библиогр.: 38.

УДК 539.142/143

Макроскопическая модель магнитных резонансов в сферических ядрах. *Баструков С.И., Молодцова И.В.* Физика элементарных частиц и атомного ядра, 1995, том 26, вып.2, с.415.

В обзоре изложены физические принципы и уравнения ядерной флюид-динамики — квантово-макроскопического метода описания мультипольных изоскалярных резонансов в терминах теории сплошных сред. Основная часть обзора посвящена коллективной модели магнитного ядерного отклика, в рамках которой изоскалярные магнитные мультипольные резонансы связываются с возбуждением длинноволновых крутильных колебаний сферического ядра. С точки зрения теории континуума существование данной ветви коллективных возбуждений свидетельствует о том, что ядерная материя обладает свойствами, присущими упругой сплошной среде. Подчеркивается, что физическая природа упругости ядерного вещества имеет существенно квантовое происхождение, поскольку является следствием фермиевского движения нуклонов и связанной с ними динамической деформации поверхности Ферми. Представлены аналитические выводы и численные оценки интегральных характеристических параметров магнитных изоскалярных резонансов: положений центроидов энергий в ядерном спектре, суммарных вероятностей возбуждения, магнитных осцилляторных сил, столкновительных ширин, вычисленных в зависимости от массового числа, атомного номера и мультипольного порядка возбуждения. Приведены коллективные переходные токовые плотности и магнитные формфакторы, аналитически рассчитанные в плосковолновом борновском приближении; численные расчеты выполнены в приближении искаженных волн. Теоретические предсказания сопоставляются с экспериментальными данными по магнитным коллективным возбуждениям сферических ядер, полученными в реакции неупругого рассеяния электронов.

Табл.4. Ил.10. Библиогр.: 111.

УДК 530.145+539.19

Гауссово-эквивалентное представление функциональных интегралов в квантовой физике. *Ефимов Г.В., Ганболд Г.* Физика элементарных частиц и атомного ядра, 1995, том.26, вып.2, с.459.

Предложен новый, регулярный метод непертурбативного вычисления широкого класса функциональных интегралов, применяемых в квантовой физике. Метод обеспечивает хорошую точность в низшем приближении, получаемом несложным путем. В случае вещественных функционалов оно представляет собой обобщение вариационного принципа. Предлагаемый метод выгодно отличается от вариационных подходов применимостью для комплексных функционалов и в теориях с расходимостями. Поправки высших порядков к низшему приближению вычисляются по регулярной схеме. Метод легко алгоритмизируется, что позволяет применять его к задачам, требующим большого объема численных расчетов.

Метод применен к ряду задач из различных областей теоретической физики: теории полярона в физике твердого тела, изучению фазового перехода в полевой модели φ^4 с расходимостями в высших порядках теории возмущений и к исследованию распространения волн в стохастических средах, где вариационные методы неприменимы. Построено гауссово-эквивалентное представление функционального интеграла полярона в пространстве размерности d и получено скейлинговое соотно-

шение для энергии полярона. Показано, что найденная собственная энергия полярона уже в нулевом приближении превосходит по точности известную вариационную оценку Фейнмана при любых значениях константы электрон-фононного взаимодействия α. Вычисленные значения следующих поправок заметно улучшают оценку для энергии полярона. В квантовой теории скалярного самодействия $g\varphi_d^4$ в двух- и трехмерном пространствах $d = 2$; 3 получены нулевое приближение для эффективного потенциала и эффективная масса скалярной частицы. Отмечено существование «нетривиального» решения для гауссова эффективного потенциала, поведение которого указывает на отсутствие фазового перехода первого рода в теории $g\varphi_2^4$. Проведен анализ этого вопроса с учетом вкладов высших поправок от негауссовой части эффективного потенциала, который убедительно указывает на существование фазового перехода второго рода в теории $g\varphi_2^4$ и на его отсутствие в случае $d = 3$. Найдено значение безразмерной критической константы $(g/2\pi m^2)_{\text{crit}} = 0{,}533$, при достижении которой наступает фазовый переход второго рода. Полученный результат согласуется с известными теоремами Б.Саймона, Р.Гриффитса и Дж.Розена (1979). В теории распространения волн в стохастических средах исследовано поведение функции Грина волнового уравнения и получено ее асимптотическое поведение на больших расстояниях.

Табл.6. Ил.3. Библиогр.: 95.

СОДЕРЖАНИЕ

CONTENTS

К СВЕДЕНИЮ АВТОРОВ

В журнале «Физика элементарных частиц и атомного ядра» (ЭЧАЯ) печатаются обзоры по актуальным проблемам теоретической и экспериментальной физики элементарных частиц и атомного ядра, проблемам создания новых ускорительных и экспериментальных установок, автоматизации обработки экспериментальных данных. Статьи печатаются на русском и английском языках. Редакция просит авторов при направлении статьи в печать руководствоваться изложенными ниже правилами.

1. Текст статьи должен быть напечатан на машинке через два интервала на одной стороне листа (обязательно представляется первый машинописный экземпляр). Поля с левой стороны должны быть не уже 3—4 см, рукописные вставки не допускаются. Экземпляр статьи должен включать аннотации и название на русском и английском языках, реферат на русском языке, УДК, сведения об авторах: фамилия и инициалы (на русском и английском языках), название института, адрес и телефон. Все страницы текста должны быть пронумерованы. Статья должна быть подписана всеми авторами. Текст статьи может быть напечатан на принтере с соблюдением тех же правил.

2. Формулы и обозначения должны быть вписаны крупно, четко, от руки темными чернилами (либо напечатаны на принтере и обязательно размечены). Желательно нумеровать только те формулы, на которые имеются ссылки в тексте. Номер формулы указывается справа в круглых скобках. Особое внимание следует обратить на аккуратное изображение индексов и показателей степеней: нижние индексы отмечаются знаком понижения ⌒, верхние — знаком повышения ⌣; штрихи необходимо четко отличать от единицы, а единицу — от запятой. Следует, по возможности, избегать громоздких обозначений и упрощать набор формул (например, применяя exp, дробь через косую черту).

Во избежание недоразумений и ошибок следует делать ясное различие между прописными и строчными буквами, одинаковыми по начертанию (V и v, U и u, W и w, O и o, K и k, S и s, C и c, P и p, Z и z), прописные подчеркивают двумя чертами снизу, строчные — двумя чертами сверху ($\underline{\underline{S}}$ и $\overline{\overline{s}}$, $\underline{\underline{C}}$ и $\overline{\overline{c}}$). Необходимо делать четкое различие между буквами e, *l*, O (большой) и o (малой) и 0 (нулем), для чего буквы $\underline{\underline{O}}$ и $\overline{\overline{o}}$ отмечают двумя черточками, а нуль оставляют без подчеркивания. Греческие буквы подчеркивают красным карандашом, векторы — синим, либо знаком $\underset{\sim}{\ }$ снизу чернилами. Не рекомендуется использовать для обозначения величин буквы готического, рукописного и других малоупотребимых в журнальных статьях шрифтов, однако если такую букву нельзя заменить буквой латинского или греческого алфавита, то ее размечают простым карандашом (обводят кружком). В случае, если написание может вызвать сомнение, необходимо на полях дать пояснение, например: ζ — «дзета», ξ — «кси», k — лат., к — русск.

3. Рисунки представляют на отдельных листах белой бумаги или кальки с указанием на обороте номера рисунка и названия статьи. Тоновые фотографии должны быть представлены в двух экземплярах, на обороте карандашом указать: «верх», «низ». Графики должны быть тщательно выполнены тушью или черными чернилами; не рекомендуется загромождать рисунок ненужными деталями: большинство надписей выносится в подпись, а на рисунке заменяется цифрами или буквами. Желательно, чтобы рисунки были готовы к прямому репродуцированию. Подписи к рисункам представляются на отдельных листах.

4. Таблицы должны быть напечатаны на отдельных листах, каждая таблица должна иметь заголовок. Следует указывать единицы измерения величин в таблицах.

5. Список литературы помещается в конце статьи. Ссылки в тексте даются с указанием номера ссылки на строке в квадратных скобках. В литературной ссылке должны быть указаны: для книг — фамилии авторов, инициалы, название книги, город, издательство (или организация),

год издания, том (часть, глава), цитируемая страница, если нужно; для статей — фамилии авторов, инициалы, название журнала, серия, год издания, том (номер, выпуск, если это необходимо), первая страница статьи. Если авторов более пяти, то указать только первые три фамилии.

Например:

1. Лезнов А.Н., Савельев М.В. — Групповые методы интегрирования нелинейных динамических систем. М.: Наука, 1985, с.208.
2. Годен М. — Волновая функция Бете: Пер. с франц. М.: Мир, 1987.
3. Turbiner A.V. — Comm.Math.Phys., 1988, vol.118, p.467.
4. Ушверидзе А.Г. — ЭЧАЯ, 1989, т.20, вып.5, с.1185.
5. Endo I., Kasai S., Harada M. et al. — Hirosima Univ. Preprint, HUPD-8607, 1986.

6. Редакция посылает автору одну корректуру. Изменения и дополнения в тексте и рисунках не допускаются. Корректура с подписью автора и датой ее подписания должна быть выслана в редакцию в минимальный срок.

Редакторы: **Е.К.Аксенова, Э.В.Ивашкевич.**
Художественный редактор **А.Л.Вульфсон.**
Корректор **Т.Е.Попеко.**

Сдано в набор 17.11.94. Подписано в печать 24.02.95. Формат 60×90/16.
Бумага офсетная № 1. Печать офсетная. Усл.печ.л. 14,8. Уч.-изд.л. 17,78.
Тираж 600. Заказ 48016. Цена 800 р.

141980 Дубна Московской области
ОИЯИ, Издательский отдел, тел. (09621) 65-165.

ISSN 0367—2026. Физика элементарных частиц и атомного ядра
1995. Том 26. Вып.2. 281—518.